ISSN 2220-315x (online)

World Journal of *Experimental Medicine*

Quarterly Volume 14 Number 1 March 20, 2024

Published by Baishideng Publishing Group Inc

World Journal of Experimental Medicine

Contents

Quarterly Volume 14 Number 1 March 20, 2024

EDITORIAL

Casu C, Orrù G. Potential of photodynamic therapy in the management of infectious oral diseases. *World J Exp Med* 2024; 14(1): 84284 [DOI: 10.5493/wjem.v14.i1.84284]

FIELD OF VISION

Kelleni MT. COVID-19 mortality paradox (United States vs Africa): Mass vaccination vs early treatment. *World J Exp Med* 2024; 14(1): 88674 [DOI: 10.5493/wjem.v14.i1.88674]

OPINION REVIEW

Milionis C, Ilias I, Lekkou A, Venaki E, Koukkou E. Future clinical prospects of C-peptide testing in the early diagnosis of gestational diabetes. *World J Exp Med* 2024; 14(1): 89320 [DOI: 10.5493/wjem.v14.i1.89320]

MINIREVIEWS

Cotterell A, Griffin M, Downer MA, Parker JB, Wan D, Longaker MT. Understanding wound healing in obesity. *World J Exp Med* 2024; 14(1): 86898 [DOI: 10.5493/wjem.v14.i1.86898]

Sridhar GR, Gumpeny L. Emerging significance of butyrylcholinesterase. *World J Exp Med* 2024; 14(1): 87202 [DOI: 10.5493/wjem.v14.i1.87202]

ORIGINAL ARTICLE

Retrospective Cohort Study

Senchukova MA, Kalinin EA, Volchenko NN. Predictors of disease recurrence after radical resection and adjuvant chemotherapy in patients with stage IIb-IIIa squamous cell lung cancer: A retrospective analysis. *World J Exp Med* 2024; 14(1): 89319 [DOI: 10.5493/wjem.v14.i1.89319]

Clinical Trials Study

Saeed EN, Faeq AK. Impact of primary percutaneous coronary intervention on ST-segment elevation myocardial infarction patients: A comprehensive analysis. *World J Exp Med* 2024; 14(1): 88541 [DOI: 10.5493/wjem.v14.i1.88541]

Observational Study

Stasi C, Pacifici M, Milli C, Profili F, Silvestri C, Voller F. Prevalence and features of SARS-CoV-2 infection in prisons in Tuscany. *World J Exp Med* 2024; 14(1): 87551 [DOI: 10.5493/wjem.v14.i1.87551]

Clinical and Translational Research

Garg G, Bharadwaj A, Chaudhary S, Gupta V. Chemical profiling of bioactive compounds in the methanolic extract of wild leaf and callus of Vitex negundo using gas chromatography-mass spectrometry. *World J Exp Med* 2024; 14(1): 88064 [DOI: 10.5493/wjem.v14.i1.88064]

World Journal of Experimental Medicine

Quarterly Volume 14 Number 1 March 20, 2024

Contents

Basic Study

Lesser T, Wolfram F, Braun C, Gottschall R. Effects of unilateral superimposed high-frequency jet ventilation on porcine hemodynamics and gas exchange during one-lung flooding. *World J Exp Med* 2024; 14(1): 87256 [DOI: 10.5493/wjem.v14.i1.87256]

Medanki S, Dommati N, Bodapati HH, Katru VNSK, Moses G, Komaraju A, Donepudi NS, Yalamanchili D, Sateesh J, Turimerla P. Artificial intelligence powered glucose monitoring and controlling system: Pumping module. *World J Exp Med* 2024; 14(1): 87916 [DOI: 10.5493/wjem.v14.i1.87916]

Mohd Nasir S, Ismail AF, Tuan Ismail TS, Wan Abdul Rahman WF, Wan Ahmad WAN, Tengku Din TADAA, Sirajudeen KNS. Hepatic and renal effects of oral stingless bee honey in a streptozotocin-induced diabetic rat model. *World J Exp Med* 2024; 14(1): 91271 [DOI: 10.5493/wjem.v14.i1.91271]

World Journal of Experimental Medicine

Quarterly Volume 14 Number 1 March 20, 2024

Contents

ABOUT COVER

Peer Reviewer of *World Journal of Experimental Medicine*, Ramya Badrachalam, MBBS, MD, Assistant Professor, Department of Biochemistry, Sri Manakula Vinayagar Medical College & Hospital, Puducherry 605107, India. drramya830@gmail.com

AIMS AND SCOPE

The primary aim of the *World Journal of Experimental Medicine* (*WJEM*, *World J Exp Med*) is to provide scholars and readers from various fields of experimental medicine with a platform to publish high-quality basic and clinical research articles and communicate their research findings online.

WJEM mainly publishes articles reporting research results and findings obtained in the field of experimental medicine and covering a wide range of topics including clinical laboratory medicine (applied and basic research in hematology, body fluid examination, cytomorphology, genetic diagnosis of hematological disorders, thrombosis and hemostasis, and blood typing and transfusion), biochemical examination (applied and basic research in laboratory automation and information system, biochemical methodology, and biochemical diagnostics), *etc*.

INDEXING/ABSTRACTING

The *WJEM* is now abstracted and indexed in PubMed, PubMed Central, Scopus, Reference Citation Analysis, China Science and Technology Journal Database, and Superstar Journals Database. The *WJEM*'s CiteScore for 2022 is 1.0 and Scopus CiteScore rank 2022: Internal medicine is 106/140.

RESPONSIBLE EDITORS FOR THIS ISSUE

NAME OF JOURNAL
World Journal of Experimental Medicine

ISSN
ISSN 2220-315x (online)

LAUNCH DATE
December 20, 2011

FREQUENCY
Quarterly

PUBLICATION DATE
March 20, 2024

PUBLISHING PARTNER
Department of Clinical Laboratory, The Affiliated Suzhou Hospital of Nanjing Medical University, Suzhou Municipal Hospital

PUBLISHING PARTNER's OFFICIAL WEBSITE
http://www.smh.cc/home2020/page/index/index.html

World Journal of Experimental Medicine

Submit a Manuscript: https://www.f6publishing.com

World J Exp Med 2024 March 20; 14(1): 84284

DOI: 10.5493/wjem.v14.i1.84284

ISSN 2220-315x (online)

EDITORIAL

Potential of photodynamic therapy in the management of infectious oral diseases

Cinzia Casu, Germano Orrù

Specialty type: Dentistry, oral surgery and medicine

Provenance and peer review: Invited article; Externally peer reviewed.

Peer-review model: Single blind

Peer-review report's scientific quality classification

Grade A (Excellent): A
Grade B (Very good): B
Grade C (Good): C
Grade D (Fair): 0
Grade E (Poor): 0

P-Reviewer: Aoun G, Lebanon; Liu HQ, China; Wu J, China

Received: July 28, 2023
Peer-review started: July 28, 2023
First decision: October 9, 2023
Revised: November 24, 2023
Accepted: December 19, 2023
Article in press: December 19, 2023
Published online: March 20, 2024

Cinzia Casu, Germano Orrù, Department of Surgical Science, Oral Biotechnology Laboratory, University of Cagliari, Cagliari 09124, Italy

Corresponding author: Cinzia Casu, MD, Adjunct Professor, Department of Surgical Science, Oral Biotechnology Laboratory, University of Cagliari, Via Ospedale 54, Cagliari 09124, Italy. ginzia.85@hotmail.it

Abstract

Photodynamic therapy (PDT) can take place in the presence of three elements: Light with an appropriate wavelength; a photosensitizer; and the presence of oxygen. This type of treatment is very effective overall against bacterial, viral and mycotic cells. In the last 10 years many papers have been published on PDT with different types of photosensitizers (*e.g.*, methylene blue, toluidine blue, indocyanine green, curcumin-based photosensitizers), different wavelengths (*e.g.*, 460 nm, 630 nm, 660 nm, 810 nm) and various parameters (*e.g.*, power of the light, time of illumination, number of sessions). In the scientific literature all types of PDT seem very effective, even if it is difficult to find a standard protocol for each oral pathology. PDT could be an interesting way to treat some dangerous oral infections refractory to common pharmacological therapies, such as candidiasis from multidrug-resistant *Candida spp*.

Key Words: Photodynamic therapy; oral infections; Photodynamic therapy *vs* candidiasis; Blue light; 460 nm; *Streptococcus mutans*

Core Tip: In recent years there are more and more multidrug resistant infections at the oral level, and this has led researchers to find alternative solutions to conventional pharmacology that have no impact on systemic health. Among these, there is photodynamic therapy, which has demonstrated efficacy both *in vitro* and *in vivo*, for treating bacterial, viral (reducing recrudescence) and fungal infections, particularly multidrug-resistant *Candida spp*.

Citation: Casu C, Orrù G. Potential of photodynamic therapy in the management of infectious oral diseases. *World J Exp Med* 2024; 14(1): 84284
URL: https://www.wjgnet.com/2220-315x/full/v14/i1/84284.htm
DOI: https://dx.doi.org/10.5493/wjem.v14.i1.84284

INTRODUCTION

There are over 780 results in PubMed when searching the keyword "Photodynamic Therapy for Oral Infection," with an exponential growth of the works published in the last 10 years. All this denotes the strong scientific interest of this instrument in the field of infectious pathologies of the oral cavity.

Photodynamic therapy (PDT) can take place in the presence of three elements: Light with an appropriate wavelength; a photosensitizer; and the presence of oxygen. When a photosensitizer is activated by light, it will either lose energy or form an oxygen triplet[1]. This second type of PDT is linked to the amount of oxygen, while the first type of PDT can work in anaerobic conditions[2]. The interaction that the photosensitizer has with oxygen can determine the formation of hydrogen peroxide, hydroxyl radicals, superoxide radical oxygen, and singlet oxygen. These products determine the killing of microorganisms due to damage to the cell membrane and their metabolic activity[1].

The maximum absorption of light by the photosensitizer occurs at a wavelength between 600 nm and 800 nm. In fact, a higher wavelength would not have enough energy to stimulate oxygen to produce radicals[1]. The penetration of the wavelength comprised between 700-1100 nm is wider than that comprised between 400-700 nm[2].

Among the infections that afflict the oral cavity, endodontic infections are caused by microorganisms that colonize the inside of the tooth and can give rise to infections in the periapical bone tissue. One of the most important microorganisms in this infectious process is *Enterococcus faecalis* (*E. faecalis*), which is also the most studied *in vitro* and *ex vivo* model. The difficulty of eradicating this microorganism responsible for endodontic re-infections and refractory infections has prompted researchers to make use of PDT in eradicating this microorganism. Researchers have found that the photosensitizer curcumin activated by LED (450 nm, 67 mW/cm^2, and 20.1 J/cm^2) has shown very interesting results in reducing the colony forming units of *E. faecalis*[1]. Other authors have tested Ce6 methyl ester (Zn(II)e6Me), a chlorophyll-derived photosensitizer activated by red light (627 nm, 75 mW, 3150 J/cm^2) for 90 s, with success against *E. faecalis*. Furthermore, an *in vitro* study found that a PDT using 500 g/mL of Chlorella plus 660 nm diode laser at an energy density of 23.43 J/cm^2 was effective against *E. faecalis* biofilms[1].

The most frequent infectious disease at the gingival level is periodontitis. It is an infectious process mediated by various microorganisms, including *Porphyromonas gingivalis* and *Aggregatibacter actinomycetemcomitans* that leads to inflammation and destruction of bone and gingival tissue with loss of stability of the dental elements. *Curcuma longa* activated by blue LED lights (450-470 nm, output power density 1.2 W/cm^2) and Ce6 have shown the most effectiveness among the natural photosensitizers[1]. PDT carried out with *Curcuma longa* and diode light at 460 nm has also shown efficacy in drug-induced gingival hypertrophy[3].

Rose bengal with a light source for illumination (375 nm, 3 mW/cm^2) could be very useful for reducing the bacterial load of *Streptococcus mutans*, the most important etiological agent of dental cavities. Ozonated water used as a photosensitizer and activated by 460 nm LED lights has also demonstrated efficacy against *Streptococcus mutans*[4].

The most frequent oral viral infectious diseases are associated with herpes simplex type 1. Clinically, this is a condition that involves the formation of vesicles filled with infectious liquid that when they explode give rise to erosion and the formation of crusts if they affect the vermilion border of the lips. In this context, the gold standard treatment is represented by topical or systemic antivirals, particularly in extensive systemic cases. However, the reduction of effectiveness of traditional pharmacological treatments has prompted several researchers to find different solutions to mitigate these infections, including PDT[5]. For example, the most common photosensitizer for the treatment of *Herpes simplex* infection is methylene blue at concentrations between 0.1% and 1%, activated by lights with a wavelength of 660 nm. In another *in vitro* study, indocyanine green also showed good results when activated by wavelengths of 810 nm[6,7].

Human papillomavirus (HPV) plays a prominent role in causing viral infections in the mouth. According to the World Health Organization reports, it is estimated that in developed countries a growing prevalence of HPV-related cancer is reported each year, particularly for males. There are over 200 subtypes of HPV, but some of these can trigger malignant tissue transformations, including HPV 16. Surgical excision and histological evaluation represent the treatment of choice. Sometimes these lesions can reach considerable dimensions, are located in sites that are difficult to reach and can be recurring. These reasons have led clinicians to try PDT on the oral cavity in a patient with a large squamous papilloma in the soft palate. In this case, a formulation containing 5-aminolevulenic acid is injected at the perilesional level and activated with wavelengths of 630 nm at a power of 100 J/cm^2 and at 300 mW/cm^2 of power density for 6 min. After two sessions, the lesion healed[8].

PDT has also been proposed in the treatment of oral lesions from coronavirus disease 2019. In fact, *in vitro* studies have shown that methylene blue was able to inhibit the severe acute respiratory syndrome coronavirus 2 spike protein and its angiotensin converting enzyme-2 receptor. It was also used to treat the typical crusted lip lesions associated with coronavirus disease 19 at very low concentrations[9].

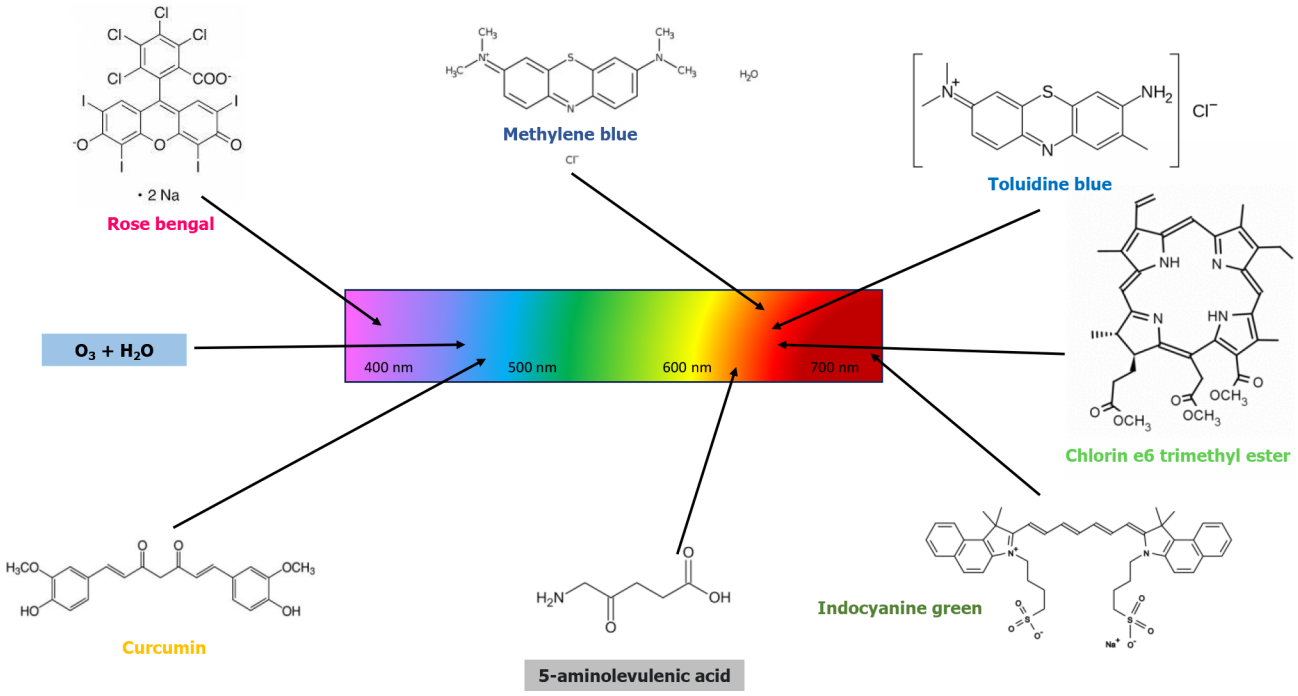

Figure 1 Schematic representation of the main photosensitizers used in oral medicine with the respective wavelength of excitation pointed in the visible light spectrum.

PDT FOR ORAL CANDIDIASIS

Oral candidiasis, as previously mentioned, is an infection that increasingly shows resistance to the main commercial antifungals, such as azoles. PDT was proposed 15 years ago as an alternative, especially in relapsing cases of oral candidiasis. Among the most tested photosensitizers, methylene blue, which is associated with laser and non-red laser lights, has demonstrated excellent antifungal properties at different concentrations[10-13]. Toluidine blue has also been widely proposed in different concentrations for the treatment of *Candida* infections in the oral cavity. A recent review on the subject has highlighted that most of these are *in vitro* studies, where the parameters used are very different between the various studies, even if almost all report the efficacy of PDT. In addition to the more common *Candida albicans*, it has also been tested against different species of *Candida* in some studies, such as *Candida glabrata, Candida krusei, Candida parapsilosis and Candida tropicalis*. Toluidine blue has been shown to be effective against all types of *Candida spp.* mentioned [14]. Most of the *in vitro* studies evaluated both the activity of PDT in its planktonic form and in the biofilm of the fungus. The prevailing method was that of microplates[14].

A recent compound, indocyanine green, activated by a light with a wavelength of 808 nm has also been proposed as a photosensitizer. In fact, by comparing this approach with a traditional treatment based on nystatin, a significant infection reduction was observed, which was similar to the healthy group control patient[15]. The same result was reported in another study on refractory subprosthetic candidiasis in which PDT showed better results than the group treated only pharmacologically[16]. Furthermore, in another study, PDT with indocyanine green was shown to be more effective *in vitro* than PDT performed with methylene blue[17].

Other photosensitizers tested *in vitro* against *Candida* were erythrosine and rose bengal, activated by green diode lights around 532 nm[18,19]. Erythrosine was also effective against *Candida dubliniensis*, demonstrating good efficacy in the planktonic form but less activity on the biofilm[20]. Among the natural photosensitizers reported are 5-aminolevulenic acid[21] and derivatives from *Curcuma longa*, which was first carried out in 2013[22]. In a study using LED light at 460 nm, 5-aminolevulenic acid showed *in vitro* antifungal activity higher than that of methylene blue, which was activated by red light at 660 nm[23]. A photosensitizer based on *Curcuma longa*/3% hydrogen peroxide, activated by polarized light (wavelength from 380 to 3400 nm), showed greater antifungal activity than activation with LED light at 460 nm (the wavelength most widely used in PDT to activate curcumin)[24]. Furthermore, PDT has also shown efficacy in other oral pathologies, perhaps by virtue of its antimicrobial action against microorganisms that colonize the damaged mucosal surfaces[25] or which may be at the basis of the pathogenic process[26]. The main photosensitizers used in PDT *vs* oral infections, with relative wavelength of activation, are summarized in Figure 1.

CONCLUSION

The increasing resistance to antibiotics, antifungals and antivirals, the side effects of the drugs themselves on some categories of patients and the possibility of resolving some infections in a single session have led researchers to propose

the use of PDT as a treatment tool for refractory infections of the oral cavity. The wide variability of the parameters used, including the wavelength, the type of photosensitizer, the pre-illumination and irradiation times, makes it difficult to have standard protocols for the treatment of each oral pathology. Further studies will be needed to find the most suitable protocols for each type of oral infection.

ACKNOWLEDGEMENTS

Cinzia Casu performed this research activity in the framework of the International PhD in Innovation Sciences and Technologies at the University of Cagliari, Italy.

FOOTNOTES

Co-corresponding authors: Cinzia Casu and Germano Orrù.

Author contributions: Casu C contributed to ideas and writing of the work; Orrù G contributed to bibliographic support, creation of the figure and final revision; Casu C and Orrù G are both corresponding authors because they have different areas of expertise (Casu C is a clinician with expertise in oral pathology, and Orrù G is a biologist with expertise in microbiology and molecular biology); All authors read and approved the final manuscript.

Conflict-of-interest statement: All the authors declare having no conflicts of interest.

Country/Territory of origin: Italy

ORCID number: Cinzia Casu 0000-0002-7962-2712.

S-Editor: Liu JH
L-Editor: Filipodia
P-Editor: Yuan YY

REFERENCES

1 **Afrasiabi S**, Partoazar A, Chiniforush N, Goudarzi R. The Potential Application of Natural Photosensitizers Used in Antimicrobial Photodynamic Therapy against Oral Infections. *Pharmaceuticals (Basel)* 2022; **15** [PMID: 35745686 DOI: 10.3390/ph15060767]
2 **Gao J**, Chen Z, Li X, Yang M, Lv J, Li H, Yuan Z. Chemiluminescence in Combination with Organic Photosensitizers: Beyond the Light Penetration Depth Limit of Photodynamic Therapy. *Int J Mol Sci* 2022; **23** [PMID: 36293406 DOI: 10.3390/ijms232012556]
3 **Casu C**, Murgia MS, Orrù G, Scano A. Photodynamic therapy for the successful management of cyclosporine-related gum hypertrophy: A novel therapeutic option. *J Public Health Res* 2022; **11**: 22799036221116177 [PMID: 36226306 DOI: 10.1177/22799036221116177]
4 **Casu C**, Orrù G, Fais S, Mazur M, Grassi R, Grassi RF, Nardi GM. Efficacy of ozonated water as a PS in photodynamic therapy: A tool for dental caries management? An *in vitro* study. *J Public Health Res* 2023; **12**: 22799036231182267 [PMID: 37378003 DOI: 10.1177/22799036231182267]
5 **La Selva A**, Negreiros RM, Bezerra DT, Rosa EP, Pavesi VCS, Navarro RS, Bello-Silva MS, Ramalho KM, Aranha ACC, Braz-Silva PH, Fernandes KPS, Bussadori SK, Horliana ACRT. Treatment of herpes labialis by photodynamic therapy: Study protocol clinical trial (SPIRIT compliant). *Medicine (Baltimore)* 2020; **99**: e19500 [PMID: 32195950 DOI: 10.1097/MD.0000000000019500]
6 **Khalil M**, Hamadah O. Association of Photodynamic Therapy and Photobiomodulation As a Promising Treatment of Herpes Labialis: A Systematic Review. *Photobiomodul Photomed Laser Surg* 2022; **40**: 299-307 [PMID: 35483089 DOI: 10.1089/photob.2021.0186]
7 **Namvar MA**, Vahedi M, Abdolsamadi HR, Mirzaei A, Mohammadi Y, Azizi Jalilian F. Effect of photodynamic therapy by 810 and 940 nm diode laser on Herpes Simplex Virus 1: An *in vitro* study. *Photodiagnosis Photodyn Ther* 2019; **25**: 87-91 [PMID: 30447412 DOI: 10.1016/j.pdpdt.2018.11.011]
8 **Jin J**, Zhang Y, Zhiyue L. Successful treatment of oral human papilloma by local injection 5-aminolevulinic acid-mediated photodynamic therapy: A case report. *Photodiagnosis Photodyn Ther* 2019; **26**: 134-136 [PMID: 30890459 DOI: 10.1016/j.pdpdt.2019.03.011]
9 **Betsy J**, Prasanth CS. Can photodynamic therapy be repurposed to treat oral lesions of COVID-19? *Photodiagnosis Photodyn Ther* 2021; **33**: 102175 [PMID: 33422697 DOI: 10.1016/j.pdpdt.2021.102175]
10 **Freire F**, Ferraresi C, Jorge AO, Hamblin MR. Photodynamic therapy of oral Candida infection in a mouse model. *J Photochem Photobiol B* 2016; **159**: 161-168 [PMID: 27074245 DOI: 10.1016/j.jphotobiol.2016.03.049]
11 **Javed F**, Samaranayake LP, Romanos GE. Treatment of oral fungal infections using antimicrobial photodynamic therapy: a systematic review of currently available evidence. *Photochem Photobiol Sci* 2014; **13**: 726-734 [PMID: 24686309 DOI: 10.1039/c3pp50426c]
12 **Boltes Cecatto R**, Siqueira de Magalhães L, Fernanda Setúbal Destro Rodrigues M, Pavani C, Lino-Dos-Santos-Franco A, Teixeira Gomes M, Fátima Teixeira Silva D. Methylene blue mediated antimicrobial photodynamic therapy in clinical human studies: The state of the art.

Photodiagnosis Photodyn Ther 2020; **31**: 101828 [PMID: 32473398 DOI: 10.1016/j.pdpdt.2020.101828]

13 **Martins Jda S**, Junqueira JC, Faria RL, Santiago NF, Rossoni RD, Colombo CE, Jorge AO. Antimicrobial photodynamic therapy in rat experimental candidiasis: evaluation of pathogenicity factors of Candida albicans. *Oral Surg Oral Med Oral Pathol Oral Radiol Endod* 2011; **111**: 71-77 [PMID: 21176823 DOI: 10.1016/j.tripleo.2010.08.012]

14 **Wiench R**, Skaba D, Matys J, Grzech-Leśniak K. Efficacy of Toluidine Blue-Mediated Antimicrobial Photodynamic Therapy on Candida spp. A Systematic Review. *Antibiotics (Basel)* 2021; **10** [PMID: 33806003 DOI: 10.3390/antibiotics10040349]

15 **Tavangar A**, Khozeimeh F, Razzaghi-Abyaneh M, Sherkat S. Sensitivity of Four Various Candida Species to Photodynamic Therapy Mediated by Indocyanine Green, an *in vitro* Study. *J Dent (Shiraz)* 2021; **22**: 118-124 [PMID: 34150948 DOI: 10.30476/DENTJODS.2020.81817.0]

16 **Afroozi B**, Zomorodian K, Lavaee F, Zare Shahrabadi Z, Mardani M. Comparison of the efficacy of indocyanine green-mediated photodynamic therapy and nystatin therapy in treatment of denture stomatitis. *Photodiagnosis Photodyn Ther* 2019; **27**: 193-197 [PMID: 31185323 DOI: 10.1016/j.pdpdt.2019.06.005]

17 **Azizi A**, Amirzadeh Z, Rezai M, Lawaf S, Rahimi A. Effect of photodynamic therapy with two photosensitizers on Candida albicans. *J Photochem Photobiol B* 2016; **158**: 267-273 [PMID: 27064379 DOI: 10.1016/j.jphotobiol.2016.02.027]

18 **Costa AC**, Rasteiro VM, Pereira CA, Rossoni RD, Junqueira JC, Jorge AO. The effects of rose bengal- and erythrosine-mediated photodynamic therapy on Candida albicans. *Mycoses* 2012; **55**: 56-63 [PMID: 21668520 DOI: 10.1111/j.1439-0507.2011.02042.x]

19 **Freire F**, Costa AC, Pereira CA, Beltrame Junior M, Junqueira JC, Jorge AO. Comparison of the effect of rose bengal- and eosin Y-mediated photodynamic inactivation on planktonic cells and biofilms of Candida albicans. *Lasers Med Sci* 2014; **29**: 949-955 [PMID: 24013675 DOI: 10.1007/s10103-013-1435-x]

20 **Costa AC**, de Campos Rasteiro VM, Pereira CA, da Silva Hashimoto ES, Beltrame M Jr, Junqueira JC, Jorge AO. Susceptibility of Candida albicans and Candida dubliniensis to erythrosine- and LED-mediated photodynamic therapy. *Arch Oral Biol* 2011; **56**: 1299-1305 [PMID: 21704304 DOI: 10.1016/j.archoralbio.2011.05.013]

21 **AlGhamdi AS**, Qamar Z, AlSheikh R, Al Hinai MTA, Abdul NS, Aljoghaiman EA, Ali S. Clinical efficacy of 5-aminolevulinic acid-mediated photodynamic therapy *vs* topical antifungal agent and surgical excision for the treatment of hyperplastic candidiasis. *Photodiagnosis Photodyn Ther* 2023; **41**: 103258 [PMID: 36592782 DOI: 10.1016/j.pdpdt.2022.103258]

22 **Dovigo LN**, Carmello JC, de Souza Costa CA, Vergani CE, Brunetti IL, Bagnato VS, Pavarina AC. Curcumin-mediated photodynamic inactivation of Candida albicans in a murine model of oral candidiasis. *Med Mycol* 2013; **51**: 243-251 [PMID: 22934533 DOI: 10.3109/13693786.2012.714081]

23 **Daliri F**, Azizi A, Goudarzi M, Lawaf S, Rahimi A. In vitro comparison of the effect of photodynamic therapy with curcumin and methylene blue on Candida albicans colonies. *Photodiagnosis Photodyn Ther* 2019; **26**: 193-198 [PMID: 30914389 DOI: 10.1016/j.pdpdt.2019.03.017]

24 **Casu C**, Orrù G, Scano A. Curcumin/H2O2 photodynamically activated: an antimicrobial time-response assessment against an MDR strain of Candida albicans. *Eur Rev Med Pharmacol Sci* 2022; **26**: 8841-8851 [PMID: 36524503 DOI: 10.26355/eurrev_202212_30556]

25 **Casu C**, Mannu C. Atypical Afta Major Healing after Photodynamic Therapy. *Case Rep Dent* 2017; **2017**: 8517470 [PMID: 29085681 DOI: 10.1155/2017/8517470]

26 **Scano A**, Casu C, Orrù G, Coni P. Editorial - Epigenetic mechanisms in oral cancer: new diagnostic and therapeutic strategies. *Eur Rev Med Pharmacol Sci* 2022; **26**: 7318-7320 [PMID: 36314301 DOI: 10.26355/eurrev_202210_30000]

World Journal of Experimental Medicine

Submit a Manuscript: https://www.f6publishing.com

World J Exp Med 2024 March 20; 14(1): 88674

DOI: 10.5493/wjem.v14.i1.88674

ISSN 2220-315x (online)

FIELD OF VISION

COVID-19 mortality paradox (United States *vs* Africa): Mass vaccination *vs* early treatment

Mina Thabet Kelleni

Specialty type: Infectious diseases

Provenance and peer review: Invited article; Externally peer reviewed.

Peer-review model: Single blind

Peer-review report's scientific quality classification
Grade A (Excellent): 0
Grade B (Very good): 0
Grade C (Good): C
Grade D (Fair): 0
Grade E (Poor): 0

P-Reviewer: Liu YC, China

Received: October 4, 2023
Peer-review started: October 4, 2023
First decision: December 6, 2023
Revised: December 16, 2023
Accepted: January 4, 2024
Article in press: January 4, 2024
Published online: March 20, 2024

Mina Thabet Kelleni, Department of Pharmacology, College of Medicine, Minia University, Minya 61111, Egypt

Corresponding author: Mina Thabet Kelleni, MD, PhD, Assistant Professor, Pharmacology Department, College of Medicine, Minia University, Main Road Shalaby Land, PO Box 61519, Minia, Egypt. mina.kelleni@mu.edu.eg

Abstract

The coronavirus disease 2019 (COVID-19) mortality rate in 55 African countries is almost 4.5 times lower than in the coronavirus disease 2019 (COVID-19) despite Africa having over 4.2 times more people. This mortality paradox is also evident when comparing Nigeria, a heavily populated, poorly vaccinated and weakly mandated country to Israel, a small, highly vaccinated and strictly mandated country. Nigeria has almost 4 times lower COVID mortality than Israel. In this Field of Vision perspective, I explain how this paradox has evolved drawing upon my academic, clinical and social experience. Since April 2020, I've developed and been using the Egyptian immune-modulatory Kelleni's protocol to manage COVID-19 patients including pediatric, geriatric, pregnant, immune-compromised and other individuals suffering from multiple comorbidities. It's unfortunate that severe acute respiratory syndrome coronavirus 2 is still evolving accompanied by more deaths. However in Africa, we've been able to live without anxiety or mandates throughout the pandemic because we trust science and adopted early treatment using safe, and effective repurposed drugs that have saved the majority of COVID-19 patients. This article represents an African and Egyptian tale of honor.

Key Words: COVID-19; Early treatment; Kelleni's Protocol; Mandates; Mortality Paradox; SARS-CoV-2; Nucleic acid based vaccines

Core Tip: Coronavirus disease 2019 (COVID-19) has claimed the lives of millions of people worldwide. Paradoxically, the highest mortality numbers were encountered in countries that adopted the Western approach of mass nucleic acid based vaccination and rapidly approved drugs such as remdesivir, molnupiravir and nirmatrelvir-ritonavir (Paxlovid). In contrast, most developing countries that adopted early treatment using uniquely repurposed safe immune-modulatory drugs, as best scientifically documented in Kelleni's protocol, experienced the lowest COVID-19 mortality rates. In this field of vision perspective, I aim to explain the COVID-19 mortality paradox by demonstrating our African scientific approach which rejected compulsory vaccination with nucleic acid based vaccines as well as many other Western mandates. Early treatment using Kelleni's protocol has saved the lives of geriatric, immune-compromised and other comorbid COVID-19 patients, while young and otherwise healthy patients lost their lives in developed countries like the United States.

Citation: Kelleni MT. COVID-19 mortality paradox (United States *vs* Africa): Mass vaccination *vs* early treatment. *World J Exp Med* 2024; 14(1): 88674
URL: https://www.wjgnet.com/2220-315x/full/v14/i1/88674.htm
DOI: https://dx.doi.org/10.5493/wjem.v14.i1.88674

INTRODUCTION

As of October 1, 2023 severe acute respiratory syndrome coronavirus 2 (SARS-CoV-2) is still evolving and the potential to return to square one remains valid[1]. Unfortunately, very few lessons have been learned since November 2019, if any[2] despite the fact that coronavirus disease 2019 (COVID-19) global mortality has approached seven million people, to be noted that this abstract and underestimated number[3] can never reflect the personal suffering of millions of families. Moreover, the repeated COVID-19 imposed lockdowns have severely affected the global economy[4] and have led to increased poverty[5]. Additionally, numerous psychological disorders have affected children who have been isolated at home or constrained at schools as well as adults who have experienced repeated lockdowns[6]. Several mandates especially compulsory vaccination have been strictly implemented, resulting in job loss, defamation, stigmatization, intimidation or censorship of individuals who refused to comply[7,8] or exposed potential fraud[8,9].

Remarkably, most African countries, including Egypt, have managed to avoid this catastrophic situation. We were fortunate as we initially had no access to the newly introduced "experimental" nucleic acid based (mRNA and adenovector-ed) vaccines and other expensive "experimental" drugs such as remdesivir, molnupiravir, Paxlovid and numerous monoclonal antibodies[10-12]. These drugs were very rapidly approved and distributed first in Western and wealthy countries despite scientific concerns about their outbalanced risk-benefit ratio[11], their evolutionary pressure leading to more virulent SARS-CoV-2 variants[3], biased approval standards[9,13], and even delayed carcinogenicity risk [11,14,15].

Furthermore, we, Africans, have defied many mandates and have enjoyed a relatively COVID-free life. Nonetheless, the total number of COVID-19 deaths in 55 African countries as of October 1, 2023 was almost 4.5 times lower than in the United States, despite the fact that Africa has over 4.2 times more people than the United States[3] (Figure 1). Similarly, the mortality paradox is quite evident when comparing Nigeria, a heavily populated country with over 216 million people, relatively low vaccination rates and weak mandates to Israel, a small country with less than 10 million people, high vaccination rates and strict mandates. Nigeria has almost 4 times lower COVID deaths compared to Israel. Similar observation can also be made when examining the case of Haiti, a Caribbean with a population of over 11 million people. Despite having a negligible COVID-19 vaccination rate, with only 5% of the population choosing to receive it, Haiti has experienced almost no COVID burden or mortality[3]. This perspective aims to provide some reasons that may explain this paradox while drawing upon my academic, clinical and social experience.

EARLY COVID-19 TREATMENT USING KELLENI'S PROTOCOL IN EGYPT HAS PERFECT SUCCESS RATE

My first correspondence regarding COVID-19 was sent to the New England Journal of Medicine in March 2020 (ID 20-06753), but it was rejected without comment. In this correspondence, I aimed to expose what I called a pseudoscientific global scam that denied millions of patients access to lifesaving nonsteroidal anti-inflammatory drugs (NSAIDs), including ibuprofen, for the management of their COVID-19[16]. For months, nearly a dozen reputable journals denied me the opportunity for a peer review. However, an honorable editor in chief and the editorial board of a reputable journal offered me this opportunity and my work was eventually published[17,18].

Meanwhile, in April 2020, my first peer-reviewed publication was released. It explained for the first time globally why nitazoxanide is best suitable to manage COVID-19 and why it's superior to ivermectin regarding safety and efficacy[19]. It has also explained why azithromycin should be the antibiotic of choice when COVID-19 patients need one and a pioneering protocol was first suggested[19]. At that time, there was no ivermectin "obsession". However, when the full real-life immune-modulatory Kelleni's protocol using safe, effective and economic repurposed drugs was first fully published as a preprint in June 2020 (after prior preprints were published in May 2020); many editors of reputable

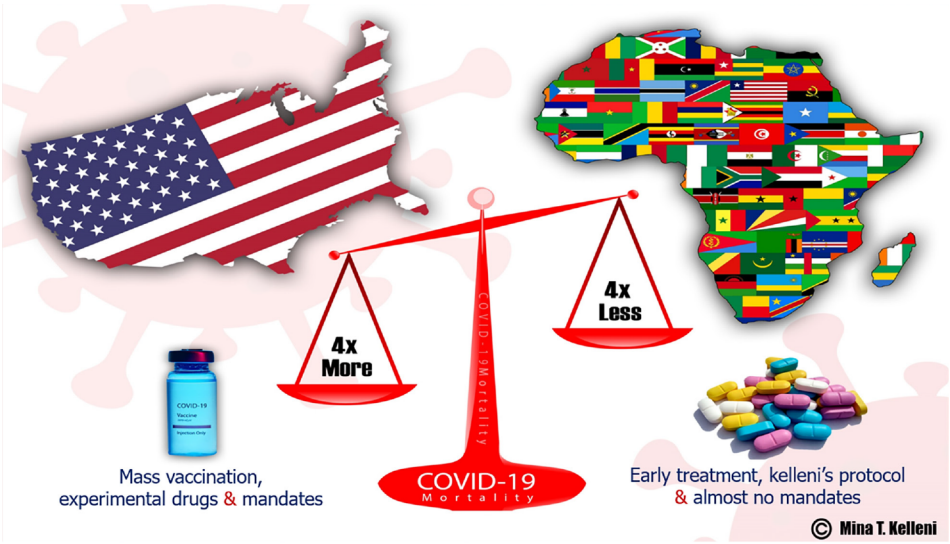

Figure 1 The coronavirus disease 2019 mortality paradox. The United States has tackled coronavirus disease 2019 (COVID-19) by heavily relying on mass vaccination, rapidly approving experimental drugs and implementing strict mandates. In contrast, Africa has chosen to adopt early treatment using safe repurposed drugs as best scientifically revealed in Kelleni's protocol and has abandoned mass vaccination and mandates. Despite Africa having a population over four times larger than the United States, its COVID-19 death toll has been four times lower.

medical journals were still skeptical. They repeatedly denied me fair opportunity for peer review. Additionally, my call to adopt randomized clinical trials of my protocol was completely ignored, despite hundreds of emails sent to scientists, ministers of health, prime ministers, journalists, the United States Food and Drug Administration (FDA) and other health care officials. I've kept records of these attempts, urging them to consider that an Egyptian and African protocol is safely, effectively and economically saving the lives of Egyptian patients of all ages as later was evident by numerous publications published at reputable journals[16,18,20-23]. Unfortunately, I've never received a single response from any of these hundreds of official recipients around the world, regardless of the number of reputable publications supporting my claims. This made me realize that during times panic and pandemic, medicine in Western countries serves politics rather than people. Ironically, I also realized that most ministers of health in the West are not physicians or scientists and their main aim is probably to win votes rather than save lives.

However, since April 2020, myself and many of colleagues who read my early publications and adopted the simple clinical approach of Kelleni's protocol, have almost saved every single life that was not previously exposed to remdesivir and the iatrogenic high dose of methylprednisolone used in hospitals that claimed to adopt the Western protocols[24]. Many of these cases suffered from moderate to severe COVID-19[21,23,25]. Notably, it took me almost a year and a half to have some of my COVID-19 preprints peer reviewed and published. In these numerous papers I've explained why the highly economic and extremely safe immune-modulatory Kelleni's protocol is highly effective and I've also demonstrated the molecular, genetic, immune mechanisms[16,22,26] together with real-life case reports of tens of patients including severe COVID-19 cases and how I used a personalized approach in their management[21,25]. Hence, this is how the name Kelleni's protocol has been coined[18,20,27].

Notably, at the start of the pandemic, I was working in Saudi Arabia, away from my family and patients in Egypt. This is why I initially relied on telemedicine. However, I soon resigned and returned home to be among the impoverished Egyptian patients and near my family members. I reopened my traditional clinic focusing mainly on COVID-19 and Post COVID syndrome; I named it Kelleni's COVID Clinic. I have been fully dedicated to the clinic until mid-December 2022 when knowledge about my protocol has spread, especially after appearing in three TV shows. At that point, I decided to take a break, return to telemedicine and traditional medicine in charitable clinics to have more time to resume my academic activity and share my updated clinically gained knowledge globally[1,3,20,27,28]. Importantly, my family; especially my parents in their 80s and my young daughters were the guiding light in my quest for a safe cure, as well as to repurpose a safe old vaccine which we all received it once[29]. Fortunately, I soon realized that we don't need a vaccine for this highly evolving respiratory virus. Early treatment using the immune-modulatory Kelleni's protocol has remained the most effective tool against all SARS-CoV-2 variants and subvariants.

IN AFRICA WE AVOIDED HOSPITALS THAT ADOPTED THE WESTERN COVID-19 PROTOCOLS

Moreover, it was quite astonishing to encounter, at a very early stage in the pandemic, how almost every time an Egyptian celebrity or high ranking official was treated in governmental or private hospitals using Western protocols that included remdesivir and dexamethasone, the ultimate outcome was death or, at best, disability[24]. Meanwhile, geriatric people with multiple co-morbidities were safely treated using Kelleni's protocol mostly at home[21,25]. Subsequently, the "business" of monoclonal antibodies have flourished[24], followed by the introduction of relatively unsafe and potentially ineffective yet highly profitable drugs like favipiravir and molnupiravir[10,12]. These drugs were widely

introduced to the African pharmaceutical market without most of the Western restrictions, and there was no fear of legal consequences. I claim that the Western COVID pharmaceutical industry has gained hundreds of billions of dollars while exploiting people's fear and ignorance. Notably, Western top politicians protected and nourished this business using mandates, along with a fierce media that defamed or at best ignored any attempt to expose potential corruption. They simply ignored the loss of precious souls and probably considered them collateral damage, or at best a necessary sacrifice to save the globe[7]. Notably, I've been permanently banned from Twitter twice and temporarily banned from Facebook seven times whenever I argued against the dogma of "perfectly safe and effective nucleic acid based vaccination". No matter how badly the Western countries were being severly hit by COVID-19, not a single stakeholder, politician or journalist replied to my repeatedly sent updated emails and scientific publications, except for one thank you email from a high-ranking FDA official after I've exposed another very recent potential scam[28].

I repeatedly argued, with fervent decline of any opportunity for peer review, that mass vaccination campaigns, drugs like remdesivir, dexamethasone, favipiravir, molnupiravir, monoclonal antibodies as well as Paxlovid are inducing the evolution of more and more virulent immune-evasive SARS-CoV-2 variants that could prolong and worsen the global misery and division in which we live[3,12]. Meanwhile, I also repeatedly advocated for the use of immune-modulatory drugs such as those used in Kelleni's and Expanded Kelleni's protocol[1,18,20,25,27] as the right approach to treat and abort SARS-CoV-2 infection and end this pandemic. Moreover, I occasionally used Kelleni's protocol (nitazoxanide and/or NSAIDs) in successful post-exposure prophylaxis of close contacts of SARS-CoV-2 patients. I've also administered the immune-modulatory Bacillus Calmette-Guérin vaccine to myself and my family to boost our natural immunity[29]. We're not and have never been "antivaxers" as stigmatized by the biased sponsored media, indeed we are the ones who trust real science[3].

IN AFRICA WE DEFIED THE UNSCIENTIFIC MANDATES

As mentioned previously, in Africa we enjoyed our lives during most of the pandemic after only a few months of the initial global panic. My father, who is in his eighth decade of life, has seldom put a mask on his face despite my early recommendation to wear one. The vast majority of poor people in Africa have acted similarly, either because they can't afford the additional costs of "masks" or, like my father, because they simply want to enjoy breathing without restrictions as they have done all their lives and they trust their natural immunity. Later, I allowed my two little daughters not to wear masks, which is a voluntary choice in most Egyptian kindergartens and schools. I considered the inevitable infection as a natural vaccine when early properly treated[3].

However, we had a very difficult time when some African governments wished to sell imported vaccines and distribute late "gifts" coming from rich countries. These countries falsely promoted another scam, claiming that their overall failure with the new vaccines/boosters and the increasing number of death among "vaccinated" people was because of the unvaccinated individuals, including those living in poor Africa. Unfortunately, some African governments threatened poor employees with their jobs if they were not vaccinated and people were denied entry of any governmental facility unless they showed a vaccination certificate. Ironically, many employees were forced to sign a legal document stating that "they received the vaccine of their own free will and exempting the government and vaccine manufacturers from any adverse effect whether known unknown and whether immediate or future". Moreover, there was absolute silence and denial when we early witnessed the deaths of numerous young healthy adults, including health care professionals, soon after receiving the "vaccines"[11]. While some Western governments later paid huge compensations for "COVID vaccine victims" or their families, this has never been and probably will never be an option for most of the poor people in Africa, as it's almost impossible to find a civil court that will condemn a sovereign mandate that led to these tragedies. In Egypt, one private newspaper initially published my call not to mandate these vaccines and in some YouTube videos and one TV show, I urged the consideration of a personalized risk benefit ratio, but to no avail.

During this struggle, I've published several preprints that highlighted the potential hazards of mandate nucleic acid based jabs including a call to immediately suspend Pfizer-BioNTech mRNA vaccine though knowing that this was almost impossible. I even suggested to the manufacturers that they should decrease the dose of the vaccine in order to mitigate some risks and they later practically adopted this approach in the "boosters". However, after a year of absolute denial of peer review from numerous medical journals, an article has been published to explain why I consider mandatory nucleic acid based vaccination a crime against humanity as it poses potential hazards in both the short term for some victims and the long term for others[11]. Fortunately, some African health care workers, despite their low rank, acted with mercy and provided people with the required governmental papers confirming vaccination while secretly disposing these vaccines in the trash.

In contrast, it was disheartening to witness high-ranking officials in the West ignore to fairly investigate the claims made by whistle blowers who exposed severe medical malpractice in Pfizer-BioNTech mRNA clinical trials[9]. The denial of people's free will in deciding whether or not to be injected with a new technology was another global tragedy. Furthermore, when an editor of the well-known Journal "Science" falsely and shamelessly promoted vaccine mandates among college students, he denied me the opportunity to present a counterargument and I preprinted it. Even the European Court of Human Rights ruled that compulsory vaccination with nucleic acid based vaccines would not violate human rights law[11].

I argue that the COVID mortality paradox has originated when a biased scientist and his followers manipulated desperate American and other Western politicians to approve, integrate and mandate highly profitable drugs[10,30] and vaccines with outbalanced risk benefit ratio, at least for currently proven and undisputed numerous victims[11,15,31-34]. Although these serious adverse effects labeled as rare, yet can't be predicted[31,35,36]. Some have described it as a

"Russian roulette" game and I agree especially considering that Africa has managed COVID-19 better without nucleic acid based vaccines. Additionally, there may be a yet unknown and properly uninvestigated or dismissed as co-incidence adverse effects associated with these vaccines as mentioned earlier. Moreover, the ongoing evolution and mutation of SARS-CoV-2 may be directly and indirectly attributed to the suppressed natural immunity and the administration of pro-mutant vaccines and drugs. I strongly suggest that these biased stakeholders, not SARS-CoV-2, are responsible for most of the COVID-19 mortality, which primarily affects their own citizens in their home countries. These stakeholders should be held accountable and prosecuted[11].

IN AFRICA WE ENJOY A HEALTHIER LIFESTYLE

Despite poverty being a major problem in Africa, one can buy large quantities of antioxidant-rich fruits and vegetables for just one United States dollar[37]. This highly healthy and nutritious food comes at with minimal cost and it was a huge surprise when I travelled abroad and found how expensive similar items are in Western countries. Additionally, air and water pollution are much lower in many African countries compared to the West, and obesity is also less prevalent in Africa. All these factors, along with simpler mental and better spiritual well-being, contribute to better natural immunity in African citizens compared to their Western counterparts.

CONCLUSION

Africa has been fortunate to avoid the expedited, toxic, ineffective and potentially mutagenic Western COVID-19 interventions. These interventions, including experimental vaccines and drugs developed or repurposed by biased Western scientists, have been promoted by politicians, pharmaceutical companies and other stakeholders who control most of the mainstream media and social networks. On the other hand, early treatment using Kelleni's protocol has successfully managed every Egyptian COVID patient regardless of its initial case severity. Unfortunately, the majority of the world remains blind to the possibility of being manipulated by these stakeholders who are well aware that if this possibility is thoroughly examined, they might face serious ethical and legal consequences beyond losing their political, academic or financial positions.

ACKNOWLEDGEMENTS

I would like to acknowledge the example set by my great grandfather, Saint Athanasius of Alexandria, also known as "contra-mundum". In the fourth century AD, he chose to stand firm with my brave Coptic ancestors against a corrupt and powerful global coalition that included emperors, potentates and top-ranked bishops. Together we, Egyptians, defended what we believed to be right, noble and just. Despite being an apparently powerless minority, we eventually emerged victorious. I would also like to express my gratitude to OSF Preprints for preprinting an earlier version of this article which included many other citations supporting the claims mentioned.

FOOTNOTES

Author contributions: Kelleni MT is a sole author.

Conflict-of-interest statement: The author declares that he has no conflict of interest.

Country/Territory of origin: Egypt

ORCID number: Mina Thabet Kelleni 0000-0001-6290-6025.

S-Editor: Liu JH
L-Editor: A
P-Editor: Yu HG

REFERENCES

1 **Kelleni MT**. The African Kelleni's roadmap using nitazoxanide and broad-spectrum antimicrobials to abort returning to COVID-19 square one. *Inflammopharmacology* 2023; **31**: 3335-3338 [PMID: 37326756 DOI: 10.1007/s10787-023-01263-4]

2 **Nkengasong JN**. COVID-19: unprecedented but expected. *Nat Med* 2021; **27**: 364 [PMID: 33723449 DOI: 10.1038/s41591-021-01269-x]

3 **Kelleni MT**. Evolution of SARS CoV-2 Omicron subvariants BF.7 and XBB.1.5: Time to follow Africa and abort all COVID restrictions. *J Infect* 2023; **86**: 405 [PMID: 36702311 DOI: 10.1016/j.jinf.2023.01.027]

4 **Yamaka W**, Lomwanawong S, Magel D, Maneejuk P. Analysis of the Lockdown Effects on the Economy, Environment, and COVID-19 Spread: Lesson Learnt from a Global Pandemic in 2020. *Int J Environ Res Public Health* 2022; **19** [PMID: 36232169 DOI: 10.3390/ijerph191912868]

5 **Dzawanda B**, Matsa M, Nicolau M. A catastrophic threat to the already vulnerable towards 2030: Impact of COVID-19 lockdown on livelihood outcome of informal cross border traders in Gweru, Zimbabwe. *Soc Sci Humanit Open* 2022; **6**: 100316 [PMID: 35959465 DOI: 10.1016/j.ssaho.2022.100316]

6 **Martínez-Vélez NA**, Arroyo-Belmonte M, Tiburcio M, Natera-Rey G, Fernández-Torres M, Sánchez-Hernández GY. Psycho-Emotional Factors Associated with Depressive Symptoms during Lockdown Due to the COVID-19 Pandemic in the Mexican Population. *Int J Environ Res Public Health* 2023; **20** [PMID: 36901346 DOI: 10.3390/ijerph20054331]

7 **Shir-Raz Y**, Elisha E, Martin B, Ronel N, Guetzkow J. Censorship and Suppression of Covid-19 Heterodoxy: Tactics and Counter-Tactics. *Minerva* 2022; 1-27 [PMID: 36340971 DOI: 10.1007/s11024-022-09479-4]

8 **Elisha E**, Guetzkow J, Shir-Raz Y, Ronel N. Suppressing Scientific Discourse on Vaccines? Self-perceptions of researchers and practitioners. *HEC Forum* 2022; 1-19 [PMID: 35587319 DOI: 10.1007/s10730-022-09479-7]

9 **Thacker PD**. Covid-19: Researcher blows the whistle on data integrity issues in Pfizer's vaccine trial. *BMJ* 2021; **375**: n2635 [PMID: 34728500 DOI: 10.1136/bmj.n2635]

10 **Kelleni MT**. Tocilizumab, Remdesivir, Favipiravir, and Dexamethasone Repurposed for COVID-19: a Comprehensive Clinical and Pharmacovigilant Reassessment. *SN Compr Clin Med* 2021; **3**: 919-923 [PMID: 33644693 DOI: 10.1007/s42399-021-00824-4]

11 **Kelleni MT: SARS CoV-2 Vaccination Autoimmunity**, Antibody Dependent Covid-19 Enhancement and Other Potential Risks: Beneath the Tip of the Iceberg. International Journal of Pulmonary & Respiratory Sciences 2021; 5 [DOI: 10.19080/ijoprs.2021.05.555658]

12 **Kelleni MT**. Paxlovid and Molnupiravir Approved to Manage COVID-19: A Countdown for SARS CoV-2 Variant Apocalypse. OSF (preprint) 1031219/osfio/qsfkh 2021 [DOI: 10.31219/osf.io/qsfkh]

13 **Fraiman J**, Erviti J, Jones M, Greenland S, Whelan P, Kaplan RM, Doshi P. Serious adverse events of special interest following mRNA COVID-19 vaccination in randomized trials in adults. *Vaccine* 2022; **40**: 5798-5805 [PMID: 36055877 DOI: 10.1016/j.vaccine.2022.08.036]

14 **Seneff S**, Nigh G, Kyriakopoulos AM, McCullough PA. Innate immune suppression by SARS-CoV-2 mRNA vaccinations: The role of G-quadruplexes, exosomes, and MicroRNAs. *Food Chem Toxicol* 2022; **164**: 113008 [PMID: 35436552 DOI: 10.1016/j.fct.2022.113008]

15 **Parry PI**, Lefringhausen A, Turni C, Neil CJ, Cosford R, Hudson NJ, Gillespie J. 'Spikeopathy': COVID-19 Spike Protein Is Pathogenic, from Both Virus and Vaccine mRNA. *Biomedicines* 2023; **11** [PMID: 37626783 DOI: 10.3390/biomedicines11082287]

16 **Kelleni MT**. Early use of non-steroidal anti-inflammatory drugs in COVID-19 might reverse pathogenesis, prevent complications and improve clinical outcomes. *Biomed Pharmacother* 2021; **133**: 110982 [PMID: 33197762 DOI: 10.1016/j.biopha.2020.110982]

17 **Kelleni MT**. ACEIs, ARBs, ibuprofen originally linked to COVID-19: the other side of the mirror. *Inflammopharmacology* 2020; **28**: 1477-1480 [PMID: 32920716 DOI: 10.1007/s10787-020-00755-x]

18 **Kelleni MT**. NSAIDs and Kelleni's protocol as potential early COVID-19 treatment game changer: could it be the final countdown? *Inflammopharmacology* 2022; **30**: 343-348 [PMID: 34822026 DOI: 10.1007/s10787-021-00896-7]

19 **Kelleni MT**. Nitazoxanide/azithromycin combination for COVID-19: A suggested new protocol for early management. *Pharmacol Res* 2020; **157**: 104874 [PMID: 32360581 DOI: 10.1016/j.phrs.2020.104874]

20 **Kelleni MT**. Real-life practice of the Egyptian Kelleni's protocol in the current tripledemic: COVID-19, RSV and influenza. *J Infect* 2023; **86**: 154-225 [PMID: 36513168 DOI: 10.1016/j.jinf.2022.12.007]

21 **Kelleni MT**. NSAIDs/Nitazoxanide/Azithromycin Immunomodulatory Protocol Used in Adult, Geriatric, Pediatric, Pregnant, and Immunocompromised COVID-19 Patients: A Real-World Experience. *CJM* 2021; **3**: 121-143 [DOI: 10.33844/cjm.2021.60511]

22 **Kelleni MT**. COVID-19, Ebola virus disease, and Nipah virus infection reclassification as novel acute immune dysrhythmia syndrome (n-AIDS): potential crucial role for immunomodulators. *Immunol Res* 2021; **69**: 457-460 [PMID: 34357535 DOI: 10.1007/s12026-021-09219-y]

23 **Sobhy A**, Saleh LA, AbdelAtty MEI, Refaat SA, M K. Early Use of Ibuprofen in Moderate Cases of COVID-19 Might be a Promising Agent to Attenuate the Severity of Disease: A Randomized Controlled Trial. *The Open Anesthesia Journal* 2023 [DOI: 10.2174/25896458-v17-e230403-2022-26]

24 **Kelleni MT**. Recent Western Updates in COVID-19 Pharmacotherapy (January - April 3, 2022): An Afro-Egyptian Perspective. OSF (preprint) 1031219/osfio/txb2m 2022 [DOI: 10.31219/osf.io/txb2m]

25 **Kelleni MT**. Personalized Expanded Kelleni's Immunomodulatory COVID-19 Protocol Safely Used to Manage Severe COVID-22: A Case-Report. OSF (preprint) 1031219/osfio/ysfr2 2022 [DOI: 10.31219/osf.io/ysfr2]

26 **Kelleni MT**. NSAIDs/nitazoxanide/azithromycin repurposed for COVID-19: potential mitigation of the cytokine storm interleukin-6 amplifier *via* immunomodulatory effects. *Expert Rev Anti Infect Ther* 2022; **20**: 17-21 [PMID: 34088250 DOI: 10.1080/14787210.2021.1939683]

27 **Kelleni MT**. Real-world practice of the Egyptian Kelleni's protocol amid changing tropism of SARS-CoV-2 omicron BA.5.2.1.7, XBB 1.5 and CH.1.1 subvariants: a multi-purpose protocol. *Inflammopharmacology* 2023; **31**: 1559-1560 [PMID: 36928633 DOI: 10.1007/s10787-023-01180-6]

28 **Kelleni MT**. Peg-interferon Lambda Single Dose Treatment for COVID-19: A Call to Avoid another Hydroxychloroquine Fiasco (Version 3). OSF (preprint) 1031219/osfio/5xd6q 2023 [DOI: 10.31219/osf.io/5xd6q]

29 **Kelleni MT**. Repurposing BCG Vaccine to Protect my Parents, Children, and my Family against COVID-19: A Real-life Experience. OSF (preprint) 1031219/osfio/z2qw6 2022 [DOI: 10.31219/osf.io/z2qw6]

30 **Kelleni MT**. Remdesivir-gate for COVID-19. Acta Sci Gastrointest Disord 3(8):01 2020 [DOI: 10.22541/au.160677059.91320681/v1]

31 **Maiese A**, Baronti A, Manetti AC, Di Paolo M, Turillazzi E, Frati P, Fineschi V. Death after the Administration of COVID-19 Vaccines Approved by EMA: Has a Causal Relationship Been Demonstrated? *Vaccines (Basel)* 2022; **10** [PMID: 35214765 DOI: 10.3390/vaccines10020308]

32 **Patel YR**, Louis DW, Atalay M, Agarwal S, Shah NR. Cardiovascular magnetic resonance findings in young adult patients with acute myocarditis following mRNA COVID-19 vaccination: a case series. *J Cardiovasc Magn Reson* 2021; **23**: 101 [PMID: 34496880 DOI: 10.1186/s12968-021-00795-4]

33 **Helms JM**, Ansteatt KT, Roberts JC, Kamatam S, Foong KS, Labayog JS, Tarantino MD. Severe, Refractory Immune Thrombocytopenia Occurring After SARS-CoV-2 Vaccine. *J Blood Med* 2021; **12**: 221-224 [PMID: 33854395 DOI: 10.2147/JBM.S307047]

34 **Eom H**, Kim SW, Kim M, Kim YE, Kim JH, Shin HY, Lee HL. Case Reports of Acute Transverse Myelitis Associated With mRNA Vaccine for COVID-19. *J Korean Med Sci* 2022; **37**: e52 [PMID: 35191229 DOI: 10.3346/jkms.2022.37.e52]

35 **García-Grimshaw M**, Ceballos-Liceaga SE, Hernández-Vanegas LE, Núñez I, Hernández-Valdivia N, Carrillo-García DA, Michel-Chávez A, Galnares-Olalde JA, Carbajal-Sandoval G, Del Mar Saniger-Alba M, Carrillo-Mezo RA, Fragoso-Saavedra S, Espino-Ojeda A, Blaisdell-Vidal C, Mosqueda-Gómez JL, Sierra-Madero J, Pérez-Padilla R, Alomía-Zegarra JL, López-Gatell H, Díaz-Ortega JL, Reyes-Terán G, Arauz A, Valdés-Ferrer SI. Neurologic adverse events among 704,003 first-dose recipients of the BNT162b2 mRNA COVID-19 vaccine in Mexico: A nationwide descriptive study. *Clin Immunol* 2021; **229**: 108786 [PMID: 34147649 DOI: 10.1016/j.clim.2021.108786]

36 **Oueijan RI**, Hill OR, Ahiawodzi PD, Fasinu PS, Thompson DK. Rare Heterogeneous Adverse Events Associated with mRNA-Based COVID-19 Vaccines: A Systematic Review. *Medicines (Basel)* 2022; **9** [PMID: 36005648 DOI: 10.3390/medicines9080043]

37 **Kelleni MT**. Resveratrol-zinc nanoparticles or pterostilbene-zinc: Potential COVID-19 mono and adjuvant therapy. *Biomed Pharmacother* 2021; **139**: 111626 [PMID: 33894625 DOI: 10.1016/j.biopha.2021.111626]

World Journal of Experimental Medicine

Submit a Manuscript: https://www.f6publishing.com

World J Exp Med 2024 March 20; 14(1): 89320

DOI: 10.5493/wjem.v14.i1.89320

ISSN 2220-315x (online)

OPINION REVIEW

Future clinical prospects of C-peptide testing in the early diagnosis of gestational diabetes

Charalampos Milionis, Ioannis Ilias, Anastasia Lekkou, Evangelia Venaki, Eftychia Koukkou

Specialty type: Medicine, research and experimental

Provenance and peer review: Invited article; Externally peer reviewed.

Peer-review model: Single blind

Peer-review report's scientific quality classification

Grade A (Excellent): A
Grade B (Very good): 0
Grade C (Good): C, C, C
Grade D (Fair): 0
Grade E (Poor): 0

P-Reviewer: Arumugam VA, India; Gong F, China; Wu J, China

Received: October 27, 2023
Peer-review started: October 27, 2023
First decision: November 30, 2023
Revised: December 11, 2023
Accepted: December 28, 2023
Article in press: December 28, 2023
Published online: March 20, 2024

Charalampos Milionis, Ioannis Ilias, Anastasia Lekkou, Evangelia Venaki, Eftychia Koukkou, Department of Endocrinology, Diabetes, and Metabolism, 'Elena Venizelou' General Hospital, Athens 11521, Greece

Corresponding author: Charalampos Milionis, MD, PhD, Consultant Physician-Scientist, Department of Endocrinology, Diabetes, and Metabolism, 'Elena Venizelou' General Hospital, Elena Venizelou Square 2, Athens 11521, Greece. pesscharis@hotmail.com

Abstract

Gestational diabetes is typically diagnosed in the late second or third trimester of pregnancy. It is one of the most common metabolic disorders among expectant mothers, with potential serious short- and long-term complications for both maternal and offspring health. C-peptide is secreted from pancreatic beta-cells into circulation in equimolar amounts with insulin. It is a useful biomarker to estimate the beta-cell function because it undergoes negligible hepatic clearance and consequently it has a longer half-life compared to insulin. Pregnancy induces increased insulin resistance due to physiological changes in hormonal and metabolic homeostasis. Inadequate compensation by islet beta-cells results in hyperglycemia. The standard oral glucose tolerance test at 24-28 wk of gestation sets the diagnosis. Accumulated evidence from prospective studies indicates a link between early pregnancy C-peptide levels and the risk of subsequent gestational diabetes. Elevated C-peptide levels and surrogate glycemic indices at the beginning of pregnancy could prompt appropriate strategies for secondary prevention.

Key Words: C-peptide; Gestational diabetes; Secondary prevention; Pregnancy; Clinical laboratory techniques

Core Tip: Understanding the diagnostic role of C-peptide measurements in predicting hyperglycemia during pregnancy can facilitate timely interventions in clinical practice, potentially preventing gestational diabetes in a subset of predisposed women. Further research is necessary to confirm the utility of C-peptide testing in pregnancy and define the appropriate diagnostic thresholds.

Citation: Milionis C, Ilias I, Lekkou A, Venaki E, Koukkou E. Future clinical prospects of C-peptide testing in the early diagnosis of gestational diabetes. *World J Exp Med* 2024; 14(1): 89320
URL: https://www.wjgnet.com/2220-315x/full/v14/i1/89320.htm
DOI: https://dx.doi.org/10.5493/wjem.v14.i1.89320

INTRODUCTION

Gestational diabetes (GD) presents a mounting global public health challenge, with its prevalence varying from 7.1% to 27.6% across different International Diabetes Federation regions[1]. Its epidemiological pattern parallels that of type 2 diabetes mellitus (T2DM) in the same ethnic groups[2]. Typically emerging in the late second or third trimester, GD heightens the risk of various adverse maternal and fetal effects. Moreover, women with a history of GD face an elevated susceptibility to developing T2DM later in life. However, this relative risk is considerably variable and hinges on factors like the amount of time after delivery, ethnicity, age, body mass index, family history of diabetes, and previous affected pregnancies[3].

Maintaining optimal blood sugar levels is crucial to managing pregnant women with GD. Identifying early those at risk of dysglycemia during pregnancy is challenging because it can enable timelier interventions and, in turn, foster more effective glycemic control. Early diagnosis and treatment of GD can lead to improved maternal metabolic profiles and the creation of favorable intrauterine conditions for fetal development. Managing dysglycemia before the 20th week of pregnancy may contribute to a decreased incidence of a composite of adverse neonatal outcomes[4].

GD can be regarded as a pre-gravid subclinical glycemic dysregulation unmasked in late gestation[5]. Presently, blood glucose, insulin, and occasionally triglycerides are widely used in clinical practice to determine insulin resistance through the calculation of various indices[6]. However, these methods suffer from significant variability in defining appropriate threshold levels, making it challenging to estimate optimal cut-off points[7]. Given the specific physiological conditions of pregnancy, diagnosing glucose intolerance in pregnant women typically relies on blood glucose measurements in the fasting state and after glucose load.

Accurate identification of GD is of paramount significance. The standard approach involves an oral glucose tolerance test (OGTT) in the late second or early third trimester. Still, various physiological factors, including previous physical activity, preparatory diet, fasting duration, rate of intestinal glucose absorption, hydration status, and stress, can influence the glycemic response to oral glucose load. Moreover, technical inadequacies such as errors in sample handling and a lack of analytical standardization can compromise the reliability of this test[8]. It is also worth noting that postprandial blood sugar measurements in pregnant women only detect a manifested disturbance of glucose metabolism. Consequently, exploring the use of other biochemical markers that are more accurate and timelier in revealing dysglycemia during pregnancy is essential.

In contrast, C-peptide measurement has rarely been employed for diagnostic purposes in assessing insulin resistance. Using C-peptide as a biochemical marker is promising. Yet, its current role is limited to differentiating between type 1 diabetes mellitus (T1DM) and T2DM in cases of ambiguous hyperglycemia, as well as in the differential diagnosis of hypoglycemia. However, C-peptide testing could be instrumental in several other facets of diabetes care, including estimating the progression of insulin resistance (and deficiency), predicting the onset of T2DM, and evaluating the risk of diabetic complications. This review particularly focuses on the potential utilization of C-peptide testing in early pregnancy to assess the risk of GD. It also analyzes the rationale for the practical integration of C-peptide testing in the clinical setting for this purpose.

METHODLOGY

With the aim of providing an overview of the use of C-peptide determination in the early diagnosis of GD, a search in the database of PubMed was performed between October and November 2023. It used the terms ‘C-peptide’, ‘gestational diabetes’, ‘early diagnosis’, and ‘biomarkers’ in all possible combinations. Table 1 shows the relevant literature search. The selected articles included studies that explored novel clinical applications of C-peptide testing with a special focus on pregnancy. For a better understanding of the relevant physiology, review papers that explained the applicability of C-peptide measurements, analyzed aspects of insulin synthesis and secretion, or described the nosological entity of GD were also used after a targeted literature search.

A narrative review can be defined as a thorough report of a body of literature that also includes interpretation and critique[9]. This method lacks cumbersome restrictions, which makes it suitable for the in-depth analysis of a particular topic, especially when existing data are incomplete[10]. The utility of C-peptide measurements in pregnancy has been researched sparingly. Hence, this article used a narrative approach to summarize the existing evidence on the underlying physiology of glucose homeostasis, elaborate on the importance of early diagnosis of dysglycemia, and speculate on possible preventive strategies. Although a narrative review may suffer from data selection bias, a purposeful search of the literature can mitigate this disadvantage and allow for a comprehensive investigation of the desired topic.

Table 1 Search details in PubMed

Query	Results
Search: ((gestational diabetes) AND (early diagnosis)) AND (biomarkers)	344
Search: ((C-peptide) AND (early diagnosis)) AND (biomarkers)	96
Search: ((C-peptide) AND (gestational diabetes)) AND (biomarkers)	64
Search: ((C-peptide) AND (gestational diabetes)) AND (early diagnosis)	32
Search: (((C-peptide) AND (gestational diabetes)) AND (early diagnosis)) AND (biomarkers)	9

PHYSIOLOGY OF INSULIN SYNTHESIS AND SECRETION-BIOLOGICAL ACTION OF C-PEPTIDE

Insulin, a peptide hormone, is produced through the classical process of protein synthesis. The human insulin gene is located on the short arm of chromosome 11. It is transcribed into preproinsulin mRNA in the nucleus of pancreatic beta-cells in the islets of Langerhans. This mRNA is transferred to the cytoplasm, where it is translated into a 110-amino-acid precursor peptide (preproinsulin) in the rough endoplasmic reticulum. Preproinsulin is cleaved to proinsulin with the removal of the signal peptide almost immediately after synthesis. Proinsulin is a single 86-amino-acid chain containing the A and B chains of insulin (with 21 and 30 amino acids, respectively) and a 35-residue connecting segment (the C-peptide and four intervening amino acids). As proinsulin folds, the A and B chains form three disulfide bonds (two bridges between the A and B chains and an intra-chain bridge within the A chain). Proinsulin is then packaged into clathrin-coated secretory vesicles in the Golgi apparatus. Loss of the clathrin coating and conversion of proinsulin into insulin indicate maturation for exocytosis[11,12]. Figure 1 represents the process of insulin synthesis and secretion by the pancreatic beta-cell.

C-peptide, consisting of 31 amino acids, initially links the A and B chains of insulin within proinsulin, aiding correct protein folding and disulfide bond formation. In the Golgi apparatus, proinsulin is cleaved at two sites along the peptide chain through prohormone convertases 1 and 2, with carboxypeptidase E removing two pairs of amino acids from the protein's ends. This process yields equimolar quantities of C-peptide and active insulin stored together in secretory vesicles in the cytoplasm of pancreatic beta-cells. Glucose and other secretagogues (leucine, arginine, acetylcholine, incretins, and vagal nerve stimulation) stimulate the co-release of both insulin and C-peptide into the bloodstream. Mature secretory vesicles might contain small amounts of proinsulin or partially split products that evade cleavage[11,12]. Figure 2 depicts the molecular structure of proinsulin.

Following secretion, insulin and C-peptide are routed through the portal circulation into the liver, where half of the pancreatic insulin undergoes first-pass hepatic clearance. Insulin is also metabolized in the kidney and the placenta. In contrast, C-peptide is only limitedly processed in the liver. It is primarily metabolized in the kidney, with a small fraction excreted unchanged in the urine (5%-10%). Consequently, the half-life of C-peptide is around 30 min, roughly ten times longer than that of endogenous insulin (approximately 3 min). Moreover, the molar ratio of insulin to C-peptide in peripheral circulation is less than 1. The stability of C-peptide in the bloodstream supports its clinical utility as a reliable marker of islet beta-cell function[13].

Besides its contribution to insulin structure, the exact biological actions of C-peptide in normal physiology remain only partially understood[14]. Available data indicate that C-peptide may bind to the cell membrane, possibly *via* a surface receptor coupled with a G-protein. Then, the latter triggers a signaling cascade that results in several effects, including elevation in the concentration of intracellular calcium, activation of the sodium-potassium adenosine triphosphatase (Na^+-K^+-ATPase), increased transcription of endothelial nitric oxide synthetase, stimulation of phosphoinositide 3-kinase, and activation of mitogen-activated protein kinases pathways, in multiple cell types from various tissues[15,16]. Non-receptor-mediated mechanisms of the C-peptide's biological action have also been implied.

C-peptide likely exerts anti-inflammatory, anti-apoptotic, vasodilatory, and antioxidant effects in the vascular endothelium, either directly or through interactions with erythrocytes and immune cells. It may also participate in fine-tuning insulin signaling[17]. However, further research is necessary to confirm these presumptive functions, as well as their physiological role and clinical significance.

PATHOPHYSIOLOGY, DIAGNOSIS, AND CLINICAL IMPLICATIONS OF GESTATIONAL DIABETES

In pregnant women, hormonal and metabolic changes significantly influence carbohydrate metabolism, adapting to the nutritional demands of the growing fetus. The flow of glucose from maternal to fetal circulation relies on the gradient across the blood-placental barrier. Placental and other hormones (progesterone, estrogen, placental lactogen, leptin, cortisol, and growth hormone) induce insulin resistance, maintaining adequate maternal plasma glucose levels and ensuring unmarred glucose flow to the fetus. Heightened lipolysis in the adipose tissue of pregnant women favors fatty acid utilization by maternal tissues, increasing glucose availability for the fetus[18,19]. Changes in cytokine and adipokine production, circulating exosomes (both total and placenta-derived), and alterations in the gut microbiota might also contribute to increased insulin resistance during pregnancy[20]. Compensatory mechanisms involve expansion, proliferation, and possibly neogenesis of pancreatic beta-cells, leading to a two- to three-fold rise in insulin production[21,22].

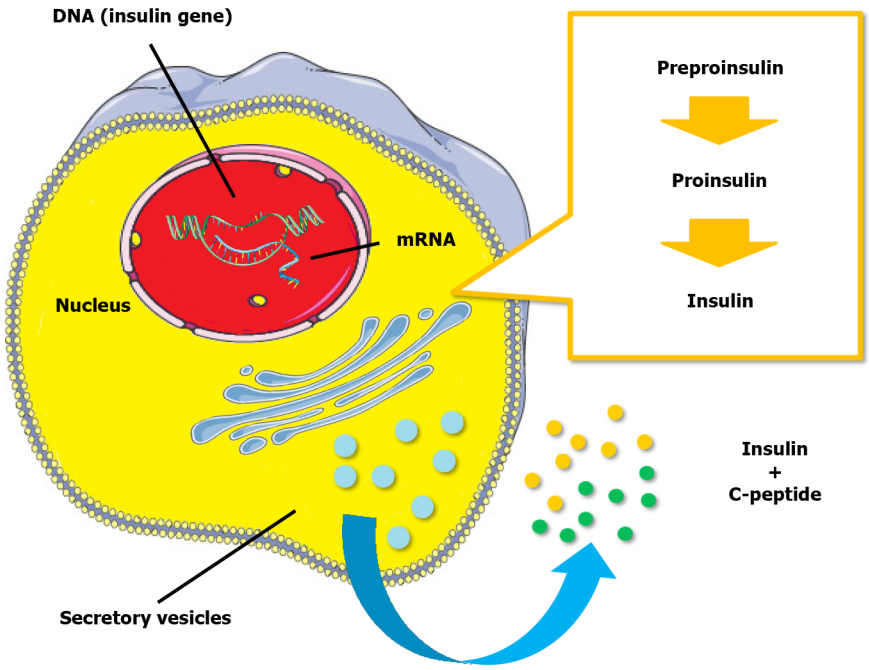

Figure 1 Insulin synthesis and secretion by the pancreatic beta-cell.

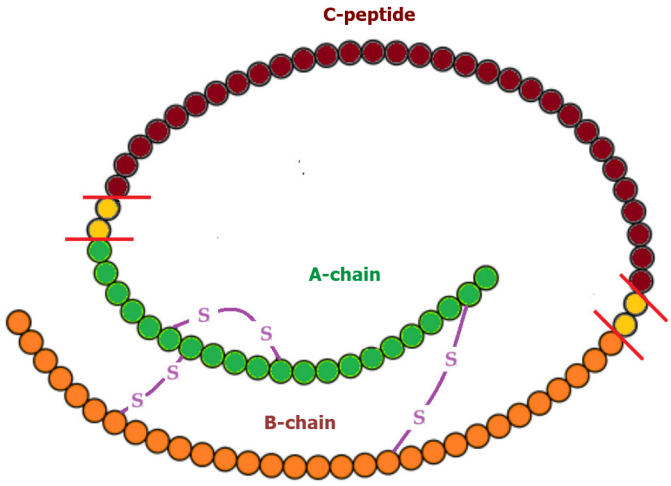

Figure 2 The molecule of proinsulin with its components.

Maternal insulin sensitivity returns to pre-pregnancy levels shortly after parturition.

GD manifests as pregnancy-related hyperglycemia resulting from insufficient pancreatic insulin secretion against heightened blood glucose levels due to the hormonal and metabolic homeostasis of pregnancy. It often arises from an underlying predisposition to beta-cell dysfunction in the presence of latent insulin resistance. Hormonal and metabolic changes during pregnancy exacerbate this state. Defects may occur at any stage of beta-cell function, including glucose sensing, proinsulin synthesis, post-translational modifications, and vesicle storage and exocytosis. Insulin resistance arises from disruptions in various phases of insulin signaling. As insulin resistance peaks in the third trimester, hyperglycemia typically becomes apparent around this time[18,19].

Early screening before the 15th week of gestation is crucial, especially for women with risk factors, to identify undiagnosed preexisting diabetes. Risk factors include advanced age, excessive weight, specific ethnicities (Indian, Southeast Asian, Arab, Mediterranean, Afro-Caribbean), family history of T2DM, previous macrosomic neonate delivery, and polycystic ovarian syndrome[23]. The gold-standard diagnostic approach is the OGTT at 24-28 wk, with different hyperglycemia thresholds indicating varying degrees of complication risk[24]. Adverse outcomes associated with GD include preeclampsia, preterm delivery, need for cesarean section, shoulder dystocia, neonatal hypoglycemia, neonatal jaundice, and increased birth weight[25].

Pre-pregnancy lifestyle modifications (exercise and diet) may serve as primary prevention against GD[26]. Similar interventions in early gestation might prevent subsequent GD in high-risk individuals[27,28]. Nonetheless, no widely accepted strategy currently exists for secondary prevention (after conception) in the general pregnant population. An

ideal diagnostic tool capable of detecting the condition prior to the onset of overt hyperglycemia, possibly in the first trimester, could enable timely interventions before adverse metabolic effects act on the fetus. Proper management of GD, including dietary plans, behavioral adjustments, and, if necessary, insulin therapy, can improve perinatal outcomes (tertiary prevention)[29]. Figure 3 outlines the timeline for potential diagnostic and therapeutic interventions in GD.

MEASUREMENT OF C-PEPTIDE – METHODS AND CLINICAL APPLICATIONS

C-peptide testing serves as an important laboratory tool for evaluating pancreatic beta-cell function and finding application as a biochemical marker for insulin secretion assessment in clinical settings. It is preferred over insulin measurements in some instances owing to its slower degradation rate, which provides a broader time window to evaluate fluctuating beta-cell function. C-peptide is less affected by hemolysis, and its determination has a well-established standardization process[30]. Additionally, its measurement avoids the risk of cross-reactivity of immunoassays between endogenous and synthetic insulin[31].

Estimating C-peptide involves basal, random, and stimulated blood measurements. Fasting blood samples are obtained after an 8-10-h overnight fast, whereas random blood specimens can be drawn at any time during the day regardless of the last mealtime. Both of these approaches are simple and flexible and can be performed in an outpatient or inpatient setting. However, fasting C-peptide values might not capture subtle postprandial fluctuations. In addition, random C-peptide levels often require confirmation with stimulation methods. The latter include measurements at specific time intervals after glucose intake, glucagon administration, or a mixed meal[32]. Stimulation tests should be conducted primarily in diagnostically challenging cases, considering the potential inconveniences for both patients and personnel. C-peptide is prone to enzymatic proteolytic cleavage in serum gel or plain sample tubes but remains stable in whole blood specimens in ethylenediaminetetraacetic acid-prepared tubes for up to 24 h at room temperature[33].

Normal plasma C-peptide concentration in the fasting state ranges around 0.9-1.8 ng/mL, rising to 3-9 ng/mL postprandially in non-diabetic, non-obese individuals[34]. Elevated C-peptide blood levels may indicate insulin resistance, insulinoma, or kidney disease, whereas low concentrations are typical in T1DM or sometimes in T2DM.

Urinary C-peptide testing is a non-invasive procedure. It involves collecting samples in boric acid, which maintains C-peptide stability for up to 3 d at room temperature. In individuals with normal urinary function, the urinary C-peptide quantity represents 5%-10% of the total secretion by the pancreas. While 24-h urine collection provides a relatively accurate estimation of pancreatic secretion over an extended period, it can be time-consuming and inconvenient for the patient. The determination of spot urinary C-peptide concentration is less reliable because of the variability in the beta-cell secretory activity over the day. Nevertheless, the C-peptide to creatinine ratio in a spot sample correlates well with 24-h collection values, making it an attractive option for estimating islet beta-cell function. Gender differences should be considered due to variations in urinary creatinine levels between men and women[32].

C-peptide measurement is a key element in the differential diagnosis of hypoglycemia. When hypoglycemic episodes are confirmed, evaluating C-peptide blood concentration is essential. Low C-peptide levels alongside high insulin levels suggest factitious hypoglycemia due to excessive exogenous insulin administration. Elevated C-peptide levels in the presence of high insulin concentration should prompt consideration of stimulating insulin autoantibodies, insulinoma, or intoxication with insulin secretagogues (sulfonylureas or meglitinides)[35]. Furthermore, C-peptide is valuable for assessing insulin secretory reserve in patients with diabetes. In T1DM, C-peptide values decline rapidly during the initial 3-5 years since onset, with concentrations lower than 0.4 ng/mL indicative of pancreatic beta-cell failure and insulin deficiency[36].

There are some pitfalls associated with C-peptide testing. Its measurement in patients with chronic kidney failure is problematic due to the compromised renal metabolism. Cross-reactions with proinsulin and its partially processed forms, including C-peptide fragments, may lead to an overestimation of C-peptide concentration. High levels of antibodies binding to proinsulin or C-peptide can also yield falsely elevated readings with indirect immunoassays. While modern assays demonstrate high accuracy in quantifying blood C-peptide[37], awareness of the applied laboratory method remains crucial.

POTENTIAL FUTURE USES OF C-PEPTIDE TESTING IN PREDICTING GESTATIONAL DIABETES

The escalating incidence of GD presents a growing global health challenge due to its potentially severe implications for both the mother and the offspring. Consequently, strategies for prevention, early identification, and optimal treatment are of utmost importance. As previously highlighted, the emergence of GD often results from an underlying deficit of islet beta-cells within a setting of pregnancy-induced insulin resistance. Thus, the early assessment of pancreatic beta-cell function, if feasible, holds significant promise for predicting the onset of this metabolic dysregulation. While the idea of employing C-peptide testing to evaluate insulin secretory capacity in pregnant women is appealing, it has not yet been extensively trialed in routine clinical practice. The theoretical advantage of C-peptide assessment, compared to the OGTT, lies in the potential for an earlier diagnosis (secondary prevention) of a pregnant woman's predisposition to developing GD. This early assessment could allow for tailored interventions before the onset of glycemic dysregulation.

C-peptide can be readily measured in the serum of pregnant women, both in the fasting state and after stimulation. Given that glucose serves as the primary stimulus for endogenous insulin secretion, adjusting C-peptide levels based on blood sugar values using appropriate indices appears reasonable. Evaluating pancreatic beta-cell function through overnight fasting serum samples is readily comparable both within an individual over time and among different

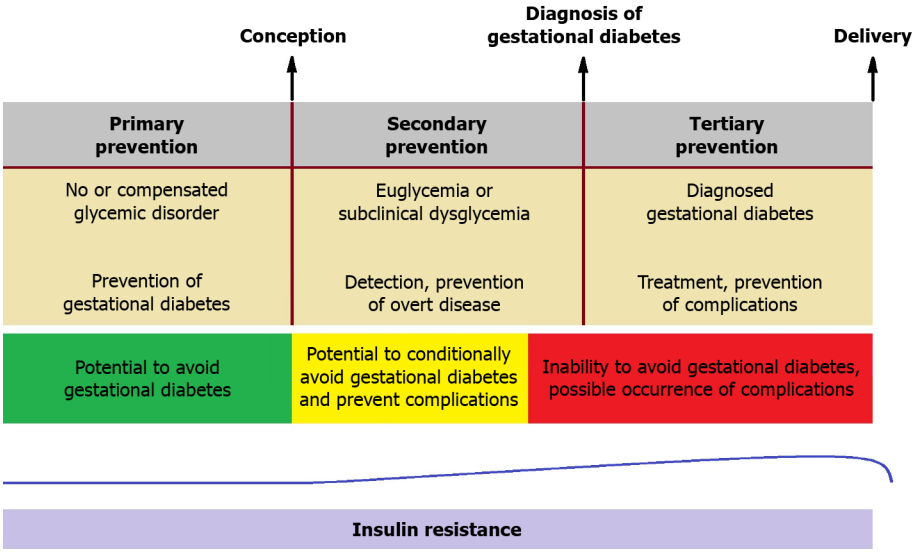

Figure 3 The different stages of prevention in treating gestational diabetes and the development of insulin resistance during pregnancy. Primary prevention can only be sought before conception. Secondary prevention is feasible during the period from conception to around the 20th week of gestation, after which prevention of hyperglycemia is not possible and only complications can be potentially avoided; There is a substantial increase in insulin resistance from gestational week 15 until week 35. Then, it remains stable (or slightly decreases) until delivery and returns to the pre-pregnancy state a few days after parturition.

individuals, as basal insulin secretion remains relatively stable during fasting periods. However, post-stimulation examination reveals the maximum insulin secretory capacity of islet beta-cells, especially in the presence of insulin resistance. Hence, calculating the C-peptide (in ng/mL) to glucose (in mg/dL) ratio (multiplied by 100) in both fasting and post-stimulation serum samples could serve as a well-fitted marker for determining declining insulin secretion[38]. This approach holds promise for identifying pregnant women at high risk of developing GD early in their pregnancy.

Examining C-peptide levels in the urine represents a potentially attractive method for estimating islet beta-cell preserved function. While a substantial correlation exists between 24-h urinary excretion quantity and serum concentration, inter- and intra-personal differences in renal C-peptide clearance must be considered. Of course, collecting a 24-h urine sample can pose practical challenges. Correcting urinary C-peptide concentration for the respective creatinine levels facilitates the use of spot specimens in daily practice, albeit with presumably lower diagnostic accuracy[39]. Assessing C-peptide values in the urine during the initial weeks of gestation could serve as an alternative or complementary tool for evaluating the risk of subsequent hyperglycemia, with the necessary consideration of renal hemodynamic changes in pregnancy.

DISCUSSION

Recent efforts have concentrated on the early detection and management of glycemic dysregulation during pregnancy [40]. A large number of first-trimester biochemical markers have been tested for this purpose. These include glycemic, metabolic, inflammatory, hormonal, adipocyte-derived, and other molecules. Some of them may be useful for identifying women at high risk of developing GD. To apply the relevant findings in practice, further clinical trials as well as cost-effectiveness analyses of the use of these novel biomarkers are needed[41].

The potential integration of C-peptide testing for the early diagnosis of GD could prove to be a vital screening strategy. While current guidelines do not endorse its use for diagnosis during pregnancy, the future application of C-peptide measurement may hold promise for detecting abnormal glycemic homeostasis before the clinical manifestation of GD. This review offers valuable insights into the correlation between C-peptide levels and the progression of glucose intolerance in pregnancy. In this perspective, C-peptide testing could serve as a springboard for secondary prevention interventions during the period after conception but before the onset of frank hyperglycemia.

Pregnancy can be regarded as a stressful state that challenges a woman's glycemic regulatory reserves. Physiological insulin resistance during pregnancy leads to adaptive changes in pancreatic beta-cell function, including increased insulin synthesis, heightened glucose-stimulated insulin secretion, elevated levels of glucokinase and glucose transporters (Glut-2 and Glut-5), increased glucose metabolism, and enhanced expression of soluble N-ethylmaleimide-sensitive factor attachment protein receptor proteins[42]. Failure of these cellular processes to adapt to the insulin demands of pregnancy results in disrupted glucose homeostasis. The OGTT conducted between 24 and 28 wk of pregnancy primarily serves tertiary prevention since the diagnosis of GD with this method is only established after the occurrence of hyperglycemia. Thus, the search for predictive biomarkers for secondary prevention that could potentially prevent hyperglycemia and subsequent complications at an earlier stage becomes imperative.

In the absence of pre-pregnancy hyperglycemia, current guidelines recommend diagnosing GD in the late second or early third trimester. Detecting and treating the disorder at this stage can have significant positive effects, albeit in a

relatively small proportion of cases[25]. Therefore, it is significant to identify biomarkers that can assist in the prediction of GD at an earlier phase, primarily in the first trimester, triggering appropriate monitoring and treatment. Ideally, candidate laboratory tests for this purpose should be relatively affordable, readily available, automated, and minimally invasive[43].

GD is nowadays considered to be part of a progressive metabolic dysfunction that predates conception. A chronic beta-cell defect leads to elevated glycemia during pregnancy. Inadequate compensatory pancreatic secretion in the face of insulin resistance during the latter half of gestation results in hyperglycemia, which characterizes GD[42]. Assessing C-peptide concentration in the serum (or in the urine) and calculating relevant mathematical indices offers an optimal means of evaluating the amount of insulin secretion and sensitivity. Existing evidence suggests that elevated fasting C-peptide levels in early pregnancy are associated with a higher risk of subsequent GD, independently of factors such as maternal age, family history of diabetes, pre-pregnancy body weight, and parity[44-48]. Thus, the evaluation of C-peptide values, possibly in combination with other biochemical parameters, can potentially identify early glycemic disturbances from the initial weeks of pregnancy. Early diagnosis expands the time frame for targeted interventions that may prevent the onset of GD. However, further basic and clinical tests are required to validate these assumptions and determine the precise diagnostic cut-offs.

The pursuit of developing screening tests capable of detecting a disorder before the development of symptoms or at a stage when treatment is potentially more effective remains a longstanding goal in research and clinical practice. Managing GD is no exception to this objective. Following the Hyperglycemia and Adverse Pregnancy Outcome (HAPO) study, which demonstrated a relationship between glucose levels after oral glucose load and adverse pregnancy outcomes[49], the OGTT at the late stages of pregnancy has become a cornerstone of diagnosis. However, advanced age, increased body weight, and family or personal history of GD may conditionate this approach. In addition, an earlier and more specific detection could improve glycemic progression and maternal and neonatal outcomes[50]. Novel indices that incorporate fasting and stimulated C-peptide values could be employed to assess glucose homeostasis and stratify the risk of hyperglycemia earlier in pregnancy[51]. Identifying appropriate biomarkers is an important milestone for designing effective prevention strategies and enhancing the health and well-being of both mothers and offspring. Prospective studies should be conducted to determine whether early interventions, such as lifestyle modifications, in the first trimester can impact the development of GD, the necessity for medical treatment, and perinatal outcomes.

CONCLUSION

GD is a common complication of pregnancy, with a rising incidence. Its consequences are far-reaching, associated with short-term adverse maternal and neonatal outcomes and long-term metabolic implications for both the mother and offspring. Biomarkers to identify women susceptible to the development of GD are useful to target prevention and prompt treatment. Unfortunately, the already well-known clinical risk factors lack specificity, while the OGTT offers a rather late diagnosis. The addition of novel biomarkers to predictive strategies for gestational diabetes may improve clinicians' ability to identify pregnant women at risk of hyperglycemia prior to its development. This review concluded that the use of C-peptide as a biomarker is based on the comprehension of the pathophysiologic mechanisms of insulin resistance during gestation, and hence, it may provide further aid in the prediction of the relevant risk. However, the present article is a narrative review. As such, it has inherent flaws because of non-completely standardized methods of literature search, potential bias in the appraisal of retrieved data, and subjectivity in the interpretation of findings. Further research is certainly needed to validate C-peptide testing as a diagnostic tool in pregnancy.

FOOTNOTES

Author contributions: Milionis C conceived the subject of the paper, prepared and revised the text, and approved the final version of the article; Ilias I and Lekkou A provided feedback on the content of the paper, made amendments to the text, and approved the final version of the article; Koukkou E and Venaki E supervised the writing of the paper, guided the revisions, and approved the final version of the article.

Conflict-of-interest statement: All the authors report no relevant conflicts of interest for this article.

Country/Territory of origin: Greece

ORCID number: Charalampos Milionis 0000-0003-2442-3772; Ioannis Ilias 0000-0001-5718-7441; Evangelia Venaki 0000-0001-8942-2039; Eftychia Koukkou 0000-0002-1433-3151.

S-Editor: Li L
L-Editor: A

P-Editor: Yuan YY

REFERENCES

1 **Wang H**, Li N, Chivese T, Werfalli M, Sun H, Yuen L, Hoegfeldt CA, Elise Powe C, Immanuel J, Karuranga S, Divakar H, Levitt N, Li C, Simmons D, Yang X; IDF Diabetes Atlas Committee Hyperglycaemia in Pregnancy Special Interest Group. IDF Diabetes Atlas: Estimation of Global and Regional Gestational Diabetes Mellitus Prevalence for 2021 by International Association of Diabetes in Pregnancy Study Group's Criteria. *Diabetes Res Clin Pract* 2022; **183**: 109050 [PMID: 34883186 DOI: 10.1016/j.diabres.2021.109050]

2 **Ben-Haroush A**, Yogev Y, Hod M. Epidemiology of gestational diabetes mellitus and its association with Type 2 diabetes. *Diabet Med* 2004; **21**: 103-113 [PMID: 14984444 DOI: 10.1046/j.1464-5491.2003.00985.x]

3 **Dennison RA**, Chen ES, Green ME, Legard C, Kotecha D, Farmer G, Sharp SJ, Ward RJ, Usher-Smith JA, Griffin SJ. The absolute and relative risk of type 2 diabetes after gestational diabetes: A systematic review and meta-analysis of 129 studies. *Diabetes Res Clin Pract* 2021; **171**: 108625 [PMID: 33333204 DOI: 10.1016/j.diabres.2020.108625]

4 **Simmons D**, Immanuel J, Hague WM, Teede H, Nolan CJ, Peek MJ, Flack JR, McLean M, Wong V, Hibbert E, Kautzky-Willer A, Harreiter J, Backman H, Gianatti E, Sweeting A, Mohan V, Enticott J, Cheung NW; TOBOGM Research Group. Treatment of Gestational Diabetes Mellitus Diagnosed Early in Pregnancy. *N Engl J Med* 2023; **388**: 2132-2144 [PMID: 37144983 DOI: 10.1056/NEJMoa2214956]

5 **Catalano PM**. Trying to understand gestational diabetes. *Diabet Med* 2014; **31**: 273-281 [PMID: 24341419 DOI: 10.1111/dme.12381]

6 **Gutch M**, Kumar S, Razi SM, Gupta KK, Gupta A. Assessment of insulin sensitivity/resistance. *Indian J Endocrinol Metab* 2015; **19**: 160-164 [PMID: 25593845 DOI: 10.4103/2230-8210.146874]

7 **Tahapary DL**, Pratisthita LB, Fitri NA, Marcella C, Wafa S, Kurniawan F, Rizka A, Tarigan TJE, Harbuwono DS, Purnamasari D, Soewondo P. Challenges in the diagnosis of insulin resistance: Focusing on the role of HOMA-IR and Tryglyceride/glucose index. *Diabetes Metab Syndr* 2022; **16**: 102581 [PMID: 35939943 DOI: 10.1016/j.dsx.2022.102581]

8 **Bogdanet D**, O'Shea P, Lyons C, Shafat A, Dunne F. The Oral Glucose Tolerance Test-Is It Time for a Change?-A Literature Review with an Emphasis on Pregnancy. *J Clin Med* 2020; **9** [PMID: 33121014 DOI: 10.3390/jcm9113451]

9 **Greenhalgh T**, Thorne S, Malterud K. Time to challenge the spurious hierarchy of systematic over narrative reviews? *Eur J Clin Invest* 2018; **48**: e12931 [PMID: 29578574 DOI: 10.1111/eci.12931]

10 **Furley P**, Goldschmied N. Systematic vs. Narrative Reviews in Sport and Exercise Psychology: Is Either Approach Superior to the Other? *Front Psychol* 2021; **12**: 685082 [PMID: 34305741 DOI: 10.3389/fpsyg.2021.685082]

11 **Maddaloni E**, Bolli GB, Frier BM, Little RR, Leslie RD, Pozzilli P, Buzzetti R. C-peptide determination in the diagnosis of type of diabetes and its management: A clinical perspective. *Diabetes Obes Metab* 2022; **24**: 1912-1926 [PMID: 35676794 DOI: 10.1111/dom.14785]

12 **Novac C**, Radulian G, Orzan A, Balgradean M. Short Update on C-Peptide and its Clinical Value. *Maedica (Bucur)* 2019; **14**: 53-58 [PMID: 31123514 DOI: 10.26574/maedica.2019.14.1.53]

13 **Vejrazkova D**, Vankova M, Lukasova P, Vcelak J, Bendlova B. Insights into the physiology of C-peptide. *Physiol Res* 2020; **69**: S237-S243 [PMID: 33094622 DOI: 10.33549/physiolres.934519]

14 **Landreh M**, Jörnvall H. Biological activity *vs* physiological function of proinsulin C-peptide. *Cell Mol Life Sci* 2021; **78**: 1131-1138 [PMID: 32959070 DOI: 10.1007/s00018-020-03636-2]

15 **Wahren J**, Larsson C. C-peptide: new findings and therapeutic possibilities. *Diabetes Res Clin Pract* 2015; **107**: 309-319 [PMID: 25648391 DOI: 10.1016/j.diabres.2015.01.016]

16 **Hills CE**, Brunskill NJ. Intracellular signalling by C-peptide. *Exp Diabetes Res* 2008; **2008**: 635158 [PMID: 18382618 DOI: 10.1155/2008/635158]

17 **Yosten GL**, Kolar GR. The Physiology of Proinsulin C-Peptide: Unanswered Questions and a Proposed Model. *Physiology (Bethesda)* 2015; **30**: 327-332 [PMID: 26136546 DOI: 10.1152/physiol.00008.2015]

18 **Sharma AK**, Singh S, Singh H, Mahajan D, Kolli P, Mandadapu G, Kumar B, Kumar D, Kumar S, Jena MK. Deep Insight of the Pathophysiology of Gestational Diabetes Mellitus. *Cells* 2022; **11** [PMID: 36078079 DOI: 10.3390/cells11172672]

19 **Plows JF**, Stanley JL, Baker PN, Reynolds CM, Vickers MH. The Pathophysiology of Gestational Diabetes Mellitus. *Int J Mol Sci* 2018; **19** [PMID: 30373146 DOI: 10.3390/ijms19113342]

20 **Kampmann U**, Knorr S, Fuglsang J, Ovesen P. Determinants of Maternal Insulin Resistance during Pregnancy: An Updated Overview. *J Diabetes Res* 2019; **2019**: 5320156 [PMID: 31828161 DOI: 10.1155/2019/5320156]

21 **Egan AM**, Dow ML, Vella A. A Review of the Pathophysiology and Management of Diabetes in Pregnancy. *Mayo Clin Proc* 2020; **95**: 2734-2746 [PMID: 32736942 DOI: 10.1016/j.mayocp.2020.02.019]

22 **Moyce BL**, Dolinsky VW. Maternal β-Cell Adaptations in Pregnancy and Placental Signalling: Implications for Gestational Diabetes. *Int J Mol Sci* 2018; **19** [PMID: 30400566 DOI: 10.3390/ijms19113467]

23 **Rodrigo N**, Glastras SJ. The Emerging Role of Biomarkers in the Diagnosis of Gestational Diabetes Mellitus. *J Clin Med* 2018; **7** [PMID: 29882903 DOI: 10.3390/jcm7060120]

24 **ElSayed NA**, Aleppo G, Aroda VR, Bannuru RR, Brown FM, Bruemmer D, Collins BS, Hilliard ME, Isaacs D, Johnson EL, Kahan S, Khunti K, Leon J, Lyons SK, Perry ML, Prahalad P, Pratley RE, Seley JJ, Stanton RC, Gabbay RA; on behalf of the American Diabetes Association. 2. Classification and Diagnosis of Diabetes: Standards of Care in Diabetes-2023. *Diabetes Care* 2023; **46**: S19-S40 [PMID: 36507649 DOI: 10.2337/dc23-S002]

25 **Buchanan TA**, Xiang AH, Page KA. Gestational diabetes mellitus: risks and management during and after pregnancy. *Nat Rev Endocrinol* 2012; **8**: 639-649 [PMID: 22751341 DOI: 10.1038/nrendo.2012.96]

26 **Zhang C**, Tobias DK, Chavarro JE, Bao W, Wang D, Ley SH, Hu FB. Adherence to healthy lifestyle and risk of gestational diabetes mellitus: prospective cohort study. *BMJ* 2014; **349**: g5450 [PMID: 25269649 DOI: 10.1136/bmj.g5450]

27 **Sadiya A**, Jakapure V, Shaar G, Adnan R, Tesfa Y. Lifestyle intervention in early pregnancy can prevent gestational diabetes in high-risk pregnant women in the UAE: a randomized controlled trial. *BMC Pregnancy Childbirth* 2022; **22**: 668 [PMID: 36042401 DOI: 10.1186/s12884-022-04972-w]

28 **Koivusalo SB**, Rönö K, Klemetti MM, Roine RP, Lindström J, Erkkola M, Kaaja RJ, Pöyhönen-Alho M, Tiitinen A, Huvinen E, Andersson S, Laivuori H, Valkama A, Meinilä J, Kautiainen H, Eriksson JG, Stach-Lempinen B. Gestational Diabetes Mellitus Can Be Prevented by Lifestyle Intervention: The Finnish Gestational Diabetes Prevention Study (RADIEL): A Randomized Controlled Trial. *Diabetes Care* 2016; **39**: 24-30 [PMID: 26223239 DOI: 10.2337/dc15-0511]

29 **ElSayed NA**, Aleppo G, Aroda VR, Bannuru RR, Brown FM, Bruemmer D, Collins BS, Hilliard ME, Isaacs D, Johnson EL, Kahan S, Khunti K, Leon J, Lyons SK, Perry ML, Prahalad P, Pratley RE, Jeffrie Seley J, Stanton RC, Gabbay RA; on behalf of the American Diabetes Association. 15. Management of Diabetes in Pregnancy: Standards of Care in Diabetes-2023. *Diabetes Care* 2023; **46**: S254-S266 [PMID: 36507645 DOI: 10.2337/dc23-S015]

30 **Hörber S**, Achenbach P, Schleicher E, Peter A. Harmonization of immunoassays for biomarkers in diabetes mellitus. *Biotechnol Adv* 2020; **39**: 107359 [PMID: 30802485 DOI: 10.1016/j.biotechadv.2019.02.015]

31 **Ghazal K**, Brabant S, Prie D, Piketty ML. Hormone Immunoassay Interference: A 2021 Update. *Ann Lab Med* 2022; **42**: 3-23 [PMID: 34374345 DOI: 10.3343/alm.2022.42.1.3]

32 **Leighton E**, Sainsbury CA, Jones GC. A Practical Review of C-Peptide Testing in Diabetes. *Diabetes Ther* 2017; **8**: 475-487 [PMID: 28484968 DOI: 10.1007/s13300-017-0265-4]

33 **McDonald TJ**, Perry MH, Peake RW, Pullan NJ, O'Connor J, Shields BM, Knight BA, Hattersley AT. EDTA improves stability of whole blood C-peptide and insulin to over 24 h at room temperature. *PLoS One* 2012; **7**: e42084 [PMID: 22860060 DOI: 10.1371/journal.pone.0042084]

34 **Yosten GL**, Maric-Bilkan C, Luppi P, Wahren J. Physiological effects and therapeutic potential of proinsulin C-peptide. *Am J Physiol Endocrinol Metab* 2014; **307**: E955-E968 [PMID: 25249503 DOI: 10.1152/ajpendo.00130.2014]

35 **Wong SL**, Priestman A, Holmes DT. Recurrent hypoglycemia from insulin autoimmune syndrome. *J Gen Intern Med* 2014; **29**: 250-254 [PMID: 23979685 DOI: 10.1007/s11606-013-2588-9]

36 **Becht FS**, Walther K, Martin E, Nauck MA. Fasting C-peptide and Related Parameters Characterizing Insulin Secretory Capacity for Correctly Classifying Diabetes Type and for Predicting Insulin Requirement in Patients with Type 2 Diabetes. *Exp Clin Endocrinol Diabetes* 2016; **124**: 148-156 [PMID: 26824281 DOI: 10.1055/s-0035-1565177]

37 **Oh J**, Kim JH, Park HD. Clinical Utility and Cross-Reactivity of Insulin and C-Peptide Assays by the Lumipulse G1200 System. *Ann Lab Med* 2018; **38**: 530-537 [PMID: 30027696 DOI: 10.3343/alm.2018.38.6.530]

38 **Saisho Y**. Postprandial C-Peptide to Glucose Ratio as a Marker of β Cell Function: Implication for the Management of Type 2 Diabetes. *Int J Mol Sci* 2016; **17** [PMID: 27196896 DOI: 10.3390/ijms17050744]

39 **Jones AG**, Hattersley AT. The clinical utility of C-peptide measurement in the care of patients with diabetes. *Diabet Med* 2013; **30**: 803-817 [PMID: 23413806 DOI: 10.1111/dme.12159]

40 **Schaefer-Graf U**, Napoli A, Nolan CJ; Diabetic Pregnancy Study Group. Diabetes in pregnancy: a new decade of challenges ahead. *Diabetologia* 2018; **61**: 1012-1021 [PMID: 29356835 DOI: 10.1007/s00125-018-4545-y]

41 **Powe CE**. Early Pregnancy Biochemical Predictors of Gestational Diabetes Mellitus. *Curr Diab Rep* 2017; **17**: 12 [PMID: 28229385 DOI: 10.1007/s11892-017-0834-y]

42 **Ernst S**, Demirci C, Valle S, Velazquez-Garcia S, Garcia-Ocaña A. Mechanisms in the adaptation of maternal β-cells during pregnancy. *Diabetes Manag (Lond)* 2011; **1**: 239-248 [PMID: 21845205 DOI: 10.2217/dmt.10.24]

43 **Omazić J**, Viljetić B, Ivić V, Kadivnik M, Zibar L, Müller A, Wagner J. Early markers of gestational diabetes mellitus: what we know and which way forward? *Biochem Med (Zagreb)* 2021; **31**: 030502 [PMID: 34658643 DOI: 10.11613/BM.2021.030502]

44 **Fu J**, Retnakaran R. The life course perspective of gestational diabetes: An opportunity for the prevention of diabetes and heart disease in women. *EClinicalMedicine* 2022; **45**: 101294 [PMID: 35198924 DOI: 10.1016/j.eclinm.2022.101294]

45 **Yang X**, Ye Y, Wang Y, Wu P, Lu Q, Liu Y, Yuan J, Song X, Yan S, Qi X, Wang YX, Wen Y, Liu G, Lv C, Yang CX, Pan A, Zhang J, Pan XF. Association between early-pregnancy serum C-peptide and risk of gestational diabetes mellitus: a nested case-control study among Chinese women. *Nutr Metab (Lond)* 2022; **19**: 56 [PMID: 35996181 DOI: 10.1186/s12986-022-00691-3]

46 **Chen X**, Stein TP, Steer RA, Scholl TO. Individual free fatty acids have unique associations with inflammatory biomarkers, insulin resistance and insulin secretion in healthy and gestational diabetic pregnant women. *BMJ Open Diabetes Res Care* 2019; **7**: e000632 [PMID: 31245005 DOI: 10.1136/bmjdrc-2018-000632]

47 **Falcone V**, Kotzaeridi G, Breil MH, Rosicky I, Stopp T, Yerlikaya-Schatten G, Feichtinger M, Eppel W, Husslein P, Tura A, Göbl CS. Early Assessment of the Risk for Gestational Diabetes Mellitus: Can Fasting Parameters of Glucose Metabolism Contribute to Risk Prediction? *Diabetes Metab J* 2019; **43**: 785-793 [PMID: 30877716 DOI: 10.4093/dmj.2018.0218]

48 **Qiu C**, Vadachkoria S, Meryman L, Frederick IO, Williams MA. Maternal plasma concentrations of IGF-1, IGFBP-1, and C-peptide in early pregnancy and subsequent risk of gestational diabetes mellitus. *Am J Obstet Gynecol* 2005; **193**: 1691-1697 [PMID: 16260212 DOI: 10.1016/j.ajog.2005.04.015]

49 **Metzger BE**, Lowe LP, Dyer AR, Trimble ER, Chaovarindr U, Coustan DR, Hadden DR, McCance DR, Hod M, McIntyre HD, Oats JJ, Persson B, Rogers MS, Sacks DA; HAPO Study Cooperative Research Group. Hyperglycemia and adverse pregnancy outcomes. *N Engl J Med* 2008; **358**: 1991-2002 [PMID: 18463375 DOI: 10.1056/NEJMoa0707943]

50 **Lorenzo-Almorós A**, Hang T, Peiró C, Soriano-Guillén L, Egido J, Tuñón J, Lorenzo Ó. Predictive and diagnostic biomarkers for gestational diabetes and its associated metabolic and cardiovascular diseases. *Cardiovasc Diabetol* 2019; **18**: 140 [PMID: 31666083 DOI: 10.1186/s12933-019-0935-9]

51 **Stopp T**, Feichtinger M, Rosicky I, Yerlikaya-Schatten G, Ott J, Egarter HC, Schatten C, Eppel W, Husslein P, Mittlböck M, Tura A, Göbl CS. Novel Indices of Glucose Homeostasis Derived from Principal Component Analysis: Application for Metabolic Assessment in Pregnancy. *J Diabetes Res* 2020; **2020**: 4950584 [PMID: 32337294 DOI: 10.1155/2020/4950584]

World Journal of Experimental Medicine

Submit a Manuscript: https://www.f6publishing.com

World J Exp Med 2024 March 20; 14(1): 86898

DOI: 10.5493/wjem.v14.i1.86898

ISSN 2220-315x (online)

MINIREVIEWS

Understanding wound healing in obesity

Asha Cotterell, Michelle Griffin, Mauricio A Downer, Jennifer B Parker, Derrick Wan, Michael T Longaker

Specialty type: Medicine, research and experimental

Provenance and peer review: Invited article; Externally peer reviewed.

Peer-review model: Single blind

Peer-review report's scientific quality classification

Grade A (Excellent): 0
Grade B (Very good): B
Grade C (Good): 0
Grade D (Fair): 0
Grade E (Poor): 0

P-Reviewer: Mostafavinia A, Iran

Received: July 13, 2023
Peer-review started: July 13, 2023
First decision: September 19, 2023
Revised: September 30, 2023
Accepted: January 11, 2024
Article in press: January 11, 2024
Published online: March 20, 2024

Asha Cotterell, Michelle Griffin, Division of Plastic and Reconstructive Surgery, Stanford University, Palo Alto, CA 94301, United States

Mauricio A Downer, Jennifer B Parker, Stanford University School of Medicine, Stanford University School of Medicine, Palo Alto, CA 94301, United States

Derrick Wan, Michael T Longaker, Department of Surgery, Stanford University School of Medicine, Hagey Laboratory for Pediatric Regenerative Medicine, Palo Alto, CA 94301, United States

Corresponding author: Michael T Longaker, Department of Surgery, Stanford University School of Medicine, Hagey Laboratory for Pediatric Regenerative Medicine, 291 Campus Drive, Palo Alto, CA 94301, United States. mgriff12@stanford.edu

Abstract

Obesity has become more prevalent in the global population. It is associated with the development of several diseases including diabetes mellitus, coronary heart disease, and metabolic syndrome. There are a multitude of factors impacted by obesity that may contribute to poor wound healing outcomes. With millions worldwide classified as obese, it is imperative to understand wound healing in these patients. Despite advances in the understanding of wound healing in both healthy and diabetic populations, much is unknown about wound healing in obese patients. This review examines the impact of obesity on wound healing and several animal models that may be used to broaden our understanding in this area. As a growing portion of the population identifies as obese, understanding the underlying mechanisms and how to overcome poor wound healing is of the utmost importance.

Key Words: Obesity; Wound healing; Adipokines; Tissue fibrosis; Diabetes; Preclinical animal models; Hypertrophic skin scarring; Wound tension; Metabolic syndrome

Core Tip: Obesity induces a chronic low-grade inflammatory state through increased release of adipokines, cytokines, and chemokines from excess adipose tissue. The chronic low-grade inflammation is thought to contribute to a dampened immune response during the inflammatory phase of wound healing leading to delayed wound healing. While there are several animal models used to study wound healing, they have not been widely applied to studying the effects of obesity on wound healing leading to a gap in the literature on this topic.

Citation: Cotterell A, Griffin M, Downer MA, Parker JB, Wan D, Longaker MT. Understanding wound healing in obesity. *World J Exp Med* 2024; 14(1): 86898
URL: https://www.wjgnet.com/2220-315x/full/v14/i1/86898.htm
DOI: https://dx.doi.org/10.5493/wjem.v14.i1.86898

INTRODUCTION

Obesity has become more common over the past 40 years, with approximately 33% of the population being classified as overweight or obese[1]. In adults, obesity is defined as a body mass index of 30.0 kg/m^2 or greater[2-4]. Obesity accounts for up to 7% of total healthcare costs in developed nations, classifying it as a significant expenditure of national healthcare budgets[3]. Obesity is associated with the development of several diseases including diabetes mellitus, coronary heart disease, hypertension, and certain forms of cancer, and has been associated with a decreased lifetime expectancy[2-4]. Delayed wound healing seen in patients with diabetes mellitus, commonly associated with obesity, can be attributed to changes in the macro- and microvasculature, decreased production of growth factors, and poor quality of granulation tissue[5,6]. Impaired wound healing can be caused by changes in the four phases of wound healing – hemostasis, inflammation, proliferation, and remodeling (Figure 1).

Due to the significant rise in obesity worldwide, it is important to understand the role that that this disease may have on wound healing. The purpose of this review is to highlight the impact of obesity on cutaneous wound healing and discuss future studies that must be performed to advance our understanding of the subject. We also aim to review the phases of wound healing and how they are impacted in obese states.

Physiologic changes in the human body due to obesity

There are several physiologic changes that occur in the body as the result of obesity. In the respiratory system, impaired diaphragmatic relaxation and chest expansion due to additional adipose tissue result in hyperventilation as well as decreased vital capacity and tidal volumes[7,8]. Fibroblasts, which require partial pressure of oxygen greater than 15 mmHg for proper function, are unable to produce collagen in the wound edges in obese patients where the pressure of arterial oxygen (PaO_2) is near 0 mmHg[8]. In the cardiovascular system, there is excess workload on the heart to supply oxygen to all tissues of the body. Patients with longstanding obesity may eventually develop heart failure, resulting in decreased cardiac output, reduced blood volume, and impaired circulation. It is known that adipose tissue is not well vascularized and is more susceptible to ischemia and hypoxia when compared to the epidermis[7]. It is important to explore these changes in vascularity and asses how they may contribute to wound healing outcomes.

Changes in vascularity

In addition to alterations in respiratory physiology and cardiac function, macro- and microvasulature is also impacted in the obese state. It is well documented that adipose tissue has decreased vascularity when compared to other tissues in the body[7,9]. This decrease in vascularity may contribute to the poor wound healing outcomes seen in this population. The increase in adipose tissue is also negatively correlated with angiogenesis[9]. Glucocorticoids have been well documented as inhibitors of angiogenesis. Elevated levels of 11β-hydroxysteroid dehydrogenase type 1, a glucocorticoid-amplifying enzyme, has been associated with obesity[9]. In addition to affecting angiogenesis, glucocorticoids have also been associated with altering immune responses.

Changes in immune responses

It is crucial to consider changes in immune function, as alterations at baseline may have significant impact on homeostasis. A number of studies have been published elucidating the connections between obesity and a pro-inflammatory state[10]. These alterations in immune function are mediated by adipocyte hypertrophy in conjunction with infiltration of pro-inflammatory cell types including $CD8^+$ T-cells, $CD4^+$ T-cells, and M1 macrophages[10]. In addition to changes in immune cell activation, elevated levels of glucocorticoids are seen in both obese humans and mice, likely due to increased stress on the body[11]. This chronic stress on the body is also associated with chronic low-grade inflammation[9]. Studies in obese mice have demonstrated progressive increases in proinflammatory cytokines due to activation of invariant natural killer T cells by excess lipids[9]. Elevated cytokines include tumor necrosis factor alpha (TNF-α), leptin, interleukin (IL-6), and transforming growth factor beta (TGF-β) which are all involved at varying stages of the wound healing process[9].

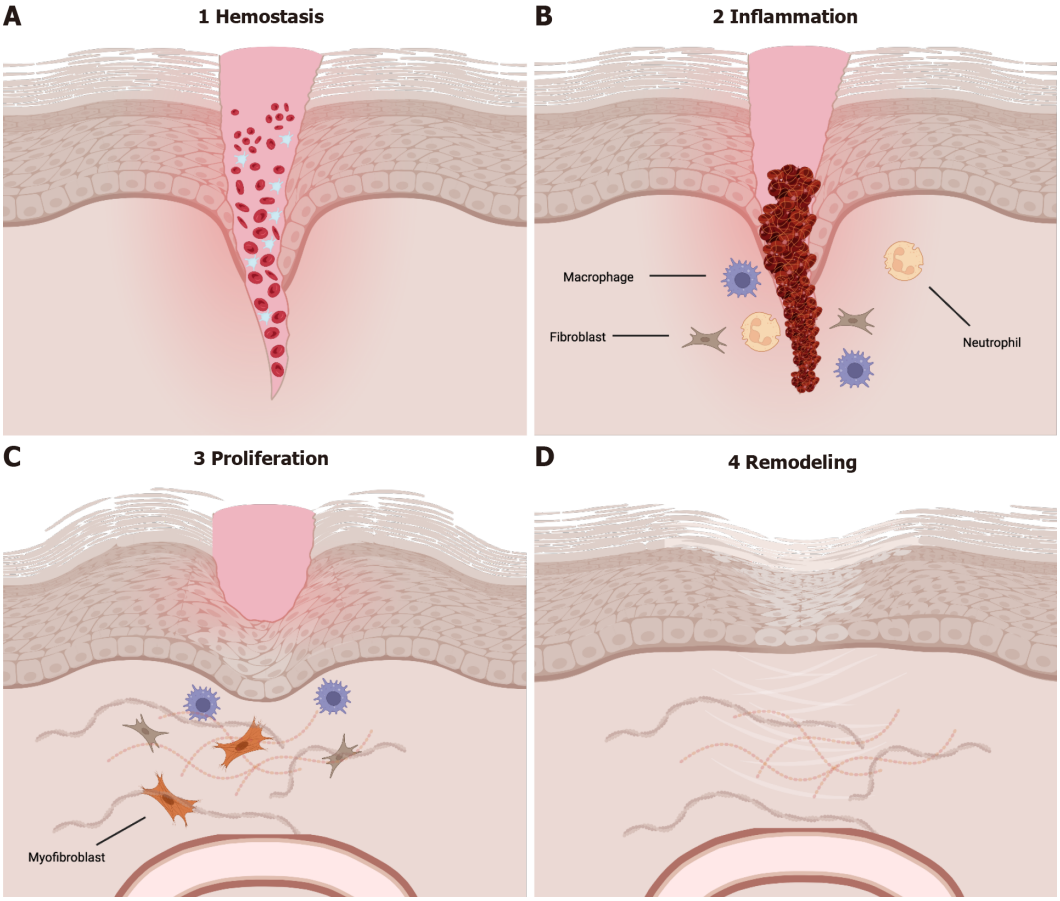

Figure 1 The four phases of wound healing. Wound healing is divided into 4 distinct phases that have overlap. A: Hemostasis, B: Inflammation, C: Proliferation, D: Remodeling. Cell-to-cell interactions mediated by both cytokines and chemokines are imperative for the transitions between phases. During hemostasis, platelets and fibrin function to form a plug to stop bleeding. Hemostasis is followed by the inflammatory phase which is characterized by release of cytokines, most notably from macrophages, that are imperative for induction of the proliferative phase. During proliferation, the body is focused on neovascularization and re-epithelialization of the wound surface. The final phase, remodeling, takes place over months to years and is currently not well characterized. Produced using BioRender.com.

PHASES OF WOUND HEALING

Given the physiologic changes seen in obesity, it is possible that they may have direct impact on the wound healing process. To understand possible mechanisms of interaction, one must be familiar with the wound healing process under normal physiologic conditions. Briefly, the first phase of wound healing, hemostasis, occurs when there is damage to endothelial cells. Following hemostasis, the inflammatory phase begins in which there is edema and an influx of inflammatory cells. The inflammatory phase is then followed by both proliferation and remodeling, the latter of which can take place for over two years[12].

Hemostasis

Hemostasis, the first phase of wound healing, occurs due to endothelial damage and can last from minutes to hours. Immediately upon injury, damaged blood vessels will vasoconstrict and both the intrinsic and extrinsic coagulation cascades are activated by nearby platelets and endothelial cells[13]. The thrombus that forms is rich in platelets, collagen, fibronectin, and thrombin; it serves a scaffold for neutrophils, monocytes, and other invading cells leading to the release of cytokines, growth factors, and local vasoconstrictors such as serotonin[13]. Following hemostasis, release of histamine induces migration of inflammatory cells to the site of injury, thus marking the beginning of the inflammatory phase.

The inflammatory phase

The inflammatory phase generally begins shortly after initial injury and the hemostasis phase[14]. The inflammatory phase is critical to the wound healing process as it marks recruitment of the innate immune system. Within the first 48 to 96 h after injury, monocytes are recruited from the surrounding tissue and transform into macrophages[13]. These activated macrophages are necessary for the transition from the inflammatory phase to the proliferative phase. Macrophages release vascular endothelial growth factor, fibroblast growth factor, and TNF-α to stimulate angiogenesis in addition to TGF-β, epidermal growth factor, and platelet-derived growth factor for fibroplasia[13]. Neutrophils, the predominant cell type during this phase, are recruited to the site of injury *via* IL-8 released from platelets during degranulation, and secrete IL-1, TNF-α, and TGF-β[13]. In the skin following injury, toll-like receptors are expressed on host cells

leading to the activation of two distinct pathways - the nuclear factor kappa beta and mitogen-activated protein kinase pathways. The activation of these pathways is the hallmark of the inflammatory phase[15]. As the inflammatory phase resolves, the body begins the proliferative phase. Healing may begin only after the inflammatory phase is done[16].

The proliferative phase

During the proliferative phase, the body prioritizes restoring the local vascular network and re-epithelializing the wound surface[15]. Keratinocytes begin migrating from the edges of the wound bed while epithelial stem cells begin proliferating in reactions influenced by both chemical and mechanical signals from both anti- and pro-inflammatory cells, inducing fibroplasia. During fibroplasia, fibroblasts become activated, transition to myofibroblasts and secrete components of the extracellular matrix that promote wound contraction, contributing to formation of a persistent scar[17]. These signals lead to the development of granulation tissue, which is largely comprised of collagen III, new blood vessels, and fibroblasts. Fibroblasts are the predominant cell type in granulation tissue and respond to cytokines released from macrophages to induce re-epithelialization[18]. Fibroblasts release keratinocyte growth factor 1 and 2 in addition to IL-6, and these cytokines stimulate local keratinocytes to migrate, proliferate, and differentiate in the wound bed[13]. Research has shown that wounds deficient in IL-6 have decreased collagen deposition, epithelialization, and angiogenesis[18]. Given the intricacies involved in the four phases of wound healing, it is important to note how these phases of wound healing are affected by obesity.

FACTORS AFFECTING WOUND HEALING IN OBESITY

There are several factors that may contribute to poor wound healing found in obese populations (Figure 2). Patients with obesity are in a persistent inflammatory state; because of this, these patients have a prolonged inflammatory phase contributing to poor wound healing outcomes (Figure 3)[16].

Adipokines

Adipokines are cytokines produced by adipose tissue that affect metabolism, reproduction, and satiety. Currently known adipokines include leptin, adiponectin, and resistin[19]. Leptin, the most studied, regulates food intake and energy expenditure *via* the central nervous system. It has been shown to be effective in improving metabolic dysfunction in patients with either lipodystrophy or congenital leptin deficiencies[20,21]. Leptin has also been shown to be structurally similar to IL-2 and growth hormone 1, suggesting that it may have pro-inflammatory activity; it has been shown to increase the production of TNF-α and IL-6 by monocytes[22]. Interestingly, leptin levels also increase in serum in response to pro-inflammatory stimuli including TNF-α[22].

Leptin is not the only proinflammatory adipokine that has been extensively studied in recent decades. Resistin, another proinflammatory adipokine, has been shown to induce insulin resistance in mice. However, it is unclear if these effects exist in humans as well[21]. In mice, it has been shown that deficiencies of this adipokine in ob/ob mice lead to increase obesity despite improved glucose tolerance and insulin sensitivity[23].

In addition to pro-inflammatory adipokines, there are also anti-inflammatory adipokines of which adiponectin is one that has been relatively well studied. Adiponectin, almost exclusively produced and secreted by adipocytes, has become well studied for its anti-inflammatory, anti-apoptotic, and insulin-sensing properties[21]. It has been shown to protect against several disorders associated with obesity; adiponectin expression has also been found to have decreased levels in patients with obesity[18,21]. In addition to the impact of adipokines on wound healing, cytokines and chemokines have also been implicated in the pathogenesis of chronic wounds in obese and pre-diabetic populations.

Cytokines and chemokines

Adipose tissue is also an important source of cytokines, and there are many cytokines and chemokines that influence wound healing in obesity. Proinflammatory cytokines including monocyte chemotactic protein-1, TNF-α, IL-1, IL-6, and IL-8, are notably increased in obesity (Table 1)[21,24,25]. Patients and mice with increased percentages of adipose tissue produce more of these pro-inflammatory cytokines at baseline leading to a state of chronic low-grade inflammation. Alterations in serum levels of these cytokines, chemokines, and adipokines may drive the underlying physiologic processes that contribute to poor wound healing outcomes in obese patients.

Wound tension, tissue pressure, and hematoma formation

In addition to chemical mediators impacting wound healing, a number of mechanical forces also impact wound healing in obesity. Due to excess adipose tissue, there is increased tension on wounds; this increased tension is frequently associated with hypertrophic scarring and stretched scars[16,26]. Increased tissue pressure is also seen due to excess adipose tissue, both in unwounded and wounded cutaneous skin[16,27]. This increased pressure is associated with reduced perfusion and vascularity[27]. Furthermore, hematoma formation is a complication frequently seen in patients due to excess tissue pressure. Given the multitude of complications associated with obesity, it is imperative to understand what impact obesity plays in the wound healing process.

Table 1 Cytokines produced by adipose tissue that may contribute to low-grade inflammation

TNF-α	Secreted by macrophages, natural killer cells, and lymphocytes[13]. Crucial in formation and maintenance of granulomas[30]
IL-1	Produced by various cell types including macrophages, fibroblasts, and epithelial cells[13]. Stimulates fibroblast and keratinocyte growth and collagen synthesis by fibroblasts
IL-6	Secreted by various cell types including macrophages and adipocytes[13]. An important mediator of the acute phase response and regulator of glucose homeostasis in obesity
IL-8	Produced by various cell types including macrophages, epithelial cells, and endothelial cells[13]. Primarily recruits neutrophils and other granulocytes to sites of tissue injury
MCP-1	Also known as CCL2. Primarily secreted by monocytes, macrophages, and dendritic cells[13]. Attracts monocytes, memory T cells, and dendritic cells to sites of inflammation produced by either tissue injury or inflammation

TNF-α: Tumor necrosis factor alpha; IL: Interleukin; MCP-1: Monocyte chemoattractant protein-1.

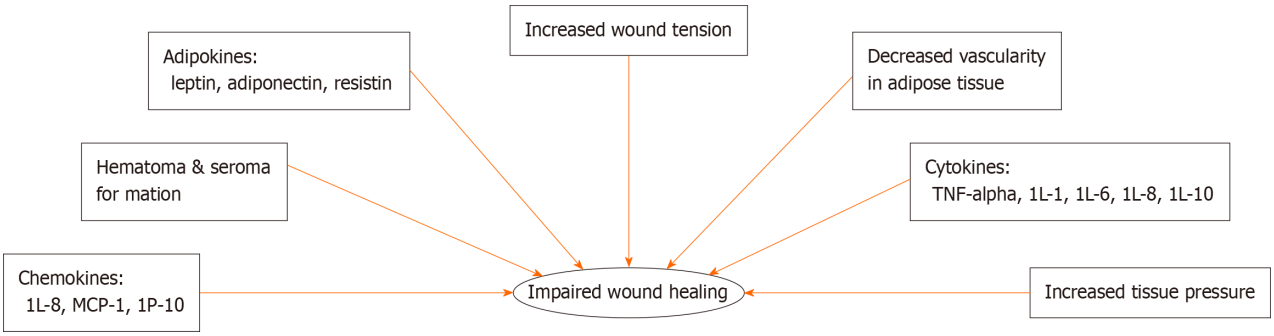

Figure 2 Factors related to wound healing impairment in obesity. Obesity is characterized by a chronic inflammatory state that is associated with changes mediated by varying levels of adipokines, chemokines, and cytokines. In addition to these chemical signals, physiologic changes including increased tissue pressure and decreased vascularity of adipose tissue also contribute to poor wound healing outcomes. MCP-1: Monocyte chemoattractant protein-1; IP-10: Interferon-gamma-inducible protein 10; TNF-α: Tumor necrosis factor alpha; IL: Interleukin.

OBESITY AND IMPACT ON WOUND HEALING

As previously discussed, patients with obesity have persistently elevated levels of pro-inflammatory cytokines in serum. This elevated immune response at baseline may likely cause a dampened immune response during the inflammatory phase of wound healing resulting in the chronic, slow-healing wounds frequently seen in this population.

ANIMAL MODELS USED TO STUDY WOUND HEALING

To study wound healing, it is essential to create animal models that mimic wound healing in human skin. There are three main models to study this process – the hypertrophic wound model, the wound-induced hair follicle neogenesis (WIHN) model, and the excisional wound model (Figure 4). Although many animal species are used to study healing, this review will only discuss advantages and disadvantages of murine models. Mice and rats are popular for these animal models as they are widely available and relatively inexpensive. However, skin in these animals contain myofibroblasts, which allow their wounds to heal *via* contraction rather than through re-epithelialization and granulation as seen in human skin.

Hypertrophic skin model

Cutaneous incisional mouse wounds rapidly heal with minimal fibrosis and will not result in hypertrophic scarring during the normal wound healing process; thus, strategies have been developed to induce hypertrophic scar formation. Hypertrophic scars are associated with excessive scarring due to severe trauma and delayed wound healing. These scars may result in skin disfiguration and restriction of joint mobility[28,29]. In humans, hypertrophic scars develop within 4-8 wk following wound closure and growth may persist for 6 months before gradual recession[29,30]. Understanding the pathophysiology of these scars is imperative for the development of restorative treatments. Therefore, the Incisional wound model in mice has been adapted to generate pathologic scarring with mechanical tension devices, and termed the Hypertrophic skin model. Advantages of this model include low cost and reproducible production of a hypertrophic scar. Disadvantages include generation of a hypertrophic scar thinner than humans and requirement of a specially designed device to generate mechanical tension.

In this model, a 2-cm full thickness incisional wound is made on the mouse dorsal surface, and a loading device is sutured on either side of the wound bed to create tension[29,31]. Due to this external mechanical tension, a hypertrophic scar that is more similar in both histology and morphology to human cutaneous scars is created in mouse skin. Scars

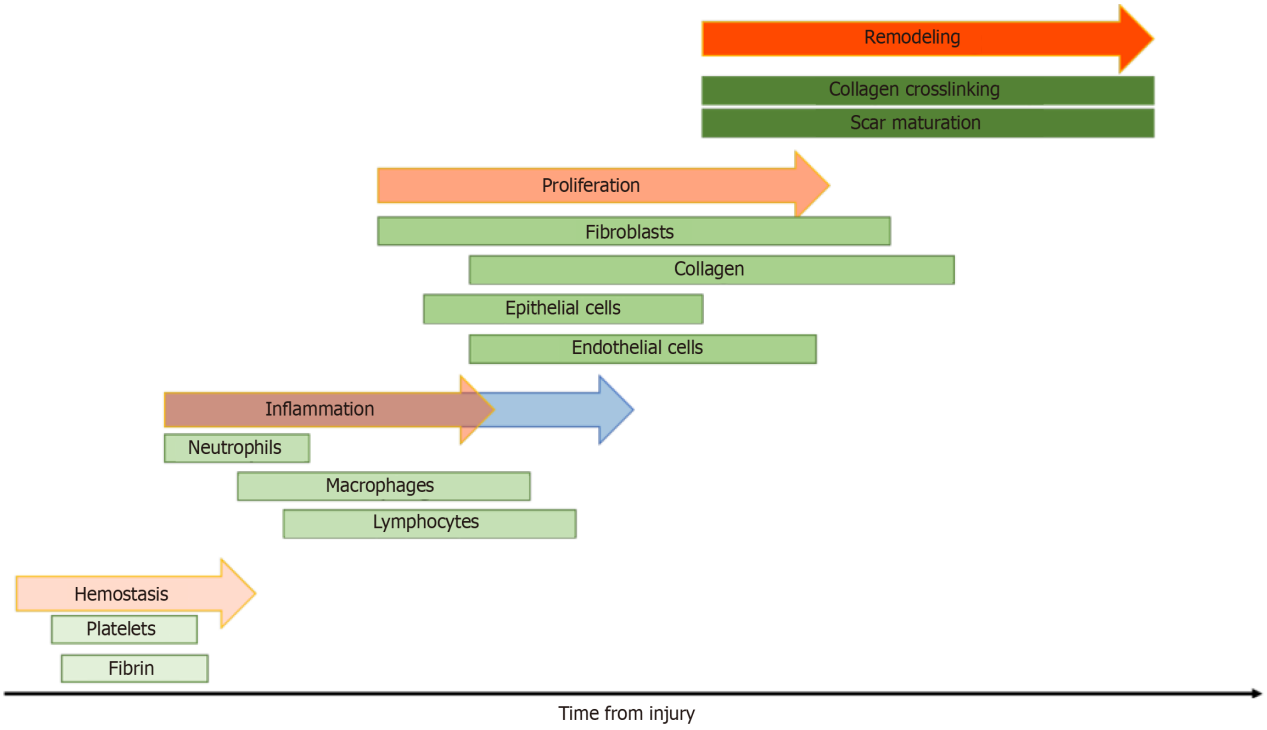

Figure 3 A timeline of the four phases of wound healing. Each phase of wound healing is mediated by a distinct population of cells. While the phases have significant overlap, alterations in levels of cytokines or cell types in any phase may cause delayed wound healing. The inflammatory phase is notably extended in obese patients (blue arrow), this is thought to contribute to poor healing outcomes in this population.

studied using this model demonstrate epidermal thickening with loss of adnexal structures and hair follicles, mast cell infiltrate (similar to what is seen in human HTS), hypervascularity, collagen whorls, and increased cellularity[31]. The increased cellularity observed is accompanied by a significant decrease in cellular apoptosis mediated by upregulation of Akt, a pro-survival marker[31].

WIHN model

Humans regenerate neither terminal nor vellus hair following large full-thickness wounds, presenting a significant clinical issue. Hair follicle regeneration is a complex process that requires coordination between multiple tissues including epidermis, dermis, muscles, and nerves. WIHN is a powerful tool used to study de novo skin regeneration following large full-thickness trauma[32]. Murine primary hair follicles are analogous to human terminal hair, while secondary hair follicles are analogous to human vellus hair, making mice a prime animal to study changes in hair growth following large full-thickness trauma. Advantages of this model include low cost, the ability to study regeneration following adult skin wounding, and development of a model to test therapeutics to activate regenerative wound healing [33]. Disadvantages of this model include variability between mouse strains, environmental conditions, age of mice, and need for creation of large wound size for the animal[33].

This model has shown that wound stiffness modulates hair follicle neogenesis and is partially regulated through mechanotransduction pathways[32]. WIHN observed using this model shows decreased focal adhesion kinase, α-smooth muscle actin, extracellular matrix expression, and cytoskeletal signaling with increased cell survival and increased levels of phospho-signal transducer and activator of transcription 3 and ephrin tyrosine kinase A3 in the central wound area [32]. These characteristics provide a wound environment that is optimal for promoting tissue regeneration following injury occurs only in the central wound area[32-34].

Excisional wound model

Through the use of splints, excisional wound models have been used in mice to create an animal model that more closely mimics the wound healing process in human skin[34]. The full-thickness excisional wound model is the most commonly used model to study wound healing. These wounds extend through the panniculosus carnosus, and a silicone splint is fixed around the wound to minimize contraction. Splinting increases time to complete wound closure and the amount of granulation tissue produced with no significant changes to the capacity for epithelialization[35]. The use of splinting in mice to study the wound healing process has been widely used and has contributed significantly to what we know about the wound healing process[35-37]. Advantages of this model include ease of access to the wound bed to study the effects of pharmaceuticals, biomaterials, and other agents to augment the wound healing process and assess cellular populations in granulation tissue at various stages of healing using histological and immunofluorescence techniques[35-37].

All of these models have their own unique set of advantages and disadvantages (Table 2). Nevertheless, each has contributed greatly to what we know about wound healing in healthy animals, yet there is a lack of studies using these models in understanding the effects of obesity on wound healing. Before applying these tools, we must first understand

Table 2 Animal models used in wound healing, advantages and disadvantages

Animal model	Advantages	Disadvantages
Hypertrophic wound model	Low cost	Hypertrophic scar different from human[27,29]
	Allows for production of hypertrophic scar[28,29]	Requires special device[28,29]
		Labor intensive: Frequent care to maintain tension and device placement[31]
Wound-induced hair follicle neogenesis (WIHN) model	Low cost	
	Regeneration following adult wounding with minimal recovery of hair follicles at the scar center[32,48]	High variability: Mouse strains, environmental conditions, age of mice, and wound size)[33]
	Test therapeutics to activate regenerative wound healing [33]	May not translate to human injury[48]
Excisional wound model	Low cost	Labor intensive: Frequent dressing changes to maintain tension[35]
	Wound healing similar to human[35]	
	Allows for fibroblast lineage tracing[49]	

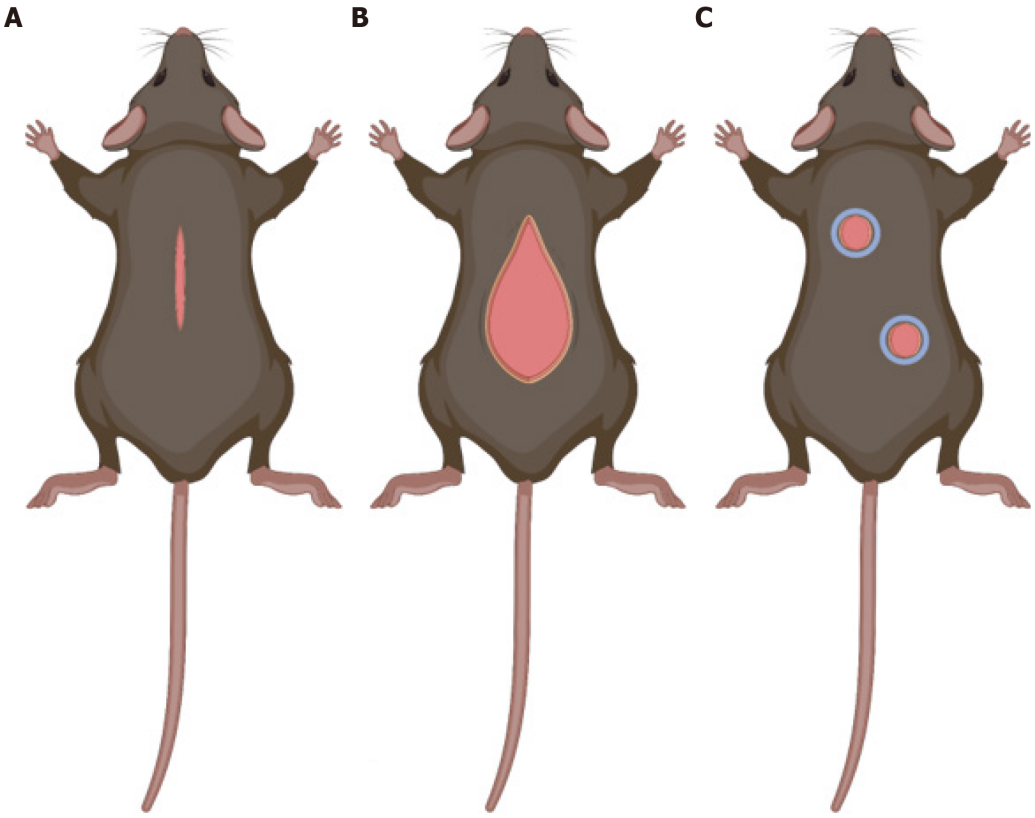

Figure 4 Schematic of three major models of wound healing. A: Hypertrophic wound model. This model allows for use of a device to produce constant tension in the wound bed to produce healing with a hypertrophic scar similar to what is seen in areas of high tension on the body; B: Wound-induced hair follicle neogenesis model. This model is used to investigate regeneration in the setting of large full-thickness trauma; C: Excisional wound model. This model is the most commonly used model to study wound healing and is popular for its ability to investigate the role of various therapeutics to augment wound healing in a similar manner to what is seen in human skin. Produced using BioRender.com.

existing models to study obesity.

ANIMAL MODELS TO STUDY OBESITY

Several models have been developed in mice to study the impact of obesity on varying physiological processes including the use of genetic mutations and diet-induced obesity models. As described above, these animal models can be used in

conjunction with existing wound healing models to examine the influence obesity has on wound healing under varying conditions. First, we will take a look at diet-induced obesity models.

Diet-induced obesity in mice

Human studies have also shown that high-fat diet diets with over 30% kilocalories (kcal) from fat can easily induce obesity[38]. Therefore, it is important to study obesity in this context as the dramatic rise in worldwide obesity over such a short period of time cannot be attributed to genetics[38]. In mice, a positive relationship has been found between dietary fat consumption and both body weight and fat gain[39,40]. To produce dietary-induced obesity in mice, diets contain between 40% and 60% kcal from fat. Similarly to human studies, the amount of dietary fat in the diet is associated with reduced glucose tolerance and increased white adipose tissue, blood glucose levels, and body weight over a 12-wk study period[39]. As previously mentioned, an advantage of diet-induced obesity models is that they may mimic development of obesity similarly to what is observed in humans. In addition to the low costs associated with this model, potential disadvantages of this model include length of time required to induce obesity. Diet-induced obesity models also display leptin insensitivity, which may be caused by persistently elevated leptin levels[41]. To further determine the effects of leptin on obesity, models have been developed to study changes in leptin metabolism.

Genetic models of obesity

The use of ob/ob mice (leptin-deficient due to obese gene mutation) and db/db mice (leptin-resistant due to diabetes gene mutation in the leptin receptor) have allowed researchers to investigate the pathogenesis of both obesity and type 2 diabetes mellitus[41]. Although the mechanisms by which these mutations cause obesity are different, mice display similar phenotypes including hyperphagia, hyperglycemia, obesity, and decreased metabolism[42,43]. Ob/ob mice display altered lipid metabolism in the liver associated with higher incidence of inflammatory infiltrate and hepatic steatosis, while db/db mice display lower hepatic inflammation with increased inflammatory tone in adipose tissue[43]. These genetic mouse models of obesity are easily replicated as the strains are readily available for purchase and are useful to study genetic impact on obesity, however they are limited in their ability to study obesity that arises due to environmental factors.

ANIMAL STUDIES OF OBESE WOUND HEALING

While studies using the hypertrophic skin, WIHN, and excisional splinted wound models in ob/ob, db/db, or diet-induced obesity mice have not been widely published to date, there have been studies in both mice and rats investigating the effects of obesity on cutaneous wound repair[44-47]. These data have shown significant changes in inflammatory cell infiltrate, tissue organization, and gene expression in cutaneous skin wounds[44-47]. While these studies give insight on the wound healing process in obesity, one limitation is the lack of splinting in excisional wounds. Without splinting, there is reduced mechanical tension on wounds, which reduces granulation tissue in the wound similar to what is seen in human wounds[35-37]. In an analysis between genetic and diet-induced obesity, researchers found that genetic murine models displayed wound healing capacity similar to that of diabetes mellitus in humans with reduced tissue responses in diet-induced mice with reduced serum levels of TGF-β and elevated TNF-α[47]. These results suggest that diet-induced obesity models may be better suited to study the effects of obesity on wound healing.

FUTURE DIRECTIONS

The wound healing process in healthy patients is well documented and is conserved between both humans and animal models used to study wound healing[12-14,17,48,49]. The effects of diabetes mellitus on wound healing have been well documented in both human and animal studies. Despite the growing body of literature surrounding wound healing, there is a gap in the literature investigating the effects of obesity on wound healing and how best to augment it in this population. Understanding the wound healing process in obesity is imperative as care requires knowledge of the physiologic demands of the body[7-9].

While there are a number of models used to study wound healing, these powerful tools have not yet been applied to study wound healing in the context of obesity. Studies using either the WIHN, excisional wound, or hypertrophic wound models should be applied to existing animal models of obesity to deepen our knowledge of the effects of obesity on wound healing. Obesity induces a chronic low-grade inflammatory response with increased production of pro-inflammatory adipokines, cytokines, and chemokines that contribute to poor wound healing phenomena seen in this population [8,11,21,44,47]. Much is known about these important proteins in the context of both obesity and normal wound healing. With an increasing number of studies assessing alterations in the both inflammatory responses and wound healing in obese mice and patients, it is imperative to continue these investigations. Future experimentation must center on altering levels of these proteins to determine if it is possible to augment wound healing outcomes in obese and overweight populations.

CONCLUSION

Approximately one third of the global population is classified as obese or overweight. With millions of patients sustaining cutaneous wounds annually, it is imperative to investigate the impact of obesity on wound healing and how to augment cutaneous wound healing in this growing population. Dysregulation of inflammatory responses due to production of pro-inflammatory mediators at baseline may contribute to poor wound healing outcomes.

ACKNOWLEDGEMENTS

The authors thank the Hagey Laboratory for Pediatric Regenerative Medicine for its continued support of our research.

FOOTNOTES

Author contributions: Cotterell A and Griffin M conceptualized and designed the research; Cotterell A, Griffin M, Downer MA, and Parker JB conducted the investigation and completed the writing of the original draft; Griffin M, Downer MA, Parker JB, Wan D, and Longaker MT reviewed and edited the manuscript; all authors reviewed the final draft.

Conflict-of-interest statement: There is no conflict of interest associated with any of the senior author or other coauthors contributed their efforts in this manuscript.

Country/Territory of origin: United States

ORCID number: Michelle Griffin 0000-0002-2027-547X.

S-Editor: Qu XL
L-Editor: A
P-Editor: Zhao YQ

REFERENCES

1 **Chooi YC**, Ding C, Magkos F. The epidemiology of obesity. *Metabolism* 2019; **92**: 6-10 [PMID: 30253139 DOI: 10.1016/j.metabol.2018.09.005]
2 **Ogden CL**, Yanovski SZ, Carroll MD, Flegal KM. The epidemiology of obesity. *Gastroenterology* 2007; **132**: 2087-2102 [PMID: 17498505 DOI: 10.1053/j.gastro.2007.03.052]
3 **Kopelman PG**. Obesity as a medical problem. *Nature* 2000; **404**: 635-643 [PMID: 10766250 DOI: 10.1038/35007508]
4 **Pi-Sunyer X**. The medical risks of obesity. *Postgrad Med* 2009; **121**: 21-33 [PMID: 19940414 DOI: 10.3810/pgm.2009.11.2074]
5 **Greenhalgh DG**. Wound healing and diabetes mellitus. *Clin Plast Surg* 2003; **30**: 37-45 [PMID: 12636214 DOI: 10.1016/s0094-1298(02)00066-4]
6 **Brem H**, Tomic-Canic M. Cellular and molecular basis of wound healing in diabetes. *J Clin Invest* 2007; **117**: 1219-1222 [PMID: 17476353 DOI: 10.1172/jci32169]
7 **Wilson JA**, Clark JJ. Obesity: impediment to wound healing. *Crit Care Nurs Q* 2003; **26**: 119-132 [PMID: 12744592 DOI: 10.1097/00002727-200304000-00006]
8 **Groszek DM**. Promoting wound healing in the obese patient. *AORN J* 1982; **35**: 1132-1138 [PMID: 6179475 DOI: 10.1016/s0001-2092(07)62477-6]
9 **Pierpont YN**, Dinh TP, Salas RE, Johnson EL, Wright TG, Robson MC, Payne WG. Obesity and surgical wound healing: a current review. *ISRN Obes* 2014; **2014**: 638936 [PMID: 24701367 DOI: 10.1155/2014/638936]
10 **Kalupahana NS**, Moustaid-Moussa N, Claycombe KJ. Immunity as a link between obesity and insulin resistance. *Mol Aspects Med* 2012; **33**: 26-34 [PMID: 22040698 DOI: 10.1016/j.mam.2011.10.011]
11 **Dallman MF**, Pecoraro NC, La Fleur SE, Warne JP, Ginsberg AB, Akana SF, Laugero KC, Houshyar H, Strack AM, Bhatnagar S, Bell ME. Glucocorticoids, chronic stress, and obesity. *Prog Brain Res* 2006; **153**: 75-105 [PMID: 16876569 DOI: 10.1016/s0079-6123(06)53004-3]
12 **Gurtner GC**, Werner S, Barrandon Y, Longaker MT. Wound repair and regeneration. *Nature* 2008; **453**: 314-321 [PMID: 18480812 DOI: 10.1038/nature07039]
13 **Broughton G 2nd**, Janis JE, Attinger CE. The basic science of wound healing. *Plast Reconstr Surg* 2006; **117**: 12S-34S [PMID: 16799372 DOI: 10.1097/01.prs.0000225430.42531.c2]
14 **Eming SA**, Martin P, Tomic-Canic M. Wound repair and regeneration: mechanisms, signaling, and translation. *Sci Transl Med* 2014; **6**: 265sr6 [PMID: 25473038 DOI: 10.1126/scitranslmed.3009337]
15 **Landén NX**, Li D, Ståhle M. Transition from inflammation to proliferation: a critical step during wound healing. *Cell Mol Life Sci* 2016; **73**: 3861-3885 [PMID: 27180275 DOI: 10.1007/s00018-016-2268-0]

16 **Guo S**, Dipietro LA. Factors affecting wound healing. *J Dent Res* 2010; **89**: 219-229 [PMID: 20139336 DOI: 10.1177/0022034509359125]

17 **Zangooei MH**, Jalili S. Protein fold recognition with a two-layer method based on SVM-SA, WP-NN and C4.5 (TLM-SNC). *Int J Data Min Bioinform* 2013; **8**: 203-223 [PMID: 24010268 DOI: 10.1504/ijdmb.2013.055507]

18 **Lin ZQ**, Kondo T, Ishida Y, Takayasu T, Mukaida N. Essential involvement of IL-6 in the skin wound-healing process as evidenced by delayed wound healing in IL-6-deficient mice. *J Leukoc Biol* 2003; **73**: 713-721 [PMID: 12773503 DOI: 10.1189/jlb.0802397]

19 **Fasshauer M**, Blüher M. Adipokines in health and disease. *Trends Pharmacol Sci* 2015; **36**: 461-470 [PMID: 26022934 DOI: 10.1016/j.tips.2015.04.014]

20 **Oral EA**, Simha V, Ruiz E, Andewelt A, Premkumar A, Snell P, Wagner AJ, DePaoli AM, Reitman ML, Taylor SI, Gorden P, Garg A. Leptin-replacement therapy for lipodystrophy. *N Engl J Med* 2002; **346**: 570-578 [PMID: 11856796 DOI: 10.1056/nejmoa012437]

21 **Ouchi N**, Parker JL, Lugus JJ, Walsh K. Adipokines in inflammation and metabolic disease. *Nat Rev Immunol* 2011; **11**: 85-97 [PMID: 21252989 DOI: 10.1038/nri2921]

22 **Santos-Alvarez J**, Goberna R, Sánchez-Margalet V. Human leptin stimulates proliferation and activation of human circulating monocytes. *Cell Immunol* 1999; **194**: 6-11 [PMID: 10357875 DOI: 10.1006/cimm.1999.1490]

23 **Qi Y**, Nie Z, Lee YS, Singhal NS, Scherer PE, Lazar MA, Ahima RS. Loss of resistin improves glucose homeostasis in leptin deficiency. *Diabetes* 2006; **55**: 3083-3090 [PMID: 17065346 DOI: 10.2337/db05-0615]

24 **Wang T**, He C. Pro-inflammatory cytokines: The link between obesity and osteoarthritis. *Cytokine Growth Factor Rev* 2018; **44**: 38-50 [PMID: 30340925 DOI: 10.1016/j.cytogfr.2018.10.002]

25 **Vendrell J**, Broch M, Vilarrasa N, Molina A, Gómez JM, Gutiérrez C, Simón I, Soler J, Richart C. Resistin, adiponectin, ghrelin, leptin, and proinflammatory cytokines: relationships in obesity. *Obes Res* 2004; **12**: 962-971 [PMID: 15229336 DOI: 10.1038/oby.2004.118]

26 **Meyer M**, McGrouther DA. A study relating wound tension to scar morphology in the pre-sternal scar using Langers technique. *Br J Plast Surg* 1991; **44**: 291-294 [PMID: 2059787 DOI: 10.1016/0007-1226(91)90074-t]

27 **Fleischmann E**, Kurz A, Niedermayr M, Schebesta K, Kimberger O, Sessler DI, Kabon B, Prager G. Tissue oxygenation in obese and non-obese patients during laparoscopy. *Obes Surg* 2005; **15**: 813-819 [PMID: 15978153 DOI: 10.1381/0960892054222867]

28 **Kloeters O**, Tandara A, Mustoe TA. Hypertrophic scar model in the rabbit ear: a reproducible model for studying scar tissue behavior with new observations on silicone gel sheeting for scar reduction. *Wound Repair Regen* 2007; **15** Suppl 1: S40-S45 [PMID: 17727466 DOI: 10.1111/j.1524-475X.2007.00224.x]

29 **Li J**, Wang J, Wang Z, Xia Y, Zhou M, Zhong A, Sun J. Experimental models for cutaneous hypertrophic scar research. *Wound Repair Regen* 2020; **28**: 126-144 [PMID: 31509318 DOI: 10.1111/wrr.12760]

30 **Gauglitz GG**, Korting HC, Pavicic T, Ruzicka T, Jeschke MG. Hypertrophic scarring and keloids: pathomechanisms and current and emerging treatment strategies. *Mol Med* 2011; **17**: 113-125 [PMID: 20927486 DOI: 10.2119/molmed.2009.00153]

31 **Aarabi S**, Bhatt KA, Shi Y, Paterno J, Chang EI, Loh SA, Holmes JW, Longaker MT, Yee H, Gurtner GC. Mechanical load initiates hypertrophic scar formation through decreased cellular apoptosis. *FASEB J* 2007; **21**: 3250-3261 [PMID: 17504973 DOI: 10.1096/fj.07-8218com]

32 **Harn HI**, Chiu PY, Lin CH, Chen HY, Lai YC, Yang FS, Wu CC, Tang MJ, Chuong CM, Hughes MW. Topological Distribution of Wound Stiffness Modulates Wound-Induced Hair Follicle Neogenesis. *Pharmaceutics* 2022; **14** [PMID: 36145674 DOI: 10.3390/pharmaceutics14091926]

33 **Xue Y**, Lim CH, Plikus MV, Ito M, Cotsarelis G, Garza LA. Wound-Induced Hair Neogenesis Model. *J Invest Dermatol* 2022; **142**: 2565-2569 [PMID: 36153062 DOI: 10.1016/j.jid.2022.07.013]

34 **Harn HI**, Wang SP, Lai YC, Van Handel B, Liang YC, Tsai S, Schiessl IM, Sarkar A, Xi H, Hughes M, Kaemmer S, Tang MJ, Peti-Peterdi J, Pyle AD, Woolley TE, Evseenko D, Jiang TX, Chuong CM. Symmetry breaking of tissue mechanics in wound induced hair follicle regeneration of laboratory and spiny mice. *Nat Commun* 2021; **12**: 2595 [PMID: 33972536 DOI: 10.1038/s41467-021-22822-9]

35 **Wong VW**, Sorkin M, Glotzbach JP, Longaker MT, Gurtner GC. Surgical approaches to create murine models of human wound healing. *J Biomed Biotechnol* 2011; **2011**: 969618 [PMID: 21151647 DOI: 10.1155/2011/969618]

36 **Lintel H**, Abbas DB, Lavin CV, Griffin M, Guo JL, Guardino N, Churukian A, Gurtner GC, Momeni A, Longaker MT, Wan DC. Transdermal deferoxamine administration improves excisional wound healing in chronically irradiated murine skin. *J Transl Med* 2022; **20**: 274 [PMID: 35715816 DOI: 10.1186/s12967-022-03479-4]

37 **Mascharak S**, desJardins-Park HE, Davitt MF, Griffin M, Borrelli MR, Moore AL, Chen K, Duoto B, Chinta M, Foster DS, Shen AH, Januszyk M, Kwon SH, Wernig G, Wan DC, Lorenz HP, Gurtner GC, Longaker MT. Preventing Engrailed-1 activation in fibroblasts yields wound regeneration without scarring. *Science* 2021; **372** [PMID: 33888614 DOI: 10.1126/science.aba2374]

38 **Hariri N**, Thibault L. High-fat diet-induced obesity in animal models. *Nutr Res Rev* 2010; **23**: 270-299 [PMID: 20977819 DOI: 10.1017/S0954422410000168]

39 **Takahashi M**, Ikemoto S, Ezaki O. Effect of the fat/carbohydrate ratio in the diet on obesity and oral glucose tolerance in C57BL/6J mice. *J Nutr Sci Vitaminol (Tokyo)* 1999; **45**: 583-593 [PMID: 10683810 DOI: 10.3177/jnsv.45.583]

40 **Bourgeois F**, Alexiu A, Lemonnier D. Dietary-induced obesity: effect of dietary fats on adipose tissue cellularity in mice. *Br J Nutr* 1983; **49**: 17-26 [PMID: 6821685 DOI: 10.1079/bjn19830006]

41 **Lin S**, Thomas TC, Storlien LH, Huang XF. Development of high fat diet-induced obesity and leptin resistance in C57Bl/6J mice. *Int J Obes Relat Metab Disord* 2000; **24**: 639-646 [PMID: 10849588 DOI: 10.1038/sj.ijo.0801209]

42 **Coleman DL**. Obese and diabetes: two mutant genes causing diabetes-obesity syndromes in mice. *Diabetologia* 1978; **14**: 141-148 [PMID: 350680 DOI: 10.1007/BF00429772]

43 **Suriano F**, Vieira-Silva S, Falony G, Roumain M, Paquot A, Pelicaen R, Régnier M, Delzenne NM, Raes J, Muccioli GG, Van Hul M, Cani PD. Novel insights into the genetically obese (ob/ob) and diabetic (db/db) mice: two sides of the same coin. *Microbiome* 2021; **9**: 147 [PMID: 34183063 DOI: 10.1186/s40168-021-01097-8]

44 **Min KK**, Neupane S, Adhikari N, Sohn WJ, An SY, Kim JY, An CH, Lee Y, Kim YG, Park JW, Lee JM, Suh JY. Effects of resveratrol on bone-healing capacity in the mouse tooth extraction socket. *J Periodontal Res* 2020; **55**: 247-257 [PMID: 31797379 DOI: 10.1111/jre.12710]

45 **Slavkovsky R**, Kohlerova R, Tkacova V, Jiroutova A, Tahmazoglu B, Velebny V, Rezačová M, Sobotka L, Kanta J. Zucker diabetic fatty rat: a new model of impaired cutaneous wound repair with type II diabetes mellitus and obesity. *Wound Repair Regen* 2011; **19**: 515-525 [PMID: 21649785 DOI: 10.1111/j.1524-475X.2011.00703.x]

46 **Nascimento AP**, Costa AM. Overweight induced by high-fat diet delays rat cutaneous wound healing. *Br J Nutr* 2006; **96**: 1069-1077 [PMID:

17181882 DOI: 10.1017/bjn20061955]

47 **Seitz O**, Schürmann C, Hermes N, Müller E, Pfeilschifter J, Frank S, Goren I. Wound healing in mice with high-fat diet- or ob gene-induced diabetes-obesity syndromes: a comparative study. *Exp Diabetes Res* 2010; **2010**: 476969 [PMID: 21318183 DOI: 10.1155/2010/476969]

48 **Talbott HE**, Mascharak S, Griffin M, Wan DC, Longaker MT. Wound healing, fibroblast heterogeneity, and fibrosis. *Cell Stem Cell* 2022; **29**: 1161-1180 [PMID: 35931028 DOI: 10.1016/j.stem.2022.07.006]

49 **Diegelmann RF**, Evans MC. Wound healing: an overview of acute, fibrotic and delayed healing. *Front Biosci* 2004; **9**: 283-289 [PMID: 14766366 DOI: 10.2741/1184]

World Journal of Experimental Medicine

Submit a Manuscript: https://www.f6publishing.com

World J Exp Med 2024 March 20; 14(1): 87202

DOI: 10.5493/wjem.v14.i1.87202

ISSN 2220-315x (online)

MINIREVIEWS

Emerging significance of butyrylcholinesterase

Gumpeny R Sridhar, Lakshmi Gumpeny

Specialty type: Medicine, research and experimental

Provenance and peer review: Invited article; Externally peer reviewed.

Peer-review model: Single blind

Peer-review report's scientific quality classification

Grade A (Excellent): 0
Grade B (Very good): B, B
Grade C (Good): 0
Grade D (Fair): D
Grade E (Poor): 0

P-Reviewer: Emran TB, Bangladesh; Teixeira KN, Brazil

Received: July 28, 2023
Peer-review started: July 28, 2023
First decision: September 5, 2023
Revised: October 4, 2023
Accepted: January 5, 2024
Article in press: January 5, 2024
Published online: March 20, 2024

Gumpeny R Sridhar, Department of Endocrinology and Diabetes, Endocrine and Diabetes Centre, Visakhapatnam 530002, Andhra Pradesh, India

Lakshmi Gumpeny, Department of Internal Medicine, Gayatri Vidya Parishad Institute of Healthcare and Medical Technology, Visakhapatnam 530048, Andhra Pradesh, India

Corresponding author: Gumpeny R Sridhar, FRCP, Adjunct Professor, Department of Endocrinology and Diabetes, Endocrine and Diabetes Centre, 15-12-15 Krishnanagar, Visakhapatnam 530002, Andhra Pradesh, India. sridharvizag@gmail.com

Abstract

Butyrylcholinesterase (BChE; EC 3.1.1.8), an enzyme structurally related to acetylcholinesterase, is widely distributed in the human body. It plays a role in the detoxification of chemicals such as succinylcholine, a muscle relaxant used in anesthetic practice. BChE is well-known due to variant forms of the enzyme with little or no hydrolytic activity which exist in some endogamous communities and result in prolonged apnea following the administration of succinylcholine. Its other functions include the ability to hydrolyze acetylcholine, the cholinergic neurotransmitter in the brain, when its primary hydrolytic enzyme, acetylcholinesterase, is absent. To assess its potential roles, BChE was studied in relation to insulin resistance, type 2 diabetes mellitus, cognition, hepatic disorders, cardiovascular and cerebrovascular diseases, and inflammatory conditions. Individuals who lack the enzyme activity of BChE are otherwise healthy, until they are given drugs hydrolyzed by this enzyme. Therefore, BChE is a candidate for the study of loss-of-function mutations in humans. Studying individuals with variant forms of BChE can provide insights into whether they are protected against metabolic diseases. The potential utility of the enzyme as a biomarker for Alzheimer's disease and the response to its drug treatment can also be assessed.

Key Words: Esterase; Acetylcholinesterase; Variant; Cholinergic; Metabolic syndrome; Cognition; Knockout model

Core Tip: Butyrylcholinesterase (BChE), a hepatic enzyme, hydrolyzes the muscle relaxant succinylcholine. Individuals with variant forms of the enzyme are healthy until they are administered succinylcholine during anesthesia. The enzyme may have regulatory roles in lipid metabolism, cholinergic response, and Alzheimer's disease. People with variant forms of the enzyme are natural human knockout models and can be followed up to study the metabolic impact of harboring variant forms of BChE.

Citation: Sridhar GR, Gumpeny L. Emerging significance of butyrylcholinesterase. *World J Exp Med* 2024; 14(1): 87202
URL: https://www.wjgnet.com/2220-315x/full/v14/i1/87202.htm
DOI: https://dx.doi.org/10.5493/wjem.v14.i1.87202

INTRODUCTION

Butyrylcholinesterase (BChE), belonging to the esterase group of enzymes, is a part of the serine hydrolase superfamily[1,2]. Esterases hydrolyze compounds that contain ester, amide, and thioester bonds[1]. BChE (EC 3.1.1.8) and acetylcholinesterase (AChE, EC 3.1.1.7) share a similar three-dimensional structure[3]. BChE is believed to have resulted from a duplication of an ancestral *AChE* gene[4]. AChE is responsible for the hydrolysis of acetylcholine at the neuromuscular junction. The roles of BChE are less well-defined: It hydrolyzes succinylcholine and bambuterol, which are used as muscle relaxants in anesthesiology[1].

EVOLUTIONARY ASPECTS AND CHEMISTRY

The *BChE* gene (HGNC: 983; MIM: 177100) exists across life forms[5] including invertebrates[6]. The concentrations of BChE exceed those of AChE in most tissues except the brain and muscle[3]. In the AChE knockout mouse model, BChE can compensate for the lack of AChE[7,8]. A convergent evolutionary mechanism is believed to have occurred between AChE and BChE[6].

BChE, which is mapped on chromosome 3 (3q26), exists in four molecular forms in plasma. The tetrameric form comprises nearly 90% of total plasma cholinesterase activity[2]. In a monomer, it consists of a common α/β hydrolase fold, flanked by α helices. The active site gorge volume of BChE is larger than that of AChE[9] and is shaped like a bowl [2]. AChE, though, has nearly 40% more aromatic residues. The active gorge consists of an acylation site for catalysis and pockets for choline-binding. It is rimmed by a peripheral anionic site. The catalytic activity of BChE depends on H-bond stabilization. In simulation studies, inhibitors were shown to reach the catalytic cavity due to the flexible entrance of the gorge[10].

TISSUE DISTRIBUTION

BChE is found in the lungs, plasma, brain, and heart. The highest levels of *BChE* mRNA are found in the liver, followed by the lung and the brain[4], where it is present at neuromuscular junctions. BChE is also expressed in brain astrocytes. The close association of neurons and glia has been termed the 'tripartite synapse', whereby glia exchange information with neurons[11].

BIOLOGICAL ROLES OF BUTYRYLCHOLINESTERASE

The role of BuChE in anaesthetic practice is well-recognized as a degrading enzyme of neuromuscular blockers succinylcholine and mivarurium[12]. Mutant forms of the enzyme have low or absent activity, resulting in prolonged apnea with the use of these muscle relaxants.

BChE levels are low in systemic conditions like liver disease, renal disease, malnutrition, malignancies, and burns[13].

It participates in the first-phase detoxification reaction against natural and exogenous toxins[14] (Table 1).

In the brain, BChE is present in the glial cells near the hippocampus and amygdala[15]. It may interact with ghrelin in the brain; in mice, increased expression of BChE is associated with low blood levels of ghrelin and reduced aggressive behavior[16].

ASSOCIATION OF BUTYRYLCHOLINESTERASE AND ENVIRONMENTAL TOXINS

BChE activity is principally found in 'tissues of first contact', such as the lungs, liver, skin, and blood. It plays a role in the activation of pro-drugs as well as in metabolizing drugs to inactive forms[17]. The biotransformation ability changes due

Table 1 Potential roles of butyrylcholinesterase

Known functions	Metabolism of drugs and toxins (*e.g.*, succinylcholine, carbamates, glucoalkaloids)	
	Affected by dietary fats	
	Influences the expression of metabolic syndrome, *via* action on lipids	
Associations and predictors of outcomes in disease states	Nutritional status	
	Hepatic disorders	
	Cardiovascular disease	Acute coronary syndrome
		Acute myocardial infarction
	Injuries to brain and cerebrovascular and disease	Ischemic brain stroke
		Traumatic brain injury
	Alzheimer's disease	Predisposition
		Onset
		Response to anticholinesterase medications
	Pre-eclampsia	
	Inflammatory and infections	Sepsis
		HIV infection
		Hansen's disease
	Other conditions	Wilsons disease
		Chronic obstructive pulmonary disease

HIV: Human immunodeficiency virus.

to alterations in the macromolecular structure of the enzyme[17].

Other potential toxins that are inactivated by BChE include carbamates and plants containing glucoalkaloids[18,19].

To derive reference ranges of AChE and BChE, their levels were measured in 387 young and healthy individuals (201 men and 186 women aged between 18 and 45 years)[18], which is useful for comparison in pathological states[20].

Gene polymorphisms of *BChE* were studied in relation to groundwater fluoride toxicity[21]. In clinically healthy adults from Pakistan, fluorosis was associated with elevated BChE activity[21].

BUTYRYLCHOLINESTERASE, METABOLIC SYNDROME, AND DIABETES MELLITUS

BChE activity in rats was influenced by dietary fat[22], perhaps due to increased release from hepatocytes[23]. Among subjects with type 2 diabetes from southern India, the plasma levels of BChE were inversely related to serum cholesterol ($P < 0.05$)[24]. The enzyme may not directly cause metabolic syndrome but may serve as a marker for this condition[25].

Similar associations were reported between BChE activity and weight in children[26]. Plasma BChE was proposed as a marker of chronic low-grade inflammation[27]. In Japanese subjects (171 with type 2 diabetes and 88 controls), serum BChE correlated with adiposity, serum lipids, and HOMA-R[28]. To assess the risk of mortality with the levels of BChE, 813 subjects were followed up from 1985-1987 to 1996. Those in the lowest quintile of BChE activity had higher mortality [29]. Body mass index mediates changes in BChE activity in healthy young men and women (age: 18-25 years)[30].

There are other interesting observations. Extracts from the fruit melanocarpa affected BChE activity[31]. Elevated BChE levels predicted the development of type 2 diabetes[32] and its vascular complication[33]. Increased levels of BChE may be associated with lower AChE levels, which play an anti-inflammatory role[34]. Exposure to BChE protects cultured pancreatic cells by reduced formation of toxic amylin oligomer[35].

BUTYRYLCHOLINESTERASE AND COGNITION

Alzheimer's disease (AD) that often accompanies aging is the most common cause of cognitive decline[36]. According to the cholinergic hypothesis, degeneration of cholinergic neurons in the basal forebrain results in cognitive dysfunction in

AD[37]. Other conditions that occur *via* the cholinergic system include amyloid deposition, tau phosphorylation, neuroinflammation, and vascular damage (Pozzi *et al*[38], 2022). Acetylcholine, the neurochemical transmitter in the cholinergic synapses, is inactivated by AChE, and to a lesser extent by BuChE. The cholinergic system is part of the cholinergic anti-inflammatory pathway. The cholinergic hypothesis received additional support by the finding that cholinesterase inhibitor drugs which increase acetylcholinesterase at the synaptic cleft are effective in the management of AD[39].

Apart from its role in the cholinergic hypothesis, BuChE has been implicated in the deposition of amyloid. Amyloid hypothesis proposes that abnormal folding of β-amyloid protein may contribute to the pathogenesis of AD[40]. A variant form of the enzyme, called K-variant (Ala567Thr (A539T), may act synergistically with others such as the ε4 allele of apolipoprotein E and iron as a risk factor for AD[41,42].

BUTYRYLCHOLINESTERASE IN RELATION TO OTHER CONDITIONS

Liver disorders and malnutrition

BChE measurement is sometimes included in the panel of liver function tests due to its hepatic origin. It is an indicator of acute hepatitis or cirrhosis of the liver[14].

BChE levels are altered by inflammatory processes: They are low in acute inflammation and normalize once inflammation resolves[43]. BChE levels were low in malnourished children and in subjects with visceral undernutrition[44,45]. It can be used as a marker of nutritional status among the elderly[46].

Coronary artery disease

Acute coronary syndrome encompasses a range of conditions from angina pectoris to irreversible damage of the myocardium. BChE levels could differentiate healthy subjects from those with acute myocardial infarction (AMI). BChE activity was lower in acute myocardial infarction (AMI) (n = 85) compared with controls (n = 45) (P < 0.001)[47,48]. Similar observations were reported by Sulzgruber *et al*[49] in 2015. Higher BChE levels were associated with greater mortality-free survival in acute coronary syndrome. The strongest effect was observed among people aged 45-65 years. Similar findings of mortality were reported in subjects undergoing veno-arterial extracorporeal membrane oxygenation treatment after cardiac surgery[50].

Disorders of the brain

In ischemic brain stroke, BChE levels were measured in 33 subjects with acute ischemic stroke within 12 h of onset and in 29 controls. Stroke subjects had lower BChE activity compared to controls[51].

Among 188 patients with traumatic brain injury within 72 h of injury, non-survivors (n = 42; 22.3%) had lower levels of BChE activity[52]; they had an acute decrease of enzyme activity.

Pre-eclampsia

Pre-eclampsia, which occurs in pregnancy, is characterized by hypertension, proteinuria, and other maternal-related dysfunctions. BChE levels were measured in 198 unrelated women having pre-eclampsia and 101 unrelated women with normal pregnancy. Pre-eclampsia was associated with lower BChE activity[53].

Sepsis

Sepsis, presenting with acute organ dysfunction, is a common cause of mortality in the intensive care setting. To identify the severity of sepsis, BChE levels were used as a biomarker. Those who died within 90 d of admission had lower levels of BChE. Admission levels of the enzyme could predict those who survived 90 d[54]. Measurement of BChE could complement other ways of predicting the outcome of patients admitted in intensive care units. Using a newer definition of sepsis, 'life-threatening organ dysfunction due to a dysregulated host response to infection', Peng *et al*[55] showed that lower levels of BChE activity are an independent risk factor for the 30-d death rate in sepsis-3 patients.

Infections

The 6-mo outcome of subjects receiving highly active antiretroviral therapy for HIV infection was assessed in relation to the levels of BChE. Low levels of BChE were seen in 25.5% (129/505) of subjects with infection. In the first year, 16.6% of patients died (n = 84). Low BChE levels were associated with a survival of (64.5 +/- 4.5)% at one year compared to (87.6 +/- 1.8)% in those with normal levels[56].

In Hansen's disease, genotyping of an atypical BChE allele (70G; rs1799807) and five additional single nucleotide polymorphisms (SNPs) reported higher allele (70G) and genotypic (70DG) frequencies in rs1799807. Atypical variants of the enzyme could predispose to infection[57], by interfering with the inflammatory response against the infective agent. Similarly, children with foot and mouth disease caused by enterovirus 71 infection had increased BChE levels[58].

Fertility

BChE was measured in idiopathic unexplained infertility, a day before and a day after intrauterine insemination. A positive correlation between BChE levels and total antioxidant activity on the day before the procedure was observed[59].

Other conditions

BChE was measured in untreated Wilson's disease and in chronic obstructive pulmonary disease. Pilot studies showed that along with ceruloplasmin, BChE could be used as a biomarker in Wilson's disease[60]. In chronic obstructive pulmonary disease (n = 153), BChE levels were elevated[61].

Studies in animals

Dogs with hypercortisolism had elevated serum BChE activity, related either to a direct effect of glucocorticoids or to changes in lipid metabolism associated with hypercortisolism[62]. Elevated salivary levels of BChE were reported in dogs with parvovirus infections[63].

The underlying pathogenic mechanism in all these disparate conditions appears to involve dysregulation of the inflammatory response leading to adverse outcome.

Cholinergic control of inflammation

Inflammation is part of a physiological response that is protective against noxious environmental factors. In a recent review, Medzhitov[64] proposed that inflammation ensures that homeostasis is maintained, and tissues retain their functional and structural integrity. It is regulated by the immune system, hormones, and neural signals.

The vagus nerve conveys information from the brain to attenuate the inflammatory process. It integrates signals from the hypothalamic-pituitary-adrenal axis and through the cholinergic anti-inflammatory pathway[65]. Bonaz *et al*[66] proposed that the anti-inflammatory properties of the vagus nerve may suggest the therapeutic implications of stimulating the nerve.

BChE may also influence the outcomes of coronavirus disease 2019 (COVID-19) *via* its effect on chronic low-grade inflammation. It could also serve as a biomarker for COVID-19 outcome; subjects with COVID-19 may be studied in subjects with variant forms of BChE[34,64].

BChE activity was predictive of 28-d mortality in critically ill COVID-19 patients[67]. A recent report indicates higher mortality in subjects with low or declining levels of serum BChE during hospitalization[68].

KNOCKOUT ANIMAL MODELS TO ELUCIDATE FUNCTION OF GENES

In functional genomics, gene knockout animal models are used to determine the function of genes. When a specific gene is inactivated, the resultant phenotype can provide information about its function[69]. Humans with loss-of-function genes give better insights than animal models[70]. The differences may relate to the other gene regulators upstream or downstream as well as environmental factors[71].

MacArthur *et al*[72] reported that a healthy person has an average of 100 inactivated genes, of which 20 are homozygous. A whole-exome sequencing study among European populations (n = 1432) reported that of loss-of-function mutations, nearly 45% (n = 76) were newly identified[73]. Narasimhan *et al*[74] studied the effects of rare gene knockouts in adults born of consanguineous marriage. Exome sequencing data in 3222 adults of Pakistani origin domiciled in Britain were linked to their lifelong health records. They did not find any relationship between those with loss-of-function genes and their consultation for health issues or prescription medication use. The latter two were taken as surrogate markers for their state of health.

Loss-of-function mutations can result from: (1) Nonsense SNPs leading to a premature stop codon, producing a truncated protein sequence; (2) splicing can be affected by an SNP at a canonical splice site; (3) an insertion or deletion variant located in the gene coding region can disrupt the full-length transcript leading to frameshifts; and (4) loss-of-function mutations can arise from the loss of an initiation codon[75].

Individuals with loss-of-function mutations who are apparently healthy were referred to as 'experiments of nature'. Studying them could help in the search for new drug targets and in identifying or exploring whether such mutated genes could have beneficial effects[76].

The nascent field of studying natural human knockouts and the genotype-phenotype correlation can provide insights into population genetics and the evolution of genes[69,71].

Butyrylcholinesterase and its variants qualify as natural human knockouts: Other than prolonged apnea following exposure to succinylcholine, individuals with variant forms of BChE are apparently healthy[77].

SIGNIFICANCE OF STUDYING BUTYRYLCHOLINESTERASE VARIANTS

Unlike other gene knockout animal models, variants of BChE have a high prevalence in isolated ethnic groups: Mainly south Indian from the Vysya community, and certain Eskimos in western Alaska[34]. Li *et al*[78] developed an animal *BChE* gene knockout model to test drug toxicity. The model had a normal phenotype unless exposed to the drug. Altered cognitive functions were associated with normal nicotinic receptor function, though the muscarinic receptor function was altered in the knockout model. Preliminary studies on the effect of (R)-bambuterol, a specific and reversible inhibitor of BChE, suggested that it may be used in the treatment of early cognitive decline[79].

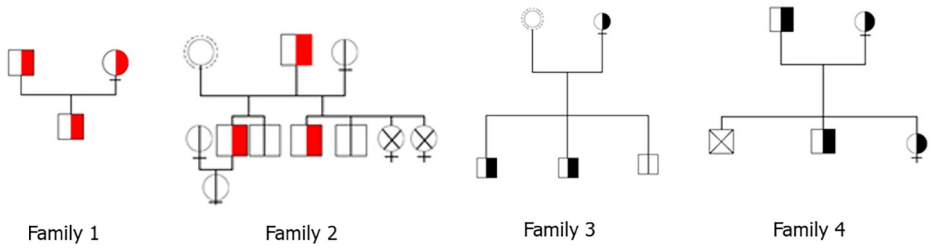

Figure 1 Phenotype of variant butyrylcholinesterase, families 1-4.

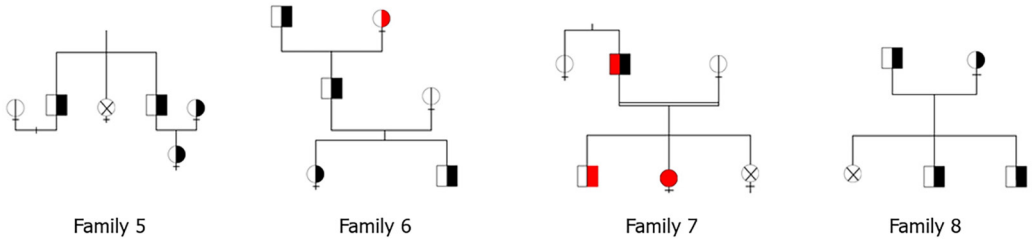

Figure 2 Phenotype of variant butyrylcholinesterase, families 5-8.

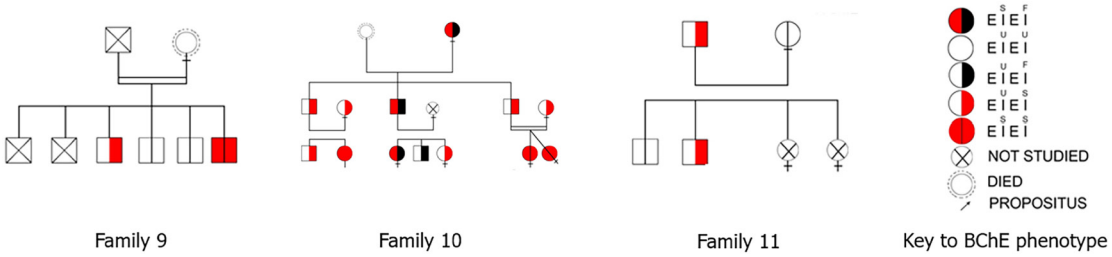

Figure 3 Phenotype of variant butyrylcholinesterase, families 9-11. BChE: Butyrylcholinesterase.

BUTYRYLCHOLINESTERASE VARIANTS IN HUMANS

Lockridge *et al* reviewed the naturally occurring genetic variants of BChE[80]. Thirty-four loss-of-function mutations were identified; all of them were tolerated, meaning that having a nonfunctional gene was compatible with life. Humans harboring silent *BChE* genes are healthy and fertile[77]. Lando *et al*[81] reported that among healthy blood donors (n = 2609), 59 had low plasma BChE activity.

In the Netherlands Organisation for Applied Research Prins Mauritis Laboratory and Centers for Disease Control and Prevention, the frequency of BChE mutations was 9 out of 121000 alleles. Some of the mutants resulted in a complete absence of enzyme activity[80].

The commonest missense mutation, the K-variant [Ala567Thr (AS39T)], is associated with a 30% lower BChE plasma activity compared to native BChE. It is due to an unknown mutation in a regulatory region[81]. Other variants are less common except in communities such as south Indian Vysyas or Eskimos, where genotyping is not possible. Estimating dibucaine and fluoride numbers could serve as a surrogate. Family studies in the south Indian state of Andhra Pradesh showed various phenotypic forms of BChE deficiency in inbred families (oral presentation at the 12th International Meeting on Cholinesterases-Sixth International Conference on Paraoxonases at Elche (Alicante, Spain) in 2015: GR Sridhar, G Nirmala, Premlata S, Satyanarayana M. Variant butyrylcholinesterase in South India (Figures 1-4).

BChE activity increases with the progression of AD and may eventually replace the function of AChE[82]. Individuals with the BChE-K variant could have deleterious outcomes when donepezil is given to patients with mild cognitive impairment. It can therefore serve as a pharmacogenetic marker in the choice of drugs for cognitive impairment[82].

The reasons why non-functional proteins persisted include: (1) The active enzyme can compensate for the absent enzyme; (2) it might have acquired new beneficial functions; and (3) the enzyme may be involved in a pathway regulated by other molecules or enzyme that can substitute for it.

As mentioned earlier, succinylcholine is hydrolyzed by BChE. Administration of succinylcholine to a homozymous knockout mouse model for BChE [$BChE^{-/-}$] resulted in rapid death; heterozygous model [$BChE^{+/-}$] had less severe manifestations and recovered within 30 min[78]. $AChE^{-/-}$ animals suffered greater toxicity to succinylcholine exposure than $BChE^{-/-}$ mice.

Table 2 Potential areas for studies in subjects with variant forms of butyrylcholinesterrase and therapeutic potential of the enzyme
Follow up of asymptomatic individuals for any protective or predictive role in cardiovascular disease and Alzheimer's disease
Production from transgenic sources as a pharmacologic agent
Potential drug target

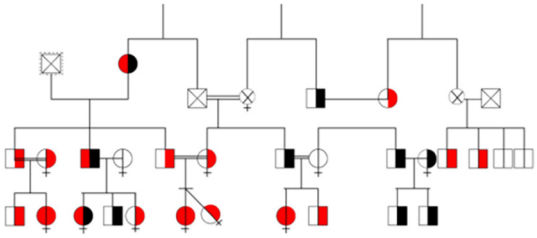

See key in figure 3

Figure 4 Consanguinity (=) in families 7, 8, 9, and 10.

BChE is a natural drug target in which drug side effects can be minimized by knocking out its gene[83]. Knowledge from knockout models could be used to assess the effects of drugs such as donepezil in cognitive impairment.

CONCLUSION

BChE serves a critical role in the hydrolysis of esters. Unlike AChE with which it shares structural and functional properties, BChE acts on a broader number of substrates, but has lower catalytic efficiency on acetylcholine[83]. Novel ligands and mutants of BChE were developed for use in the treatment of cocaine toxicity and neurological diseases[84]. Its roles extend into cardiovascular health; recent clinical studies suggest a correlation between increased plasma BChE activity and longevity in patients with severe cardiovascular disease[16].

BChE also serves as a prognostic marker for liver and non-liver diseases, protein-energy malnutrition, and obesity by reflecting the availability of amino acidic substrates[46]. It is also involved in neurodegenerative disorders, particularly AD. BChE not only co-regulates cholinergic transmission by hydrolyzing acetylcholine alongside AChE, but potentially interferes with the course of AD. Inhibitors of BChE are therefore used in the treatment of AD and other disorders of cognition by ameliorating cholinergic deficiency[85].

Recent findings show that BChE regulates substrates such as cocaine and ghrelin. Recombinant BChE mutants and viral gene therapy are being developed against cocaine addiction, and in exploring the role of BChE in obesity[86] (Table 2).

As a therapeutic agent, phase I trials showed the safety of pure BChE, thereby giving an option in preventing nerve agent toxicity. Gene therapy using vectors that allow long-term expression of BChE after a single injection is being explored[87].

Animal studies have illustrated that pretreatment with BChE can prevent adverse effects from lethal doses of nerve agents like soman, sarin, and VX[88]. Other technologies employed to synthesise BChE include glycosylation and PEGylation that can enhance its pharmacokinetics[86].

Not all loss-of-function gene variants manifest in the same way; they may range from being mildly deleterious to neutral and sometimes, even advantageous[89]: In populations where consanguinity and Mendelian disorders are common, population-wide rapid exome sequencing may be beneficial[90,91].

BChE's multi-faceted nature, as a pharmacological target and tool, deepens our understanding of biological pathways in health and disease. Further phenotype-genotype studies will throw light on its potential effects. In this context, subjects with variant forms of BChE serve as critical comparators in such studies.

FOOTNOTES

Author contributions: The two authors contributed equally to the writing of the manuscript.

Conflict-of-interest statement: Both authors declare that they have no conflict of interest to disclose.

Country/Territory of origin: India

ORCID number: Gumpeny R Sridhar 0000-0002-7446-1251; Lakshmi Gumpeny 0000-0002-1368-745X.

S-Editor: Liu JH
L-Editor: Wang TQ
P-Editor: Yu HG

REFERENCES

1 **Fukami T**, Yokoi T. The emerging role of human esterases. *Drug Metab Pharmacokinet* 2012; **27**: 466-477 [PMID: 22813719 DOI: 10.2133/dmpk.dmpk-12-rv-042]
2 **Masson P**, Carletti E, Nachon F. Structure, activities and biomedical applications of human butyrylcholinesterase. *Protein Pept Lett* 2009; **16**: 1215-1224 [PMID: 19508180 DOI: 10.2174/092986609789071207]
3 **Li B**, Stribley JA, Ticu A, Xie W, Schopfer LM, Hammond P, Brimijoin S, Hinrichs SH, Lockridge O. Abundant tissue butyrylcholinesterase and its possible function in the acetylcholinesterase knockout mouse. *J Neurochem* 2000; **75**: 1320-1331 [PMID: 10936216 DOI: 10.1046/j.1471-4159.2000.751320.x]
4 **Johnson G**, Moore SW. Why has butyrylcholinesterase been retained? Structural and functional diversification in a duplicated gene. *Neurochem Int* 2012; **61**: 783-797 [PMID: 22750491 DOI: 10.1016/j.neuint.2012.06.016]
5 **Sridhar GR**, Lakshmi PV, Rao AA. Phylogenetic tree construction of butyrylcholinesterase sequences in life forms. *J Assoc Physicians India* 2006; **54**: 122-123 [PMID: 16715615]
6 **Pezzementi L**, Nachon F, Chatonnet A. Evolution of acetylcholinesterase and butyrylcholinesterase in the vertebrates: an atypical butyrylcholinesterase from the Medaka Oryzias latipes. *PLoS One* 2011; **6**: e17396 [PMID: 21364766 DOI: 10.1371/journal.pone.0017396]
7 **Masson P**, Lockridge O. Butyrylcholinesterase for protection from organophosphorus poisons: catalytic complexities and hysteretic behavior. *Arch Biochem Biophys* 2010; **494**: 107-120 [PMID: 20004171 DOI: 10.1016/j.abb.2009.12.005]
8 **Mesulam MM**, Guillozet A, Shaw P, Levey A, Duysen EG, Lockridge O. Acetylcholinesterase knockouts establish central cholinergic pathways and can use butyrylcholinesterase to hydrolyze acetylcholine. *Neuroscience* 2002; **110**: 627-639 [PMID: 11934471 DOI: 10.1016/s0306-4522(01)00613-3]
9 **Masson P**, Lushchekina S, Schopfer LM, Lockridge O. Effects of viscosity and osmotic stress on the reaction of human butyrylcholinesterase with cresyl saligenin phosphate, a toxicant related to aerotoxic syndrome: kinetic and molecular dynamics studies. *Biochem J* 2013; **454**: 387-399 [PMID: 23782236 DOI: 10.1042/BJ20130389]
10 **De Boer D**, Nguyen N, Mao J, Moore J, Sorin EJ. A Comprehensive Review of Cholinesterase Modeling and Simulation. *Biomolecules* 2021; **11** [PMID: 33920972 DOI: 10.3390/biom11040580]
11 **Perea G**, Navarrete M, Araque A. Tripartite synapses: astrocytes process and control synaptic information. *Trends Neurosci* 2009; **32**: 421-431 [PMID: 19615761 DOI: 10.1016/j.tins.2009.05.001]
12 **Delacour H**, Dedome E, Courcelle S, Hary B, Ceppa F. Butyrylcholinesterase deficiency. *Ann Biol Clin (Paris)* 2016; **74**: 279-285 [PMID: 27237801 DOI: 10.1684/abc.2016.1141]
13 **Andersson ML**, Møller AM, Wildgaard K. Butyrylcholinesterase deficiency and its clinical importance in anaesthesia: a systematic review. *Anaesthesia* 2019; **74**: 518-528 [PMID: 30600548 DOI: 10.1111/anae.14545]
14 **Pohanka M**. Butyrylcholinesterase as a biochemical marker. *Bratisl Lek Listy* 2013; **114**: 726-734 [PMID: 24329513 DOI: 10.4149/bll_2013_153]
15 **Darvesh S**, Grantham DL, Hopkins DA. Distribution of butyrylcholinesterase in the human amygdala and hippocampal formation. *J Comp Neurol* 1998; **393**: 374-390 [PMID: 9548556]
16 **Brimijoin S**, Chen VP, Pang YP, Geng L, Gao Y. Physiological roles for butyrylcholinesterase: A BChE-ghrelin axis. *Chem Biol Interact* 2016; **259**: 271-275 [PMID: 26915976 DOI: 10.1016/j.cbi.2016.02.013]
17 **Sisková K**, Bilka F, Adameová A, Balazová A, Mydla M, Pauliková I. Influence of lipid imbalance on butyrylcholinesterase activity and biotransformation efficiency. *Pharmazie* 2012; **67**: 345-350 [PMID: 22570941]
18 **Nielsen SD**, Schmidt JM, Kristiansen GH, Dalsgaard TK, Larsen LB. Liquid Chromatography Mass Spectrometry Quantification of α-solanine, α-chaconine, and Solanidine in Potato Protein Isolates. *Foods* 2020; **9** [PMID: 32252270 DOI: 10.3390/foods9040416]
19 **McGehee DS**, Krasowski MD, Fung DL, Wilson B, Gronert GA, Moss J. Cholinesterase inhibition by potato glycoalkaloids slows mivacurium metabolism. *Anesthesiology* 2000; **93**: 510-519 [PMID: 10910502 DOI: 10.1097/00000542-200008000-00031]
20 **Karasova JZ**, Maderycova Z, Tumova M, Jun D, Rehacek V, Kuca K, Misik J. Activity of cholinesterases in a young and healthy middle-European population: Relevance for toxicology, pharmacology and clinical praxis. *Toxicol Lett* 2017; **277**: 24-31 [PMID: 28465191 DOI: 10.1016/j.toxlet.2017.04.017]
21 **Bibi S**, Habib R, Shafiq S, Abbas SS, Khan S, Eqani SAMAS, Nepovimova E, Khan MS, Kuca K, Nurulain SM. Influence of the chronic groundwater fluoride consumption on cholinergic enzymes, ACHE and BCHE gene SNPs and pro-inflammatory cytokines: A study with Pakistani population groups. *Sci Total Environ* 2023; **880**: 163359 [PMID: 37030382 DOI: 10.1016/j.scitotenv.2023.163359]
22 **Van Lith HA**, Haller M, Van Tintelen G, Van Zutphen LF, Beynen AC. Plasma esterase-1 (ES-1) activity in rats is influenced by the amount and type of dietary fat, and butyryl cholinesterase activity by the type of dietary fat. *J Nutr* 1992; **122**: 2109-2120 [PMID: 1432252 DOI: 10.1093/jn/122.11.2109]
23 **Van Lith HA**, Haller M, Van Tintelen G, Lemmens AG, Van Zutphen LF, Beynen AC. Fat intake and clofibrate administration have interrelated effects on liver cholesterol concentration and serum butyryl cholinesterase activity in rats. *J Nutr* 1992; **122**: 2283-2291 [PMID: 1432266 DOI: 10.1093/jn/122.11.2283]
24 **Sridhar GR**, Nirmala G, Apparao A, Madhavi AS, Sreelatha S, Rani JS, Vijayalakshmi P. Serum butyrylcholinesterase in type 2 diabetes

mellitus: a biochemical and bioinformatics approach. *Lipids Health Dis* 2005; **4**: 18 [PMID: 16150144 DOI: 10.1186/1476-511X-4-18]

25 **Han Y**, Ma Y, Liu Y, Zhao Z, Zhen S, Yang X, Xu Z, Wen D. Plasma cholinesterase is associated with Chinese adolescent overweight or obesity and metabolic syndrome prediction. *Diabetes Metab Syndr Obes* 2019; **12**: 685-702 [PMID: 31190929 DOI: 10.2147/DMSO.S201594]

26 **Rodríguez-Fuentes GA**, Arcega-Cabrera Fl, Fargher LF. Plasma and erythrocyte cholinesterase activities in children from Yucatan, Mexico: relationship with anthropometry and obesity. *Asian J Pharm Clin Res* 2015; **8**: 224-228 [DOI: 10.1016/j.scitotenv.2015.10.152]

27 **Rao AA**, Sridhar GR, Das UN. Elevated butyrylcholinesterase and acetylcholinesterase may predict the development of type 2 diabetes mellitus and Alzheimer's disease. *Med Hypotheses* 2007; **69**: 1272-1276 [PMID: 17553629 DOI: 10.1016/j.mehy.2007.03.032]

28 **Iwasaki T**, Yoneda M, Nakajima A, Terauchi Y. Serum butyrylcholinesterase is strongly associated with adiposity, the serum lipid profile and insulin resistance. *Intern Med* 2007; **46**: 1633-1639 [PMID: 17917325 DOI: 10.2169/internalmedicine.46.0049]

29 **Calderon-Margalit R**, Adler B, Abramson JH, Gofin J, Kark JD. Butyrylcholinesterase activity, cardiovascular risk factors, and mortality in middle-aged and elderly men and women in Jerusalem. *Clin Chem* 2006; **52**: 845-852 [PMID: 16527886 DOI: 10.1373/clinchem.2005.059857]

30 **Stojanov M**, Stefanović A, Džingalašević G, Mandić-Radić S, Prostran M. Butyrylcholinesterase activity in young men and women: association with cardiovascular risk factors. *Clin Biochem* 2011; **44**: 623-626 [PMID: 21402063 DOI: 10.1016/j.clinbiochem.2011.03.028]

31 **Duchnowicz P**, Ziobro A, Rapacka E, Koter-Michalak M, Bukowska B. Changes in Cholinesterase Activity in Blood of Adolescent with Metabolic Syndrome after Supplementation with Extract from Aronia melanocarpa. *Biomed Res Int* 2018; **2018**: 5670145 [PMID: 29780825 DOI: 10.1155/2018/5670145]

32 **Sato KK**, Hayashi T, Maeda I, Koh H, Harita N, Uehara S, Onishi Y, Oue K, Nakamura Y, Endo G, Kambe H, Fukuda K. Serum butyrylcholinesterase and the risk of future type 2 diabetes: the Kansai Healthcare Study. *Clin Endocrinol (Oxf)* 2014; **80**: 362-367 [PMID: 23418907 DOI: 10.1111/cen.12171]

33 **Yu R**, Ye X, Wang X, Wu Q, Jia L, Dong K, Zhu Z, Bao Y, Hou X, Jia W. Serum cholinesterase is associated with incident diabetic retinopathy: the Shanghai Nicheng cohort study. *Nutr Metab (Lond)* 2023; **20**: 26 [PMID: 37138337 DOI: 10.1186/s12986-023-00743-2]

34 **Sridhar GR**. Butyrylcholinesterase, variants and metabolic syndrome. *Adipobiology* 2018; **9**: 19-27 [DOI: 10.14748/adipo.v9.4984]

35 **Shenhar-Tsarfaty S**, Bruck T, Bennett ER, Bravman T, Aassayag EB, Waiskopf N, Rogowski O, Bornstein N, Berliner S, Soreq H. Butyrylcholinesterase interactions with amylin may protect pancreatic cells in metabolic syndrome. *J Cell Mol Med* 2011; **15**: 1747-1756 [PMID: 20807286 DOI: 10.1111/j.1582-4934.2010.01165.x]

36 **Sridhar GR**, Lakshmi G, Nagamani G. Emerging links between type 2 diabetes and Alzheimer's disease. *World J Diabetes* 2015; **6**: 744-751 [PMID: 26069723 DOI: 10.4239/wjd.v6.i5.744]

37 **Jasiecki J**, Wasąg B. Butyrylcholinesterase Protein Ends in the Pathogenesis of Alzheimer's Disease-Could BCHE Genotyping Be Helpful in Alzheimer's Therapy? *Biomolecules* 2019; **9** [PMID: 31601022 DOI: 10.3390/biom9100592]

38 **Pozzi FE**, Conti E, Appollonio I, Ferrarese C, Tremolizzo L. Predictors of response to acetylcholinesterase inhibitors in dementia: A systematic review. *Front Neurosci* 2022; **16**: 998224 [PMID: 36203811 DOI: 10.3389/fnins.2022.998224]

39 **Sridhar GR**. Acetylcholinesterase inhibitors (Galantamine, Rivastigmine, and Donepezil). In P. Riederer, G. Laux *et al* (eds.), NeuroPsychopharmacotherapy. *Springer Nature Switzerland AG* 20211 [DOI: 10.1007/978-3-319-56015-1_418-1]

40 **Reid GA**, Darvesh S. Butyrylcholinesterase-knockout reduces brain deposition of fibrillar β-amyloid in an Alzheimer mouse model. *Neuroscience* 2015; **298**: 424-435 [PMID: 25931333 DOI: 10.1016/j.neuroscience.2015.04.039]

41 **Ratis RC**, Dacoregio MI, Simão-Silva DP, Mateus RP, Machado LPB, Bonini JS, da Silva WCFN. Confirmed Synergy Between the ε4 Allele of Apolipoprotein E and the Variant K of Butyrylcholinesterase as a Risk Factor for Alzheimer's Disease: A Systematic Review and Meta-Analysis. *J Alzheimers Dis Rep* 2023; **7**: 613-625 [PMID: 37483326 DOI: 10.3233/ADR-220084]

42 **Jasiecki J**, Targońska M, Wasąg B. The Role of Butyrylcholinesterase and Iron in the Regulation of Cholinergic Network and Cognitive Dysfunction in Alzheimer's Disease Pathogenesis. *Int J Mol Sci* 2021; **22** [PMID: 33670778 DOI: 10.3390/ijms22042033]

43 **Assis CRD**, Linhares AG, Cabrera MP, Oliveira VM, Silva KCC, Marcuschi M, Maciel Carvalho EVM, Bezerra RS, Carvalho LB Jr. Erythrocyte acetylcholinesterase as biomarker of pesticide exposure: new and forgotten insights. *Environ Sci Pollut Res Int* 2018; **25**: 18364-18376 [PMID: 29797194 DOI: 10.1007/s11356-018-2303-9]

44 **Dabke AT**, Pohowalla JN, Inamdar S, Singh SD, Mathur PS. Serum cholinesterase and histopathology of the liver in severe protein calorie malnutrition. *Indian J Pediatr* 1972; **39**: 151-157 [PMID: 4629953 DOI: 10.1007/BF02750872]

45 **Camarero González E**, Muñoz Leira V, Iglesias Guerrero M, Fernández Alvarez JA, Cabezas-Cerrato J. [Protein-energy malnutrition: its effects on 4 metabolic parameters]. *Nutr Hosp* 1995; **10**: 158-160 [PMID: 7612711]

46 **Santarpia L**, Grandone I, Contaldo F, Pasanisi F. Butyrylcholinesterase as a prognostic marker: a review of the literature. *J Cachexia Sarcopenia Muscle* 2013; **4**: 31-39 [PMID: 22956442 DOI: 10.1007/s13539-012-0083-5]

47 **Kocabaş**, Ramazan, Erenler, Ali Kemal, Yetim, Mücahit, Doğan, Tolga and Erdemli, Hacı Kemal. Butyrylcholinesterase as an additional marker in the diagnostic network of acute myocardial infarction. *Laboratoriums Medizin* 2016; **40**: 147-152 [DOI: 10.1515/Labmed-2015-0086]

48 **Nechaeva N**, Prokopkina T, Makhaeva G, Rudakova E, Boltneva N, Dishovsky C, Eremenko A, Kurochkin I. Quantitative butyrylcholinesterase activity detection by surface-enhanced Raman spectroscopy. *Sensors and Actuators B: Chemical* 2018; **259**: 75-82 [DOI: 10.1016/j.snb.2017.11.174]

49 **Sulzgruber P**, Koller L, Reiberger T, El-Hamid F, Forster S, Rothgerber DJ, Goliasch G, Wojta J, Niessner A. Butyrylcholinesterase predicts cardiac mortality in young patients with acute coronary syndrome. *PLoS One* 2015; **10**: e0123948 [PMID: 25933219 DOI: 10.1371/journal.pone.0123948]

50 **Distelmaier K**, Winter MP, Rützler K, Heinz G, Lang IM, Maurer G, Koinig H, Steinlechner B, Niessner A, Goliasch G. Serum butyrylcholinesterase predicts survival after extracorporeal membrane oxygenation after cardiovascular surgery. *Crit Care* 2014; **18**: R24 [PMID: 24479557 DOI: 10.1186/cc13711]

51 **Vaisi-Raygani A**, Tavilani H, Zahrai M, Rahimi Z, Sheikh N, Aminian M, Pourmotabbed T. Serum butyrylcholinesterase activity and phenotype associations with lipid profile in stroke patients. *Clin Biochem* 2009; **42**: 210-214 [PMID: 19028482 DOI: 10.1016/j.clinbiochem.2008.10.025]

52 **Zhang QH**, Li AM, He SL, Yao XD, Zhu J, Zhang ZW, Sheng ZY, Yao YM. Serum Total Cholinesterase Activity on Admission Is Associated with Disease Severity and Outcome in Patients with Traumatic Brain Injury. *PLoS One* 2015; **10**: e0129082 [PMID: 26107885 DOI: 10.1371/journal.pone.0129082]

53 **Rahimi Z**, Ahmadi R, Vaisi-Raygani A, Rahimi Z, Bahrehmand F, Parsian A. Butyrylcholinesterase (BChE) activity is associated with the risk

of preeclampsia: influence on lipid and lipoprotein metabolism and oxidative stress. *J Matern Fetal Neonatal Med* 2013; **26**: 1590-1594 [PMID: 23650977 DOI: 10.3109/14767058.2013.795534]

54 **Zivkovic AR**, Decker SO, Zirnstein AC, Sigl A, Schmidt K, Weigand MA, Hofer S, Brenner T. A Sustained Reduction in Serum Cholinesterase Enzyme Activity Predicts Patient Outcome following Sepsis. *Mediators Inflamm* 2018; **2018**: 1942193 [PMID: 29853783 DOI: 10.1155/2018/1942193]

55 **Peng ZL**, Huang LW, Yin J, Zhang KN, Xiao K, Qing GZ. Association between early serum cholinesterase activity and 30-day mortality in sepsis-3 patients: A retrospective cohort study. *PLoS One* 2018; **13**: e0203128 [PMID: 30161257 DOI: 10.1371/journal.pone.0203128]

56 **Xu L**, Zhu B, Huang Y, Yang Z, Sun J, Xu Y, Zheng J, Kinloch S, Yin MT, Weng H, Wu N. Butyrylcholinesterase Levels on Admission Predict Severity and 12-Month Mortality in Hospitalized AIDS Patients. *Mediators Inflamm* 2018; **2018**: 5201652 [PMID: 29736152 DOI: 10.1155/2018/5201652]

57 **Gomes HJ**, Souza RL, Prevedello FC, Mira MT, Chautard-Freire-Maia EA. Investigation of Association between Susceptibility to Leprosy and SNPs inside and near the BCHE Gene of Butyrylcholinesterase. *J Trop Med* 2012; **2012**: 184819 [PMID: 22523498 DOI: 10.1155/2012/184819]

58 **Cheng BN**, Jin YL, Chen BQ, Zhu LY, Xu ZC, Shen T. Serum cholinesterase: a potential assistant biomarker for hand, foot, and mouth disease caused by enterovirus 71 infection. *Infect Dis Poverty* 2016; **5**: 27 [PMID: 27025584 DOI: 10.1186/s40249-016-0124-y]

59 **Haghnazari L**, Vaisi-Raygani A, Keshvarzi F, Ferdowsi F, Goodarzi M, Rahimi Z, Baniamerian H, Tavilani H, Vaisi-Raygani H, Pourmotabbed T. Effect of Acetylcholinesterase and Butyrylcholinesterase on Intrauterine Insemination, Contribution to Inflammations, Oxidative Stress and Antioxidant Status; A Preliminary Report. *J Reprod Infertil* 2016; **17**: 157-162 [PMID: 27478769]

60 **Hefter H**, Arslan M, Kruschel TS, Novak M, Rosenthal D, Meuth SG, Albrecht P, Hartmann CJ, Samadzadeh S. Pseudocholinesterase as a Biomarker for Untreated Wilson's Disease. *Biomolecules* 2022; **12** [PMID: 36551217 DOI: 10.3390/biom12121791]

61 **Ben Anes A**, Ben Nasr H, Garrouch A, Bennour S, Bchir S, Hachana M, Benzarti M, Tabka Z, Chahed K. Alterations in acetylcholinesterase and butyrylcholinesterase activities in chronic obstructive pulmonary disease: relationships with oxidative and inflammatory markers. *Mol Cell Biochem* 2018; **445**: 1-11 [PMID: 29234928 DOI: 10.1007/s11010-017-3246-z]

62 **Tvarijonaviciute A**, Caldin M, Martinez-Subiela S, Tecles F, Pastor J, Ceron JJ. Serum paraoxonase 1 and butyrylcholinesterase in dogs with hyperadrenocorticism. *Vet J* 2015; **203**: 262-263 [DOI: 10.1016/j.tvjl.2014.12.002]

63 **Kocatürk M**, Tecles F, Yalçın E, Cihan H, Tural M, Levent P, Cansev M, Cerón JJ, Yilmaz Z. Changes in choline and cholinesterase in saliva of dogs with parvovirus infection. *Res Vet Sci* 2021; **134**: 147-149 [PMID: 33385977 DOI: 10.1016/j.rvsc.2020.12.012]

64 **Medzhitov R**. The spectrum of inflammatory responses. *Science* 2021; **374**: 1070-1075 [PMID: 34822279 DOI: 10.1126/science.abi5200]

65 **Sridhar G**, Lakshmi G. Influence of butyrylcholinesterase on the course of COVID-19. *Biomedical Reviews* 2021; **32**: 37-46 [DOI: 10.14748/bmr.v31.7712]

66 **Bonaz B**, Sinniger V, Pellissier S. Anti-inflammatory properties of the vagus nerve: potential therapeutic implications of vagus nerve stimulation. *J Physiol* 2016; **594**: 5781-5790 [PMID: 27059884 DOI: 10.1113/JP271539]

67 **Espeter F**, Künne D, Garczarek L, Kuhlmann H, Skarabis A, Zivkovic AR, Brenner T, Schmidt K. Critically Ill COVID-19 Patients Show Reduced Point of Care-Measured Butyrylcholinesterase Activity-A Prospective, Monocentric Observational Study. *Diagnostics (Basel)* 2022; **12** [PMID: 36140551 DOI: 10.3390/diagnostics12092150]

68 **Markuskova L**, Javorova Rihova Z, Fazekas T, Martinkovicova A, Havrisko M, Dingova D, Solavova M, Rabarova D, Hrabovska A. Serum butyrylcholinesterase as a marker of COVID-19 mortality: Results of the monocentric prospective observational study. *Chem Biol Interact* 2023; **381**: 110557 [PMID: 37209860 DOI: 10.1016/j.cbi.2023.110557]

69 **Borger P**. Natural Knockouts: Natural Selection Knocked Out. *Biology (Basel)* 2017; **6** [PMID: 29231847 DOI: 10.3390/biology6040043]

70 **Alkuraya FS**. Natural human knockouts and the era of genotype to phenotype. *Genome Med* 2015; **7**: 48 [PMID: 26029266 DOI: 10.1186/s13073-015-0173-z]

71 **Narasimhan VM**, Xue Y, Tyler-Smith C. Human Knockout Carriers: Dead, Diseased, Healthy, or Improved? *Trends Mol Med* 2016; **22**: 341-351 [PMID: 26988438 DOI: 10.1016/j.molmed.2016.02.006]

72 **MacArthur DG**, Balasubramanian S, Frankish A, Huang N, Morris J, Walter K, Jostins L, Habegger L, Pickrell JK, Montgomery SB, Albers CA, Zhang ZD, Conrad DF, Lunter G, Zheng H, Ayub Q, DePristo MA, Banks E, Hu M, Handsaker RE, Rosenfeld JA, Fromer M, Jin M, Mu XJ, Khurana E, Ye K, Kay M, Saunders GI, Suner MM, Hunt T, Barnes IH, Amid C, Carvalho-Silva DR, Bignell AH, Snow C, Yngvadottir B, Bumpstead S, Cooper DN, Xue Y, Romero IG; 1000 Genomes Project Consortium, Wang J, Li Y, Gibbs RA, McCarroll SA, Dermitzakis ET, Pritchard JK, Barrett JC, Harrow J, Hurles ME, Gerstein MB, Tyler-Smith C. A systematic survey of loss-of-function variants in human protein-coding genes. *Science* 2012; **335**: 823-828 [PMID: 22344438 DOI: 10.1126/science.1215040]

73 **Kaiser VB**, Svinti V, Prendergast JG, Chau YY, Campbell A, Patarcic I, Barroso I, Joshi PK, Hastie ND, Miljkovic A, Taylor MS; Generation Scotland; UK10K, Enroth S, Memari Y, Kolb-Kokocinski A, Wright AF, Gyllensten U, Durbin R, Rudan I, Campbell H, Polašek O, Johansson Å, Sauer S, Porteous DJ, Fraser RM, Drake C, Vitart V, Hayward C, Semple CA, Wilson JF. Homozygous loss-of-function variants in European cosmopolitan and isolate populations. *Hum Mol Genet* 2015; **24**: 5464-5474 [PMID: 26173456 DOI: 10.1093/hmg/ddv272]

74 **Narasimhan VM**, Hunt KA, Mason D, Baker CL, Karczewski KJ, Barnes MR, Barnett AH, Bates C, Bellary S, Bockett NA, Giorda K, Griffiths CJ, Hemingway H, Jia Z, Kelly MA, Khawaja HA, Lek M, McCarthy S, McEachan R, O'Donnell-Luria A, Paigen K, Parisinos CA, Sheridan E, Southgate L, Tee L, Thomas M, Xue Y, Schnall-Levin M, Petkov PM, Tyler-Smith C, Maher ER, Trembath RC, MacArthur DG, Wright J, Durbin R, van Heel DA. Health and population effects of rare gene knockouts in adult humans with related parents. *Science* 2016; **352**: 474-477 [PMID: 26940866 DOI: 10.1126/science.aac8624]

75 **Xu YC**, Guo YL. Less Is More, Natural Loss-of-Function Mutation Is a Strategy for Adaptation. *Plant Commun* 2020; **1**: 100103 [PMID: 33367264 DOI: 10.1016/j.xplc.2020.100103]

76 **Kaiser J**. The hunt for missing genes. *Science* 2014; **344**: 687-689 [PMID: 24833372 DOI: 10.1126/science.344.6185.687]

77 **Manoharan I**, Boopathy R, Darvesh S, Lockridge O. A medical health report on individuals with silent butyrylcholinesterase in the Vysya community of India. *Clin Chim Acta* 2007; **378**: 128-135 [PMID: 17182021 DOI: 10.1016/j.cca.2006.11.005]

78 **Li B**, Duysen EG, Carlson M, Lockridge O. The butyrylcholinesterase knockout mouse as a model for human butyrylcholinesterase deficiency. *J Pharmacol Exp Ther* 2008; **324**: 1146-1154 [PMID: 18056867 DOI: 10.1124/jpet.107.133330]

79 **Liu W**, Cao Y, Lin Y, Tan KS, Zhao H, Guo H, Tan W. Enhancement of Fear Extinction Memory and Resistance to Age-Related Cognitive Decline in Butyrylcholinesterase Knockout Mice and (R)-Bambuterol Treated Mice. *Biology (Basel)* 2021; **10** [PMID: 34062954 DOI: 10.3390/biology10050404]

80 **Lockridge O**, Norgren RB Jr, Johnson RC, Blake TA. Naturally Occurring Genetic Variants of Human Acetylcholinesterase and Butyrylcholinesterase and Their Potential Impact on the Risk of Toxicity from Cholinesterase Inhibitors. *Chem Res Toxicol* 2016; **29**: 1381-1392 [PMID: 27551784 DOI: 10.1021/acs.chemrestox.6b00228]

81 **Lando G**, Mosca A, Bonora R, Azzario F, Penco S, Marocchi A, Panteghini M, Patrosso MC. Frequency of butyrylcholinesterase gene mutations in individuals with abnormal inhibition numbers: an Italian-population study. *Pharmacogenetics* 2003; **13**: 265-270 [PMID: 12724618 DOI: 10.1097/00008571-200305000-00005]

82 **Sokolow S**, Li X, Chen L, Taylor KD, Rotter JI, Rissman RA, Aisen PS, Apostolova LG. Deleterious Effect of Butyrylcholinesterase K-Variant in Donepezil Treatment of Mild Cognitive Impairment. *J Alzheimers Dis* 2017; **56**: 229-237 [PMID: 27911294 DOI: 10.3233/JAD-160562]

83 **Ha ZY**, Mathew S, Yeong KY. Butyrylcholinesterase: A Multifaceted Pharmacological Target and Tool. *Curr Protein Pept Sci* 2020; **21**: 99-109 [PMID: 31702488 DOI: 10.2174/1389203720666191107094949]

84 **Sridhar GR**. Proteins of the Esterase Family: Patents for Some Proteins in Search of Metabolic Functions. Recent Patents on Biomarkers, 2011; 1: 205-212. Available from: https://www.ingentaconnect.com/content/ben/rpbm/2011/00000001/00000003/art00004

85 **Geula C**, Darvesh S. Butyrylcholinesterase, cholinergic neurotransmission and the pathology of Alzheimer's disease. *Drugs Today (Barc)* 2004; **40**: 711-721 [PMID: 15510242 DOI: 10.1358/dot.2004.40.8.850473]

86 **Lockridge O**. Review of human butyrylcholinesterase structure, function, genetic variants, history of use in the clinic, and potential therapeutic uses. *Pharmacol Ther* 2015; **148**: 34-46 [PMID: 25448037 DOI: 10.1016/j.pharmthera.2014.11.011]

87 **Lockridge O**, Duysen EG, Masson P. Butyrylcholinesterase: overview, structure, and function. *Anticholinesterase Pesticides* 2011; **10**: 25-41

88 **Zhang P**, Jain P, Tsao C, Sinclair A, Sun F, Hung HC, Bai T, Wu K, Jiang S. Butyrylcholinesterase nanocapsule as a long circulating bioscavenger with reduced immune response. *J Control Release* 2016; **230**: 73-78 [PMID: 27063423 DOI: 10.1016/j.jconrel.2016.04.008]

89 **MacArthur DG**, Tyler-Smith C. Loss-of-function variants in the genomes of healthy humans. *Human Molecular Genetics* 2010; **19**: R125-R130

90 **Monies D**, Abouelhoda M, AlSayed M, Alhassnan Z, Alotaibi M, Kayyali H, Al-Owain M, Shah A, Rahbeeni Z, Al-Muhaizea MA, Alzaidan HI, Cupler E, Bohlega S, Faqeih E, Faden M, Alyounes B, Jaroudi D, Goljan E, Elbardisy H, Akilan A, Albar R, Aldhalaan H, Gulab S, Chedrawi A, Al Saud BK, Kurdi W, Makhseed N, Alqasim T, El Khashab HY, Al-Mousa H, Alhashem A, Kanaan I, Algoufi T, Alsaleem K, Basha TA, Al-Murshedi F, Khan S, Al-Kindy A, Alnemer M, Al-Hajjar S, Alyamani S, Aldhekri H, Al-Mehaidib A, Arnaout R, Dabbagh O, Shagrani M, Broering D, Tulbah M, Alqassmi A, Almugbel M, AlQuaiz M, Alsaman A, Al-Thihli K, Sulaiman RA, Al-Dekhail W, Alsaegh A, Bashiri FA, Qari A, Alhomadi S, Alkuraya H, Alsebayel M, Hamad MH, Szonyi L, Abaalkhail F, Al-Mayouf SM, Almojalli H, Alqadi KS, Elsiesy H, Shuaib TM, Seidahmed MZ, Abosoudah I, Akleh H, AlGhonaium A, Alkharfy TM, Al Mutairi F, Eyaid W, Alshanbary A, Sheikh FR, Alsohaibani FI, Alsonbul A, Al Tala S, Balkhy S, Bassiouni R, Alenizi AS, Hussein MH, Hassan S, Khalil M, Tabarki B, Alshahwan S, Oshi A, Sabr Y, Alsaadoun S, Salih MA, Mohamed S, Sultana H, Tamim A, El-Haj M, Alshahrani S, Bubshait DK, Alfadhel M, Faquih T, El-Kalioby M, Subhani S, Shah Z, Moghrabi N, Meyer BF, Alkuraya FS. The landscape of genetic diseases in Saudi Arabia based on the first 1000 diagnostic panels and exomes. *Hum Genet* 2017; **136**: 921-939 [PMID: 28600779 DOI: 10.1007/s00439-017-1821-8]

91 **Monies D**, Goljan E; Rapid Exome Consortium, Assoum M, Albreacan M, Binhumaid F, Subhani S, Boureggah A, Hashem M, Abdulwahab F, Abuyousef O, Temsah MH, Alsohime F, Kelaher J, Abouelhoda M, Meyer BF, Alkuraya FS. The clinical utility of rapid exome sequencing in a consanguineous population. *Genome Med* 2023; **15**: 44 [PMID: 37344829 DOI: 10.1186/s13073-023-01192-5]

World Journal of Experimental Medicine

Submit a Manuscript: https://www.f6publishing.com

World J Exp Med 2024 March 20; 14(1): 89319

DOI: 10.5493/wjem.v14.i1.89319

ISSN 2220-315x (online)

ORIGINAL ARTICLE

Retrospective Cohort Study

Predictors of disease recurrence after radical resection and adjuvant chemotherapy in patients with stage IIb-IIIa squamous cell lung cancer: A retrospective analysis

Marina A Senchukova, Evgeniy A Kalinin, Nadezhda N Volchenko

Specialty type: Oncology

Provenance and peer review: Invited article; Externally peer reviewed.

Peer-review model: Single blind

Peer-review report's scientific quality classification
Grade A (Excellent): 0
Grade B (Very good): 0
Grade C (Good): C
Grade D (Fair): D
Grade E (Poor): 0

P-Reviewer: Liu Y, China

Received: October 27, 2023
Peer-review started: October 27, 2023
First decision: December 7, 2023
Revised: December 20, 2023
Accepted: January 10, 2024
Article in press: January 10, 2024
Published online: March 20, 2024

Marina A Senchukova, Department of Oncology, Orenburg State Medical University, Orenburg 460000, Russia

Evgeniy A Kalinin, Department of Thoracic Surgery, Orenburg Regional Cancer Clinic, Orenburg 460021, Russia

Nadezhda N Volchenko, Department of Pathology, P. A. Hertzen Moscow Oncology Research Centre, National Medical Research Centre of Radiology, Moscow 125284, Russia

Corresponding author: Marina A Senchukova, MD, PhD, Professor, Department of Oncology, Orenburg State Medical University, Sovetskaya Street, 6, Orenburg 460000, Russia. masenchukova@yandex.com

Abstract

BACKGROUND

Lung cancer (LC) is a global medical, social and economic problem and is one of the most common cancers and the leading cause of mortality from malignant neoplasms. LC is characterized by an aggressive course, and in the presence of disease recurrence risk factors, patients, even at an early stage, may be indicated for adjuvant therapy to improve survival. However, combined treatment does not always guarantee a favorable prognosis. In this regard, establishing predictors of LC recurrence is highly important both for determining the optimal treatment plan for the patients and for evaluating its effectiveness.

AIM

To establish predictors of disease recurrence after radical resection and adjuvant chemotherapy in patients with stage IIb-IIIa lung squamous cell carcinoma (LSCC).

METHODS

A retrospective case-control cohort study included 69 patients with LSCC who underwent radical surgery at the Orenburg Regional Clinical Oncology Center from 2009 to 2018. Postoperatively, all patients received adjuvant chemotherapy. Histological samples of the resected lung were stained with Mayer's hematoxylin and eosin and examined under a light microscope. Univariate and multivariate analyses were used to identify predictors associated with the risk of disease

recurrence. Receiver operating characteristic curves were constructed to discriminate between patients with a high risk of disease recurrence and those with a low risk of disease recurrence. Survival was analyzed using the Kaplan-Meier method. The log-rank test was used to compare survival curves between patient subgroups. Differences were considered to be significant at $P < 0.05$.

RESULTS

The following predictors of a high risk of disease recurrence in patients with stage IIb-IIa LSCC were established: a low degree of tumor differentiation [odds ratio (OR) = 7.94, 95%CI = 1.08-135.81, $P = 0.049$]; metastases in regional lymph nodes (OR = 5.67, 95%CI = 1.09-36.54, $P = 0.048$); the presence of loose, fine-fiber connective tissue in the tumor stroma (OR = 21.70, 95%CI = 4.27-110.38, $P = 0.0002$); and fragmentation of the tumor solid component (OR = 2.53, 95%CI = 1.01-12.23, $P = 0.049$). The area under the curve of the predictive model was 0.846 (95%CI = 0.73-0.96, $P < 0.0001$). The sensitivity, accuracy and specificity of the method were 91.8%, 86.9% and 75.0%, respectively. In the group of patients with a low risk of LSCC recurrence, the 1-, 2- and 5-year disease-free survival (DFS) rates were 84.2%, 84.2% and 75.8%, respectively, while in the group with a high risk of LSCC recurrence the DFS rates were 71.7%, 40.1% and 8.2%, respectively ($P < 0.00001$). Accordingly, in the first group of patients, the 1-, 2- and 5-year overall survival (OS) rates were 94.7%, 82.5% and 82.5%, respectively, while in the second group of patients, the OS rates were 89.8%, 80.1% and 10.3%, respectively ($P < 0.00001$).

CONCLUSION

The developed method allows us to identify a group of patients at high risk of disease recurrence and to adjust to ongoing treatment.

Key Words: Lung cancer; Lung squamous cell carcinoma; Adjuvant chemotherapy; Radical resection; Disease recurrence risk factors

Core Tip: This study identified the following independent predictors of a high risk of disease recurrence in patients with stage IIb-IIIa lung squamous cell carcinoma treated by radical resection and adjuvant chemotherapy: a low degree of tumor differentiation, metastases in regional lymph nodes, the presence of loose, fine-fiber connective tissue in the tumor stroma and fragmentation of the tumor solid component. The area under the curve of the predictive model was 0.846. The sensitivity, accuracy and specificity of the methods were 91.8%, 86.9% and 75.0%, respectively. The developed method allows us to identify a group of patients at high risk of disease relapse and to adjust the treatment.

Citation: Senchukova MA, Kalinin EA, Volchenko NN. Predictors of disease recurrence after radical resection and adjuvant chemotherapy in patients with stage IIb-IIIa squamous cell lung cancer: A retrospective analysis. *World J Exp Med* 2024; 14(1): 89319

URL: https://www.wjgnet.com/2220-315x/full/v14/i1/89319.htm

DOI: https://dx.doi.org/10.5493/wjem.v14.i1.89319

INTRODUCTION

Lung cancer (LC) is a global medical, social and economic problem and is one of the most common cancers and the leading cause of mortality from malignant neoplasms worldwide[1,2]. Despite advances in the diagnosis and treatment of this pathology, the 5-year survival rate of patients with LC does not exceed 20%[3]. The 5-year survival rate of patients who received radical therapy is higher and is approximately 35% in men and 44% in women[4,5]. Low survival rates are associated with late diagnosis of the disease and the presence of underlying severe disease in elderly patients, which significantly limits the choice of treatment methods, as well as the insufficient effectiveness of systemic therapy in a significant proportion of patients with advanced LC.

It is important to note that LC is a heterogeneous disease. The two major histologic subtypes are non-small-cell lung cancer (NSCLC) and small-cell lung cancer. NSCLC accounts for approximately 85% of all LC cases and includes lung squamous cell carcinoma (LSCC), lung adenocarcinoma and lung large cell carcinoma[6]. The different histological subtypes differ in metabolism, microenvironment, prognosis and treatment regimens[6]. Despite significant differences between subtypes, surgical resection and chemotherapy are the standard treatments for patients with stage IB-IIIA NSCLC[5]. Because NSCLC has an aggressive course, adjuvant therapy is indicated to improve survival even in patients with stage IB disease and risk factors[7,8]. However, combination treatment does not always guarantee a favorable disease prognosis. Despite radical treatment, some patients with NSCLC experience disease recurrence, the frequency of which ranges from 25% to 65%, depending on the stage of the disease[9,10]. Postoperative recurrences in NSCLC can occur even at an early stage, which leads to decreased patient survival. Thus, life expectancy after local relapse averages

12 to 26 months, and in patients with distant metastases, life expectancy is 7 to 8 months[11,12]. In addition, the presence of disease recurrence is associated with higher healthcare costs[12].

Thus, reducing mortality from NSCLC seems to be one of the most important tasks of modern healthcare. To successfully solve this problem, both timely diagnosis and effective treatment are important. However, the effectiveness of LC treatment depends, among other things, on an accurate assessment of the disease prognosis. Currently, assessments of the risk of disease recurrence and indications for adjuvant therapy in NSCLC patients are based on clinical and morphological characteristics of the disease, including age, tumor size, race, sex, histological type, grade, T stage, N stage, type of surgery and adjuvant therapy[5,13]. Unfortunately, the existing classifications do not allow prediction of the effect of drug therapy, and disease prognosis in patients with similar clinical and morphological characteristics may differ. Meanwhile, assessing the effect of combination therapy in individual NSCLC patients is highly important for determining the optimal treatment plan and assessing its effectiveness[14]. Determining the risk of disease recurrence in patients with NSCLC allows one to avoid prescribing ineffective treatment regimens, adjust individual treatment plans and subsequently dynamically monitor patients, thereby helping improve the results of their treatment. Thus, the search for new effective criteria for assessing the risk of LC recurrence has not lost relevance[9].

We previously established that tumor microvessels have different morphologies and clinical significance[15-17]. In addition, in squamous cell carcinoma of the cervix, we described the phenomenon of fragmentation of the tumor solid component as the presence of separate fibroblast-like cells in the solid component of the tumor. This study revealed that vessels with weak CD34 expression, located in the loose, fine-fiber connective tissue of the tumor stroma (LFFCT), vessels in the solid component of the tumor, and fragmentation of the tumor solid component were associated with a high risk of relapse of squamous cell carcinoma of the cervix I-IIA stages. The purpose of this study was to establish the prognostic significance of different types of tumor microvessels, as well as the characteristics of the stromal and parenchymal components, in patients with stage IIb-IIIa LSCC who underwent radical resection and adjuvant chemotherapy.

MATERIALS AND METHODS

Patient characteristics

This retrospective case-control cohort study included 69 patients with stage IIb-IIIa LSCC who underwent radical surgery (R0) at the Orenburg Regional Oncology Center from May 20, 2009, to December 14, 2018. The age of the patients was 61.9 ± 6.8 years (median 62 years). The study was conducted in accordance with the Helsinki Declaration and internationally recognized guidelines. Study approval was received from the Ethics Committee of Orenburg State Medical University (Russia, Orenburg). The inclusion criteria for patients were as follows: (1) Patients who underwent radical surgery (R0) in the form of lobectomy, bilobectomy or pneumonectomy; (2) the stage of the disease corresponded to IIb-IIIa; (3) the histological subtype was LSCC; (4) LSCC was the first primary tumor; (5) patients who received at least 4 cycles of adjuvant chemotherapy after surgery (etoposide - 100 mg/m^2/d on days 1, 2, and 3 and cisplatin - 80 mg/m^2/d on day 1, every 3 wk); and (6) complete follow-up data were obtained.

The exclusion criteria were as follows: (1) Patients who underwent nonradical surgery (R1); (2) patients who received neoadjuvant radiotherapy or chemotherapy; (3) patients who received steroids, nonsteroidal anti-inflammatory drugs, or antihistamines; (4) patients who had significant comorbid pathologies in the decompensation stage; and (5) patients who died within the first three months after surgery. The median follow-up period was 62.4 months.

Pathology

Sections (4 μm) were cut on a microtome and transferred to glass slides (SuperFrost® Plus, Menzel, Thermo Scientific, United States). Sections were stained with Mayer's hematoxylin and eosin (H&E) and studied *via* light microscopy (Levenhuk D740T digital microscope connected to a 5.1 MP camera, Russia). The following features of the parenchymal and stromal components of the tumor were estimated: the presence of LFFCT in the tumor stroma, the presence of capillaries in the solid component of the tumor, the presence of fragmentation of the tumor solid component, the presence of peritumoral retraction clefting, and the tumor spreading through the alveolar air spaces (AAS).

Statistical analysis

Statistical analysis was performed using Statistica 10.0 software. Quantitative data are presented as the mean ± standard deviation (SD), while categorical variables are presented as numbers and percentages (*n*, %). Clinicopathologic factors were compared between patients with and without disease relapse *via* the chi-square test. Univariate and multivariate logistic regression analyses were performed to identify potential risk factors for LSCC recurrence. Receiver operating characteristic (ROC) curves were constructed to discriminate between patients with and without recurrence of LSCC. The best threshold (cutoff) values were determined by the largest Youden's index (J = sensitivity + specificity-1). The effectiveness of the predictive models was assessed by the area under the curve (AUC). Survival was analyzed using the Kaplan-Meier method. The log-rank test was used to compare survival curves between patient subgroups. A value of $P < 0.05$ was considered to indicate statistical significance.

RESULTS

The baseline patient clinicopathological and treatment information is shown in Table 1.

Table 1 Baseline patient clinical, pathological and treatment information

Clinical and pathological data	Patients	
	n	%
Age (yr)		
< 60	23	33.3
60-69	36	52.2
≥ 70	10	14.5
Gender		
Male	67	97.1
Female	2	2.9
Tumor location		
Upper lobe	45	65.2
Middle lobe	1	1.5
Lower lobe	21	30.4
Main bronchus	2	2.9
Lateral origin		
Left	31	44.9
Right	38	55.1
Tumor localization		
Central	57	82.6
Peripheral	12	17.4
Histology		
KSCC	18	26.1
NKSCC	51	74.9
Grade		
G1	11	15.9
G2	41	59.4
G3	17	24.7
T stage		
T1b	7	10.1
T2a	30	43.5
T2b	6	8.7
T3a	26	37.7
N stage		
N0	10	14.5
N1	38	55.1
N2	31	30.4
Stage		
IIb	37	53.6
IIIa	32	46.4
Type of surgery		
Lobectomy	29	42.0
Pneumonectomy	40	58.0

KSCC: Keratinizing squamous cell carcinoma; NKSCC: Nonkeratinizing squamous cell carcinoma.

Nine patients underwent sleeve lobectomies, 6 of whom were older than 70 years. Sixty-five patients received 4 courses of adjuvant chemotherapy, 3 patients received 5 courses of adjuvant chemotherapy, and 1 patient received 6 courses of adjuvant chemotherapy.

Recurrence of LSCC was diagnosed in 49 (71.0%) patients, 43 (62.3%) of whom died from disease progression. Twenty-eight (57.1%) patients with recurrent LC were diagnosed within the first two years after surgery. The one-, two-, three-, four-, and five-year disease-free survival (DFS) rates were 85.7%, 60%, 40.8%, 34.3%, and 30.0%, respectively. The one-, two-, three-, four- and five-year overall survival (OS) rates were 95.7%, 85.7%, 68.6%, 48.6% and 37.1%, respectively.

Local relapse of LSCC was diagnosed in 22 (31.4%) patients, systemic relapse was diagnosed in 22 (31.4%), and local-systemic relapse was diagnosed in 5 (3.9%). In particular, metastases to the lungs and pleura were detected in 14 (20.0%) patients, to the mediastinum in 9 (12.9%), to the liver in 6 (8.6%), to the brain in 3 (4.3%), to the cervical lymph nodes in 1 (1.4%), bones in 4 (5.7%) and multiple disseminations in 12 (17.1%) patients. Due to relapse of LSCC, 31 patients received 1 to 4 courses of mono- or polychemotherapy. Six patients with relapsed LSCC are alive and continue to receive mono-chemotherapy. One (1.4%) patient died from nononcological pathology. Nineteen (27.5%) patients were alive without signs of disease relapse as of July 30, 2023.

Characteristics of tumor microvessels and features of parenchymal and stromal components of LSCC

The main condition for including tumor microvessels and features of the parenchymal and stromal components of the tumor in the analysis was the possibility of their detection during routine staining with Mayer's hematoxylin and eosin. In accordance with this, the presence of LFFCTL in the tumor stroma, microvessels in the tumor solid component, fragmentation of the tumor solid component, and the presence of peritumoral retraction clefting were included in the analysis. Additionally, taking into account the literature data, the analysis included indicator such as tumor spreading through the AAS.

LFFCT was most often observed along the invasive edge of the tumor and was rich in cells with large light nuclei (Figure 1). LFFCT was detected in 56 (80%) LSCC samples.

Microvessels in the tumor solid component were represented by capillaries with collapsed walls separated from the tumor cells by empty space (Figure 2A). This type of vessel was noted in 30 (42.9%) LSCC samples.

The fragmentation of the tumor solid component was characterized by the presence of isolated fibroblast-like cells in the tumor parenchyma (Figure 2B). This phenomenon was observed in 54 (77.1%) LSCC samples.

Peritumoral retraction clefting manifested as an empty space located around clusters of tumor cells (Figure 2C). This phenomenon was identified in 43 (61.4%) LSCC samples.

Tumor spread in the AAS was noted in 33 (47.1%) LSCC samples. Clusters of tumor cells were found both in unchanged alveoli (Figure 2D) and in alveoli with thickened, deformed walls. A number of observations revealed fragmentation of the tumor solid component in the alveoli.

Clinicopathological data of patients with and without recurrence of LSCC

The clinicopathological characteristics of patients with and without recurrence of LSCC are presented in Table 2.

According to the data obtained, patients who experienced disease recurrence were significantly more likely to have a low degree of tumor differentiation ($P = 0.04$) and metastases in regional lymph nodes ($P = 0.05$). Slightly more often, relapse of the disease was observed when the tumor had a low degree of differentiation ($P = 0.08$), was localized in the upper lobe ($P = 0.19$), was in the left lung ($P = 0.11$) or was nonkeratinizing squamous cell carcinoma (NKSCC) ($P = 0.19$). The recurrence rate of LSCC did not depend on the age of the patient, T stage, or extent of surgery performed.

Risk factors associated with LSCC recurrence

The results of univariate and multivariate analyses evaluating the independent factors associated with the risk of LSCC recurrence are presented in Table 3. Thus, we identified 4 independent prognostic factors associated with the risk of LSCC recurrence, namely, tumor grade, N stage, the presence of LFFCT in the tumor stroma and fragmentation of the tumor solid component.

We summarized the odds ratios (ORs) of the independent predictors for each patient. For example, for a patient with G3 (OR = 7.94), N2 (OR = 6.30), fragmentation of the tumor solid component (OR = 2.53) and absence of LFFCT in the tumor stroma (OR = 1), this number was 17.77 (7.94 + 6.30 + 2.53 + 1). On the basis of these results, ROC curves were constructed to discriminate between cases with and without LSCC relapse (Figure 3).

The AUC was 0.846 (95%CI = 0.73-0.96, $P < 0.0001$). The cutoff for discriminating between cases with and without LSCC relapse, was 26.2. If the sum of the ORs of the four independent predictors of high risk of LSCC recurrence was less than 26.2 (the first group of patients), then recurrence of LSCC was noted in 4 (21.1%) of the 19 patients. If the sum of the ORs was greater than or equal to 26.2 (the second group of patients), then recurrence of LSCC was noted in 45 (90.0%) of the 50 patients. The sensitivity, accuracy and specificity of the method were 91.8%, 86.9% and 75.0%, respectively. In the first group of patients, the 1-, 2- and 5-year DFS rates were 84.2%, 84.2% and 75.8%, respectively, while in the second group of patients, the DFS rates were 71.7%, 40.1% and 8.2%, respectively ($P < 0.00001$). Accordingly, in the first group of patients, the 1-, 2- and 5-year OS rates were 94.7%, 82.5% and 82.5%, respectively, while in the second group of patients, the OS rates were 89.8%, 80.1% and 10.3%, respectively ($P < 0.00001$). The relapse-free survival (RFS) and OS curves for these groups are shown in Figure 4.

Table 2 Characteristics of patients with and without recurrence of lung squamous cell carcinoma

	Patients with recurrence of LSCC		Patients without recurrence of LSCC		*P* value
	n	%	*n*	%	
Age (yr)					
< 60	15	30.6	8	40.0	0.72
60-69	27	55.1	9	45.0	
≥ 70	7	14.3	3	15.0	
Gender					
Male	47	95.9	20	100.0	0.359
Female	2	4.1	0	0.0	
Tumor location					
Upper lobe	35	71.5	10	50.0	0.193
Middle lobe	0	0.0	1	5.0	
Lower lobe	13	26.5	8	40.0	
Main bronchus	1	2.0	1	5.0	
Lateral origin					
Left	25	51.1	6	30.0	0.111
Right	24	48.9	14	70.0	
Tumor localization					
Central	43	87.8	14	70.0	0.08
Peripheral	6	12.2	6	30.0	
Histology					
KSCC	10	20.4	8	40.0	0.193
NKSCC	39	79.6	12	60.0	
Grade					
G1	8	16.3	3	15.0	0.040
G2	25	51.0	16	80.0	
G3	16	32.7	1	5.0	
T stage					
T1b	5	10.2	2	10.0	0.559
T2a	24	48.9	6	30.0	
T2b	4	8.2	2	10.0	
T3a	16	32.7	10	50.0	
N stage					
N0	4	8.2	6	30.0	0.05
N1	30	61.2	8	40.0	
N2	15	30.6	6	30.0	
Stage					
IIb	25	51.0	12	60.0	0.497
IIIa	24	49.0	8	40.0	
Type of surgery					
Lobectomy	19	38.8	10	50.0	0.618
Pneumonectomy	30	61.2	10	50.0	

KSCC: Keratinizing squamous cell carcinoma; NKSCC: Nonkeratinizing squamous cell carcinoma.

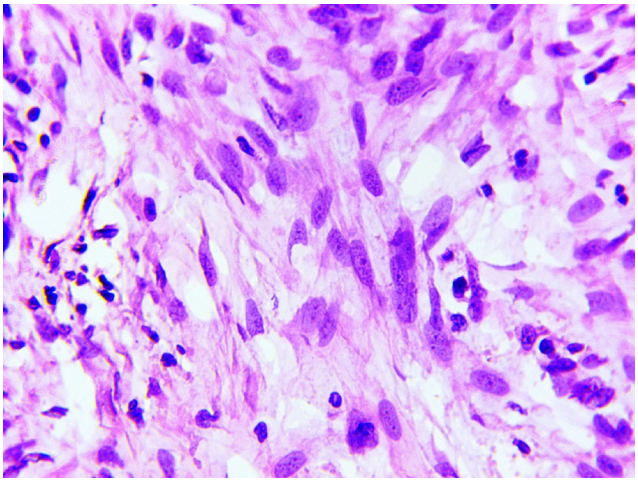

Figure 1 Loose fine-fiber connective tissue of the tumor stroma. Mayer's hematoxylin and eosin staining (× 400).

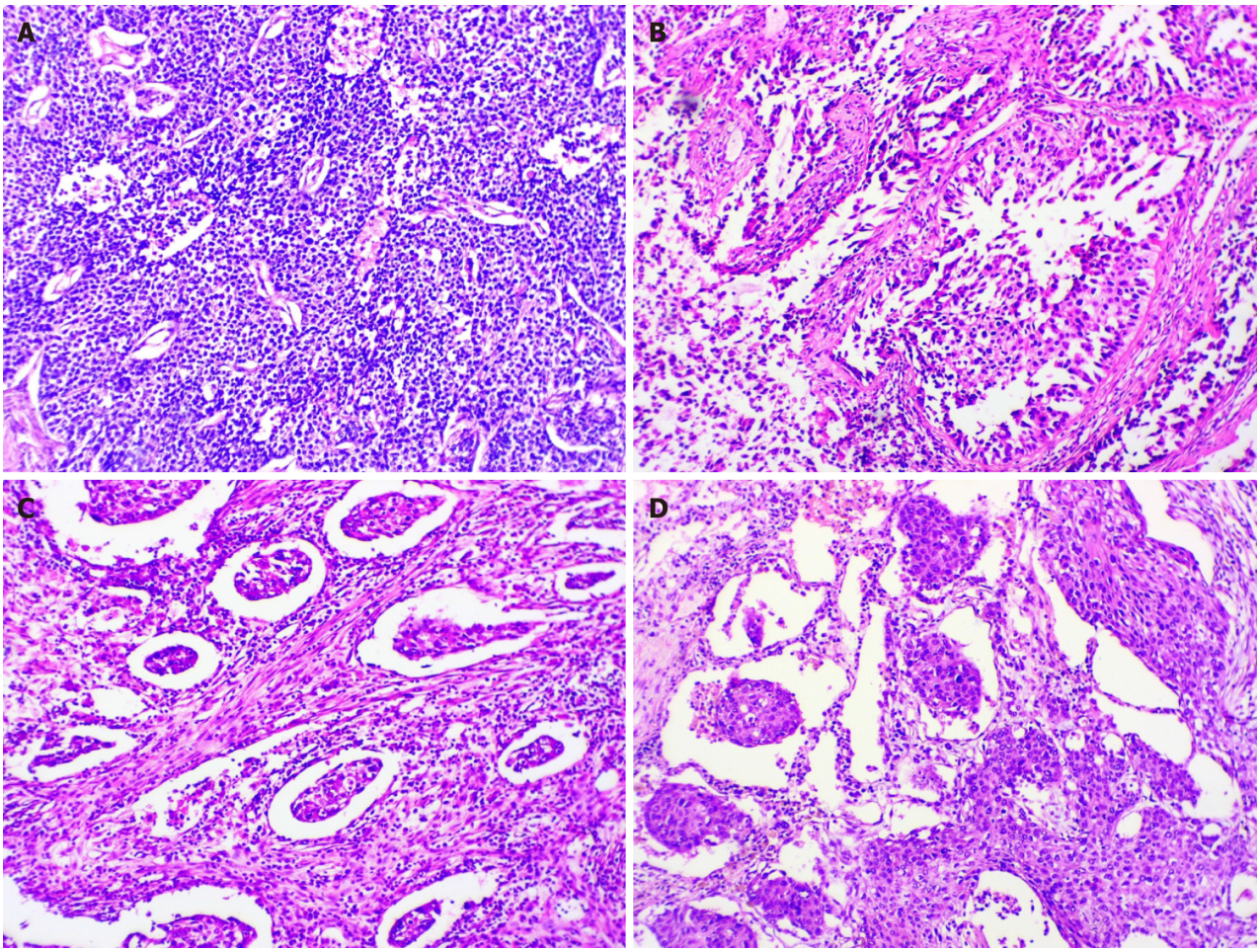

Figure 2 Features of parenchymal and stromal components of lung squamous cell carcinoma. A: Microvessels in the tumor solid component; B: The fragmentation of the tumor solid component; C: The phenomenon of peritumoral retraction clefting; D: Spread of the tumor through the alveolar air spaces. Mayer's hematoxylin and eosin staining (× 200).

DISCUSSION

Establishing independent predictors of the risk of LSCC recurrence is important both for assessing disease prognosis and understanding the mechanisms of LSCC progression, as well as for identifying factors associated with sensitivity to therapy. Currently, assessing the risk of LC recurrence is based on the traditional staging system and other clinicopathological risk factors and their combinations[18,19]. However, it is believed that the current TNM staging system is insufficient for predicting the survival of LC patients[20]. In this regard, the search for reliable predictors of the risk of LC recurrence continues. New methods for assessing the risk of relapse in patients with LC include radiomic signatures[21, 22], positron emission tomography[23,24], and machine learning models[25,26]. These methods are highly sensitive but require special equipment and trained personnel.

The inclusion of various tumor markers in the analysis can improve the accuracy of disease prognosis. Thus, in a study by Yu *et al*[20], a higher C-reactive protein-to-albumin ratio, intrapericardial pulmonary artery ligation, lymph node metastasis, and adjuvant therapy were associated with a high risk of LC recurrence in patients who underwent pneumonectomy. In turn, the independent predictors of OS in this group of patients were intrapericardial pulmonary artery and vein ligation, higher T stage, lymph node metastasis, and no adjuvant therapy. The AUCs for 1-, 3-, and 5-year DFS were 0.655, 0.726, and 0.735, respectively, and those for 1-, 3-, and 5-year OS were 0.741, 0.765, and 0.709, respectively. However, it should be noted that the patient cohort in this study was very heterogeneous and included patients with stage T0-T4 and N0-N2 disease who received both neoadjuvant and adjuvant therapy. Interestingly, the use of adjuvant therapy in this study was associated with a decrease in DFS, while its absence was associated with a decrease in OS[20].

In the study by Jiao *et al*[27], the independent predictors of a high risk of relapse in NSCLC were disease stage, T stage, N stage, histological tumor type, the presence of radiation therapy and residual tumor, and 4-and-a-half LIM domain protein 2 (FHL2), which is responsible for the proliferation, invasion and metastasis of tumor cells. The authors noted that high FHL2 levels may serve as an independent predictor of DFS in NSCLC patients. However, it is worth noting the insufficient efficiency of the proposed model since the AUCs for 1-, 3- and 5-year OS were 0.56, 0.53 and 0.51, respectively.

In stage IIIA patients receiving adjuvant chemotherapy, the independent predictors associated with decreased OS were adjuvant radiotherapy, targeted therapy, tumor size, N1p, and N2p, whereas the independent predictors associated with decreased OS were only tumor size and N2p[28]. The authors noted moderate agreement between the predicted and actual RFS and OS. The C-index was 0.656 (95%CI: 0.626-0.687) for RFS and 0.651 (95%CI: 0.611-0.691) for OS.

In early NSCLC, the independent predictors of a high risk of disease recurrence were smoking status, total lymph nodes removed, and tumor size[29]. This model was relevant only to patients with stage 1a-1b NSCLC who did not receive adjuvant therapy. It should be noted that data on the role of adjuvant therapy in the treatment of early-stage NSCLC vary widely. A study by Xu *et al*[30] revealed that in a cohort of patients with stage IB NSCLC, adjuvant chemotherapy was associated with improved survival, especially in older patients with poorly differ-entiated and undifferentiated tumors, 0-15 Lymph nodes examined, visceral pleural invasion, lobectomy and lack of radiation therapy. However, in stage IB LSCC, the effect of adjuvant chemotherapy was not statistically significant (HR = 0.84, 95%CI = 0.67-1.06, P = 0.144).

In another similar study, the authors did not observe any improvement in patient survival with or without adjuvant chemotherapy for stage IB NSCLC[31]. The inclusion of molecular markers (VEGF-C, miR-1, miR-486, miR-499, and miR-30d) in the analysis did not increase the accuracy of predicting the risk of disease relapse in patients with early-stage NSCLC[9].

A number of studies have noted correlations between immune cell levels and DFS. In particular, a study by Wu *et al* [32] showed that higher levels of CD68 and M1 macrophages are associated with worse DFS (P < 0.0001). Based on the results obtained, a nomogram was constructed that included age and sex, the presence of visceral pleural invasion, the number of lymph nodes removed, clinical stage and the immune-related risk assessment nomogram. The proposed nomogram outperformed the TNM classification and the CD68-based immune-related risk score.

It is worth noting that in most related studies, the authors considered patients with both LSCC and lung adenocarcinomas and patients with different disease stages, and with and without adjuvant therapy[27-29,31]. However, it is known that LSCC and lung adenocarcinoma are malignant tumors that differ in their biological characteristics and sensitivity to special methods of therapy. We believe that the heterogeneity of the groups can significantly affect the effectiveness of prognostic models since some markers may be associated with more aggressive characteristics of LC, for example, a higher stage of the disease and a low degree of tumor differentiation, while other factors may be associated with the sensitivity of tumor cells to systemic therapy. The latter fact is especially significant in locally advanced cancer, in which the sensitivity of tumor cells to treatment significantly affects disease prognosis. Given that lung adenocarcinoma and LSCC have different sensitivities to radiation therapy and chemotherapy, joint evaluation of these two histological types of NSCLC may significantly bias the study results. For example, the effectiveness of a particular prognostic model can be influenced by various factors, including the ratio of subgroups of patients with different histological subtypes of LC.

Unlike most related studies, our study included a fairly homogeneous cohort of patients with stage IIb-IIIa LSCC who underwent radical resection and adjuvant chemotherapy. In addition to the standard clinicopathological characteristics of LC, we also included the following markers in the analysis: The presence of LFFCT in the tumor stroma, microvessels in the tumor solid component and fragmentation of the tumor solid component. Their choice was based on the results of our previous studies. In addition, the presence of peritumoral retraction clefting and tumor spread through the AAS were included in the analysis. The connection of these factors with tumor progression and disease prognosis has been demonstrated in a number of studies. For example, a connection has been established between tumor spread through the AAS and the prognosis of lung adenocarcinoma[33]. In LSCC, tumor spread through the AAS was associated with

Table 3 Univariate and multifactorial logistic regression analysis

Characteristic	Univariate analysis OR (95%CI)	*P* value	Multivariate analysis OR (95%CI)	*P* value
Age (yr)				
< 60	1	-		
60-69	1.60 (0.51-5.02)	0.420		
≥ 70	1.24 (0.25-6.17)	0.789		
Tumor localization				
Peripheral	1	-		
Central	3.07 (0.85-11.07)	0.089		
Histology				
KSCC	1	-		
NKSCC	2.60 (0.84-8.07)	0.101		
Grade				
G1	1	-	1	-
G2	0.59 (0.13-2.54)	0.590	0.91 (0.44-4.56)	0.345
G3	6.00 (1.01-67.28)	0.021[1]	7.94 (1.08-135.81)	0.048[1]
T stage				
T1b	1	-		
T2a	1.62 (0.25-10.36)	0.622		
T2b	0.80 (0.08-8.47)	0.853		
T3	0.63 (0.10-3.95)	0.631		
N stage				
N0	1	-	1	-
N1	5.63 (1.27-24.86)	0.023[1]	5.67 (1.09-36.54)	0.048[1]
N2	3.75 (0.77-18.21)	0.101	6.30 (0.78-50.78)	0.08
Stage				
IIb	1	-		
IIIa	1.44 (0.50-4.14)	0.498		
DCs of "contact type"				
Presence	1	-		
Absence	1.61 (0.53-4.91)	0.404		
The capillaries in the tumor solid component				
Absence	1	-		
Presence	2.24 (0.74-6.79)	0.154		
LFFCT in the tumor stroma				
Absence	1	-	1	-
Presence	15.33 (3.56-66.04)	0.0002[1]	21.70 (4.27-110.38)	0.0002[1]
Fragmentation in the tumor solid component				
Absence	1	-	1	-
Presence	3.42 (1.06-11.03)	0.040[1]	2.53 (1.01-12.23)	0.049[1]
Peritumoral retraction clefting				
Absence	1	-		
Presence	0.41 (0.13-1.30)	0.13		

Tumor spread in the AAS		
Absence	1	-
Presence	1.08 (0.38-3.07)	0.883

[1]The differences between groups are statistically significant, $P < 0.05$.
AAS: Alveolar air spaces; DCs: Dilated capillaries; KSCC: Keratinizing squamous cell carcinoma; LFFCT: Loose, fine-fiber connective tissue in the tumor stroma; NKSCC: Nonkeratinizing squamous cell carcinoma.

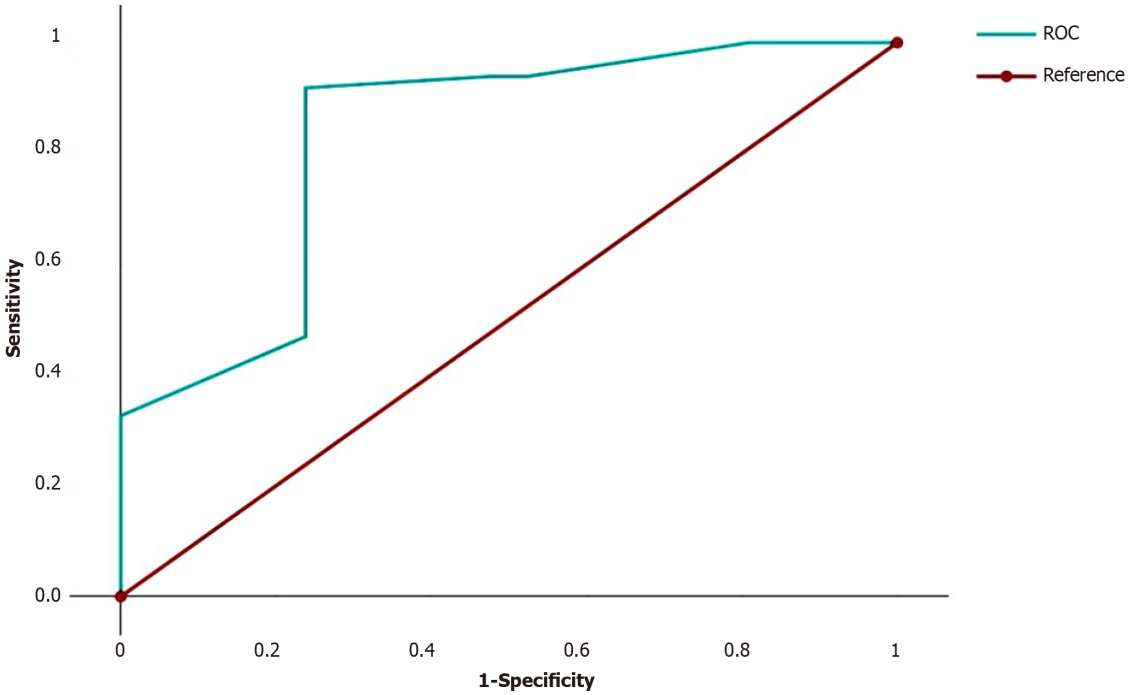

Figure 3 Receiver operating characteristic curves discriminating between cases of lung squamous cell carcinoma with and without disease recurrence. ROC: Receiver operating characteristic.

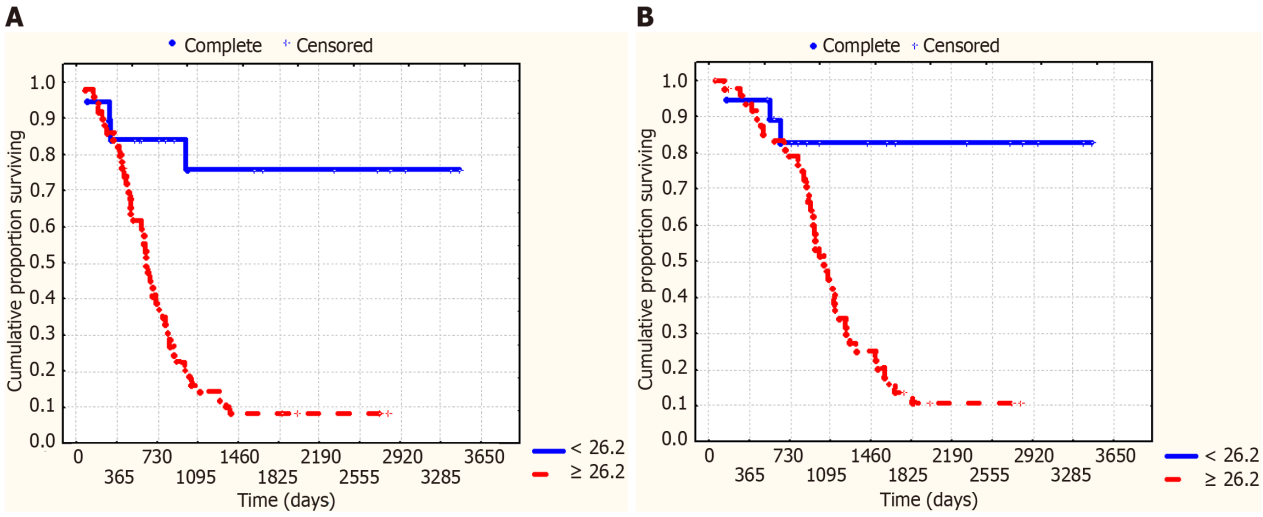

Figure 4 The relapse-free survival and overall survival curves for the patients with lung squamous cell carcinoma. A: RFS curves of patients with the sum of the odds ratios (ORs) less (red line) and more than 26.2 (blue line); B: Overall survival curves of lung squamous cell carcinoma patients with the sum of the ORs less (red line) and more than 26.2 (blue line).

disease relapse only at stage Ib[34]. In a mixed cohort of patients with stage Ib LC, a decrease in OS and RFS was also noted when the tumor spread through the AAS[35]. However, in this cohort, 67.7% of patients had lung adenocarcinoma, and only 32.3% of patients had LSCC.

The connection between peritumoral retraction clefting and the risk of disease relapse in patients with various malignancies, including breast cancer[36] and oral squamous cell carcinoma[37], has also been described. However, in LC, this phenomenon has practically not been studied. The analysis revealed 4 independent prognostic factors associated with the risk of LSCC recurrence, namely, tumor grade, N stage, the presence of LFFCT in the tumor stroma and fragmentation of the tumor solid component. The associations of tumor grade and N stage with the risk of LC relapse have been confirmed by numerous studies[20,30,38,39]. This dependence can be traced in various malignant neoplasms and is explained by the fact that low differentiation of tumor cells and a tendency to metastasize predominantly characterize the most aggressive subtypes of cancer, which are prone to recurrence. The most significant independent predictor of a high risk of LSCC recurrence was the presence of LFFCT in the tumor stroma (OR = 21.70, 95%CI = 4.27-110.38, P = 0.0002). LFFCT was most often detected in the peritumoral stroma and waswere rich in cells with large pale nuclei and weakly condensed euchromatin. We hypothesized that the described cells may be tumor-associated fibroblasts. It has been suggested that tumor-associated fibroblasts may originate from bone marrow mesenchymal stem cells, hematopoietic stem cells, tumor cells, and endothelial cells (via endothelial-mesenchymal transition) and may contribute not only to the invasion of malignant neoplasms but also to chemoresistance[40]. Previously, for stage I-IIA squamous cell carcinoma of the cervix, we found that LFFCT in the tumor stroma was significantly more common in patients with nonkeratinizing cancer (P = 0.008), a low degree of tumor differentiation (P = 0.05), a depth of tumor invasion greater than 1 cm (P = 0.007) and a high risk of disease recurrence (P = 0.004)[17].

Another independent predictor of a high risk of LSCC recurrence was fragmentation of the tumor solid component. We first described this phenomenon in squamous cell carcinoma of the cervix, defined as the presence of separate fibroblast-like cells in the solid component of the tumor. In an immunohistochemical study, the described cells showed nuclear expression of HIF-1α and Shail[17]. In squamous cell carcinoma of the cervix, the described phenomenon was significantly more often observed in the presence of disease relapse than in its absence (P = 0.01). We believe that fragmentation of the tumor solid component can promote the survival of tumor cells under hypoxic conditions through epithelial-mesenchymal transition. Notably, vessels in the tumor solid component, tumor spread through the AAS and peritumoral retraction clefting were not associated with the risk of stage IIb-IIIa LSCC recurrence.

CONCLUSION

Thus, independent predictors of a high risk of disease relapse in patients with stage IIb-IIIa LSCC after radical resection and adjuvant chemotherapy are tumor grade, N stage, the presence of LFFCT in the tumor stroma and fragmentation in the tumor solid component. The data obtained can be used to clarify the prognosis of the disease and to individualize treatment and observation. The advantages of the developed method for assessing the risk of recurrence of LSCC include its high sensitivity, accuracy and specificity, as well as ease of implementation; moreover, additional research is not needed since the determination of the presence of LFFCT in the tumor stroma and fragmentation in the tumor solid component is possible with routine histological examination by staining histological slides with Mayer hematoxylin and eosin. The main disadvantages of the present study are its single-center nature and the small number of patients. We believe that further research will not only improve the accuracy of LSCC prognosis but also improve our understanding of the mechanisms of tumor progression and drug resistance in this deadly disease.

ARTICLE HIGHLIGHTS

Research background

Establishing predictors of lung cancer (LC) recurrence is highly important both for determining the optimal treatment plan for the patients and for evaluating its effectiveness.

Research motivation

Assessment of different types of tumor microvessels, features of the tumor parenchyma and stroma can improve the accuracy of predicting the risk of lung squamous cell carcinoma (LSCC) recurrence.

Research objectives

This study aimed to establish predictors of disease recurrence after radical resection and adjuvant chemotherapy in patients with stage IIb-IIIa LSCC.

Research methods

This retrospective analysis of the treatment results of 69 patients with stage IIb-IIa LSCC who underwent radical surgery and received adjuvant chemotherapy. To establish independent predictors of the risk of LSCC recurrence, univariate and multivariate analyzes were performed, which included clinicopathological characteristics of LSCC and the features of tumor parenchyma and stroma.

Research results

The following independent predictors of a high risk of disease recurrence in patients with stage IIb-IIa LSCC were established: A low degree of tumor differentiation; metastases in regional lymph nodes; the presence of loose, fine-fiber connective tissue in the tumor stroma; and fragmentation of the tumor solid component.

Research conclusions

A method has been developed that allows us to identify a group of patients at high risk of disease recurrence and to adjust to ongoing treatment.

Research perspectives

Future studies will contribute to understanding the mechanisms of tumor progression and drug resistance of LSCC.

FOOTNOTES

Author contributions: Senchukova MA designed and performed the research, and wrote the paper; Kalinin EA acquired and analyzed the data and contributed substantially to the conception and design of the study; Volchenko NN participated in the discussion of related data, and revised and approved the final version; all the authors wrote and approved the final manuscript.

Institutional review board statement: This study was reviewed and approved by Ethics Committee of Orenburg State Medical University (Russia, Orenburg).

Informed consent statement: Patients were not required to give informed consent to the study because the study was retrospective and analysis used anonymous clinical data that were obtained after each patient agreed to treatment by written consent.

Conflict-of-interest statement: The authors have no financial relationships to disclose.

Data sharing statement: Data from patients included in the study in Statistica10 table or Excel table format can be provided upon request to the corresponding author at masenchukova@yandex.com.

STROBE statement: The authors have read the STROBE Statement – checklist of items, and the manuscript was prepared and revised according to the STROBE Statement – checklist of items.

Country/Territory of origin: Russia

ORCID number: Marina A Senchukova 0000-0001-8371-740X; Evgeniy A Kalinin 0000-0001-5329-3589; Nadezhda N Volchenko 0000-0002-4873-4455.

S-Editor: Liu JH
L-Editor: A
P-Editor: Zhao YQ

REFERENCES

1 **Sung H**, Ferlay J, Siegel RL, Laversanne M, Soerjomataram I, Jemal A, Bray F. Global Cancer Statistics 2020: GLOBOCAN Estimates of Incidence and Mortality Worldwide for 36 Cancers in 185 Countries. *CA Cancer J Clin* 2021; **71**: 209-249 [PMID: 33538338 DOI: 10.3322/caac.21660]
2 **Siegel RL**, Miller KD, Jemal A. Cancer statistics, 2020. *CA Cancer J Clin* 2020; **70**: 7-30 [PMID: 31912902 DOI: 10.3322/caac.21590]
3 **Siegel RL**, Miller KD, Fuchs HE, Jemal A. Cancer statistics, 2022. *CA Cancer J Clin* 2022; **72**: 7-33 [PMID: 35020204 DOI: 10.3322/caac.21708]
4 **Howlader N**, Forjaz G, Mooradian MJ, Meza R, Kong CY, Cronin KA, Mariotto AB, Lowy DR, Feuer EJ. The Effect of Advances in Lung-Cancer Treatment on Population Mortality. *N Engl J Med* 2020; **383**: 640-649 [PMID: 32786189 DOI: 10.1056/NEJMoa1916623]
5 **Pei Q**, Luo Y, Chen Y, Li J, Xie D, Ye T. Artificial intelligence in clinical applications for lung cancer: diagnosis, treatment and prognosis. *Clin Chem Lab Med* 2022; **60**: 1974-1983 [PMID: 35771735 DOI: 10.1515/cclm-2022-0291]
6 **Neumann JM**, Freitag H, Hartmann JS, Niehaus K, Galanis M, Griesshammer M, Kellner U, Bednarz H. Subtyping non-small cell lung cancer by histology-guided spatial metabolomics. *J Cancer Res Clin Oncol* 2022; **148**: 351-360 [PMID: 34839410 DOI: 10.1007/s00432-021-03834-w]
7 **Zhang T**, Guo Q, Zhang Y, Liu Z, Zhou S, Xu S. Meta-analysis of adjuvant chemotherapy *vs* surgery alone in T2aN0 stage IB non-small cell lung cancer. *J Cancer Res Ther* 2018; **14**: 139-144 [PMID: 29516976 DOI: 10.4103/jcrt.JCRT_862_17]
8 **Pathak R**, Goldberg SB, Canavan M, Herrin J, Hoag JR, Salazar MC, Papageorge M, Ermer T, Boffa DJ. Association of Survival With

Adjuvant Chemotherapy Among Patients With Early-Stage Non-Small Cell Lung Cancer With *vs* Without High-Risk Clinicopathologic Features. *JAMA Oncol* 2020; **6**: 1741-1750 [PMID: 32940636 DOI: 10.1001/jamaoncol.2020.4232]

9 **Thornblade LW**, Mulligan MS, Odem-Davis K, Hwang B, Waworuntu RL, Wolff EM, Kessler L, Wood DE, Farjah F. Challenges in Predicting Recurrence After Resection of Node-Negative Non-Small Cell Lung Cancer. *Ann Thorac Surg* 2018; **106**: 1460-1467 [PMID: 30031845 DOI: 10.1016/j.athoracsur.2018.06.022]

10 **Wei W**, Zhou J, Zhang Q, Liao DH, Liu QD, Zhong BL, Liang ZB, Zhang YC, Jiang R, Liu GY, Xu CY, Li Zhou H, Zhu SY, Yang N, Jiang W, Liu ZG. Postoperative intensity-modulated radiation therapy reduces local recurrence and improves overall survival in III-N2 non-small-cell lung cancer: A single-center, retrospective study. *Cancer Med* 2020; **9**: 2820-2832 [PMID: 32100444 DOI: 10.1002/cam4.2937]

11 **Mizuno T**, Arimura T, Kuroda H, Sakakura N, Yatabe Y, Sakao Y. Current outcomes of postrecurrence survival in patients after resection of non-small cell lung cancer. *J Thorac Dis* 2018; **10**: 1788-1796 [PMID: 29707333 DOI: 10.21037/jtd.2018.01.148]

12 **West H**, Hu X, Zhang S, Song Y, Chirovsky D, Gao C, Lerner A, Jiang A, Signorovitch J, Samkari A. Evaluation of disease-free survival as a predictor of overall survival and assessment of real-world burden of disease recurrence in resected early-stage non-small cell lung cancer. *J Manag Care Spec Pharm* 2023; **29**: 749-757 [PMID: 37404067 DOI: 10.18553/jmcp.2023.29.7.749]

13 **Rami-Porta R**. Future Perspectives on the TNM Staging for Lung Cancer. *Cancers (Basel)* 2021; **13** [PMID: 33920510 DOI: 10.3390/cancers13081940]

14 **Brascia D**, De Iaco G, Schiavone M, Panza T, Signore F, Geronimo A, Sampietro D, Montrone M, Galetta D, Marulli G. Resectable IIIA-N2 Non-Small-Cell Lung Cancer (NSCLC): In Search for the Proper Treatment. *Cancers (Basel)* 2020; **12** [PMID: 32722386 DOI: 10.3390/cancers12082050]

15 **Senchukova M**, Kiselevsky MV. The "cavitary" type of angiogenesis by gastric cancer. Morphological characteristics and prognostic value. *J Cancer* 2014; **5**: 311-319 [PMID: 24723973 DOI: 10.7150/jca.8716]

16 **Senchukova MA**, Nikitenko NV, Tomchuk ON, Zaitsev NV, Stadnikov AA. Different types of tumor vessels in breast cancer: morphology and clinical value. *Springerplus* 2015; **4**: 512 [PMID: 26405632 DOI: 10.1186/s40064-015-1293-z]

17 **Senchukova MA**, Makarova EV, Shurygina EI, Volchenko NN. Morphological Characteristics and Clinical Significance of Different Types of Tumor Vessels in Patients with Stages I-IIA of Squamous Cervical Cancer. *J Oncol* 2020; **2020**: 3818051 [PMID: 32849870 DOI: 10.1155/2020/3818051]

18 **Huang Y**, Liu Z, He L, Chen X, Pan D, Ma Z, Liang C, Tian J. Radiomics Signature: A Potential Biomarker for the Prediction of Disease-Free Survival in Early-Stage (I or II) Non-Small Cell Lung Cancer. *Radiology* 2016; **281**: 947-957 [PMID: 27347764 DOI: 10.1148/radiol.2016152234]

19 **Torrente M**, Sousa PA, Guerreiro GR, Franco F, Hernández R, Parejo C, Sousa A, Campo-Cañaveral JL, Pimentão J, Provencio M. Clinical factors influencing long-term survival in a real-life cohort of early stage non-small-cell lung cancer patients in Spain. *Front Oncol* 2023; **13**: 1074337 [PMID: 36910629 DOI: 10.3389/fonc.2023.1074337]

20 **Yu X**, Wang F, Yang L, Ma K, Guo X, Wang L, Du L, Yu X, Lin S, Xiao H, Sui Z, Zhang L, Yu Z. Development and validation of web-based dynamic nomograms predictive of disease-free and overall survival in patients who underwent pneumonectomy for primary lung cancer. *PeerJ* 2023; **11**: e15938 [PMID: 37637160 DOI: 10.7717/peerj.15938]

21 **Kirienko M**, Sollini M, Corbetta M, Voulaz E, Gozzi N, Interlenghi M, Gallivanone F, Castiglioni I, Asselta R, Duga S, Soldà G, Chiti A. Radiomics and gene expression profile to characterise the disease and predict outcome in patients with lung cancer. *Eur J Nucl Med Mol Imaging* 2021; **48**: 3643-3655 [PMID: 33959797 DOI: 10.1007/s00259-021-05371-7]

22 **Libling WA**, Korn R, Weiss GJ. Review of the use of radiomics to assess the risk of recurrence in early-stage non-small cell lung cancer. *Transl Lung Cancer Res* 2023; **12**: 1575-1589 [PMID: 37577298 DOI: 10.21037/tlcr-23-5]

23 **Kwon W**, Howard BA, Herndon JE, Patz EF Jr. FDG Uptake on Positron Emission Tomography Correlates with Survival and Time to Recurrence in Patients with Stage I Non-Small-Cell Lung Cancer. *J Thorac Oncol* 2015; **10**: 897-902 [PMID: 25811445 DOI: 10.1097/JTO.0000000000000534]

24 **Blumenthaler AN**, Hofstetter WL, Mehran RJ, Rajaram R, Rice DC, Roth JA, Sepesi B, Swisher SG, Vaporciyan AA, Walsh GL, Strange CD, Antonoff MB. Preoperative Maximum Standardized Uptake Value Associated With Recurrence Risk in Early Lung Cancer. *Ann Thorac Surg* 2022; **113**: 1835-1844 [PMID: 34252403 DOI: 10.1016/j.athoracsur.2021.06.017]

25 **Zhang Y**, Zheng D, Xie J, Li Y, Wang Y, Li C, Xiang J, Zhang Y, Hu H, Sun Y, Chen H. Development and Validation of Web-Based Nomograms to Precisely Predict Conditional Risk of Site-Specific Recurrence for Patients With Completely Resected Non-small Cell Lung Cancer: A Multiinstitutional Study. *Chest* 2018; **154**: 501-511 [PMID: 29758181 DOI: 10.1016/j.chest.2018.04.040]

26 **Mohamed SK**, Walsh B, Timilsina M, Torrente M, Franco F, Provencio M, Janik A, Costabello L, Minervini P, Stenetorp P, Novác˘ek V. On Predicting Recurrence in Early Stage Non-small Cell Lung Cancer. *AMIA Annu Symp Proc* 2021; **2021**: 853-862 [PMID: 35308971]

27 **Jiao Y**, Wei J, Li Z, Zhou J, Liu Y. High FHL2 mRNA expression and its prognostic value in lung cancer. *Aging (Albany NY)* 2022; **14**: 7986-8000 [PMID: 36227138 DOI: 10.18632/aging.204328]

28 **Zheng D**, Wang Y, Li Y, Sun Y, Chen H. Predicting prognosis of post-chemotherapy patients with resected IIIA non-small cell lung cancer. *J Thorac Dis* 2018; **10**: 4186-4194 [PMID: 30174863 DOI: 10.21037/jtd.2018.06.160]

29 **Merritt RE**, Abdel-Rasoul M, Fitzgerald M, D'Souza DM, Kneuertz PJ. Nomograms for Predicting Overall and Recurrence-free Survival From Pathologic Stage IA and IB Lung Cancer After Lobectomy. *Clin Lung Cancer* 2021; **22**: e574-e583 [PMID: 33234491 DOI: 10.1016/j.cllc.2020.10.009]

30 **Xu Y**, Wan B, Zhu S, Zhang T, Xie J, Liu H, Zhan P, Lv T, Song Y. Effect of Adjuvant Chemotherapy on Survival of Patients With 8th Edition Stage IB Non-Small Cell Lung Cancer. *Front Oncol* 2021; **11**: 784289 [PMID: 35155190 DOI: 10.3389/fonc.2021.784289]

31 **Moon Y**, Choi SY, Park JK, Lee KY. Prognostic factors in stage IB non-small cell lung cancer according to the 8(th) edition of the TNM staging system after curative resection. *J Thorac Dis* 2019; **11**: 5352-5361 [PMID: 32030253 DOI: 10.21037/jtd.2019.11.71]

32 **Wu XR**, Peng HX, He M, Zhong R, Liu J, Wen YK, Li CC, Li JF, Xiong S, Yu T, Zheng HB, Chen YH, He JX, Liang WH, Cai XY. Macrophages-based immune-related risk score model for relapse prediction in stage I-III non-small cell lung cancer assessed by multiplex immunofluorescence. *Transl Lung Cancer Res* 2022; **11**: 523-542 [PMID: 35529784 DOI: 10.21037/tlcr-21-916]

33 **Gutierrez-Sainz L**, López-Muñoz S, Cruz-Castellanos P, Higuera O, Esteban-Rodríguez MI, Losantos-García I, De Castro-Carpeño J. Retrospective analysis of the prognostic implications of tumor spread through air spaces in lung adenocarcinoma patients treated with surgery. *ESMO Open* 2022; **7**: 100568 [PMID: 36007450 DOI: 10.1016/j.esmoop.2022.100568]

34 **Yanagawa N**, Shiono S, Endo M, Ogata SY. Tumor spread through air spaces is a useful predictor of recurrence and prognosis in stage I lung squamous cell carcinoma, but not in stage II and III. *Lung Cancer* 2018; **120**: 14-21 [PMID: 29748009 DOI: 10.1016/j.lungcan.2018.03.018]

35 **Chen Z**, Wu X, Fang T, Ge Z, Liu J, Wu Q, Zhou L, Shen J, Zhou C. Prognostic impact of tumor spread through air spaces for T2aN0 stage IB non-small cell lung cancer. *Cancer Med* 2023; **12**: 15246-15255 [PMID: 37278137 DOI: 10.1002/cam4.6211]

36 **Li W**, Jia H, Wang S, Guo X, Zhang X, Zhang L, Wen HY, Fu L. The presence of retraction clefts correlates with lymphovascular invasion and lymph node metastasis and predicts poor outcome: Analysis of 2497 breast cancer patients. *Ann Diagn Pathol* 2022; **61**: 152047 [PMID: 36156357 DOI: 10.1016/j.anndiagpath.2022.152047]

37 **Jain D**, Tikku G, Bhadana P, Dravid C, Grover RK. The Impact of Peritumoral Retraction Clefting & Intratumoral Eosinophils on Overall Survival in Oral Squamous Carcinoma Patients. *Pathol Oncol Res* 2019; **25**: 183-189 [PMID: 29047016 DOI: 10.1007/s12253-017-0328-x]

38 **Zhang CC**, Hou RP, Feng W, Fu XL. Lymph Node Parameters Predict Adjuvant Chemoradiotherapy Efficacy and Disease-Free Survival in Pathologic N2 Non-Small Cell Lung Cancer. *Front Oncol* 2021; **11**: 736892 [PMID: 34604073 DOI: 10.3389/fonc.2021.736892]

39 **Wang W**, Zhou J. A Nomogram to Predict the Overall Survival of Patients With Resected T1-2N0-1M0 Non-Small Cell Lung Cancer and to Identify the Optimal Candidates for Adjuvant Chemotherapy in Stage IB or IIA Non-Small Cell Lung Cancer Patients. *Cancer Control* 2023; **30**: 10732748231197973 [PMID: 37703536 DOI: 10.1177/10732748231197973]

40 **Yamamoto Y**, Kasashima H, Fukui Y, Tsujio G, Yashiro M, Maeda K. The heterogeneity of cancer-associated fibroblast subpopulations: Their origins, biomarkers, and roles in the tumor microenvironment. *Cancer Sci* 2023; **114**: 16-24 [PMID: 36197901 DOI: 10.1111/cas.15609]

World Journal of Experimental Medicine

Submit a Manuscript: https://www.f6publishing.com

World J Exp Med 2024 March 20; 14(1): 88541

DOI: 10.5493/wjem.v14.i1.88541

ISSN 2220-315x (online)

ORIGINAL ARTICLE

Clinical Trials Study

Impact of primary percutaneous coronary intervention on ST-segment elevation myocardial infarction patients: A comprehensive analysis

Eza Nawzad Saeed, Abdulsatar Kamil Faeq

Specialty type: Health care sciences and services

Provenance and peer review: Unsolicited article; Externally peer reviewed.

Peer-review model: Single blind

Peer-review report's scientific quality classification

Grade A (Excellent): 0
Grade B (Very good): B
Grade C (Good): 0
Grade D (Fair): 0
Grade E (Poor): 0

P-Reviewer: He L, China

Received: September 27, 2023
Peer-review started: September 27, 2023
First decision: January 2, 2024
Revised: January 8, 2024
Accepted: February 2, 2024
Article in press: February 2, 2024
Published online: March 20, 2024

Eza Nawzad Saeed, Abdulsatar Kamil Faeq, Department of Medicine, Hawler Medical University, Erbil 44001, Kurdistan, Iraq

Corresponding author: Eza Nawzad Saeed, MBChB, Researcher, Department of Medicine, Hawler Medical University, Erbil - IRAQ 44001, Erbil 44001, Kurdistan, Iraq. demolali542@gmail.com

Abstract

BACKGROUND

Myocardial infarction, particularly ST-segment elevation myocardial infarction (STEMI), is a key global mortality cause. Our study investigated predictors of mortality in 96 STEMI patients undergoing primary percutaneous coronary intervention at Erbil Cardiac Center. Multiple factors were identified influencing in-hospital mortality. Significantly, time from symptom onset to hospital arrival emerged as a decisive factor. Consequently, our study hypothesis is: "Reducing time from symptom onset to hospital arrival significantly improves STEMI prognosis."

AIM

To determine the key factors influencing mortality rates in STEMI patients.

METHODS

We studied 96 consecutive STEMI patients undergoing primary percutaneous coronary intervention (PPCI) at the Erbil Cardiac Center. Their clinical histories were compiled, and coronary evaluations were performed *via* angiography on admission. Data included comorbid conditions, onset of cardiogenic shock, complications during PPCI, and more. Post-discharge, one-month follow-up assessments were completed. Statistical significance was set at $P < 0.05$.

RESULTS

Our results unearthed several significant findings. The in-hospital and 30-d mortality rates among the 96 STEMI patients were 11.2% and 2.3% respectively. On the investigation of independent predictors of in-hospital mortality, we identified atypical presentation, onset of cardiogenic shock, presence of chronic kidney disease, Thrombolysis In Myocardial Infarction grades 0/1/2, triple vessel disease, ventricular tachycardia/ventricular fibrillation, coronary dissection, and

the no-reflow phenomenon. Specifically, the recorded average time from symptom onset to hospital arrival amongst patients who did not survive was significantly longer (6.92 ± 3.86 h) compared to those who survived (3.61 ± 1.67 h), $P < 0.001$. These findings underscore the critical role of timely intervention in improving the survival outcomes of STEMI patients.

CONCLUSION
Our results affirm that early hospital arrival after symptom onset significantly improves survival rates in STEMI patients, highlighting the critical need for prompt intervention.

Key Words: Percutaneous coronary intervention; Impact analysis, Segment elevation; Erbil

Core Tip: Myocardial infarction, particularly the ST-segment elevation myocardial infarction (STEMI) subtype, is a leading global cause of mortality. Primary percutaneous coronary intervention is the preferred treatment, but its success depends on various factors. In a study of 96 consecutive STEMI patients at Erbil Cardiac Center, factors predicting in-hospital mortality included atypical presentation, cardiogenic shock, chronic kidney disease, TIMI grades 0/1/2, triple vessel disease, ventricular tachycardia/ventricular fibrillation, coronary dissection, and no-reflow phenomenon. Significantly, the time from symptom onset to hospital arrival emerged as a critical determinant in improving STEMI prognosis.

Citation: Saeed EN, Faeq AK. Impact of primary percutaneous coronary intervention on ST-segment elevation myocardial infarction patients: A comprehensive analysis. *World J Exp Med* 2024; 14(1): 88541
URL: https://www.wjgnet.com/2220-315x/full/v14/i1/88541.htm
DOI: https://dx.doi.org/10.5493/wjem.v14.i1.88541

INTRODUCTION

Myocardial infarction (MI), a type of coronary heart disease, is a leading cause of morbidity and mortality. This disease causes more than 15% of deaths in the world, most of them have non-ST-segment elevation MI than ST-segment MI (STEMI), men are more prone to develop MI than women, several modifiable risk factors are responsible for more than 90% of MI, these factors include hyperlipidemia, diabetes mellitus (DM), smoking, heavy alcohol consumption, physical inactivity, hypertension, psychosocial stress and a diet low in fruits and vegetables[1]. Factors that may lead to ST-segment elevation include infarction of the cardiac muscles due to occlusion of one vessel with a supply where there is obstruction, and this usually happens because of plaque rupture erosion, fissuring, or dissection, which leads to an obstructing thrombus. ST-elevation MI can be defined as a clinical syndrome in which the characteristic symptoms of MI associated with electrocardiogram (ECG) finding of ST-segment elevation in ECG associated later with elevation in biomarkers of myocardial necrosis, therefore a diagnostic ST-segment elevation is a new S.T. elevation at the J point in at least two contiguous leads > 2 mm (0.2 mV) in men or > 1.5 mm (0.15 mV) in women in leads V2-V3 and of > 1 mm (0.1mV) in other contiguous chest or limb lead[2]. It's found that timely primary percutaneous coronary intervention (PPCI) is the best treatment for ST-segment elevation MI[3]. The critical point is the time; most studies show that the preference of primary percutaneous coronary intervention (PCI) over fibrinolytic therapy is just approximately 2 h, and this depends on the duration of ischemia and the number of myocardial muscles involved with ischemia in some countries, which was named as door to balloon time has been reduced to less than 1 h[4]. At the same, some studies show that if PCI is delayed after the onset of the symptoms, the outcome will be poor; others show that delay in performing PPCI may be only significant within the first 2 to 3 h after the onset of the symptoms since this is the time where myocardial salvage is most fabulous, or in those who are risky group such as in patients with cardiogenic shock. In general, studies that didn't confirm this relationship had already depended on a small sample size[5]. This work aims to comprehensively evaluate the outcomes of PPCI in patients diagnosed with STEMI. To achieve this aim, we have set the following specific objectives. Firstly, assess the impact of PPCI on the improvement of cardiac function in patients diagnosed with STEMI, and determine and report the mortality rate among patients undergoing PPCI for STEMI. Investigate and establish associations between various risk factors and the overall outcomes of PPCI in patients diagnosed with STEMI, Analyze the association between the onset of STEMI symptoms and the timing of PPCI procedures, and their implications on patient prognosis and finally, explore correlations between the type of culprit vessel, the number of affected vessels, the occurrence of complications, and the ultimate clinical outcomes in patients with STEMI undergoing PPCI.

MATERIALS AND METHODS

The type of study in this research is an interventional study; after selecting the samples to be included according to specific criteria, the intervention will be the PCI procedure. Ninety-six consecutive cases were selected according to inclusion criteria. This study will be conducted in the Cardiac Center in Erbil city in Kurdistan Regional Government. The time frame for this study was more than four months.

Sampling

A consecutive sampling technique was used for this study because of time restriction and availability of cases with the specified criteria; in addition to that, every facility regarding investigation, treatment, and intervention is available in this center. For these reasons, this sampling technique was used.

Inclusion criteria

Cases present with myocardial infarction and apparent ST elevation on electrocardiography records. Case admitted to the hospital within the first 48 h of symptoms. The age of patients should be between 30 and 90 years. The patient agrees to participate in the study and sign the consent form.

Exclusion criteria

Age that is out of the range described. Cases received thrombolytic medications. Patients refused to participate in the study.

Procedure technique

Percutaneous coronary intervention is a surgical procedure used when there is a narrowing or stenosis in one of the coronary arteries that supply blood to the heart; this process includes coronary angioplasty and stenting, which is the process of inserting a permanent drug-eluting stent.

Tools used in the procedure: ECG; Echocardiography; Angiography and Angioplasty.

RESULTS

From the total number of patients enrolled in this study, 13 died, while eleven died during hospitalization before discharge and two died after discharge within one month of follow-up. Male to female ratio was 5:1, and no significant correlation was established between death and gender (Table 1) and age group (Table 2).

Table 1 Association of deaths during hospitalization and within one month after discharge with gender

Deaths		Gender			
		Female, %	Male, %	Total, %	*P* value
Death category	Deaths within one month	1	1	2	0.423[1]
		50.0	50.0	100.0	
	Deaths during hospitalization	2	9	11	
		18.2	81.8	100.0	
Total		3	10	13	
		23.1	76.9	100.0	

[1]Fisher's exact test.

More than one quarter (25%) of patients were hospitalized within the initial 2 h of symptom onset, up until balloon inflation, and the rest were admitted in more than 2 h, as shown in Table 3. There was a statistically significant association between total arrival time till balloon inflation and mortality. Therefore, the earlier the patient arrives, the better the outcome with a *P* value of < 0.0184. The time from symptom to hospital and door to balloon time alone was insignificant.

Most of the patients admitted with typical ischemic chest pain (89 cases), and 7 cases presented with an atypical presentation; there was a statistically significant association between syncope (8 cases), Cardiac arrest (1 case), and Ventricular arrhythmias (9 cases) with deaths inside the hospital as shown in Table 4.

Although smoking is one of the essential factors that are usually associated with deaths, in this study, there was no statistically significant association with this factor; on the other hand, dyslipidemia showed a strong association with deaths inside hospitals with a *P* value < 0.001. Chronic kidney disease was also significantly associated with in-hospital deaths, as shown in Table 5. On the other hand, outside hospital deaths, only chronic kidney disease showed a significant

Table 2 Association between age groups and deaths

Age		Death category			
		Deaths within one month, %	Deaths during hospitalization, %	Total, %	*P* value
Age groups	40-49	0	2	2	1.000[1]
		0.0	100.0	100.0	
	50-59	1	3	4	
		25.0	75.0	100.0	
	60-69	1	2	3	
		33.3	66.7	100.0	
	70-79	0	2	2	
		0.0	100.0	100.0	
	80-90	0	2	2	
		0.0	100.0	100.0	
Total		2	11	13	
		15.4	84.6	100.0	

[1]Fisher's exact test.

Table 3 Association of deaths inside and outside hospitals with time from symptom till balloon inflation

Time interval		Death category			
		Deaths till one month, %	Survival till one month, %	Total, %	*P* value
Arrival in hours	< 2	0	25	25	0.0184[1]
		0.00	30.1	26.4	
	> 2	13	58	71	
		100.0	69.87	73.95	
Total		13	83	96	
		100.0	100.0	100.0	

[1]Fisher's exact test.

association with deaths after PCI with a *P* value of < 0.002 (Table 5).

Regarding the in-hospital deaths due to cardiogenic shock systolic blood pressure is less than 90, there was a statistically significant association with this variable with a *P* value of 0.004 (Table 6). Also, deaths within one month after discharge had a significant association with cardiogenic shock with a *P* value of 0.024 (Table 6).

More than half of patients had high levels of HbA1c, and nearly 78% of cases had an average level of creatinine. However, only creatinine level had a statistically significant association with deaths with a *P* value of 0.014 (Table 7).

Regarding angiographic results, most deaths inside the hospital happened due to 3 vessel disease (3VD) with a statistically significant association, a *P* value of < 0.001, and the minor disease association was a single vessel with a *P* value of < 0.05. Central stem disease was also associated with deaths inside the hospital with a *P* value of < 0.05 (Table 8). However for deaths outside the hospital, only 3VD was associated with deaths with a *P* value < 0.05 (Table 8).

The angiographic results regarding the culprit's vessels showed that the left circumflex, left anterior descending artery, and obtuse marginal were significantly associated with deaths inside the hospital (Table 9). On the other hand, only the Left anterior descending artery was significantly associated with deaths outside the hospital within one month of discharge (Table 9).

On looking at the complications associated with deaths inside the hospital, it was found that many complications were significantly associated with death except temporary pacemakers and contrast nephropathy. Most of these associations were highly significant, with a *P* value of < 0.001, as shown in Table 10. While for deaths outside the hospital, the insignificant complications were coronary dissection and temporary pacemakers, other complications were statistically significant with a *P* value < 0.05, as shown in Table 10.

Table 4 Atypical presentation of patients

Symptoms	Status	In-hospital deaths			
		Survivals, %	Deaths, %	Total, %	*P* value
Syncope	Outside hospital (1 month)	7	1	8	0.180[1]
		8.4	50.0[2]	9.4	
	Inside hospital	8	5	13	0.006[1]
		9.40	45.50	13.50	
Cardiac arrest	Outside hospital (1 month)	1	0	1	1.000[1]
		1.2	0.0	1.2	
	Inside hospital	1	2	3	0.029[1]
		1.20	20.00	3.20	
Ventricular Arrhythmia	Outside hospital (1 month)	8	1	9	0.204[1]
		9.8	50.0	10.7	
	Inside hospital	9	4	13	0.030[1]
		10.70	40.00	13.80	
Typical pain	Outside hospital (1 month)	78	2	80	1.000[1]
		94.0	100.0	94.1	
	Inside hospital	80	9	89	0.182[1]
		94.10	81.80	92.70	

[1]Fisher's exact test.
[2]Column percent.

DISCUSSION

In this study, the hospital mortality rate of STEMI patients who underwent PPCI was (11.4 %) and the mortality rate from discharge to one month was (2.35%). However, in comparison to another study done in 2021, the in-hospital mortality was slightly lower (9.2%), and 30-d mortality was (7.7%)[6], which is slightly higher than our study since only one-quarter of our patients were admitted to the hospital within first 2 h from symptoms till needle insertion and the rest over 2 h as shown in Table 3. The time to start treatment is the most important determinant of mortality, and it consists of the time from symptom to initiation of reperfusion therapy. This embraces the time from symptom to first medical contact and the time from hospital arrival to initiation of reperfusion[7]. Notably, there was a statistically significant association between the time from starting symptoms to balloon inflation and mortality. This is due to the lack of a standard emergency medical services system by telephone and public awareness. Nearly all patients were referred from other hospitals, especially emergency hospitals in Erbil, which are not PCI-capable hospitals, and no one received thrombolysis even those delayed more than six hours. This may be due to the delay in reaching the emergency hospital. The other explanation for higher in-hospital mortality is that primary PCI was done through a femoral rather than radial approach; the radial method, as compared to the femoral access approach, is associated with a lower mortality rate (2.7% *vs* 4.7%)[8].

This study aims to identify both risk factors and variables influencing mortality among patients who have undergone primary PCI for STEMI. Men have five-fold higher than females, and sex has shown no significant effect on mortality. However, death in STEMI patients occurs more in males, though some studies have found higher mortality rates in women than men[3]. The lack of elevated risk among our female patients underscores the advantages of primary PCI for women.

Based on our results, in terms of STEMI and mortality, it was mostly related to middle-aged patients; with increased age, the risk for death becomes higher in patients who experienced a myocardial infarction[9]. This difference is justifiable Since very old patients with STEMI who did not undergo primary PCI may not reach PCI-capable hospitals and be prescribed pharmacological treatment instead.

In this study, we found that the presentation of patients to the hospital was critical; those patients who presented with typical ischemic chest pain were associated with a better survival rate, but patients who presented with syncope, ventricular arrhythmia, cardiogenic shock, and cardiac arrest were significantly associated with mortality[10].

In primary PCI patients, we observed diabetic state enhanced the probability of STEMI. In essence, diabetes did not augment mortality in hospitals and from hospital discharge to one month. Also, uncontrolled diabetes mellitus increases mortality in STEMI patients who underwent primary PCI after putting the stent; however, trials attempting to decrease macrovascular events have been unsuccessful[11]. However, better glycemic control has not led to reduction in the occurrence of cardiovascular events while ACCORD trial[11], It was linked to heightened risks of all-cause mortality and

Table 5 Risk factors associated with deaths inside and outside the hospital within one month of discharge

Symptoms	Status	Deaths in hospital				Deaths outside the hospital within one month			
		Survivals, %	Deaths, %	Total, %	*P* value	Survivals, %	Deaths, %	Total, %	*P* value
Smoking	No	40	5	45	0.92	38	2	40	0.218
		47.10	45.50	46.90		45.80	100.00	47.10	
	Yes	45	6	51		45	0	45	
		52.90	54.50	53.10		54.20	0.00	52.90	
H.T.	No	41	4	45	0.458	41	0	41	0.495
		48.20	36.40	46.90		49.40	0.00	48.20	
	Yes	44	7	51		42	2	44	
		51.80	63.60	53.10		50.60	100.00	51.80	
D.M.	No	49	3	52	0.057	48	1	49	0.671
		57.60	27.30	54.20		57.80	50.00	57.60	
	Yes	36	8	44		35	1	36	
		42.40	72.70	45.80		42.20	50.00	42.40	
Dyslipidemia	No	74	1	75	< 0.001	72	2	74	0.757
		87.10	9.10	78.10		86.70	100.00	87.10	
	Yes	11	10	21		11	0	11	
		12.90	90.90	21.90		13.30	0.00	12.90	
Family history of CAD	No	66	7	73	0.452	65	1	66	0.399
		77.60	63.60	76.00		78.30	50.00	77.60	
	Yes	19	4	23		18	1	19	
		22.40	36.40	24.00		21.70	50.00	22.40	
CKD	No	81	8	89	0.031	81	0	81	0.002
		95.30	72.70	92.70		97.60	0.00	95.30	
	Yes	4	3	7		2	2	4	
		4.70	27.30	7.30		2.40	100.00	4.70%	

CAD: Coronary artery disease; H.T.: Hupertension; D.M.: Diabetes mellitus; CKD: Chronic kidney disease.

Table 6 Association between cardiogenic shock (systolic blood pressure < 90) deaths inside and outside the hospital within one month of discharge

STEMI		Deaths in hospital				Deaths out-hospital one month			
		Survivals, %	Deaths, %	Total, %	*P* value	Survivals, %	Deaths, %	Total, %	*P* value
Cardiogenic Shock (SBP less than 90)	No	84	8	92	0.004	83	1	84	0.024
		98.80	72.70	95.80		100.00	50.00	98.80	
	Yes	1	3	4		0	1	1	
		1.20	27.30	4.20		0.00	50.00	1.20	
Total		85	11	96		83	2	85	
		100.00	100.00	100.00		100.00	100.00	100.00	

STEMI: ST-segment elevation myocardial infarction; SBP: Systolic blood pressure.

Table 7 Association between lab investigations and deaths inside and outside the hospital within one month of discharge

Lab results	Status	Deaths in-hospital				Deaths out hospital one month			
		Survivals, %	Deaths, %	Total, %	*P* value	Survivals, %	Deaths, %	Total, %	*P* value
Hb category	Low	24	3	27	0.757	22	2	24	0.208
		32.40	37.50	32.90		30.60	100.00	32.40	
	Normal	40	5	45		40	0	40	
		54.10	62.50	54.90		55.60	0.00	54.10	
	High	10	0	10		10	0	10	
		13.50	0.00	12.20		13.90	0.00	13.50	
WBC category	Low	2	1	3	0.44	2	0	2	0.533
		2.40	9.10	3.10		2.40	0.00	2.40	
	Normal	34	4	38		34	0	34	
		40.00	36.40	39.60		41.00	0.00	40.00	
	High	49	6	55		47	2	49	
		57.60	54.50	57.30		56.60	100.00	57.60	
HbA1c category	Low	32	4	36	0.539	32	0	32	0.624
		37.60	36.40	37.50		38.60	0.00	37.60	
	Normal	11	0	11		11	0	11	
		12.90	0.00	11.50		13.30	0.00	12.90	
	High	42	7	49		40	2	42	
		49.40	63.60	51.00		48.20	100.00	49.40	
S. Cr. category	Low	6	1	7	0.01	6	0	6	0.014
		7.10	9.10	7.30		7.20	0.00	7.10	
	Normal	70	5	75		70	0	70	
		82.40	45.50	78.10		84.30	0.00	82.40	
	High	9	5	14		7	2	9	
		10.60	45.50	14.60		8.40	100.00	10.60	

Hb: Hemoglobin; WBC: White blood counts.

cardiovascular-related mortality. Notably, on admission, HbA1c levels had no association with in-hospital mortality and short-term all-cause mortality outcomes in diabetic patients with STEMI undergoing primary PCI. Still, they affected long-term outcomes and major cardiovascular events, as demonstrated in another study[12].

Another major risk factor for coronary artery disease is smoking. The contribution of smoking to the prevalence of mortality rates after primary PCI is also a cause for attention. The case in this study is that smoking had no detrimental effects on mortality. Nevertheless, other studies have shown superior reperfusion following PCI in smokers. In contrast, high arterial blood pressure is associated with CAD and the incidence of complications after ACS[13,14]. However, we found that hypertension increases the risk of STEMI more than other risk factors but does not affect mortality. Furthermore, hyperlipidemia is a risk factor for coronary artery disease; it significantly affected the incidence of mortality in this study[15].

A strong association was demonstrated between mortality of STEMI in patients undergoing primary PCI and chronic kidney disease, and about half of them developed cardiogenic shock, were admitted to the intensive care unit (ICU) and associated with three-vessel disease, and had higher cardiovascular risk factors like hypertension, diabetes mellitus, and hyperlipidemia in contrast to those patients without chronic kidney diseases. The same results have appeared compared to a study of the outcome of STEMI patients with chronic kidney disease treated with primary PCI[15].

Low hemoglobin level before primary PCI was associated with a higher mortality rate, anemia was associated with cardiac arrest, congestive heart failure, cardiogenic shock and death, and anemia causing hypoxia during myocardial infarction. This hypoxia makes patients more vulnerable to spasms and arrhythmias[16]. However in this study, there was no association between anemia and mortality because the hemoglobin of all our patients was above 11 g/dL, so it was mild anemia.

Table 8 Number of vessels involved with deaths inside hospital and deaths outside hospital within one month of discharge

Number of vessels	Status	Deaths in-hospital				Deaths out hospital one month			
		Survivals, %	Deaths, %	Total, %	*P* value	Survivals, %	Deaths, %	Total, %	*P* value
SVD	No	37	10	47	0.003	35	2	37	0.187
		43.50	90.90	49.00		42.20	100.00	43.50	
	Yes	48	1	49		48	0	48	
		56.50	9.10	51.00		57.80	0.00	56.50	
2VD	No	62	9	71	0.723	60	2	62	1
		72.90	81.80	74.00		72.30	100.00	72.90	
	Yes	23	2	25		23	0	23	
		27.10	18.20	26.00		27.70	0.00	27.10	
3VD	No	71	3	74	< 0.001	71	0	71	0.025
		83.50	27.30	77.10		85.50	0.00	83.50	
	Yes	14	8	22		12	2	14	
		16.50	72.70	22.90		14.50	100.00	16.50	
Central stem disease (> 50%)	No	82	8	90	0.019	80	2	82	1
		96.50	72.70	93.80		96.40	100.00	96.50	
	Yes	3	3	6		3	0	3	
		3.50	27.30	6.30		3.60	0.00	3.50	

SVD: Singular-valued decomposition; VD: Vessel disease.

TIMI flow is one of the critical factors in determining the outcome of PCI in patients with STEMI. Good TIMI flows at the time of angiography, and PCI is a determinant of mortality in patients undergoing primary PCI. Patients with TIMI flow grade 3 are expected to have higher survival rates and fewer complications following primary PCI[17,18]. In the present study, TIMI flow grade less than three was associated with increased mortality in patients receiving primary PCI for STEMI. A significant relationship was shown between the number of involved vessels and outcome in patients who underwent primary PCI in STEMI[19]. However, the left circumflex and anterior descending arteries are affected in-hospital mortality following STEMI. This discovery validates the significance of the involvement of these arteries in myocardial infarction patients. Additionally, some studies have indicated that multi-vessel, especially 3VD and left central steam involvement in patients, increases the risk of primary PCI mortality. It is compatible with the results of this study[19].

Previous studies have proven that ventricular arrhythmia was significantly associated with in-hospital and thirty-day mortality rates[20]. Moreover, mortality from hospital discharge to one month was strongly affected by the three-vessel disease, chronic kidney disease, left anterior descending artery, cardiogenic shock, especially those are on positive inotropes and admitted to ICU on mechanical ventilation, intubated patients, patients who present to hospital with ventricular tachycardia/ventricular fibrillation or a ventricular arrhythmia that happened in Cath-lab and no-reflow less than class 2, respectively affect mortality.

CONCLUSION

This study thoroughly examines the effects of PPCI on patients diagnosed with STEMI. Through our analysis, we have uncovered numerous parameters that exert a substantial impact on patient outcomes.

The results of our study highlight the significance of crucial factors linked to the prognosis of patients undergoing percutaneous coronary intervention. Several characteristics that can be considered include delayed presentation, syncope as the initial symptom, ventricular arrhythmias, cardiogenic shock, cardiac arrest, hyperlipidemia, and chronic kidney disease. In addition, the identification of the particular coronary arteries affected, such as the left anterior descending artery, left circumflex artery or left main stem, as well as the assessment of the amount of disease (three-vessel disease), were observed to have significant impacts on the determination of outcomes.

The incidence of several complications during the PPCI operation, such as dissection, cardiogenic shock, the need for mechanical ventilation, ventricular arrhythmias, and the no-reflow phenomenon, have been found to have a significant impact on patient prognosis.

Table 9 Types of vessels involved and their association with deaths inside hospital and deaths outside hospital within one month of discharge

Vessels	Status	Deaths in-hospital				Deaths out hospital one month			
		Survivals, %	Deaths, %	Totals, %	*P* value	Survivals, %	Deaths, %	Total, %	*P* value
RCA	No	40	4	44	0.503	38	2	40	0.218
		47.10	36.40	45.80		45.80	100.00	47.10	
	Yes	45	7	52		45	0	45	
		52.90	63.60	54.20		54.20	0.00	52.90	
LCx	No	73	5	78	0.005	72	1	73	0.264
		85.90	45.50	81.30		86.70	50.00	85.90	
	Yes	12	6	18		11	1	12	
		14.10	54.50	18.80		13.30	50.00	14.10	
LAD	No	57	2	59	0.003	56	1	57	1
		67.10	18.20	61.50		67.50	50.00	67.10	
	Yes	28	9	37		27	1	28	
		32.90	81.80	38.50		32.50	50.00	32.90	
OM	No	82	9	91	0.099	80	2	82	1
		96.50	81.80	94.80		96.40	100.00	96.50	
	Yes	3	2	5		3	0	3	
		3.50	18.20	5.20		3.60	0.00	3.50	
Diagonal	No	81	9	90	0.139	79	2	81	1
		95.30	81.80	93.80		95.20	100.00	95.30	
	Yes	4	2	6		4	0	4	
		4.70	18.20	6.30		4.80	0.00	4.70	
PDA	No	84	9	93	0.034	82	2	84	1
		98.80	81.80	96.90		98.80	100.00	98.80	
	Yes	1	2	3		1	0	1	
		1.20	18.20	3.10		1.20	0.00	1.20	

RCA: Right coronary artery; LCx: Left circumflex artery; LAD: Left descending artery; OM: Obtuse Marginal; PDA: Patent ductus arteriosus.

Table 10 Complications and their association with deaths inside and outside hospitals within one month of discharge

Complications	Status	Deaths in-hospital				Deaths out hospital one month			
		Survivals, %	Deaths, %	Total, %	*P* value	Survivals, %	Deaths, %	Total, %	*P* value
Coronary dissection	No	79	7	86	0.009	78	1	79	1
		94.00	63.60	90.50		94.00	100.00	94.00	
	Yes	5	4	9		5	0	5	
		6.00	36.40	9.50		6.00	0.00	6.00	
Cardiogenic shock	No	83	5	88	< 0.001	82	1	83	0.047
		97.60	45.50	91.70		98.80	50.00	97.60	
	Yes	2	6	8		1	1	2	
		2.40	54.50	8.30		1.20	50.00	2.40	
Temporary PM	No	82	11	93	1	81	1	82	1

		97.60	100.00	97.90		97.60	100.00	97.60	
	Yes	2	0	2		2	0	2	
		2.40	0.00	2.10		2.40	0.00	2.40	
Mechanical ventilation	No	83	3	86	< 0.001	82	1	83	0.047
		97.60	27.30	89.60		98.80	50.00	97.60	
	Yes	2	8	10		1	1	2	
		2.40	72.70	10.40		1.20	50.00	2.40	
VT/VF	No	79	5	84	< 0.001	79	0	79	0.004
		92.90	45.50	87.50		95.20	0.00	92.90	
	Yes	6	6	12		4	2	6	
		7.10	54.50	12.50		4.80	100.00	7.10	
Contrast nephropathy	No	84	10	94	0.217	81	2	83	1
		98.80	90.90	97.90		97.60	100.00	97.60	
	Yes	1	1	2		2	0	2	
		1.20	9.10	2.10		2.40	0.00	2.40	
IV inotropes	No	84	6	90	< 0.001	83	1	84	0.024
		98.80	54.50	93.80		100.00	50.00	98.80	
	Yes	1	5	6		0	1	1	
		1.20	45.50	6.30		0.00	50.00	1.20	
No-reflow	No	77	4	81	< 0.001	77	0	77	0.006
		91.70	36.40	85.30		93.90	0.00	91.70	
	Yes	7	7	14		5	2	7	
		8.30	63.60	14.70		6.10	100.00	8.30	

PM: Pacemaker; VT: Ventricular tachycardia; VF: Ventricular fibrillation.

This study emphasizes the intricate nature of the parameters that influence the results of PPCI in patients with STEMI, hence emphasizing the crucial importance of prompt intervention and customized care methods that are specifically designed to address the unique risk profile of each patient. Efforts to optimize these parameters can potentially enhance the overall success of primary PPCI as a life-saving strategy for patients with STEMI.

ARTICLE HIGHLIGHTS

Research background

The Erbil Cardiac Center studied 96 patients with ST-segment elevation myocardial infarction (STEMI), treated by primary percutaneous coronary intervention (PPCI). Key factors influencing survival rates included clinical features, procedure details, and the time from symptom onset to hospital arrival. Prompt intervention significantly improved outcomes. Understanding these factors can enable better treatment strategies and public awareness campaigns, ultimately reducing mortality.

Research motivation

This study focuses on STEMI treatment, PPCI efficacy, and identifying mortality predictors. Key problems include identifying mortality predictors and determining onset-to-arrival time's role. Resolving these issues could enhance STEMI treatment, reduce time-to-treatment, and guide future STEMI and PPCI research endeavors, thereby improving patient outcomes and advancing cardiology and emergency medicine fields.

Research objectives

This STEMI study aspired to examine patient mortality rates, identify mortality predictors, and assess onset-to-door time impact. It successfully revealed specific mortality rates and predictors, and it confirmed the importance of prompt intervention. These findings provide a benchmark for treatment strategies, underscore the value of personalizing care,

and inspire research on reducing delays and further exploring mortality predictors.

Research methods

The study aimed to assess STEMI patient mortality rates, identify in-hospital mortality predictors, and uncover the impact of onset-to-hospital time using data analysis methods for a detailed evaluation. These objectives' fulfilment generates mortality benchmarks, guides new treatments, informs public health policies, and catalyzes future research, thereby contributing novel insights into STEMI patient care.

Research results

This study assessed STEMI patients, identifying mortality rates, mortality predictors, and onset-to-door time's significance on prognosis. The findings highlight early intervention importance, clarify mortality predictors, and stimulate personalized treatment plans to enhance PPCI effectiveness. Yet, underlying causes for hospital arrival delays, underlying processes of mortality predictors, and their generality across demographics need additional research.

Research conclusions

The study confirms the "time is muscle" theory, emphasizing swift intervention in STEMI cases, and broadens knowledge by identifying multiple mortality predictors. Though it proposes no new theories, methods, or phenomena, its insights improve our understanding of STEMI management. These findings don't imply confirmed hypotheses but provide a basis for future treatments and hypotheses in clinical practice.

Research perspectives

Future research should focus on reducing onset-to-door time by understanding delay causes, further exploring identified mortality predictors, verifying the study's findings in larger, diverse populations, and assessing novel STEMI treatments. Investigations may employ methods such as comprehensive data analysis, clinical trials, and patient education programs for these research directions.

FOOTNOTES

Author contributions: Faeq AK provided supervision for the project; Saeed EN was responsible for data collection and curation, reviewing and draft preparation.

Institutional review board statement: The study protocol received approval from the Institutional Review Board (IRB) at Hawler Medical University. All research procedures and data collection methodologies were conducted according to the principles of the Declaration of Helsinki and other relevant national and institutional ethical guidelines.

Clinical trial registration statement: This study is registered at college of medicine -Hawler medical university. The registration is required for complete M.Sc.

Informed consent statement: All study participants or their legal guardian provided informed written consent about personal and medical data collection prior to study enrolment.

Conflict-of-interest statement: The authors declare that they have no known competing financial interests or personal relationships that could have influenced the work reported in this paper. All authors have contributed significantly to the research and preparation of the manuscript and have approved the final version for submission. No external funding was received for this research.

Data sharing statement: Original contributions reflected in this work can be obtained from the article.

CONSORT 2010 statement: The authors have read the CONSORT 2010 statement, and the manuscript was prepared and revised according to the CONSORT 2010 statement.

Country/Territory of origin: Iraq

ORCID number: Eza Nawzad Saeed 0009-0009-1099-4292.

S-Editor: Liu JH
L-Editor: A
P-Editor: Zhao YQ

REFERENCES

1 **Jayaraj RL**, Azimullah S, Beiram R, Jalal FY, Rosenberg GA. Neuroinflammation: friend and foe for ischemic stroke. *J Neuroinflammation* 2019; **16**: 142 [PMID: 31291966 DOI: 10.1186/s12974-019-1516-2]

2 **Hwang C**, Levis JT. ECG diagnosis: ST-elevation myocardial infarction. *Perm J* 2014; **18**: e133 [PMID: 24867559 DOI: 10.7812/TPP/13-127]

3 **Keeley EC**, Hillis LD. Primary PCI for myocardial infarction with ST-segment elevation. *N Engl J Med* 2007; **356**: 47-54 [PMID: 17202455 DOI: 10.1056/NEJMct063503]

4 **Pinto DS**, Kirtane AJ, Nallamothu BK, Murphy SA, Cohen DJ, Laham RJ, Cutlip DE, Bates ER, Frederick PD, Miller DP, Carrozza JP Jr, Antman EM, Cannon CP, Gibson CM. Hospital delays in reperfusion for ST-elevation myocardial infarction: implications when selecting a reperfusion strategy. *Circulation* 2006; **114**: 2019-2025 [PMID: 17075010 DOI: 10.1161/CIRCULATIONAHA.106.638353]

5 **Nallamothu B**, Fox KA, Kennelly BM, Van de Werf F, Gore JM, Steg PG, Granger CB, Dabbous OH, Kline-Rogers E, Eagle KA; GRACE Investigators. Relationship of treatment delays and mortality in patients undergoing fibrinolysis and primary percutaneous coronary intervention. The Global Registry of Acute Coronary Events. *Heart* 2007; **93**: 1552-1555 [PMID: 17591643 DOI: 10.1136/hrt.2006.112847]

6 **Motzer R**, Alekseev B, Rha SY, Porta C, Eto M, Powles T, Grünwald V, Hutson TE, Kopyltsov E, Méndez-Vidal MJ, Kozlov V, Alyasova A, Hong SH, Kapoor A, Alonso Gordoa T, Merchan JR, Winquist E, Maroto P, Goh JC, Kim M, Gurney H, Patel V, Peer A, Procopio G, Takagi T, Melichar B, Rolland F, De Giorgi U, Wong S, Bedke J, Schmidinger M, Dutcus CE, Smith AD, Dutta L, Mody K, Perini RF, Xing D, Choueiri TK; CLEAR Trial Investigators. Lenvatinib plus Pembrolizumab or Everolimus for Advanced Renal Cell Carcinoma. *N Engl J Med* 2021; **384**: 1289-1300 [PMID: 33616314 DOI: 10.1056/NEJMoa2035716]

7 **Kim HK**, Jeong MH, Ahn Y, Kim JH, Chae SC, Kim YJ, Hur SH, Seong IW, Hong TJ, Choi DH, Cho MC, Kim CJ, Seung KB, Chung WS, Jang YS, Rha SW, Bae JH, Cho JG, Park SJ; Other Korea Acute Myocardial Infarction Registry Investigators. Hospital discharge risk score system for the assessment of clinical outcomes in patients with acute myocardial infarction (Korea Acute Myocardial Infarction Registry [KAMIR] score). *Am J Cardiol* 2011; **107**: 965-971.e1 [PMID: 21256468 DOI: 10.1016/j.amjcard.2010.11.018]

8 **Karrowni W**, Vyas A, Giacomino B, Schweizer M, Blevins A, Girotra S, Horwitz PA. Radial versus femoral access for primary percutaneous interventions in ST-segment elevation myocardial infarction patients: a meta-analysis of randomized controlled trials. *JACC Cardiovasc Interv* 2013; **6**: 814-823 [PMID: 23968700 DOI: 10.1016/j.jcin.2013.04.010]

9 **Jackson EA**, Moscucci M, Smith DE, Share D, Dixon S, Greenbaum A, Grossman PM, Gurm HS. The association of sex with outcomes among patients undergoing primary percutaneous coronary intervention for ST elevation myocardial infarction in the contemporary era: Insights from the Blue Cross Blue Shield of Michigan Cardiovascular Consortium (BMC2). *Am Heart J* 2011; **161**: 106-112.e1 [PMID: 21167341 DOI: 10.1016/j.ahj.2010.09.030]

10 **Puymirat E**, Simon T, Cayla G, Cottin Y, Elbaz M, Coste P, Lemesle G, Motreff P, Popovic B, Khalife K, Labèque JN, Perret T, Le Ray C, Orion L, Jouve B, Blanchard D, Peycher P, Silvain J, Steg PG, Goldstein P, Guéret P, Belle L, Aissaoui N, Ferrières J, Schiele F, Danchin N; USIK, USIC 2000, and FAST-MI investigators. Acute Myocardial Infarction: Changes in Patient Characteristics, Management, and 6-Month Outcomes Over a Period of 20 Years in the FAST-MI Program (French Registry of Acute ST-Elevation or Non-ST-Elevation Myocardial Infarction) 1995 to 2015. *Circulation* 2017; **136**: 1908-1919 [PMID: 28844989 DOI: 10.1161/CIRCULATIONAHA.117.030798]

11 **Gerstein HC**, Swedberg K, Carlsson J, McMurray JJ, Michelson EL, Olofsson B, Pfeffer MA, Yusuf S; CHARM Program Investigators. The hemoglobin A1c level as a progressive risk factor for cardiovascular death, hospitalization for heart failure, or death in patients with chronic heart failure: an analysis of the Candesartan in Heart failure: Assessment of Reduction in Mortality and Morbidity (CHARM) program. *Arch Intern Med* 2008; **168**: 1699-1704 [PMID: 18695086 DOI: 10.1001/archinte.168.15.1699]

12 **Sabatine MS**, Morrow DA, Giugliano RP, Burton PB, Murphy SA, McCabe CH, Gibson CM, Braunwald E. Association of hemoglobin levels with clinical outcomes in acute coronary syndromes. *Circulation* 2005; **111**: 2042-2049 [PMID: 15824203 DOI: 10.1161/01.CIR.0000162477.70955.5F]

13 **Al Ali J**, Franck C, Filion KB, Eisenberg MJ. Coronary artery bypass graft surgery versus percutaneous coronary intervention with first-generation drug-eluting stents: a meta-analysis of randomized controlled trials. *JACC Cardiovasc Interv* 2014; **7**: 497-506 [PMID: 24746647 DOI: 10.1016/j.jcin.2013.12.202]

14 **Ali WM**, Zubaid M, El-Menyar A, Al Mahmeed W, Al-Lawati J, Singh R, Ridha M, Al-Hamdan R, Alhabib K, Al Suwaidi J. The prevalence and outcome of hypertension in patients with acute coronary syndrome in six Middle-Eastern countries. *Blood Press* 2011; **20**: 20-26 [PMID: 20843191 DOI: 10.3109/08037051.2010.518673]

15 **Ismail N**, Omar SV, Ismail NA, Peters RPH. Collated data of mutation frequencies and associated genetic variants of bedaquiline, clofazimine and linezolid resistance in Mycobacterium tuberculosis. *Data Brief* 2018; **20**: 1975-1983 [PMID: 30306102 DOI: 10.1016/j.dib.2018.09.057]

16 **Mehta R**, Zhu RJ. Blue or red? Exploring the effect of color on cognitive task performances. *Science* 2009; **323**: 1226-1229 [PMID: 19197022 DOI: 10.1126/science.1169144]

17 **Sadrnia S**, Pourmoghaddas M, Hadizadeh M, Maghamimehr A, Esmaeeli M, Amirpour A, Khosravi A. Factors affecting outcome of primary percutaneous coronary intervention for acute myocardial infarction. *ARYA Atheroscler* 2013; **9**: 241-246 [PMID: 23970919]

18 **Brener SJ**, Moliterno DJ, Aylward PE, van't Hof AW, Ruzyllo W, O'Neill WW, Hamm CW, Westerhout CM, Granger CB, Armstrong PW; APEX-AMI Investigators. Reperfusion after primary angioplasty for ST-elevation myocardial infarction: predictors of success and relationship to clinical outcomes in the APEX-AMI angiographic study. *Eur Heart J* 2008; **29**: 1127-1135 [PMID: 18375399 DOI: 10.1093/eurheartj/ehn125]

19 **Jahic E**. Experience and Outcomes of Primary Percutaneous Coronary Intervention for Patients with ST-Segment Elevation Myocardial Infarction of Tertiary Care Center in Bosnia and Herzegovina. *Med Arch* 2017; **71**: 183-187 [PMID: 28974830 DOI: 10.5455/medarh.2017.71.183-187]

20 **Entezarjou A**, Mohammad MA, Andell P, Koul S. Culprit vessel: impact on short-term and long-term prognosis in patients with ST-elevation myocardial infarction. *Open Heart* 2018; **5**: e000852 [PMID: 30228908 DOI: 10.1136/openhrt-2018-000852]

World Journal of Experimental Medicine

Submit a Manuscript: https://www.f6publishing.com

World J Exp Med 2024 March 20; 14(1): 87551

DOI: 10.5493/wjem.v14.i1.87551

ISSN 2220-315x (online)

ORIGINAL ARTICLE

Observational Study

Prevalence and features of SARS-CoV-2 infection in prisons in Tuscany

Cristina Stasi, Martina Pacifici, Caterina Milli, Francesco Profili, Caterina Silvestri, Fabio Voller

Specialty type: Medicine, research and experimental

Provenance and peer review: Invited article; Externally peer reviewed.

Peer-review model: Single blind

Peer-review report's scientific quality classification

Grade A (Excellent): 0
Grade B (Very good): 0
Grade C (Good): 0
Grade D (Fair): D
Grade E (Poor): 0

P-Reviewer: Liao Z, Singapore

Received: August 21, 2023
Peer-review started: August 21, 2023
First decision: November 28, 2023
Revised: December 18, 2023
Accepted: December 26, 2023
Article in press: December 26, 2023
Published online: March 20, 2024

Cristina Stasi, Martina Pacifici, Caterina Milli, Francesco Profili, Caterina Silvestri, Fabio Voller, Epidemiology Unit, Regional Health Agency of Tuscany, Florence 50141, Italy

Cristina Stasi, Department of Medicine, Surgery and Neuroscience, University of Siena, Siena 53100, Italy

Corresponding author: Cristina Stasi, MD, PhD, Research Scientist, Epidemiology Unit, Regional Health Agency of Tuscany, Via Pietro Dazzi, 1, Florence 50141, Italy.
cristina.stasi@ars.toscana.it

Abstract

BACKGROUND

Prisons can be a reservoir for infectious diseases, including severe acute respiratory syndrome coronavirus 2 (SARS-CoV-2), due to the very intimate nature of the living spaces and the large number of people forced to share them.

AIM

To investigate the SARS-CoV-2 epidemiology in prisons, this study evaluated the infection incidence rate in prisoners who underwent nasopharyngeal swabs.

METHODS

This is an observational cohort study. Data collection included information on prisoners who underwent nasopharyngeal swab testing for SARS-CoV-2 and the results. Nasopharyngeal swab tests for SARS-CoV-2 were performed between 15 February 2021 and 31 May 2021 for prisoners with symptoms and all new arrivals to the facility. Another section included information on the diagnosis of the disease according to the International Classification of Diseases, Ninth Revision, and Clinical Modification.

RESULTS

Up until the 31 May 2021, 79.2% of the prisoner cohort (n = 1744) agreed to a nasopharyngeal swab test (n = 1381). Of these, 1288 were negative (93.3%) and 85 were positive (6.2%). A significant association [relative risk (RR)] was found only for the risk of SARS-CoV-2 infection among foreigners compared to Italians [RR = 2.4, 95% confidence interval (CI): 1.2-4.8]. A positive association with SARS-CoV-2 infection was also found for inmates with at least one nervous system disorder (RR = 4, 95%CI: 1.8-9.1). The SARS-CoV-2 incidence rate among prisoners is significantly lower than in the general population in Tuscany (standardized inci-

dence ratio 0.7, 95%CI: 0.6-0.9).

CONCLUSION
In the prisoner cohort, screening and rapid access to health care for the immigrant population were critical to limiting virus transmission and subsequent morbidity and mortality in this vulnerable population.

Key Words: SARS-CoV-2; Epidemiology; Prison; Prevalence; Foreigners; Swab tests

Core Tip: Prisons can be a reservoir for infectious diseases. Based on this premise, this study evaluated the epidemiology of severe acute respiratory syndrome coronavirus 2 (SARS-CoV-2) infection in prisons. A significant association was found in the risk of SARS-CoV-2 infection in foreigners compared to Italians, in particular those with at least one nervous system disorder. The SARS-CoV-2 incidence rate in prisoners is significantly lower than in the general population in Tuscany. In the prisoner cohort, screening and rapid access to health care for the immigrant population were critical to limiting virus transmission and subsequent morbidity and mortality in this vulnerable population.

Citation: Stasi C, Pacifici M, Milli C, Profili F, Silvestri C, Voller F. Prevalence and features of SARS-CoV-2 infection in prisons in Tuscany. *World J Exp Med* 2024; 14(1): 87551
URL: https://www.wjgnet.com/2220-315x/full/v14/i1/87551.htm
DOI: https://dx.doi.org/10.5493/wjem.v14.i1.87551

INTRODUCTION

The prison environment can be a place where infectious diseases, including severe acute respiratory syndrome coronavirus 2 (SARS-CoV-2), can be amplified and spread due to the very intimate nature of the living spaces and the large number of people forced to share them (both prisoners and prison staff).

According to the international literature, the crude incidence rate for SARS-CoV-2 calculated in the prison population (September 2020) in England[1] was 988.1/100000 population at risk and did not differ significantly from that in the general population [935.3/100000 population at risk; relative risk (RR) 1.05; $P = 0.14$]. The results from a study carried out in Massachusetts (July 2020) showed a coronavirus disease 2019 (COVID-19) positivity rate 2.91 times higher [95% confidence interval (CI): 2.69-3.14] than in the general local population and 4.80 times higher (95%CI: 4.45-5.18) than in the general United States population[2].

A recent study by Stufano *et al*[3] performed a COVID-19 screening campaign by real-time polymerase chain reaction (RT-PCR) on 515 inmates from 4 to 30 January 2022. In addition, 101 serum samples collected from healthy inmates 21 d after receiving a second dose of the BNT162b2 vaccine were tested for neutralizing antibodies against both wild-type SARS-CoV-2 and the Omicron BA.1 variant. The global prevalence of SARS-CoV-2 infection during the study period was 43.6% (RR = 0.8), significantly lower than that of unvaccinated inmates (62.7%). The proportion testing positive for SARS-CoV-2 in unvaccinated subjects was significantly higher than in the other groups ($P < 0.001$) receiving one dose (52.3%), two doses (full cycle; 45.0%), and the third dose (booster; 31.4%).

In Italy, the data published weekly by the Ministry of Justice cannot be used to calculate specific incidence or prevalence rates because of the lack of details on the cases published. However, according to the XVII Report on detention conditions-COVID-19 and the pandemic in Italy, in February 2021, published by the Antigone Association[4], the average rate of positive cases in prisons was 91.1 per 10000 inmates, compared with 68.3 per 10000 in the general population[4].

Based on these premises, this study evaluated the epidemiology of SARS-CoV-2 infection in prisons.

MATERIALS AND METHODS

This is a cross-sectional study, with health status assessed at a single point in time. The study population was represented by all the inmates present in the prisons of Tuscany on 15 February 2021. From 15 January to 10 February, web meetings were organized with the representatives of the health care facilities to explain the data entry form and the methods for completion. On 14 February 2021, the list of inmates present in the prison was drawn up, including the new arrivals on that day (at midnight on 14 February). From 15 February 2021, doctors had 3 mo to complete the health status form for all detained citizens present on 14 February 2021.

For this study, we used specific clinical data created using the Python programming language. The data was divided into different areas: Socio-demographic, health, drugs and two other areas containing specific information about suicide attempts and self-harm, including any episodes in the last year of detention, number of episodes and method.

The first area included general information such as age, sex, nationality, origin of the prisoner (outside prison, another prison, Diagnostic Therapy Centre, social care or house arrest), daily tobacco and cigarette consumption, weight and height to calculate body mass index (BMI), and the number of hours per day spent in their cell. During this data collection, we also recorded whether the prisoner had already completed a nasopharyngeal swab test for SARS-CoV-2 and the result. All prisoners who had a nasopharyngeal swab test for SARS-CoV-2 were tested between the start of the pandemic and 31 May 2021, both for presenting symptoms and for new arrivals to the facility. These were compared with nasopharyngeal swab testing for SARS-CoV-2 in the general population between the start of the pandemic and 31 May 2021. The second area included information on all disease diagnoses (one primary diagnosis and an unlimited number of secondary diagnoses) relating to both general medical health and mental/psychiatric health according to the International Classification of Diseases, Ninth Revision, and Clinical Modification.

The study was conducted in accordance with the Declaration of Helsinki (revised in Edinburgh, 2000). According to Italian legislation on data confidentiality, the dataset used is not openly available (Decree No. 196/2003). No identifiable data were used in this study.

Statistical analysis

The association between positive swabs and other health aspects was investigated using the binomial Poisson model to estimate the RR for each factor considered with respect to the baseline category. The factors considered were place of birth (Italy/abroad), BMI, and the presence of at least one disease (infectious, nervous system, psychiatric, endocrine and immune system or cardiovascular disease, considered separately).

Chi-squared tests were used to identify any significant differences at the 95% level between swab results and the presence of at least one disease (in general, psychiatric, infectious, cardiovascular, endocrine and immune system, digestive system, respiratory system, musculoskeletal and connective apparatus, genitourinary system, nervous system, traumatic, hematological, cutaneous and subcutaneous, or neoplastic).

Standardized incidence ratios (SIRs) with approximated 95%CIs were calculated in order to compare the incidence rate of SARS-CoV-2 between the local population in Tuscany and the prisoners, in general and stratified by socio-demographic characteristics (age and nationality). Approximate CI were constructed using the Wilson and Hilferty[5] (1931) approximation for chi-square percentiles. The SARS-CoV-2 incidence rate in the local population was calculated using the Tuscany SARS-CoV-2 database and the number of people who tested positive between the start of the pandemic and 31 May 2021 as a proportion of the general population aged 18 years and over.

RESULTS

At the index date (31 May 2021), 79.2% of the inmates in our cohort (n = 1744) agreed to a nasopharyngeal swab test (n = 1381). Of these, 1288 were negative (93.3%) and 85 were positive (6.2%), while the results of the swab test were not recorded in 8 cases; this was compared with the positivity rate (4.1%) recorded in the general population. Figure 1 shows the bar plot for positive swabs (%) by age group (Figure 1A). The positive swab tests were most common among inmates from Eastern Europe and Africa (Figure 1B).

A significant association (RR) was found only for the risk of SARS-CoV-2 infection in foreigners compared to Italians (Figure 2) (RR = 2.4, 95%CI: 1.2-4.8). In addition to socio-demographic characteristics, we examined the association between positive swabs and other health aspects by applying the binomial Poisson model to estimate the RR for each factor considered compared to the baseline category (Figure 2). A positive association was confirmed for inmates with at least one nervous system disorder (RR = 4, 95%CI: 1.8-9.1).

Chi-squared tests showed significant differences in swab results between inmates with at least one disease and those who were disease-free (Table 1). In particular, only 5.1% of prisoners with at least one disease had a positive swab compared to 8.3% of healthy prisoners (P < 0.05). Similar differences were found between those with at least one psychiatric, digestive system or respiratory system disease and healthy inmates.

The incidence rate of SARS-CoV-2 in prisoners is significantly lower than in the general local population in Tuscany (SIR 0.7, 95%CI: 0.6-0.9) (Table 2). In terms of age groups, the results were comparable only among prisoners aged 18-29 years.

DISCUSSION

In March 2020, the World Health Organization published the guidance document "Preparedness, prevention and control of COVID-19 in prisons and other places of detention", which provided updated information on COVID-19 case definitions, management strategies, vaccine availability and distribution procedures and indicators recommended for surveillance purposes in detention settings[6]. Although people living in close proximity to each other are likely to be more susceptible to COVID-19 than the general population, the percentage of SARS-CoV-2 infection found in the Tuscan prison was in line with that reported in other studies[7]. In fact, due to the particularly stringent prevention and control measures in place in prisons, the rate of positive cases in some studies was comparable to that in the general population. In line with our study, a recently published Italian article[8] conducted between 1 October and 31 December 2020 on 504 prisoners who underwent antigen-detecting rapid diagnostic tests showed that 21 (4.2%) were positive for viremia. In fact, Augustynowicz *et al*[9] showed that based on the results of a study conducted in Poland, infections among prison

Table 1 Chi-squared tests comparing swab positivity and health conditions

Parameter	Negative[1]	Positive[1]	*P* value
Diseases in general			
At least one disease	867 (94.9)	47 (5.1)	< 0.05
No disease	421 (91.7)	38 (8.3)	
Psychiatric			
At least one disease	435 (96.2)	17 (3.8)	< 0.05
No disease	853 (92.6)	68 (7.4)	
Infectious			
At least one disease	58 (93.6)	4 (6.4)	0.9
No disease	1230 (93.8)	81 (6.2)	
Cardiovascular			
At least one disease	157 (93.5)	11 (6.5)	0.8
No disease	1131 (93.9)	74 (6.1)	
Endocrine and immune system			
At least one disease	138 (92)	12 (8)	0.3
No disease	1150 (94)	73 (6)	
Digestive system			
At least one disease	165 (97.6)	4 (2.4)	< 0.05
No disease	1123 (93.3)	81 (6.7)	
Respiratory system			
At least one disease	65 (100)	0 (0)	< 0.05
No disease	1223 (93.5)	85 (6.5)	
Musculoskeletal and connective apparatus			
At least one disease	97 (95.1)	5 (4.9)	0.6
No disease	1191 (93.7)	80 (6.3)	
Genitourinary system			
At least one disease	56 (94.9)	3 (5.1)	0.7
No disease	1232 (93.8)	82 (6.2)	
Nervous system			
At least one disease	64 (90.1)	7 (9.9)	0.2
No disease	1224 (94)	78 (6)	
Traumas			
At least one trauma or poisoning	33 (94.3)	2 (5.7)	0.9
No traumas or poisoning	1255 (93.8)	83 (6.2)	
Blood organs			
At least one disease	11 (100)	0 (0)	0.4
No disease	1277 (93.8)	85 (6.2)	
Tumour			
At least one tumour	20 (95.2)	1 (4.8)	0.8
No tumours	1268 (93.8)	84 (6.2)	
Cutaneous and subcutaneous			
At least one disease	49 (96.1)	2 (3.9)	0.5

No disease	1239 (93.7)	83 (6.3)

[1]Data are *n* (%).

Table 2 Comparison between positive swab incidence rate in prison and in the general population in Tuscany

Parameter	SIR	95%CI
Total	0.7	0.6-0.9
Age in yr		
18-29	0.4	0.2-0.8
30-39	0.8	0.5-1.1
40-49	0.8	0.5-1.1
50-59	0.6	0.4-1
60 +	1	0.5-1.8
Nationality		
Italian	0.3	0.2-0.5
Foreign	0.5	0.3-0.7

CI: Confidence interval; SIR: Standardized incidence ratio.

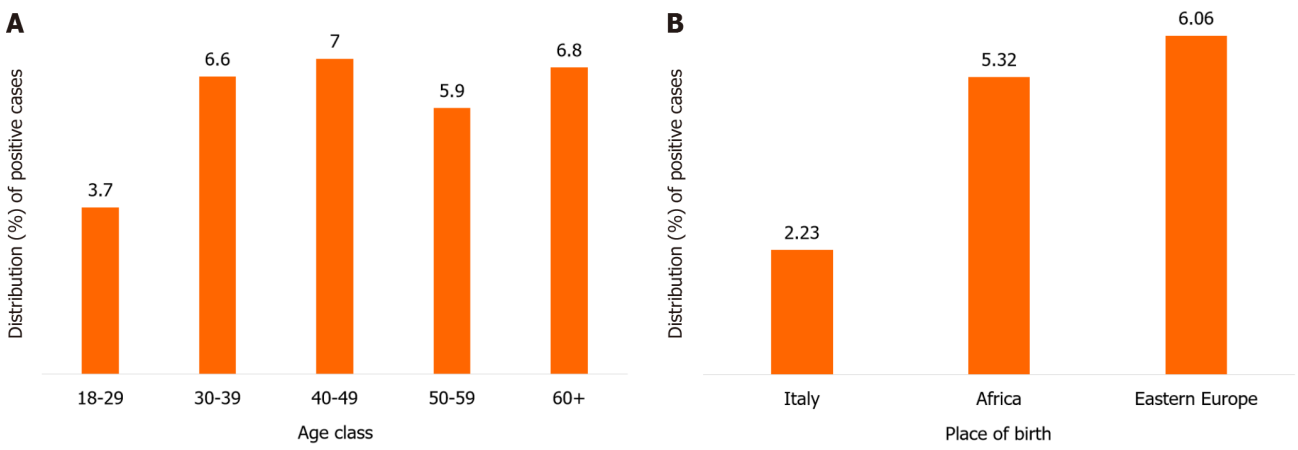

Figure 1 Distribution of severe acute respiratory syndrome coronavirus 2 positivity. A: Positive cases by age group [95% confidence interval (CI)], Tuscany, Year 2021; B: Positive cases by place of birth (95%CI), Tuscany, Year 2021.

officers and staff as well as inmates seem parallel to the epidemiological situation in the general population[9]. Contrary to our observations, a study conducted in a prison in Barcelona[10] highlighted a high percentage (24.1%) of people who tested positive by RT-PCR. Of these, 94.8% were asymptomatic. The same high prevalence was found in a study evaluating the percentage of SARS-CoV-2-infected inmates, health care professionals, and prison officers in prisons in Espírito Santo. Specifically, among 1830 individuals, the prevalence of COVID-19 infection was 11.89% among health care professionals, 22.07% among prison officers, and 31.64% among inmates[11].

In England, prison-associated cases accounted for < 1% of COVID-19 cases from 16 March to 12 October 2020[1]. In their study of incarcerated men in Canada, Kronfli *et al*[7] showed that a total of 246/1100 (22%) participants tested positive for SARS-CoV-2 antibodies. Similar to the general population, the risk increases with age. When the incidence rates among prisoners were compared with those of the general population in Tuscany, according to the different age groups, a statistically significant difference was found only in the 18-29 age group. The data from the Canadian study showed a high prevalence compared with our data (6%); moreover, the incarcerated men who tested positive had several prison-related modifiable risk factors associated with increased seropositivity, such as length of time spent in prison, employment, consumption of communal meals during incarceration, and post-prison outbreak.

Our study found a significant association in the risk of SARS-CoV-2 infection in foreigners compared with Italians, which is in line with previous studies in the general population. These studies have shown that the socioeconomic and living conditions of migrants may contribute to increased rates of SARS-CoV-2 infection, with a subsequent higher risk of

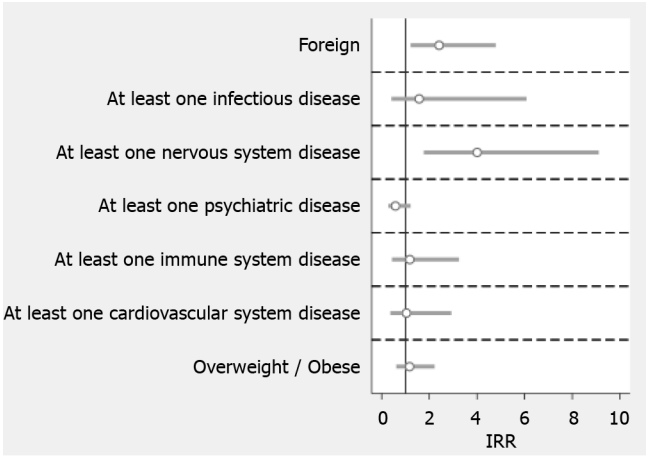

Figure 2 Association between severe acute respiratory syndrome coronavirus 2 positivity and risk factors. Association relative risk between swab positivity and other socio-economic and health factors [95% confidence interval (CI)], Tuscany, Year 2021. IRR: Incidence rate ratio.

COVID-19 mortality[12-13]. Marquez *et al*[14], analyzing the mortality patterns of the population incarcerated in Texas state prisons during both the year before (from 1 April 2019) and the 1st year (from 1 April 2020) of the COVID-19 pandemic, found that COVID-19 mortality was 1.61 and 2.12 times higher in the black and Hispanic populations, respectively, compared with the white population. A study conducted from 23 December 2020 to 19 February 2021 in Lombardy, one of the Italian regions most affected by the COVID-19 pandemic, showed that the prevalence of SARS-CoV-2 antibodies in the general population was 12.4%, with this proportion more than doubled in foreigners (23.3%) compared with Italians (9.1%)[15].

The spread of SARS-CoV-2 from October 2020 was characterized by the so-called "British" variant, a significantly more contagious variant of SARS-CoV-2 that was responsible for increasing nosocomial infections or the spread of the virus in closed environments such as prisons, despite the containment measures put in place.

Few studies have investigated the spread of SARS-CoV-2 infection during the first waves. To the best of our knowledge, this study was one of the first studies to be conducted in Italy on SARS-CoV-2 infection in a large cohort of prisoners who underwent nasopharyngeal swab testing. Therefore, its strength is the very early detection of the epidemic situation in the prison setting. Its limitation is the lack of data relating on prison and health staff during the same period in Tuscany.

In conclusion, although the control and management of SARS-CoV-2 infection in some prisons was similar to that outside, campaigns to improve disease prevention and screening, and rapid access to health care for the migrant population in prisons are critical to limiting transmission of the virus and subsequent morbidity and mortality in this vulnerable population.

CONCLUSION

In conclusion, although the control and management of SARS-CoV-2 infection in some prisons was similar to that outside, campaigns to improve disease prevention and screening, and rapid access to health care for the migrant population in prisons are critical to limiting transmission of the virus and subsequent morbidity and mortality in this vulnerable population.

ARTICLE HIGHLIGHTS

Research background

Prisons can be a reservoir for infectious diseases, including severe acute respiratory syndrome coronavirus 2 (SARS-CoV-2), due to the very intimate nature of the living spaces and the large number of people forced to share them. Therefore, in this place infectious diseases, including SARS-CoV-2, can be amplified and spread.

Research motivation

The main motivation was to improve epidemiological knowledge, aimed at better understanding what action could be taken to improve the health status of the detained population.

Research objectives

Based on these premises, this study evaluated the epidemiology of SARS-CoV-2 infection in prisons.

Research methods

This is a cross-sectional study, with health status assessed at a single point in time. The study population was represented by all the inmates present in the prisons of Tuscany on 15 February 2021. Data collection included information on prisoners who underwent nasopharyngeal swab testing for SARS-CoV-2 and the results. Nasopharyngeal swab tests for SARS-CoV-2 were performed between 15 February 2021 and 31 May 2021 for prisoners with symptoms and all new arrivals to the facility. Another section included information on the diagnosis of the disease according to the International Classification of Diseases, Ninth Revision, and Clinical Modification.

Research results

A high percentage of prisoners agreed to take the swab. This high adherence was probably due to a perception of risk. A significant association was found only for the risk of SARS-CoV-2 infection among foreigners compared to Italians but the SARS-CoV-2 incidence rate among prisoners is significantly lower than in the general population in Tuscany, probably due to the high level of attention of prison staff towards this public health problem.

Research conclusions

Although the control and management of SARS-CoV-2 infection in some prisons was similar to that outside, campaigns to improve disease prevention and screening, and rapid access to health care for the migrant population in prisons are critical to limiting transmission of the virus and subsequent morbidity and mortality in this vulnerable population.

Research perspectives

Future research is needed to definitively establish a screening program to manage organized screening programs for high-prevalence infectious diseases in the prison population.

FOOTNOTES

Author contributions: Stasi C interpreted the data, wrote the paper, and revised the manuscript critically for important intellectual content; Pacifici M analyzed and interpreted the data; Milli C collected the data; Profili F recorded the research data and revised statistical analysis; Silvestri C and Voller F conceived and designed the study and revised the manuscript critically for important intellectual content.

Institutional review board statement: The study was performed in accordance with the Declaration of Helsinki (revised in Edinburgh, 2000). According to the Italian legislation on data confidentiality, the dataset used is not openly available (Decree No. 196/2003).

Informed consent statement: No identifiable human data were used for this study.

Conflict-of-interest statement: All the authors report having no relevant conflicts of interest for this article.

Data sharing statement: No additional data are available.

Country/Territory of origin: Italy

ORCID number: Cristina Stasi 0000-0002-9146-9968; Caterina Silvestri 0000-0002-1577-2869; Fabio Voller 0000-0002-1063-415X.

S-Editor: Li L
L-Editor: Filipodia
P-Editor: Yuan YY

REFERENCES

1 **Rice WM**, Chudasama DY, Lewis J, Senyah F, Florence I, Thelwall S, Glaser L, Czachorowski M, Plugge E, Kirkbride H, Dabrera G, Lamagni T. Epidemiology of COVID-19 in Prisons, England, 2020. *Emerg Infect Dis* 2021; **27**: 2183-2186 [PMID: 34287123 DOI: 10.3201/eid2708.204920]

2 **Jiménez MC**, Cowger TL, Simon LE, Behn M, Cassarino N, Bassett MT. Epidemiology of COVID-19 Among Incarcerated Individuals and Staff in Massachusetts Jails and Prisons. *JAMA Netw Open* 2020; **3**: e2018851 [PMID: 32821919 DOI: 10.1001/jamanetworkopen.2020.18851]

3 **Stufano A**, Buonvino N, Trombetta CM, Pontrelli D, Marchi S, Lobefaro G, De Benedictis L, Lorusso E, Carofiglio MT, Vasinioti VI, Montomoli E, Decaro N, Lovreglio P. COVID-19 Outbreak and BNT162b2 mRNA Vaccination Coverage in a Correctional Facility during Circulation of the SARS-CoV-2 Omicron BA.1 Variant in Italy. *Vaccines (Basel)* 2022; **10** [PMID: 35891301 DOI: 10.3390/vaccines10071137]

4 Antigone. Oltre il virus. XVII Rapporto di Antigone sulle condizioni di detenzione. [cited 23 Dec 2023]. Available from: http://www.antoniocasella.eu/nume/Antigone_marzo21.pdf

5 **Wilson EB**, Hilferty MM. The Distribution of Chi-Square. *Proc Natl Acad Sci USA* 1931; **17**: 684-688 [PMID: 16577411 DOI: 10.1073/pnas.17.12.684]

6 **World Health Organization**, Regional Office for Europe. Preparedness, prevention and control of COVID-19 in prisons and other places of detention: Interim guidance. Feb 8, 2021. [cited 21 Dec 2023]. Available from: https://apps.who.int/iris/handle/10665/339830

7 **Kronfli N**, Dussault C, Maheu-Giroux M, Halavrezos A, Chalifoux S, Sherman J, Park H, Del Balso L, Cheng MP, Poulin S, Cox J. Seroprevalence and Risk Factors for Severe Acute Respiratory Syndrome Coronavirus 2 Among Incarcerated Adult Men in Quebec, Canada, 2021. *Clin Infect Dis* 2022; **75**: e165-e173 [PMID: 35037053 DOI: 10.1093/cid/ciac031]

8 **Mazzilli S**, Oliani F, Restivo A, Giuliani R, Tavoschi L, Ranieri R. Antigenic rapid test for SARS-CoV2 screening of individuals newly admitted to detention facilities: sensibility in an asymptomatic cohort. *J Clin Virol Plus* 2021; **1**: 100019 [PMID: 35262006 DOI: 10.1016/j.jcvp.2021.100019]

9 **Augustynowicz A**, Wójcik M, Bachurska B, Opolski J, Czerw A, Raczkiewicz D, Pinkas J. COVID-19 - Infection prevention in prisons and jails in Poland. *Ann Agric Environ Med* 2021; **28**: 621-626 [PMID: 34969220 DOI: 10.26444/aaem/140099]

10 **Marco A**, Gallego C, Pérez-Cáceres V, Guerrero RA, Sánchez-Roig M, Sala-Farré RM, Fernández-Náger J, Turu E. Public health response to an outbreak of SARS-CoV2 infection in a Barcelona prison. *Epidemiol Infect* 2021; **149**: e91 [PMID: 33849684 DOI: 10.1017/S0950268821000789]

11 **Silva AID**, Maciel ELN, Duque CLC, Gomes CC, Bianchi EDN, Cardoso OA, Lira P, Jabor PM, Zanotti RL, Sá RT, Magno Filho SJS, Zandonade E. Prevalence of COVID-19 infection in the prison system in Espírito Santo/Brazil: persons deprived of liberty and justice workers. *Rev Bras Epidemiol* 2021; **24**: e210053 [PMID: 34877995 DOI: 10.1590/1980-549720210053]

12 **Alahmad B**, AlMekhled D, Odeh A, Albloushi D, Gasana J. Disparities in excess deaths from the COVID-19 pandemic among migrant workers in Kuwait. *BMC Public Health* 2021; **21**: 1668 [PMID: 34521360 DOI: 10.1186/s12889-021-11693-w]

13 **Adams ML**, Katz DL, Grandpre J. Population-Based Estimates of Chronic Conditions Affecting Risk for Complications from Coronavirus Disease, United States. *Emerg Infect Dis* 2020; **26**: 1831-1833 [PMID: 32324118 DOI: 10.3201/eid2608.200679]

14 **Marquez N**, Moreno D, Klonsky A, Dolovich S. Racial And Ethnic Inequalities In COVID-19 Mortality Within Carceral Settings: An Analysis Of Texas Prisons. *Health Aff (Millwood)* 2022; **41**: 1626-1634 [PMID: 36343310 DOI: 10.1377/hlthaff.2022.00390]

15 **Pagani G**, Conti F, Giacomelli A, Oreni L, Beltrami M, Pezzati L, Casalini G, Rondanin R, Prina A, Zagari A, Rusconi S, Galli M. Differences in the Prevalence of SARS-CoV-2 Infection and Access to Care between Italians and Non-Italians in a Social-Housing Neighbourhood of Milan, Italy. *Int J Environ Res Public Health* 2021; **18** [PMID: 34682369 DOI: 10.3390/ijerph182010621]

World Journal of Experimental Medicine

Submit a Manuscript: https://www.f6publishing.com

World J Exp Med 2024 March 20; 14(1): 88064

DOI: 10.5493/wjem.v14.i1.88064

ISSN 2220-315x (online)

ORIGINAL ARTICLE

Clinical and Translational Research

Chemical profiling of bioactive compounds in the methanolic extract of wild leaf and callus of *Vitex negundo* using gas chromatography-mass spectrometry

Gunjan Garg, Alok Bharadwaj, Shweta Chaudhary, Veena Gupta

Specialty type: Medicine, research and experimental

Provenance and peer review: Invited article; Externally peer reviewed.

Peer-review model: Single blind

Peer-review report's scientific quality classification

Grade A (Excellent): 0
Grade B (Very good): B
Grade C (Good): C, C
Grade D (Fair): 0
Grade E (Poor): 0

P-Reviewer: Emran TB, Bangladesh; Soriano-Ursúa MA, Mexico

Received: September 8, 2023
Peer-review started: September 8, 2023
First decision: October 24, 2023
Revised: November 12, 2023
Accepted: January 30, 2024
Article in press: January 30, 2024
Published online: March 20, 2024

Gunjan Garg, Shweta Chaudhary, School of Biotechnology, Gautam Buddha University, Greater Noida 201312, Uttar Pradesh, India

Alok Bharadwaj, Biotechnology, GLA University, Mathura 281406, Uttar Pradesh, India

Veena Gupta, Division of Germplasm Conservation, Indian Council of Agricultural Research - National Bureau of Plant Genetic Resources, New Delhi 110012, New Delhi, India

Corresponding author: Alok Bharadwaj, PhD, Associate Professor, Biotechnology, GLA University, 17 Km Mile Stone, Mathura-Delhi Highway NH#1, Post-Chaumuhan District, Mathura 281406, Uttar Pradesh, India. alok.bhardwaj@gla.ac.in

Abstract

BACKGROUND

The investigation of plant-based therapeutic agents in medicinal plants has revealed their presence in the extracts and provides the vision to formulate novel techniques for drug therapy. *Vitex negundo* (*V. negundo*), a perennial herb belonging to the *Varbanaceae* family, is extensively used in conventional medication.

AIM

To determine the existence of therapeutic components in leaf and callus extracts from wild *V. negundo* plants using gas chromatography-mass spectrometry (GC-MS).

METHODS

In this study, we conducted GC-MS on wild plant leaf extracts and correlated the presence of constituents with those in callus extracts. Various growth regulators such as 6-benzylaminopurine (BAP), 2,4-dichlorophenoxyacetic acid (2,4-D), α-naphthylacetic acid (NAA), and di-phenylurea (DPU) were added to plant leaves and *in-vitro* callus and grown on MS medium.

RESULTS

The results clearly indicated that the addition of BAP (2.0 mg/L), 2,4-D (0.2 mg/mL), DPU (2.0 mg/L) and 2,4-D (0.2 mg/mL) in MS medium resulted in rapid callus development. The plant profile of *Vitex* extracts by GC-MS analysis

showed that 24, 10, and 14 bioactive constituents were detected in the methanolic extract of leaf, green callus and the methanolic extract of white loose callus, respectively.

CONCLUSION

Octadecadienoic acid, hexadecanoic acid and methyl ester were the major constituents in the leaf and callus methanolic extract. Octadecadienoic acid was the most common constituent in all samples. The maximum concentration of octadecadienoic acid in leaves, green callus and white loose callus was 21.93%, 47.79% and 40.38%, respectively. These findings demonstrate that the concentration of octadecadienoic acid doubles *in-vitro* compared to *in-vivo*. In addition to octadecadienoic acid; butyric acid, benzene, 1-methoxy-4-(1-propenyl), dospan, tridecanedialdehyde, methylcyclohexenylbutanol, chlorpyrifos, n-secondary terpene diester, anflunine and other important active compounds were also detected. All these components were only available in callus formed *in-vitro*. This study showed that the callus contained additional botanical characteristics compared with wild plants. Due to the presence of numerous bioactive compounds, the medical use of *Vitex* for various diseases has been accepted and the plant is considered an important source of therapeutics for research and development.

Key Words: Leaf extracts; Callus extracts; Methanolic extract; Octadecadienoic acid; Hexadecanoic acid; Methyl ester; Gas chromatography-mass spectrometry analysis

Core Tip: Phytopharmacological analysis of medicinal plants and their extracts can show the presence of important elements and gives insight into new methods for drug therapy. *Vitex negundo* (*L.*) is a perennial herb belonging to the *Varbanaceae* family, an aromatic small tree widely used in conventional medicine. In the present study, we report the gas chromatography-mass spectrometry analysis of leaf extracts from wild plants and correlate the existence of these components with those present in callus extracts. The medicinal application of *Vitex negundo* for various diseases has been recognized due to the identification of various bioactive compounds, and the plant is recognized as an important botanical remedy in medical research and development.

Citation: Garg G, Bharadwaj A, Chaudhary S, Gupta V. Chemical profiling of bioactive compounds in the methanolic extract of wild leaf and callus of *Vitex negundo* using gas chromatography-mass spectrometry. *World J Exp Med* 2024; 14(1): 88064
URL: https://www.wjgnet.com/2220-315x/full/v14/i1/88064.htm
DOI: https://dx.doi.org/10.5493/wjem.v14.i1.88064

INTRODUCTION

India has always been considered a treasure trove rich in medicinal plants and the application of medicinal plants in various forms has been considered a way of life[1]. Eighty percent of the world's population relies on herbal medicine as primary healthcare. These medicinal plants are an important source of secondary metabolites (SMs), which are small organic molecules that are important for the longevity of plants, but they do not play a role in the growth and development of plants. On the basis of their structures and biosynthesis, these SMs are divided into the following three categories: (1) Phenolic compounds; (2) Terpenoids; and (3) Alkaloids[2]. These SMs are beneficial to human health and effective in preventing diseases. The use of *in-vitro* propagation techniques facilitates the rapid propagation of rare and commercially important plants. The massive expansion of medicinal plants through the use of plant biotechnology has the potential to meet the pharmaceutical industry's need for raw materials for herbal preparations. Numerous medicinal plants have been extracted from the natural flora for commercial drug production[3]. The collection of phytochemicals from plant tissues has been studied for over 30 years, and the information obtained contributes to the use of cell cultures to produce the desired phytochemicals. In the last few years, the development of plant tissue culture has increased, and the corporate utility of this technique as a measure of producing precious phytochemicals has received feedback from the scientific community. Cell suspension culture has been found to be the best method for the study of biosynthesis, and callus tissue is the most abundant cell mass obtained during culture production. Cell cultures are useful tools for studying and producing important SMs[4]. Chemical evaluation of plant SMs includes qualitative, quantitative, and biochemical tests. Qualitative and quantitative drug testing can be used to identify the important bioactive components in plant samples.

Vitex negundo (*V. negundo*), is a small perennial, woody, aromatic and flowering ornamental medicinal herb, commonly known as chaste tree, belonging to the *Verbenaceae* family. This plant is deciduous in nature and has a medium height of 4-5 m. It has 3 or 5 palmate-sized flowers, with deep-violet purple aromatic flowers and rounded black-ripe fruit. Plants of *Vitex* species have different ethno-botanical and pharmacological applications. *V. negundo* contains many bioactive phytochemicals such as glycosides, phenolic compounds, flavonoids, terpenes and phytosteroids. Terpenoids are thought to be one of the most abundant metabolites in the *Vitex* plant. Chemically, they contain five carbon isoprene units,

forming monoterpenes (five carbon atoms), hemiterpenes (C5), sesquiterpenes (fifteen carbon atoms), diterpenes (twenty carbon atoms), and triterpenes (thirty carbon atoms). The leaves of *Vitex* are used to reduce breast tenderness, regulate hormones related to fertility, menstrual cycle, menstrual pain and amenorrhea symptoms. Pharmacologically, this species showed anti-oxidative, antimicrobial, anti-inflammatory and anti-tumor properties. It reduces the level of serum prolactin in hyper-prolactinemia and mastodynia. The leaves of *V. negundo* are aromatic, bitter, pungent, and have astringent, analgesic, anti-inflammatory, antipyretic, and anthelmintic properties. Literature has revealed that leaves and flowers of *Vitex* are the main sources of SMs. Leaves are a good source of alkaloids, vitamin C, carotene, glycol-nonanol, benzoic acid, β-sitosterol, flavonoids (such as luteolin-7-glycosides, ricin, iridoid glycosides, C-glycosides), terpenes oil (such as caryophyllene epoxide, δ-guaiene, and ethyl-hexadecenoate), while flowers contain oil such as α-selinene, (E)-nerolidol, carryophyllene epoxide, and germacren-4-ol. To date, there is no comprehensive record available on the phytochemical study of wild leaf and callus culture (*in-vitro*) samples obtained from this plant. Thus, to determine the therapeutic importance of *V. negundo*, a detailed comparative study of phytochemical constituents is essential. Hence, the aim of this study was to analyze and identify the phyto-constituents of wild leaves and *in-vitro* cultured leaf calluses and to spectroscopically identify bioactive compounds in crude extracts prepared in methanol by gas chromatography-mass spectrometry (GC-MS) analysis.

MATERIALS AND METHODS

Collection of plant samples

The fresh young leaves of *V. negundo* (*L.*) were collected from the National Bureau of Plant Genetic Resources (NBPGR), New Delhi. The leaves were carefully rinsed with distilled water to eliminate dust particles and dried at room temperature for 15 d until the dry weight stabilized. The dried herb was placed in liquid nitrogen, ground to a fine powder, and stored it in an airtight container until use.

Callus preparation and culture

To prepare the callus, fresh leaves were collected from plants and washed thoroughly with water to remove dust, then the surfaces were disinfected with 0.1% $HgCl_2$. Leaf explants were excised aseptically and cultured on MS medium containing 2,4-dichlorophenoxyacetic acid (2,4-D), naphthalene acetic acid (NAA), 6-benzylaminopurine (BAP), and diphenylurea (DPU). The highest and fastest response for callogenesis with a green and friable callus was observed in the MS medium with the addition of BAP (2.0 mg/L) and 2,4-D (0.2 mg/mL) (*i.e.,* M2 media); and DPU (2.0 mg/L) with 2,4-D (0.2 mg/L) (*i.e.,* M4 media). The peculiarity of the combination is the difference between the formation of green brittle and white loose calluses, respectively (Table 1). The callus of *V. negundo* (*L.*) was produced from the primary callus of leaf explants by sub-culturing on MS media (M2 and M4) enriched with standard growth regulators, *i.e.,* M2-media: BAP (2.0 mg/L) with 2,4-D (0.2 mg/mL); and M4-media: DPU (2.0 mg/L) with 2,4-D (0.2 mg/L).

Preparation of plant extracts and GC-MS analysis of bioactive compounds present in the samples

Preparation of the plant extracts was conducted by following the modified method of Anwar *et al*[5]. The fresh young leaves of *V. negundo* (*L.*) were collected from the herbal garden, NBPGR, New Delhi, and calluses were produced by subculture from leaf explants of *V. negundo* in M2 and M4 medium, which were then selected for further quantitative analysis by GC-MS. For leaf sample (LS) preparation, the leaves were carefully rinsed in tap water to eliminate dust particles, then rinsed with sterilized distilled water, dried at room temperature for 24 h, and ground to a fine powder in a mechanical grinder. For callus sample preparation, we selected 6-8-wk-old green friable callus (CS1) and white loose callus (CS2) from the M2 and M4 medium, respectively. The medium particles were removed by washing with double distilled water and then drying in an oven at 62 ± 5 °C for 28 h. Dried samples were ground to a fine powder and stored in sterilized, airtight polythene bags until use. For methanol extraction, 2 g of the powdered plant samples (LS, CS1, and CS2) were weighed and soaked in 10 mL of GC-MS grade methanol for 14 h (or incubated overnight) in a flask. The solution was thoroughly mixed with a shaker. After mixing, the solution was filtered through a Whatman No. 41 filter paper and the filtrate collected. This solution was used for GC-MS analysis.

GC analysis was performed using an Agilent gas chromatograph equipped with a split/split-less injector (230 °C) and mass spectrometer detection (230 °C). The gas used was helium (1 mL/min), and HP-5MS 5% Phenyl Methyl Silox (325 °C: 30 m × 250 μm × 0.25 μm) was employed as the capillary column. The sample (2 μL) was injected through a split-less system with the following program: 170 °C for 1 min, 250 °C for 2 min at 8 °C/min, and finally 3 °C/min at 310 °C for 2 min. The mass selective detector was operated at 70 eV in the 70-600 amu range. The final running time was 39 min, and the data were analyzed using total ion count for identification and quantification of compounds. Each extract spectrum reflects the retention time in the column, and the peaks detected correspond to the relative abundance (%) of bioactive compounds found in specific regions. By comparing the mass spectra of the detected components with the mass spectra of known components available in the National Institute of Standards and Technology library, the bioactive phytochemical compounds of *V. negundo* were identified[6]. Compound concentrations were determined from the GC peak area of the total ion current.

RESULTS

The GC-MS chromatogram spectra were achieved in all three extracts of *V. negundo i.e.*, wild *in-vivo* leaves, green-compact and white-loose *in-vitro* callus. The results showed that bioactive compounds were present in both *in-vivo* and *in-vitro* sample extracts (Figure 1). Using GC-MS analysis we detected twenty-four, ten, and fourteen bioactive compounds in the methanolic extract of wild-leaves, green, and white loose callus, respectively (Tables 2-4). The results showed that octadecadienoic acid, hexadecanoic acid and methyl esters were the main components in the methanol extract of leaves and callus. Among these, octadecadienoic acid was the most common compound in all samples[7,8]. The maximum concentration of octadecadienoic acid in leaves, green callus and white loose callus was 21.93%, 47.79% and 40.38%, respectively. Our results confirmed that the concentration of octadecadienoic acid doubled *in-vitro* compared to *in-vivo*. In earlier research, the results of GC-MS analysis revealed similar compounds to those obtained in the present study[9].

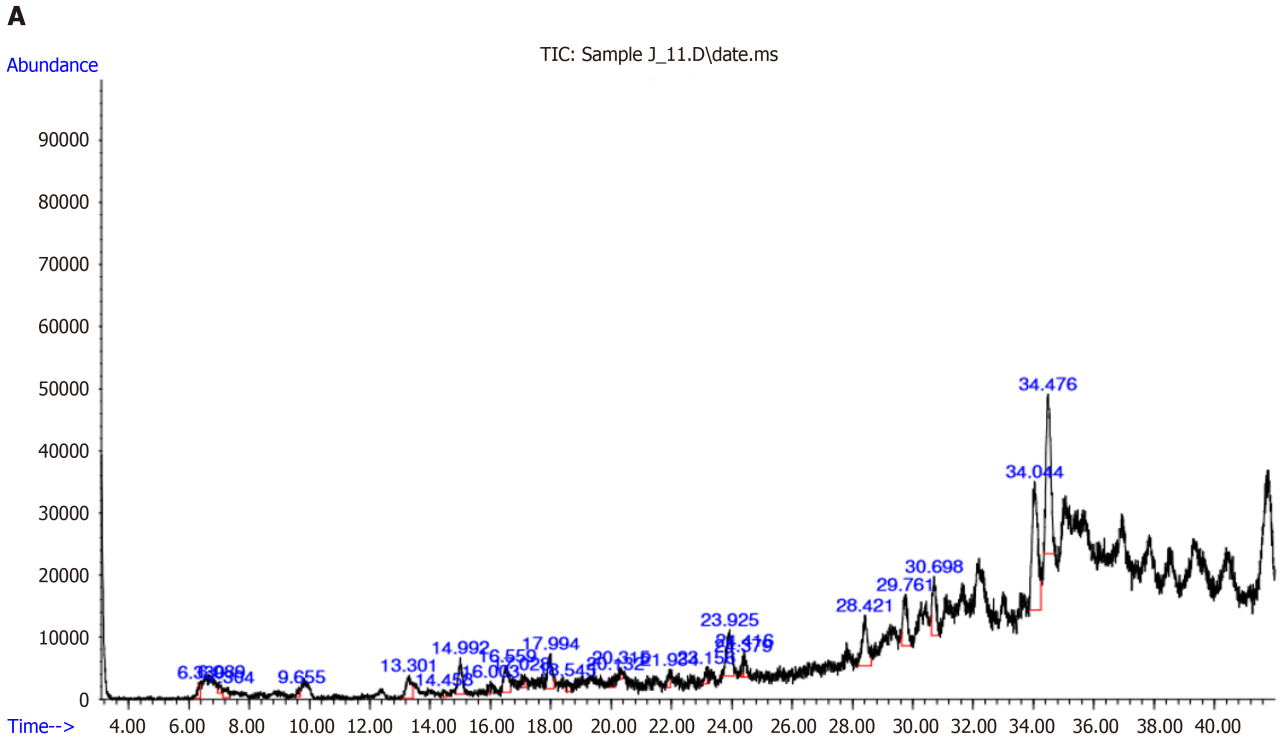

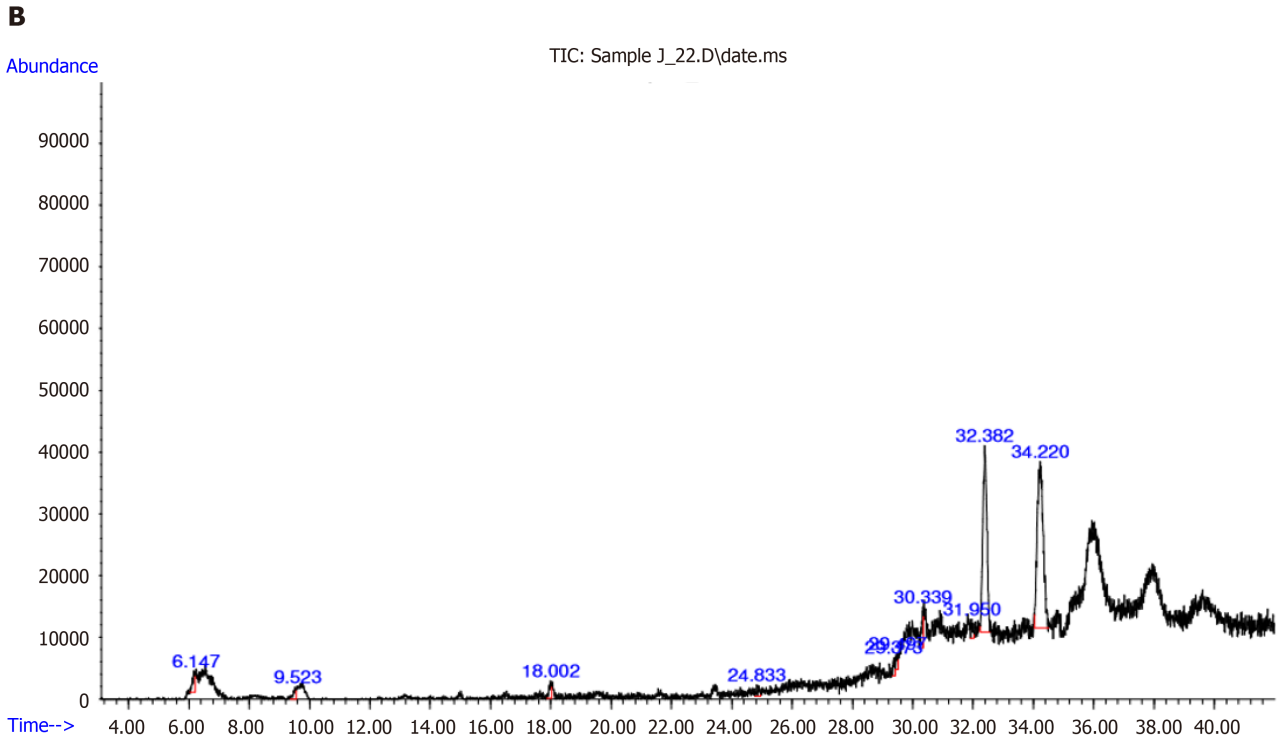

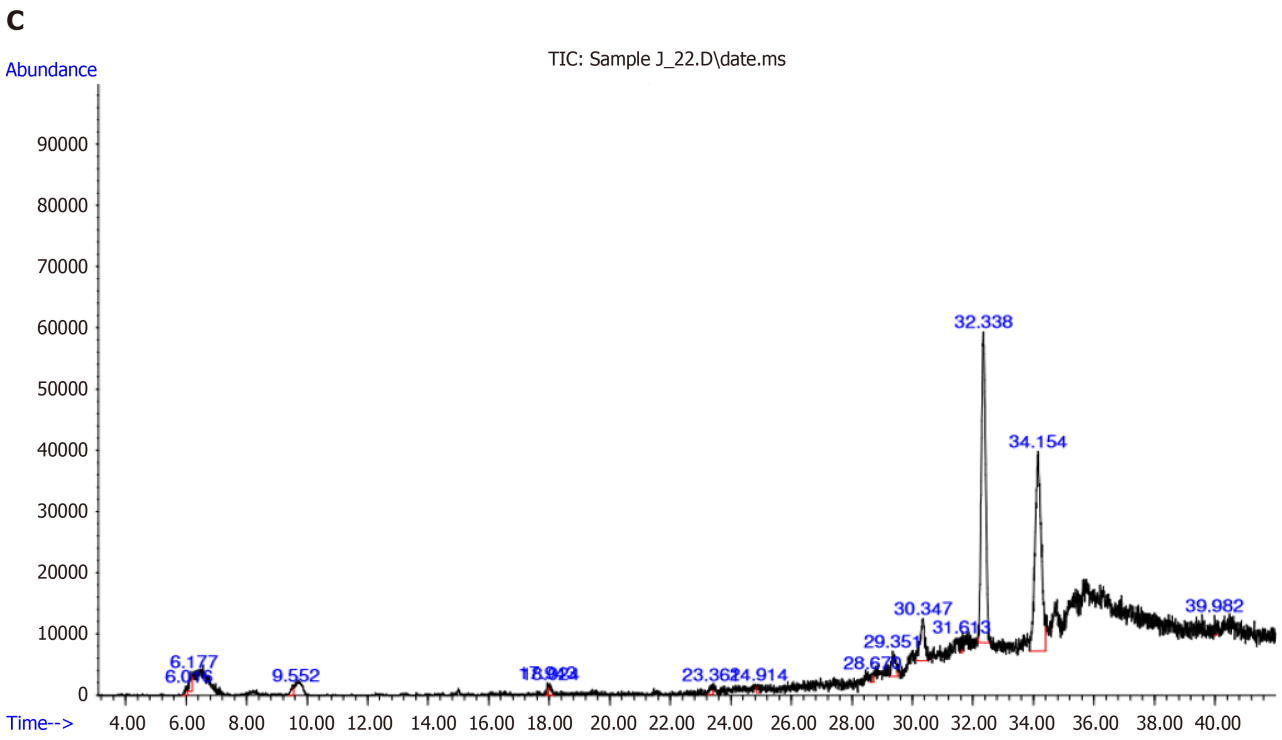

Figure 1 Gas chromatography-mass spectrometry chromatogram of the methanol extract of wild leaves, methanol extract of green callus, and methanol extract of white loose callus of *Vitex negundo* (*L.*). A: Methanol extract of wild leaves; B: Methanol extract of green callus; C: Methanol extract of white loose callus.

DISCUSSION

In *V. negundo* plants, octadecadienoic acid is present along with plant glycosides[10]. Plant glycosides are a diverse group of natural compounds found in various parts of plants, including leaves, stems, roots, and seeds. They consist of a sugar molecule (glycone) attached to a non-sugar, biologically active compound (aglycone or genin), which has both medicinal and toxic properties[11]. Along with the plants' glycosides, octadecadienoic acid develops bitterness in leaves, which frightens herbivores as the leaves are toxic or unpleasant when ingested[12]. Some important glycosides, *e.g.*, anthocyanin glycosides, along with octadecadienoic acid are responsible for the pigmentation (red, blue, and purple) in leaves, which act as stressors in plant defense against temperature stress[13].

Other bioactive constituents such as 1-oxo-dimethyl-methylene-hexahydrocyclopentanol pyran (7.91%), veridiflorol (6.79%), pyrrolo-carbazole (CAS) (6.79%), and dimethyl-phenyl (6.79% peak area) were identified in the methanolic leaf extract. It was observed that other bioactive compounds such as dursban, butyric acid, benzene, 1-methoxy-4-(1-propenyl), nor-ses-terterpene-diester, tri-decanedial, chlorpyrifos, methyl-cyclohexenyl-butanol, and anhalonine were present in good amount in *in-vitro* developed callus (both green-compact and white-loose) along with the major compounds (octadecanoic acid, hexadecanoic acid, and methyl ester) (Tables 3 and 4). The results obtained in the present study were analogous with the data obtained by Kaliyannagounder *et al*[9]. In medicinal plants, octadecadienoic acid is an important polyunsaturated fatty acid. It is also known as linoleic acid and plays several important roles in plant growth and development. Octadecadienoic acid triggers the production of defensive compounds in plants and plays a major role in plant defense mechanisms. It is considered a core-structural integral element of phospholipids that make up the lipid bi-layer of plant cell membranes. It maintains the integrity of the plant cell and controls the movement of molecules in and out of the cell along with other fatty acids. Finally, it adjusts the fluidity and stability of membranes under different environmental stresses, such as temperature extremes, drought, and pathogen attacks. Furthermore, it acts as a precursor of jasmonic acid, which is a signaling molecule involved in the plant's response to herbivores, pathogens, and other stressors in plant defense mechanisms. These findings are similar to those obtained by Ahuja *et al* [14].

Hexadecanoic acid and methyl esters have antioxidant, cholesterol-lowering, antiandrogenic, hemolytic, and alpha-reductase inhibitory properties. Hexadecanoic acid (palmitic acid) is a common saturated fatty acid, while hexadecanoic acid methyl ester (methyl palmitate) is a chemically modified derivative of palmitic acid. On the basis of data available in the literature, plant biomass with good amounts of methyl palmitate (a chemically modified derivative of hexadecanoic acid) is used in biodiesel production. The present study found that *in-vitro* grown callus (white-loose) is a good medium for the synthesis of methyl esters, and we can consider this approach in the near future as a source of renewable fuel for our future energy demands, if appropriate research is carried out[15].

In the present study, two major compounds were found *i.e.*, a sesquiterpenoid compound "viridiflorol" and anhalonine (naturally occurring alkaloid) in the *in-vitro*-derived white loose callus extract of *V. negundo*[16,17]. Viridiflorol showed anti-inflammatory, antioxidant, and anti-mycobacterium tuberculosis activity. Anhalonine is considered an important

Table 1 Effect of combinations of Plant Genetic Resources in mass spectrometry medium on callus induction in *Vitex negundo*

MS + hormone (mg/L)	Medium name	Source of explants	Number of explants inoculated	Callus response (%)	Callus genesis	Callus initiation (time/d)	Color	Texture
MS + no hormone	M1	Leaf	13	-	-	-	-	-
MS + BAP (2.0) + 2,4D (0.2)	M2	Leaf	13	15 d	+++	100%	Green	Friable
MS + BAP (2.0) + NAA (0.2)	M3	Leaf	13	15 d	++	70%	Greenish white	Friable
MS + DPU (2.0) + 2,4D (0.2)	M4	Leaf	13	15 d	+++	90%	White-yellowish	Loose
MS + DPU (2.0) + NAA (0.2)	M5	Leaf	13	15 d	+	40%	White-yellowish	Loose

MS: Mass spectrometry; BAP: 6-benzylaminopurine; NAA: α-naphthylacetic acid; DPU: Di-phenylurea.

Table 2 Bioactive components detected in the wild leaves methanol extract of *Vitex negundo* (*L.*)

Peak	Retention time	Area (%)	Name of components
1	6.330	1.12	Dimethylphosphine-D1
2	6.989	0.72	2-[2-hydroxyethyl]-9-[beta-d-ribofuranosyl] hypoxanthine
3	7.304	1.31	7-tetradecenyl-1-(N-acetyl)amine
4	9.655	0.56	1-propanol, 3-mercapto-sulfanyl-propanol
5	13.301	3.62	3-methylpyridazine pyridazine
6	14.458	0.55	2-octyldodecan-1-ol
7	14.992	3.96	3-hydroxyphenylacetylene 3-ethynylphenol
8	16.003	0.59	Z-citral 2,6-Octadienal, 3,7-dimethyl-, (Z)- (CAS)
9	16.559	03.80	1H-indenol
10	17.028	0.82	2-fluorobenzyl alcohol, benzene-methanol
11	17.994	4.28	Benzene, 1-methoxy-4-enylanisole
12	18.543	0.91	N-hexadecylpyridinium bromide
13	20.132	0.90	9-chloro-8-oxatetracyclotridecan
14	20.315	0.58	5-chlorovaleric acid, octyl ester
15	21.934	1.09	Dimethyl-2-phenyl-2-propenyl phosphite
16	23.156	0.92	4-chromanol-benzopyran-4
17	23.925	6.79	D-viridiflorol
18	24.379	0.75	8,9-epoxy-6,6-dimethyl-3,4-undecadien
19	24.416	1.51	Drimenol
20	28.421	7.91	1-oxo-5,5-dimethyl-6-methylene-hexahydrocyclopentano pyran
21	29.761	6.79	Pyrrolo-carbazole (CAS)
22	30.698	6.74	Dimethyl (phenyl) silane
23	34.044	21.93	9,12-octadecadienoic acid
24	34.476	21.84	2-hexadecen-1-OL, TETRAM

naturally occurring alkaloid. A very small amount of this compound was obtained from *Lophophora williamsii* (a rare species of cactus). It may serve as a chemical defense mechanism in some plants, and may be toxic to herbivores and pathogens. Hence, by producing anhalonine, plants may discourage herbivores and reduce the risk of damage from grazing animals. It seems that anhalonine also showed allelopathy. Such compounds are released by the plants into the soil through their root system and inhibit the growth of nearby competing plants and provide a competitive advantage

Table 3 Bioactive components detected in the green callus methanol extract of *Vitex negundo* (*L.*)

Peak	Retention time	Area (%)	Name of components
1	6.147	2.60	N-butyric-D7 acid
2	9.523	1.50	Benzyloxy-6-tetrabutyldimethyldimethylsilyl-oxy-methyl
3	18.002	1.76	Benzene, 1-methoxy-4 (CAS) anethole-p propenyl isole
4	24.833	1.23	Tridecanedial
5	29.373	1.50	Nor sesterterpene diene ester
6	29.497	1.38	But-2-enyliden-6-tert-butyl-7-methyl-tetrahydrocy
7	30.339	3.77	Hexadecanoic acid, methyl ester
8	31.950	1.63	Tricyclo-undecan-10-imine
9	32.382	36.82	Dursban
10	34.220	47.79	10,13-octadecadienoic acid, methyl ester

Table 4 Bioactive components detected in the white loose callus of methanol extract of *Vitex negundo* (*L.*)

Peak	Retention time	Area (%)	Name of components
1	6.016	0.58	Acetoxy-beta-caryophyllene
2	6.177	1.43	Anhalonine
3	9.552	0.84	1,3,5-cycloheptatriene-cyclohep-triene-cycloheptatrien
4	17.943	0.46	2,3-dichloropyridine 2, 3-dichloropyridine
5	18.024	0.83	1-methoxy-4-propenyl benzene
6	23.361	0.80	6,7-dimethyl-triazolo-triazine
7	24.914	0.51	Benzene, 2-methylthio-ethenyl
8	28.670	0.63	Spiro-decan-7-one, 1,8-dimethy epoxy-4-isopropyl
9	29.351	3.08	Methyl-cyclohex-1-enyl
10	30.347	6.31	14-pentadecynoic acid, methyl ester (CAS)
11	31.613	0.55	2,5-furandione, di hydro-dodecenylsuccinic anhydrid
12	32.338	42.98	Chlorpyrifos
13	34.154	40.38	Octadecadienoic acid, methyl ester
14	39.982	0.61	8-alpha,12-epoxy-hexanorlabdane

for the producing plant. It was noted in the present work that plants of *Vitex* grown in the *in-vivo* field condition usually inhibited the growth of weeds in their nearby area. This may be due to the presence of anhalonine, which was not detected in the methanolic extract of the wild leaf sample. The compound was present in very good amounts (peak area 1.43%) in white loose callus. Anhalonin, used as a psychotropic drug, can change the function of the nervous system and results in alterations of perception, mood, cognition, and behavior in our traditional folk medicinal/herbal system. It also showed antimicrobial properties, which protect the plants from microbial infections and diseases by acting as natural antimicrobial agent[18]. The exact role of anhalonine in plants has not been extensively studied. Detailed research on the functions of anhalonine in different plant species is continuing, and further studies are required to clarify its ecological and physiological significance in the plant system.

Similar outcomes were obtained in a previous study conducted by Lad *et al*[19]. The methanolic extract of *V. negundo* showed the presence of phytol compounds, which have other biological effects such as hypocholesterolemic cancer prevention, insecticidal, hepatoprotective, inhibition of 5-alpha reductase, anti-inflammatory, anti-rash, nematocidal, antihistamine, anti-acne, and anti-inflammatory antibiotic properties. The same bioactive SM of phytol has been previously reported to have various medicinal properties in some aquatic plant species such as *Hydrilla verticillata*, *Gracilaria*, and *Carissa carandas*[20,21]. Octadecanoic acid is a well-known example of a saturated fatty acid and possesses antihypertensive properties along with the ability to decrease low density lipoprotein cholesterol and increase high density lipoprotein cholesterol levels[22].

In the present study, octadecanoic acid was present in both leaf and callus extracts of *V. negundo*. The results of the present study were in accordance with reports on *Cleistanthus collinus*, *Goniothalamus umbrosus*, *Kigelia pinnata*, and *Melissa*

officinalis which contained n-hexadecanoic and octadecadienoic acids[23,24]. The study revealed the presence of various bioactive compounds present in all the methanolic extracts of *in-vivo* and *in-vitro* plant samples[25]. However, it has become clear from the present study that the callus contained additional phytochemicals in comparison to wild-type plants that display significant medicinal properties. Further studies such as bio-prospecting are necessary to support the biological properties and the importance of these inventive bio-molecules.

CONCLUSION

Screening of the methanolic extracts of *Vitex negundo* revealed the presence of twenty-four, ten, and fourteen bioactive compounds in the wild-leaves, green, and white loose callus, respectively. The results confirmed that octadecadienoic acid, hexadecanoic acid, and methyl ester were found to be the key constituents in the methanolic extract of leaves and callus[26]. Octadecadienoic acid was the predominant potential bioactive compound identified in all samples. Results of the present research confirmed that the concentration of octadecadienoic acid in *in-vitro* conditions was twice that in *in-vivo* conditions. Hence, in the case of *Vitex*, we can use micro-propagated plants as a potent source of phyto-compounds for commercialization without destroying the wild plant population[27,28]. A recent literature review showed that plant biomass with good amounts of methyl palmitate (a chemically modified derivative of hexadecanoic acid) is used in biodiesel production[29,30]. The findings of the present study showed that *in-vitro* grown callus is a good medium for the synthesis of methyl esters. Hence, we can consider this approach in the near future as a source renewable fuel for our future energy demands. Active sesquiterpenoid compounds such as viridiflorol and anhalonine (naturally occurring alkaloid) were found in the *in-vitro* derived white loose callus extract of *Vitex negundo*. Viridiflorol showed anti-inflammatory, antioxidant, and anti-mycobacterium tuberculosis activity, while anhalonine may be used as a psychotropic drug in animals and is also responsible for showing allelopathy in plants. This study showed that the callus contained additional botanical characteristics in comparison to wild plants. Due to the presence of numerous bioactive compounds, the medical use of *Vitex* callus for various diseases has been accepted and the plant is considered an important source of therapeutics for research and development.

ARTICLE HIGHLIGHTS

Research background

Gas chromatography-mass spectrometry (GC-MS) analysis of the methanolic leaf extract of *Vitex negundo* has been previously demonstrated in a few studies. The present study has significance as it investigated the plant-based therapeutic agents in the medicinal plant *Vitex negundo*, determined their presence in extracts and provides the vision to formulate novel techniques for drug therapy.

Research motivation

This study identified dospan, butyric acid, benzene, 1-methoxy-4-(1-propenyl), n-sec-terpene-diester, tris-decandial, chlorpyrifos, methyl-cyclohexenyl-butanol, anhalonine, and other important active compounds. These substances are only found in calluses produced *in-vitro*. The results demonstrated that callus has more botanical properties than wild plants. The medicinal application of *Vitex negundo* for various diseases has been recognized due to the identification of various bioactive compounds, and the plant is recognized as an important botanical remedy in medical research and development.

Research objectives

The exact role of anhalonine in animals and plants has not been well-studied.

Research methods

In the present study, we report a GC-MS investigation of leaf extracts from wild plants and correlate the existence of components with those present in callus extracts. Various concentrations of growth regulators such 2,4-dichlorophenoxyacetic acid (2,4-D), α-naphthaleneacetic acid, 6-benzylaminopurine (BAP), and di-phenylurea (DPU) were added to *in-vitro* callus and plant leaves and grown on MS medium. The maximum and rapid response for callogenesis with a green and friable callus was observed in the MS medium with BAP (2.0 mg/L) and 2,4-D (0.2 mg/mL) and DPU (2.0 mg/L) with 2,4-D (0.2 mg/L). The plant profile of *Vitex negundo* extracts underwent GC-MS analysis, from which 24, 10, and 14 bioactive compounds were detected from leaf, green callus, and white loose callus methanolic extracts, respectively.

Research results

Screening of the methanolic extracts of *Vitex negundo* revealed the presence of twenty-four, ten, and fourteen bioactive compounds in the wild-leaves, green, and white loose callus, respectively. Our research data confirmed that octadecadienoic acid, hexadecanoic acid, and methyl ester were the key constituents in the methanolic extract of leaves and callus. Octadecadienoic acid was the predominant potential bioactive compound identified in all samples. The results of our research confirmed that the concentration of octadecadienoic acid in *in-vitro* conditions was twice that in *in-vivo* conditions. Hence, in the case of *Vitex*, we can use micro-propagated plants as a source of potent phyto-compounds for

commercialization without destroying the wild plant population.

Research conclusions

A recent literature review showed that plant biomass with good amounts of methyl palmitate (a chemically modified derivative of hexadecanoic acid) is used in biodiesel production. In the present study, we found that *in vitro* grown callus is a good medium for the synthesis of methyl esters. Hence, we can consider this approach in the near future as a source of renewable fuel for our future energy demands. We also found the active sesquiterpenoid compound viridiflorol and anhalonine (naturally occurring alkaloid) in the *in vitro*-derived white loose callus extract of *Vitex negundo*. Viridiflorol showed anti-inflammatory, antioxidant, and anti-mycobacterium tuberculosis activity, while anhalonine may be used as a psychotropic drug in animals and is responsible for showing allelopathy in plants.

Research perspectives

Detailed research and further studies on the functions of anhalonine in different plant species are required to clarify the physiological significance of anhalonine in plants. Findings from our research show that *Vitex negundo* is a phyto-pharmaceutically important plant.

ACKNOWLEDGEMENTS

Authors are grateful to Dr. Shoor Vir Singh, Professor & Head, Department of Biotechnology at GLA University, Mathura for help and support during the present study.

FOOTNOTES

Author contributions: Garg G and Chaudhary S contributed to the conceptualization of this study, writing the original draft, reviewing, and editing; Bharadwaj A was involved in the data collection, analysis and interpretation of results; Gupta V participated in critical revision of the article, and editing.

Institutional review board statement: This study did not involve animal or human experimentation. Thus, an institutional review board statement is not required.

Clinical trial registration statement: This study did not involve animal or human experimentation. Thus, a clinical trial registration statement is not required.

Informed consent statement: This study did not involve animal or human experimentation. Thus, an informed consent statement is not required.

Conflict-of-interest statement: All the authors report no relevant conflicts of interest for this article.

Data sharing statement: No additional data to those presented in the study are available.

Country/Territory of origin: India

ORCID number: Gunjan Garg 0000-0002-6971-1981; Alok Bharadwaj 0000-0002-7383-188X; Shweta Chaudhary 0009-0000-9727-6414; Veena Gupta 0009-0005-3558-0900.

S-Editor: Wang JJ
L-Editor: Webster JR
P-Editor: Zhao YQ

REFERENCES

1 **Prasathkumar M**, Anishaa S, Dhrisyaa C, Beckya R, Sadhasivama S. Therapeutic and pharmacological efficacy of selective Indian medicinal plants - A review. *Phytomedicine Plus* 2021; **1**: 100029 [DOI: 10.1016/j.phyplu.2021.100029]

2 **Chiocchio I**, Mandrone M, Tomasi P, Marincich L, Poli F. Plant Secondary Metabolites: An Opportunity for Circular Economy. *Molecules* 2021; **26** [PMID: 33477709 DOI: 10.3390/molecules26020495]

3 **Isah T**, Umar S, Mujib A, Sharma MP, Rajasekharan PE, Zafar N, Frukh A. Secondary metabolism of pharmaceuticals in the plant in-vitro cultures, strategies, approaches and limitations to achieving higher yield. *Plant Cell Tiss Organ Cult* 2018; **132**: 239-265 [DOI:

10.1007/s11240-017-1332-2]

4 **Bhambhani S**, Kondhare KR, Giri AP. Diversity in Chemical Structures and Biological Properties of Plant Alkaloids. *Molecules* 2021; **26** [PMID: 34204857 DOI: 10.3390/molecules26113374]

5 **Anwar F**, Qayyum HM, Hussain AI, Iqbal S. Antioxidant activity of 100% and 80% methanol extracts from Barley seeds (Hordeum vulgare L.): stabilization of sunflower oil. *Grasas y Aceites* 2010; **61**: 237-243 [DOI: 10.3989/gya.087409]

6 **Tawfeeq TA**, Tawfeeq AA, Eldalawy R, Ibraheem SK. Phytochemical Analysis, GC-MS Identification, and Estimation of Antioxidant Activity of Iraqi Vitex negundo L. *J Med Chemical Sci* 2023 [DOI: 10.26655/JMCHEMSCI.2023.4.19]

7 **Fatema A**, Ubale MB, Farooqui M, Pathan AAK. Analysis of biological activity and gas chromatography-mass spectrometry study of conventional extraction of Vitex negundo (L) leaves. *Asian J Pharma Clin Res* 2019; **12**: 289 [DOI: 10.22159/ajpcr.2018.v12i1.27854]

8 **Jabeen M**, Uzair M, Siddique F, Khan MS, Hanif M, Salamatullah AM, Nafidi HA, Bourhia M. Exploring the antioxidant and anti-inflammatory potential of Wilckia maritima: In-vitro and In silico investigations. *Processes* 2023; **11**: 1497 [DOI: 10.3390/pr11051497]

9 **Kaliyannagounder S**, Chitraputhirapillai S, Raman R, Sampathrajan V, Palani N, Baskaran S. GC-MS profiling of phytocompounds in the leaves of Vitex negundo L. *Current Sci* 2023; **125**: 1250-1258

10 **Preetha SP**, Kamalabai RAS, Jayachandran KS. Qualitative and quantitative phytochemical screening of Vitex negundo L. extract using chromatographic and spectroscopic studies. *Nat Volatiles Essent Oils* 2021; **8**: 11949-11961

11 **Vignesh A**, Selvakumar S, Vasanth K. Comparative LC-MS analysis of bioactive compounds, antioxidants and antibacterial activity from leaf and callus extracts of Saraca asoca. *Phytomedicine Plus* 2022; **2**: 100167 [DOI: 10.1016/j.phyplu.2021.100167]

12 **Meena AK**, Perumal A, Kumar N, Singh R, Ilavarasan R, Srikanth N, Dhiman KS. Studies on physicochemical, phytochemicals, chromatographic profiling and estimation and in-silico study of Negundoside in roots & small branches of Vitex negundo. *Phytomedicine Plus* 2022; **2**: 100205 [DOI: 10.1016/j.phyplu.2021.100205]

13 **Bose Mazumdar Ghosh A**, Banerjee A, Chattopadhyay S. An insight into the potent medicinal plant Phyllanthus amarus Schum. and Thonn. *Nucleus (Calcutta)* 2022; **65**: 437-472 [PMID: 36407559 DOI: 10.1007/s13237-022-00409-z]

14 **Ahuja SC**, Ahuja S, Ahuja U. Nirgundi (Vitex negundo) - nature's gift to mankind. *Asian Agri-Hist* 2015; **19**: 5-32

15 **Vidana Gamage GC**, Lim YY, Choo WS. Anthocyanins From Clitoria ternatea Flower: Biosynthesis, Extraction, Stability, Antioxidant Activity, and Applications. *Front Plant Sci* 2021; **12**: 792303 [PMID: 34975979 DOI: 10.3389/fpls.2021.792303]

16 **Brahma S**, Nath B, Basumatary B, Das B, Saikia P, Patir K, Basumatary S. Biodiesel production from mixed oils: A sustainable approach towards industrial biofuel production. *Chemical Engineering J Advances* 2022; **10**: 100284 [DOI: 10.1016/j.ceja.2022.100284]

17 **Dwivedi MK**, Shukla R, Sharma NK, Manhas A, Srivastava K, Kumar N, Singh PK. Evaluation of ethnopharmacologically selected Vitex negundo L. for In vitro antimalarial activity and secondary metabolite profiling. *J Ethnopharmacol* 2021; **275**: 114076 [PMID: 33789139 DOI: 10.1016/j.jep.2021.114076]

18 **Meena S**, Kanthaliya B, Joshi A, Khan F, Choudhary S, Arora J. In-vitro Production of Alkaloids. In: Nutraceuticals Production from Plant Cell Factory. *Singapore: Springer Nature* 2022; 143-168

19 **Lad H**, Dixit D, Joshi A, Bhatnagar D. Antioxidant and antiinflammatory effects of Vitex negundo on FREUND'S complete adjuvant induced arthritis. *Int J Pharm Pharm Sci* 2015

20 **Prabha SP**, Karthik C, Chandrika SH. Phytol-A biosurfactant from the aquatic weed *Hydrilla verticillate*. *Biocatal Agric Biotechnol* 2019; **17**: 736-742 [DOI: 10.1016/j.bcab.2019.01.026]

21 **Ram M**, Rao MR, Anisha G, Prabhu K, Shil S, Vijayalakshmi N. Preliminary phytochemical and gas chromatography-mass spectrometry study of one medicinal plant Carissa carandas. *Drug Invit Today* 2019; **12**: 1629-1630

22 **Uthaug MV**, Davis AK, Haas TF, Davis D, Dolan SB, Lancelotta R, Timmermann C, Ramaekers JG. The epidemiology of mescaline use: Pattern of use, motivations for consumption, and perceived consequences, benefits, and acute and enduring subjective effects. *J Psychopharmacol* 2022; **36**: 309-320 [PMID: 33949246 DOI: 10.1177/02698811211013583]

23 **Azemi NA**, Azemi AK, Abu-Bakar L, Sevakumaran V, Muhammad TST, Ismail N. Effect of Linoleic Acid on Cholesterol Levels in a High-Fat Diet-Induced Hypercholesterolemia Rat Model. *Metabolites* 2022; **13** [PMID: 36676979 DOI: 10.3390/metabo13010053]

24 **Praveen Kumar P**, Kumaravel S, Lalitha C. Screening of antioxidant activity, total phenolics and GC-MS study of Vitex negundo. *Afr J Biochem Res* 2010; **4**: 191-195

25 **Haridasan P**, Gokuldas M, Ajaykumar AP. Antifeedant effects of Vitex negundo L. leaf extracts on the stored product pest, Tribolium castaneum H. (Coleoptera: Tenebrionidae). *Int J Pharm Pharm Sci* 2017; **9**: 17-22 [DOI: 10.22159/IJPPS.2017V9I3.15600]

26 **Othman RA**, Moghadasian MH. Beyond cholesterol-lowering effects of plant sterols: clinical and experimental evidence of anti-inflammatory properties. *Nutr Rev* 2011; **69**: 371-382 [PMID: 21729090 DOI: 10.1111/j.1753-4887.2011.00399.x]

27 **Godara P**, Dulara BK, Barwer N, Chaudhary NS. Comparative GC-MS analysis of bioactive phyto chemicals from different plant parts and callus of Leptadenia reticulata. *Pharmacogn J* 2019 [DOI: 10.5530/PJ.2019.1.22]

28 **Preetha SP**, Salomee Kamalabai RA, Jayachandran KS. Qualitative and quantitative phytochemical screening of Vitex negundo L. extract using chromatographic and spectroscopic studies. *Nat Volatiles Essent Oil* 2021; **8**

29 **Deka C**, Basumatary S. High quality biodiesel from yellow oleander (Thevetia peruviana) seed oil. *Biomass Bioenergy* 2011; **35**: 1797-1803 [DOI: 10.1016/j.biombioe.2011.01.007]

30 **Jumina J**, Kurniawan YS, Lubis AB, Larasati EI, Purwono B, Triono S. Utilization of vanillin to prepare sulfated Calix[4]resorcinarene as efficient organocatalyst for biodiesel production based on methylation of palmitic acid and oleic acid. *Heliyon* 2023; **9**: e16100 [PMID: 37251819 DOI: 10.1016/j.heliyon.2023.e16100]

World Journal of Experimental Medicine

Submit a Manuscript: https://www.f6publishing.com

World J Exp Med 2024 March 20; 14(1): 87256

DOI: 10.5493/wjem.v14.i1.87256

ISSN 2220-315x (online)

ORIGINAL ARTICLE

Basic Study

Effects of unilateral superimposed high-frequency jet ventilation on porcine hemodynamics and gas exchange during one-lung flooding

Thomas Lesser, Frank Wolfram, Conny Braun, Reiner Gottschall

Specialty type: Medicine, research and experimental

Provenance and peer review: Unsolicited article; Externally peer reviewed.

Peer-review model: Single blind

Peer-review report's scientific quality classification

Grade A (Excellent): 0
Grade B (Very good): 0
Grade C (Good): C, C
Grade D (Fair): 0
Grade E (Poor): 0

P-Reviewer: Liu Y, China

Received: September 13, 2023
Peer-review started: September 13, 2023
First decision: November 21, 2023
Revised: November 30, 2023
Accepted: December 29, 2023
Article in press: December 29, 2023
Published online: March 20, 2024

Thomas Lesser, Frank Wolfram, Department of Thoracic and Vascular Surgery, SRH Wald Klinikum Gera, Gera D-07548, Germany

Conny Braun, Central Experimental Animal Facility, Jena University Hospital, Jena 07743, Germany

Reiner Gottschall, Department of Anaesthesiology and Intensive Care, Jena University Hospital, Jena 07747, Germany

Corresponding author: Thomas Lesser, MD, Adjunct Professor, Department of Thoracic and Vascular Surgery, SRH Wald Klinikum Gera, No. 122 Street of Peace, Gera D-07548, Germany. thomas.lesser@srh.de

Abstract

BACKGROUND

Superimposed high-frequency jet ventilation (SHFJV) is suitable for respiratory motion reduction and essential for effective lung tumor ablation. Fluid filling of the target lung wing one-lung flooding (OLF) is necessary for therapeutic ultrasound applications. However, whether unilateral SHFJV allows adequate hemodynamics and gas exchange is unclear.

AIM

To compared SHFJV with pressure-controlled ventilation (PCV) during OLF by assessing hemodynamics and gas exchange in different animal positions.

METHODS

SHFJV or PCV was used alternatingly to ventilate the non-flooded lungs of the 12 anesthetized pigs during OLF. The animal positions were changed from left lateral position to supine position (SP) to right lateral position (RLP) every 30 min. In each position, ventilation was maintained for 15 min in both modalities. Hemodynamic variables and arterial blood gas levels were repeatedly measured.

RESULTS

Unilateral SHFJV led to lower carbon dioxide removal than PCV without abnormally elevated carbon dioxide levels. SHFJV slightly decreased oxygenation in SP and RLP compared with PCV; the lowest values of PaO_2 and PaO_2/FiO_2 ratio were found in SP [13.0; interquartile range (IQR): 12.6-5.6 and 32.5 (IQR: 31.5-38.9) kPa]. Conversely, during SHFJV, the shunt fraction was higher in all animal

positions (highest in the RLP: 0.30).

CONCLUSION

In porcine model, unilateral SHFJV may provide adequate ventilation in different animal positions during OLF. Lower oxygenation and CO_2 removal rates compared to PCV did not lead to hypoxia or hypercapnia. SHFJV can be safely used for lung tumor ablation to minimize ventilation-induced lung motion.

Key Words: One-lung ventilation; Unilateral superimposed high-frequency jet ventilation; One-lung flooding

Core Tip: Lung cancer prognosis is among the most unfavourable of all cancers. Therefore, there is a need to improve local lung cancer therapy while avoiding surgery. One-lung flooding (OLF) involves unilateral lung filling with saline, which generates a suitable acoustic pathway for the transthoracic application of High-intensity focused ultrasound (HIFU) in the lung. Breathing and lung movement during HIFU procedures can result in incomplete tumor ablation or collateral damage. Superimposed high-frequency jet ventilation (SHFJV) can reduce respiratory motion. However, it is unclear whether unilateral SHFJV allows adequate haemodynamics and gas exchange. In this porcine model, unilateral SHFJV may provide adequate ventilation to animals in different positions during OLF. Lower oxygenation and carbon dioxide removal rates compared to pressure controlled ventilation did not lead to hypoxia or hypercapnia. SHFJV can safely minimise ventilation-induced lung motion during lung tumor ablation.

Citation: Lesser T, Wolfram F, Braun C, Gottschall R. Effects of unilateral superimposed high-frequency jet ventilation on porcine hemodynamics and gas exchange during one-lung flooding. *World J Exp Med* 2024; 14(1): 87256
URL: https://www.wjgnet.com/2220-315x/full/v14/i1/87256.htm
DOI: https://dx.doi.org/10.5493/wjem.v14.i1.87256

INTRODUCTION

Thermal ablation of tumors in solid organs is one of the most promising and dynamic procedures in clinical oncology[1]. However, of all the minimally invasive ablation therapies, ultrasound ablation is the only non-invasive approach to ablate the targeted tumor at depth without any needle insertion. High-intensity focused ultrasound (HIFU) is currently used to treat solid tumors, including those of the liver, breast, pancreas, kidney, and prostate[2-7]. In terms of limitations, organ movement during HIFU procedures can lead to incomplete target ablation or collateral damage[8]. Besides strategies for respiratory motion compensation such as breath hold, gating, and tumor tracking techniques[9], high-frequency jet ventilation (HFJV) utilizes very low tidal volumes, which in turn are associated with smaller respiratory movement of the lung, mediastinum and diaphragm compared with conventional ventilation[10]. Many reports describe the use of HFJV for minimally invasive treatment of tumors with different techniques and thermal ablation in the lung, liver and kidney, including percutaneous, laparoscopic, and open approaches[11,12]. However, under HFJV, a mild to moderate deterioration of gas exchange and the development of atelectasis has been observed[13,14]. Jet ventilation is the pulsed release of gas portions with high kinetic energy through adapted small-lumen tubes into the airways open to the outside. This resulted in a high gross gas volume. Simultaneous coaxial inflow and outflow are the most effective gas-transport mechanisms under jet ventilation. Because there is no gas-tight connection between the jet ventilator and the airway, intravenous anesthesia is necessary. Ventilation was indirectly measured using arterial, end-tidal, or transcutaneous CO_2 measurements. The pulse frequency can be low, high, or combined superimposed HFJV (SHFJV) and is used for various clinical applications. The frequency-dependent shortening of exhalation time enables positive end-expiratory pressure (PEEP). Peak airway pressure remains comparatively low. In addition to the ventilation frequency, other adjustable jet parameters, such as jet (driving) pressure, inspiration duration, and oxygen concentration, and the individual thorax-lung mechanics, determine gas exchange[15].

For lung tumor ablation with ultrasound, a new method for complete lung sonography has been developed[16]. This so-called one-lung flooding (OLF) involves unilateral lung filling with saline after general anesthesia and double-lumen tube intubation, which generates a suitable acoustic pathway for the transthoracic application of HIFU in the lung and liver[17,18]. Saline filling of one lung requires one-lung ventilation (OLV) of the contralateral lung. In this study, we decided to use body weight-based SHFJV for OLV. Two jet streams with different frequencies were simultaneously applied using this technique. A continuous high-frequency jet stream was superimposed during the inspiratory and expiratory phases of low-frequency jet ventilation (Figure 1).

The low-frequency jet stream resulted in phased airway pressure changes analogous to conventional ventilation with 12-20/min, providing the upper pressure level. A high-frequency jet stream with a 100-900 cycles/min frequency generates a lower pressure level (*i.e.*, the PEEP)[19]. Compared to HFJV, SHFJV increases minute ventilation and facilitates carbon dioxide removal[20]. It may also increase end-expiratory lung volume and tidal volume, improving oxygenation[21-23].

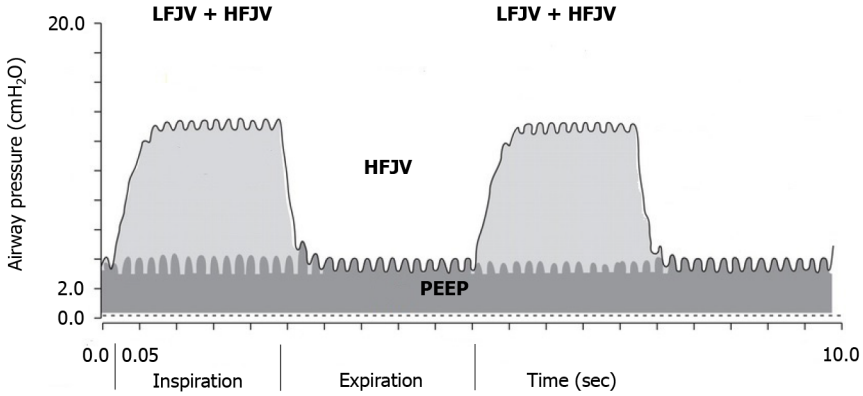

Figure 1 Illustration of superimposed high-frequency jet ventilation with typical pressure curves of continuous high-frequency jet ventilation and two cycles of simultaneous low-frequency jet ventilation. The low-frequency jet ventilation provides the upper pressure level, and the high-frequency jet ventilation generates the lower pressure level (*i.e.*, the positive end-expiratory pressure). PEEP: Positive end-expiratory pressure; HFJV: High-frequency jet ventilation; LFJV: Low-frequency jet ventilation.

However, studies on the unilateral SHFJV are limited. It is unclear whether unilateral SHFJV ensures adequate gas exchange during OLF. This study aimed to investigate the effects of unilateral SHFJV on hemodynamics and gas exchange during OLF compared to standard pressure-controlled ventilation (PCV). Depending on the driving pressure (DP), the low-frequency jet stream results in phased upper airway pressure changes, causing more or less large movement of the ventilated system and adjacent organs[24]. To keep the movement as low as possible, the DP of the low-frequency jet stream was chosen to be lower than the usual setting.

The patient position may be different because of the diverse forms of clinical application of HIFU treatment. Ultrasound-guided HIFU treatment requires a lateral position with the target lung above, whereas, for magnetic resonance-guided HIFU treatment, the target lung must be positioned below because the transducer is usually integrated into the magnetic resonance table. To consider different clinical applications, the effects of unilateral SHFJV during OLF on hemodynamics and gas exchange compared with PCV were investigated in different animal positions.

MATERIALS AND METHODS

Animals

Seventeen juvenile female pigs (German Landrace) with a mean age of 13.6 wk (range: 12-16 wk) and a mean weight of 37.5 kg (range: 36-42 kg) were included in this study. The animals were maintained in groups and housed at the facility for four days before the study to acclimate them to their surroundings. Before the experiments, the animals were confirmed to be healthy by a veterinarian. The Veterinary Department of the Thuringian State Authority approved the present study for Food Protection and Fair Trading (TLLV Reg. 22-2684-04-WKG-16-002). All procedures were performed in the laboratories at the Central Experimental Animal Facility of Jena University Hospital in compliance with the National Animal Protection Act.

Anaesthesia and instrumentation

Ketamine (25 mg/kg) and midazolam (0.2 mg/kg) were administered intramuscularly as premedicants. After intravenous catheter placement in the ear vein and a bolus injection of propofol (3 mg/kg) and fentanyl (2.7 μg/kg), tracheal intubation was performed using a single-lumen endotracheal tube (6.5 mm ID; Dahlhausen, Köln, Germany). PCV was initiated (Servo 900 C; Siemens AG, Erlangen, Germany) with the following settings: fraction of inspired oxygen (FiO_2), 0.4; P_{insp} 15 cm H_2O; inspiratory to expiratory (I:E) ratio, 1:1.9; ventilatory frequency, 20/min; and PEEP, 4 cm H_2O. These settings were maintained throughout the experiment (and adjusted as necessary to maintain an end-expiratory CO_2 tension of 35-45 mmHg), except for FiO_2, which was increased to 1.0 for denitrogenation of the lungs before OLF. Intravenous anesthesia was initiated and maintained using a continuous intravenous infusion of propofol (6 mg/kg^{-1} h^{-1}) and hourly boluses of fentanyl (2.7 μg/kg). After confirming that anesthesia was deep enough, pancuronium bromide (0.06 mg/kg hourly) maintained neuromuscular block. Electrocardiography and peripheral capillary oxygen saturation (SpO_2) were monitored throughout the procedure (Datex AS/3, Datex-Ohmeda, Helsinki, Finland). Subsequently, the right common carotid artery and internal jugular vein are exposed through a cervical incision. An arterial catheter (Arterial Leader Cath, 2.7 Fr; Vygon, Ecouen, France) was placed using a sterile technique and advanced 10 cm into the central common carotid artery for invasive arterial pressure measurement and blood gas sampling. For mixed venous blood sampling and pulmonary artery pressure measurement, a flow-directed pulmonary artery catheter (6 Fr; Swan Ganz; Edwards Lifesciences, Irvine, CA, United States) was inserted through an introducer sheath (8 Fr; Arrow International, Reading, PA, United States) in the right internal jugular vein. Urinary bladder catheterization was performed. The core temperature of the animals was measured using a rectal probe. Warmed infusions and coffering of the animals using a convective warming system (WarmTouch 5800, Mallinckrodt Medical, Hennef, Germany) were used to maintain

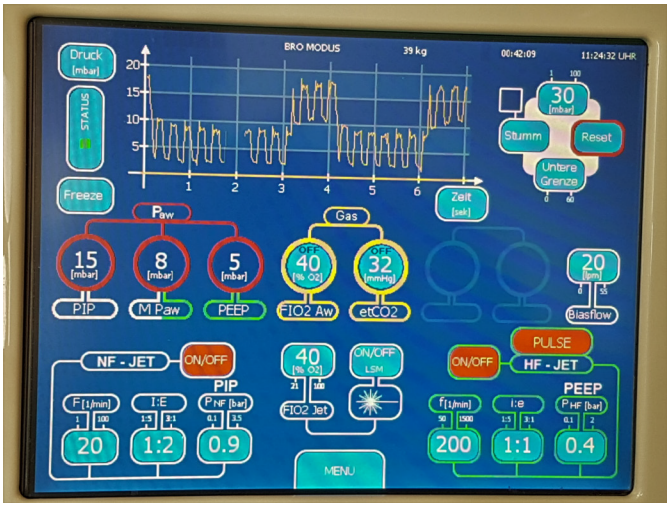

Figure 2 The TwinStream™ ICU monitor displays the selected superimposed high-frequency jet ventilation setting.

normothermia. With the pig in the supine position (SP), a 35-Fr left-sided double-lumen endobronchial tube (DLT) designed for use in pigs and specifically made for this study (Medicoplast International GmbH, Illingen, Germany)[25] was placed using an airway exchange catheter (11.0 Fr, 100 cm, extra-firm with a soft tip; COOK Deutschland GmbH, Mönchengladbach, Germany). The correct position of the DLT was confirmed using a fiber optic bronchoscope (BF 3C30; Olympus, Tokyo, Japan). A cuff controller (VBM Medizintechnik GmbH, Sulz a.N., Germany) was used to maintain a constant pressure of 50 cm H_2O within both the endobronchial and tracheal cuffs. The ventilator was connected to the DLT with unchanged settings. At the end of the experiment, the animals were euthanized under deep anesthesia by injecting pentobarbital sodium.

Interventions

OLF: Immediately before OLF, the animals underwent two-lung ventilation (TLV) with a FiO_2 of 1.0 for 20 min to denitrogenate the lungs. The animals were then placed in the left lateral decubitus position (LLP) with the lung flooded in the dependent position, and the left (bronchial) lumen of the DLT disconnected from the ventilator. An infusion system was immediately connected to the left limb of the DLT, and the left lung was slowly filled (single filling) with degassed, warmed (37 °C) isotonic saline flowing passively from an infusion bottle suspended 50 cm above heart level. The volume to be infused was estimated as one-half the functional residual capacity of the lungs (12.5 mL/kg)[26,27]. Complete saline filling was monitored with transcutaneous lung ultrasound (Flex Focus 800; BK Medical, Arhus, Denmark).

PCV

Before and after OLF, both lungs were conventionally ventilated using the ventilator set at the beginning of the experiment (see above). During OLF, OLV of the non-flooded right lung was performed without changing the setting.

Unilateral SHFJV

The inspiratory hold maneuver was performed immediately before the transition from PCV to jet ventilation. A jet ventilator (TwinStream™ ICU; Carl Reiner GmbH, Vienna, Austria) in bronchoscopy mode was connected to the right (tracheal) lumen of the DLT using a special adapter (jet converter, I.D. 15 mm; Carl Reiner GmbH, Vienna, Austria). A bias flow of warmed, humidified gas at 20 L min^{-1} with ventilator-identically FiO_2 was connected to a jet converter (AIRcon Gen2; WILAmed GmbH, Kammerstein, Germany). The exhaled gas was hygienically filtered (DARTM Mechanical Filter Large; Covidien Ltd., Mansfield, MA, United States). The low-frequency jet stream component is primarily responsible for CO_2 elimination but causes in-and expiratory movements similar to those during conventional ventilation. The extent of the movement depends on the basic/outlet DP of the low-frequency jet stream component. A previous study found that an SHFJV with a DP of 0.9 bar for the low-frequency jet stream reduces diaphragm and lung motion significantly[24]. Based on that, we found in a pilot study on three animals that this DP may ensure an acceptable gas exchange. This study aimed to verify these preliminary findings. The ventilator settings for the low-frequency jet component were 20/min, I/E = 1:2, and a basic/outlet DP of 0.9 bar. The high-frequency jet component had a 200/min frequency, an I/E ratio of 1:1, and DP of 0.4 bar. FiO_2 was set at 0.4. The low- and high-frequency components were applied simultaneously (Figure 2).

Independent of the arterial partial pressure of carbon dioxide monitoring, end-expiratory CO_2 tension measurements were performed every 5 min (integrated ventilator end-expiratory CO_2 module). When the end-expiratory CO_2 tension exceeded 45 mmHg, the DP of the low-frequency jet stream increased stepwise by 0.1 bar to a maximum of 1.3 bar.

Experimental protocol

The left lung was flooded in the experimental group (OLF, n = 12), and the right lung was ventilated successively using different modes. After OLF, the animal's position was changed every 30 min from the LLP to the SP and then to the right

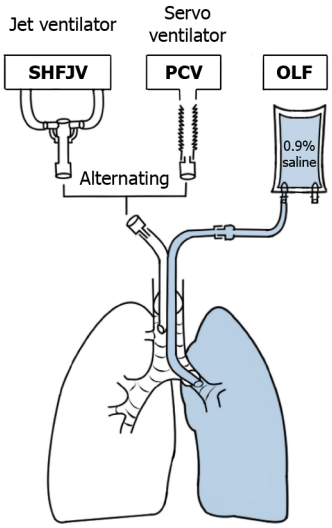

Figure 3 Experimental set-up. SHFJV: Superimposed high-frequency jet ventilation; PCV: Pressure-controlled ventilation; OLF: One-lung flooding.

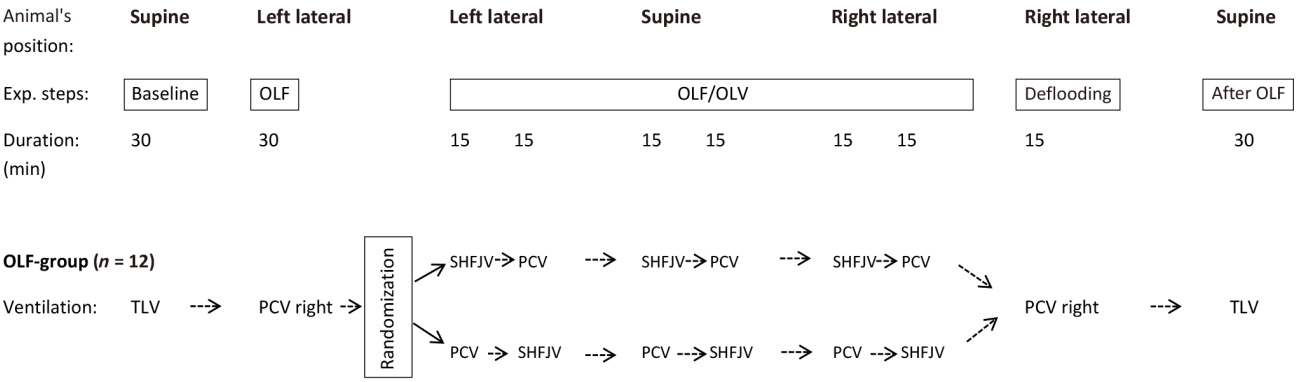

Figure 4 Flow scheme of the experimental protocol. SHFJV: Superimposed high-frequency jet ventilation. In the control group (n = 5) both lungs were ventilated with pressure-controlled ventilation (two-lung ventilation) throughout the experimental time without lung flooding, but the position change was the same. OLF: One-lung flooding (left lung); OLV: One-lung ventilation; TLV: Two-lung ventilation; PCV: Pressure-controlled ventilation.

lateral position (RLP). Thereafter, the fluid was passively drained from the left lung, followed by conventional ventilation of both lungs (TLV) over 30 min with the animals in SP. The order in which the animals were positioned was defined as the flooding that worked best when the lung to be flooded was below it. The risk of fluid overflow in the event of tube dislocation was the greatest in the RLP; therefore, this position was used at the end of the experiment. A unilateral SHFJV or PCV was alternately used during OLF to ventilate the right lung. Ventilation modes were applied successively, and ventilation was maintained for 15 min in all modalities (Figures 3 and 4).

To minimise the influence of time point in ventilation mode on gas exchange efficacy associations with animal position, the order of the ventilation modes was randomised using a computer-generated method (Excel; Microsoft, Redmond, WA, United States). As a result, six animals underwent SHFJV or PCV at the beginning of a new body position and six each at the end of the position holding time. In the control group (n = 5), both lungs were ventilated with PCV throughout the experimental period without lung flooding; however, the position changes were the same.

Data measurements

Heart rate (HR); systolic, diastolic, and median arterial pressures (MAP); systolic, diastolic, and median pulmonary arterial pressure (sPAP, dPAP, mPAP); central venous pressure; and SpO_2 were continuously recorded using a multiparameter patient monitor (Datex AS/3; Datex-Ohmeda, Helsinki, Finland). Arterial and mixed venous blood gases were measured at baseline, during both types of ventilation after 15 min of equilibration in each body position, and after deflooding and TLV for immediate analyses of PaO_2, SaO_2, arterial partial pressure of carbon dioxide ($PaCO_2$), pH, PvO_2, SvO_2, $PvCO_2$, and hemoglobin using a blood gas analyzer (Rapidpoint 405; Siemens Healthcare, Erlangen, Germany). Peak inspiratory airway pressure was measured simultaneously using a respirator. For the pulmonary right-to-left shunt fraction (Qs/Qt) calculation, the alveoloarterial oxygen difference ($AaDO_2$) and oxygen content in the arterial and mixed venous blood (CaO_2, CvO_2) were used[28].

Eq1: $$\mathrm{Qs/Qt} = \frac{AaDO_2 \times 0.0031}{AaDO_2 \times 0.0031 + (CaO_2 - CvO_2)}$$

Chest X-ray was performed before, during and after OLF.

Statistical data analysis

All data were analyzed using statistical software (MedCalc 19.1.7; MedCalc LTD, Ostend, Belgium) and Excel (Microsoft, Redmond, United States). Because CO_2 removal is the main problem with jet ventilation, we used the $PaCO_2$ as the primary outcome variable. Based on the assumption that a difference in $PaCO_2$ of at least 2 kPa with a standard deviation of 0.7 kPa would be clinically relevant, we performed a power calculation (Two-Sample *T*-test Power Analysis). Ten animals were required for a $P < 0.05$, with a power of at least 80%. A total of 12 pigs were chosen to compensate for dropouts and increase the likelihood of significant findings for other important outcome variables, such as the PaO_2 and shunt fraction (Qs/Qt). Statistical analysis of hemodynamic and blood gas variables was performed using the non-parametric Mann-Whitney-*U* test for continuous data to test the significance between independent groups (*i.e.*, PCV *vs* SHFJV during OLF in each animal position). The Wilcoxon test was used between the dependent groups (baseline *vs* OLF/OLV and TLV), and an analysis of variance using the Friedman test was performed for analysis within the OLF/OLV groups (left *vs* SP *vs* right position). All data are presented as medians and interquartile range [Q1 Q3] (IQR). Ventilation modes were applied successively for each animal position in a randomised order. Because no differences were observed between different time points using the same ventilation mode, the collected data were merged (the Mann-Whitney-*U* test was used to compare data for each given ventilation mode at the beginning ($n = 6$) *vs* at the end ($n = 6$) of each body position). The SHFJV and PCV data reported in Tables 1 and 2 and Figures 5 and 6 are the merged data from the two-time points after 15 min of ventilation in a given ventilation mode.

RESULTS

One animal was excluded from the study because it died of acute cardiac death prior to OLF. None of the animals died during OLF.

Hemodynamics

The observed values are listed in Table 1. MAP was 10 mmHg higher under SHFJV in the SP compared with PCV [90.0 (IQR: 88.0-91.0) *vs* 80.0 (IQR: 64.0-89.0) mmHg, $P = 0.015$]. HR, sPAP, dPAP, and mPAP were slightly increased during SHFJV in the RLP [105.0 (IQR: 99.0-112.0) *vs* 95.0 (IQR: 91.0-99.0) bpm, $P = 0.01$; 43.0 (IQR: 38.0-45.0) *vs* 35.0 (IQR: 33.0-40.0) mmHg, $P = 0.03$; 25.0 (IQR: 23.0-29.0) *vs* 21.0 (IQR: 19.0-22.0) mmHg, $P = 0.02$; 31.0 (IQR: 28.0-34.0) *vs* 28.0 (IQR: 26.0-29.0) mmHg, $P = 0.048$], but were normalized after deflooding and TLV.

Gas exchange

The observed values are presented in Table 2, Figures 5 and 6. Unilateral SHFJV increased $PaCO_2$ compared with PCV in all animal positions with the highest value in the RLP [6.2 (IQR: 5.8-6.8) *vs* 4.7 (IQR: 4.3-4.9) kPa, $P = 0.002$]. There was a slightly decreased pH-value in RLP during SHFJV compared with PCV [7.38 (IQR: 7.36-7.39) *vs* 7.46 (IQR: 7.44-7.48), $P = 0.02$]. SHFJV slightly decreased oxygenation in the SP and RLP compared to PCV. The lowest PaO_2 level was found in the SP [13.0 (IQR: 12.6-15.6) kPa, $P = 0.006$], the greatest difference between SHFJV and PCV was measured in the RLP [13.6 (IQR: 11.4-17.3) *vs* 19.8 (IQR: 18.5-20.3) kPa, $P = 0.003$]. SaO_2 was slightly decreased during SHFJV in the SP and RLP compared with PCV [97.6 (IQR: 96.4-98.7) *vs* 99.7 (IQR: 98.8-99.7), $P = 0.01$; 97.6 (IQR: 94.3-99.2) *vs* 99.7 (IQR: 99.7-99.7)%, $P = 0.002$]. We observed a moderate decrease of PaO_2/FiO_2 ratio during SHFJV in all animal positions, with the lowest value in SP [32.5 (IQR: 31.5-38.9) kPa, $P = 0.006$] and the greatest difference between SHFJV and PCV in the RLP [33.9 (IQR: 28.7-43.2) *vs* 48.0 (IQR: 46.2-50.8) kPa, $P = 0.003$] (Figure 5). There was an increase in shunt fraction (Q_s/Q_t) from 0.17 (IQR: 0.14-0.22) to 0.24 (IQR: 0.20-0.25) in LLP ($P = 0.02$), from 0.18 (IQR: 0.11-0.21) to 0.24 (IQR: 0.22-0.27) in SP ($P = 0.01$), from 0.20 (IQR: 0.17-0.25) to 0.30 (IQR: 0.22-0.34) in RLP ($P = 0.04$) under SHFJV compared to PCV (Figure 6). All values were normalized after deflooding and TLV.

Airway pressures

Peak inspiratory pressure was 1.7-fold higher under PCV than under SHFJV during OLF [median (min-max): 25 (21.2-40.0) *vs* 15 (14.0-20.0) cm H_2O]. In eight animals, the DP for the low-frequency jet stream during SHFJV increased (between 1.0-1.3 bar) due to the end-expiratory CO_2 tension exceeding 45 mmHg. Most often, a pressure increase was necessary for RLP (one animal 1.1 bar, at two animals 1.2 bar, and three animals 1.3 bar).

Chest X-ray

In all animals, the correct DLT position without dystelectatic lung tissue, particularly in the left upper lobe, was verified (Figure 7A). During OLF, the entire left lung was homogeneous and opaque. The right lung was normally aerated without signs of fluid overflow (Figure 7B). Thirty minutes after OLF, both lungs were aerated normally. Neither dystelectasis nor opacification was observed (Figure 7C).

Table 1 Observed haemodynamic values. Values are medians with interquartile range for controls, pressure-controlled ventilation and superimposed high-frequency jet ventilation at baseline, one-lung flooding/one-lung ventilation in different animal positions and after one-lung flooding

Variable	Mode	Baseline (TLV)	OLF/OLV			After OLF (TLV)
		SP	LLP	SP	RLP	SP
HR (bpm)	CO-group	98.0 (89.5-105.0)	100.0 (98.5-104.0)	97.0 (89.5-102.0)	100.0 (97.0-102.5)	97.0 (90.0-100.5)
	PCV	104 (98.3-109.8)	92.0 (85.5-99.3)[a]	95.0 (91.0-103.0)[a]	95.0 (91.0-99.0)[a]	91.0 (86.0-98.0)[a]
	SHFJV[b]		91.0 (85.0-100.3)	90.0 (85.0-95.0)	105.0 (99.0-112.0)[c]	
MAP (mmHg)	CO-group	80.0 (72.5-90.5)	78.0 (71.0-82.5)	75.0 (67.5-82.5)	71.0 (62.0-80.5)	71.0 (58.0-77.0)
	PCV	84.5 (80.3-91.8)	89.0 (85.3-92.8)	80.0 (64.0-89.0)	88.0 (68.0-101.0)	98.0 (91.0-107.0)[a]
	SHFJV		90.5 (88.3-94.0)	90.0 (88.0-91.0)[c]	93.0 (87.0-97.0)	
sPAP (mmHg)	CO-group[b]	31 (29.5-32.0)	29 (26.5-29.5)	30 (29.0-33.0)	31 (29.0-32.5)	30 (28.0-32.0)
	PCV	30.5 (29.0-31.8)	35 (32.0-38.0)[a]	35 (34.0-36.0)[a]	35 (33.0-40.0)[a]	36 (28.0-38.0)
	SHFJV[b]		34 (31.0-39.0)	37 (35.0-39.0)	43 (38.0-45.0)[c]	
dPAP (mmHg)	CO-group	20 (17.5-22.5)	19 (16.5-21.5)	20 (16.5-23.0)	21 (19.5-23.5)	19 (17.5-21.5)
	PCV	21 (19.3-22.0)	22 (20.0-23.8)	21 (20.0-23.0)	21 (19.0-22.0)	22 (19.0-24.0)
	SHFJV[b]		20 (18.3-24.5)	22 (21.0-23.0)	25 (23.0-29.0)[c]	
mPAP (mmHg)	CO-group	24 (22.0-25.5)	23 (20.0-25.5)	24 (21.5-28.0)	24 (21.5-25.0)	22 (20.0-23.0)
	PCV	25 (24.0-26.0)	28 (26.0-30.3)[a]	28 (26.0-28.0)[a]	28 (26.0-29.0)[a]	22 (19.0-24.0)[a]
	SHFJV		27 (25.0-30.3)	30 (28.0-32.0)	31 (28.0-34.0)[c]	

[a]$P < 0.05$ *vs* difference from baseline.

[b]$P < 0.05$ *vs* difference between left lateral position, supine position, and right lateral position.

[c]$P < 0.05$ *vs* difference between the superimposed high-frequency jet ventilation and pressure-controlled ventilation (PCV). In the control-group, both lungs were ventilated with PCV throughout the experimental period without lung flooding; however, the position change was the same.

SHFJV: Superimposed high-frequency jet ventilation; PCV: Pressure-controlled ventilation; OLF: One-lung flooding; OLV: One-lung ventilation; TLV: Two-lung ventilation; LLP: Left lateral position; SP: Supine position; RLP: Right lateral position; HR: Heart rate; MAP: Median arterial pressure; sPAP: Systolic pulmonary arterial pressure; dPAP: Diastolic pulmonary arterial pressure; mPAP: Median pulmonary arterial pressure.

DISCUSSION

The present study is the first to investigate the effects of unilateral SHFJV on hemodynamics and gas exchange during OLF in relation to the animal position. We found a slight impairment in gas exchange with the SHFJV compared to the PCV, especially in the RLP (flooded lung above). Considering the well-accepted thresholds for PaO_2 (< 8.0 kPa), $PaCO_2$ (> 6.7 kPa), and pH (< 7.35)[29], unilateral SHFJV provides blood gases and hemodynamics in a clinically acceptable range.

Ventilation-induced tumor motion is a significant source of ineffective radiotherapy or percutaneous tumor ablation with HIFU[30,31]. The rationale for using jet ventilation instead of PCV during OLF is to minimize the movement of the flooded lung caused by the contralateral ventilated lung. In a previous study, we showed that SHFJV reduces diaphragm, bronchus, and mediastinal motion compared to PCV during OLF[24]. However, whether unilateral SHFJV ensures adequate gas exchange, especially when a very low DP is needed to maintain low organ movement, is unknown. Based on the pilot study, we chose a DP of 0.9 and 0.4 bar for the low- and high-frequency jet component, which is lower than in the usual clinical use (1.0-3.5 and 0.7-3.5 bar, respectively)[32-34]. The moderate increase of $PaCO_2$ during unilateral SHFJV compared to PCV (6.2 *vs* 4.7 kPa) can be explained by the low DP of the low-frequency jet component because ventilation (*i.e.* CO_2 removal) is produced by the low frequency. This hypothesis was supported by the measured peak inspiratory pressure under PCV, which was 1.7-fold higher than that under SHFJV. We showed that, in the case of increased end-expiratory CO_2 tension, normalization was achieved in a few minutes by a gradual increase in the DP by 0.1 bar from 0.9 to a maximal 1.3 bar. This was necessary six times for eight animals in the RLP. In a pilot study, we found that increasing the DP in the low-frequency mode up to 1.3 bar caused no relevant increase in diaphragm motion.

Unilateral SHFJV resulted in a slight decrease of PaO_2 and PaO_2/FiO_2 ratio in SP (13.0 and 32.5 kPa, respectively) and RLP (13.6 and 33.9 kPa, respectively); however, the lowest values remained in the physiological range. The lowest SaO_2 was 97.6%. The lower oxygenation can be explained by the increase in right-to-left shunt perfusion compared to PCV. We found an increase during SHFJV in all animal position (+ 0.07 in LLP, + 0.06 in SP, + 0.10 in RLP, Figure 6). We believe that these findings may be caused by a ventilation/perfusion imbalance in the ventilated lung. On the one hand, pulmonary-arterial perfusion is blocked in the flooded lung, causing a blood diversion from the flooded to the ventilated lung. On the other hand, under SHFJV with low peak inspiratory pressure, dystelectatic lung areas can easily develop,

Table 2 Observed gas exchange values. Values are medians with interquartile range for controls, pressure-controlled ventilation and superimposed high-frequency jet ventilation at baseline, one-lung flooding/one-lung ventilation in different animal positions and after one-lung flooding

Variable	Mode	Baseline (TLV)		OLF/OLV		after OLF (TLV)
		SP	LLP	SP	RLP	SP
PaO_2 (kPa)	CO-group	20.8 (19.7-21.7)	22.0 (21.4-25.1)	20.5 (20.0-21.4)	23.6 (22.0-24.1)	22.5 (21.4- 24.3)
	PCV	20.6 (18.6-22.7)	18.8 (15.3-20.4)[a]	17.6 (14.7-19.1)[a]	19.8 (18.5-20.3)	22.3 (19.9-23.1)
	SHFJV		14.5 (11.2-20.9)	13.0 (12.6-15.6)[c]	13.6 (11.4-17.3)[c]	
SaO_2 (%)	CO-group	99.7 (99.7-99.8)	99.7 (99.7-99.8)	99.7 (99.7-99.9)	99.7 (99.7-99.9)	99.7 (99.7-99.8)
	PCV	99.7 (99.6-99.8)	99.7 (99.1-99.9)	99.7 (98.8-99.7)	99.7 (99.7-99.7)	99.7 (99.6-99.8)
	SHFJV		98.3 (94.7-99.7)	97.6 (96.4-98.7)[c]	97.6 (94.399.2)[c]	
$PaCO_2$ (kPa)	CO-group	5.3 (5.0-5.4)	4.9 (4.7-5.0)	4.8 (4.7-4.9)	4.6 (4.54.8)	4.6 (4.3-4.8)
	PCV	5.0 (4.8-6.0)	4.7 (4.3-4.9)[a]	4.7 (4.3-5.2)[a]	4.7 (4.3-4.9)	4.6 (4.5-4.8)
	SHFJV[b]		5.8 (5.5-6.3)[c]	5.7 (5.5-6.0)[c]	6.2 (5.8-6.8)[c]	
pH	CO-group	7.46 (7.43-7.49)	7.47 (7.45-7.49)	7.46 (7.43-7.48)	7.44 (7.4-7.46)	7.47 (7.44-7.49)
	PCV	7.46 (7.44-7.48)	7.46 (7.44-7.48)	7.47 (7.45-7.49)	7.46 (7.44-7.48)	7.47 (7.45-7.49)
	SHFJV[b]		7.41 (7.39- 7.43)	7.4 (7.39-7.41)	7.38 (7.36-7.39)[c]	

[a]$P < 0.05$ *vs* difference from baseline.
[b]$P < 0.05$ *vs* difference between left lateral position, supine position, and right lateral position.
[c]$P < 0.05$ *vs* difference between the superimposed high-frequency jet ventilation and pressure-controlled ventilation (PCV). In the control-group, both lungs were ventilated with PCV throughout the experimental period without lung flooding; however, the position change was the same.
SHFJV: Superimposed high-frequency jet ventilation; PCV: Pressure-controlled ventilation; OLF: One-lung flooding; OLV: One-lung ventilation; TLV: Two-lung ventilation; LLP: Left lateral position; SP: Supine position; RLP: Right lateral position; PaO_2: Arterial partial pressure of oxygen; SaO_2: Arterial oxygen saturation; $PaCO_2$: Arterial partial pressure of carbon dioxide; pH: Hydrogen ion concentration.

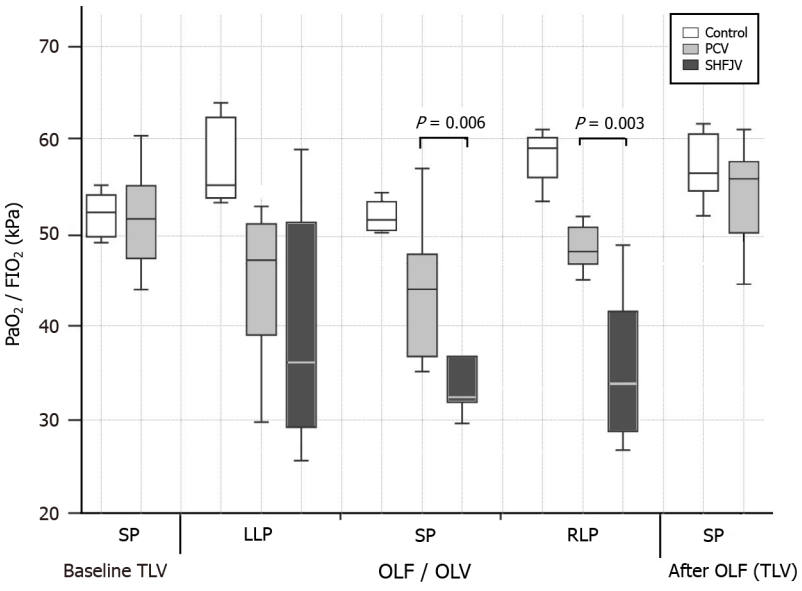

Figure 5 Boxplot of arterial partial pressure of oxygen/ fraction of inspired oxygen ratio for controls, pressure-controlled ventilation and superimposed high-frequency jet ventilation at baseline, one-lung flooding/one-lung ventilation in different animal positions and after one-lung flooding. In the supine and right lateral decubitus position after one-lung flooding, PaO_2/FiO_2 ratio during superimposed high-frequency jet ventilation was significantly lower than during PCV. SHFJV: Superimposed high-frequency jet ventilation; PCV: Pressure-controlled ventilation; OLF: One-lung flooding; OLV: One-lung ventilation; TLV: Two-lung ventilation; LLP: Left lateral position; SP: Supine position; RLP: Right lateral position; PaO_2/FiO_2: Arterial partial pressure of oxygen/fraction of inspired oxygen (Horowitz index).

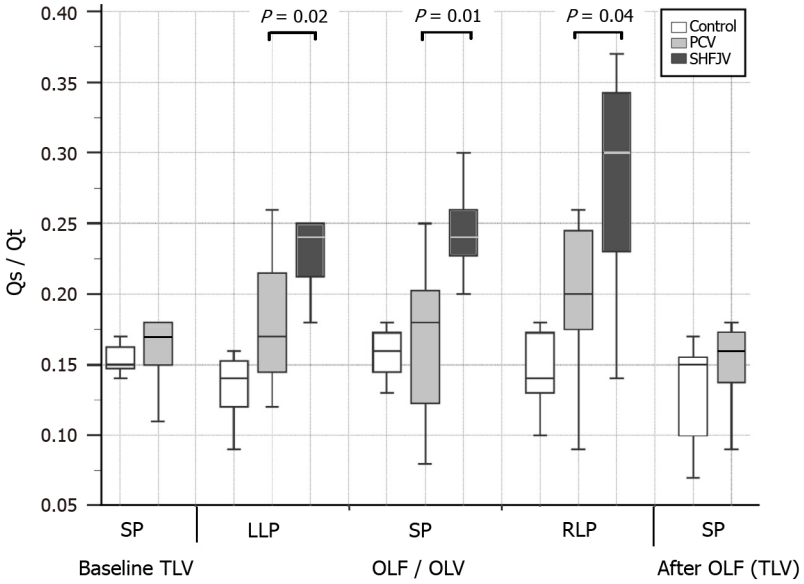

Figure 6 Boxplot of shunt fraction for controls, pressure-controlled ventilation and superimposed high-frequency jet ventilation at baseline, one-lung flooding/one-lung ventilation in different animal positions and after one-lung flooding. In all positions after one-lung flooding, Qs/Qt during superimposed high-frequency jet ventilation was significantly higher than during pressure-controlled ventilation. SHFJV: Superimposed high-frequency jet ventilation; PCV: Pressure-controlled ventilation; OLF: One-lung flooding; OLV: One-lung ventilation; TLV: Two-lung ventilation; LLP: Left lateral position; SP: Supine position; RLP: Right lateral position; Qs/Qt: Right-to-left shunt fraction.

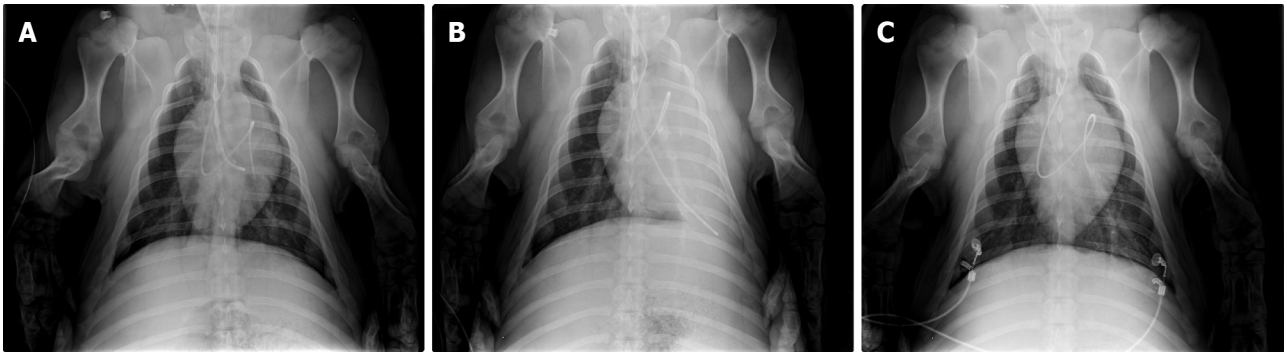

Figure 7 Chest X-ray. A: Before one-lung flooding. Correct position of the left-sided double-lumen endobronchial tube was confirmed using a fiber optic bronchoscope. Pulmonary artery catheter was placed in the left pulmonary artery; B: after one-lung flooding of the left lung wing. A pulmonary artery catheter placed in the left pulmonary artery. An endobronchial catheter placed in the left lower bronchus and inserted through the left lumen of the tube; C: 30 min after fluid drainage and conventional ventilation of both lungs. The X-ray shows normally aerated lung wings.

especially because interlobar collateral airways (pores of Kohn and Lambert´s canals) were not found in the lungs of pigs [35]. In the RLP, where the ventilated lung lies below, the chest wall and lung compliance are reduced, and the weight of the flooded lung can accentuate the development of dystelectatic areas in dependent ventilated lungs. The weight of the flooded lung could have less of an impact on humans because pigs do not have a mediastinum comparable to that of humans.

We used an FiO_2 of 0.4 in both ventilation methods to avoid absorption atelectasis, as our experimental time was very long. Other studies on SHFJV application in patients and animal models used a higher FiO_2 of 0.4[13,14,32]. An increase of FiO_2 or DP of the high-frequency jet component is a reliable option to compensate for reduced oxygenation due to dystelectases or atelectases. The unilateral SHFJV resulted in a slight increase in heart rate, systemic arterial pressure, and pulmonary artery pressure, predominantly in the RLP, which can be regarded as clinically irrelevant.

This study has several limitations that should be considered. We compared the two ventilation techniques using a porcine model. Lung volume and lung-chest wall compliance differ from those in adult humans. However, porcine and human cardiorespiratory physiologies are generally quite similar[35]. This study was performed on healthy pigs. The OLF and unilateral SHFJV methods are used for performing focused ultrasound ablation of lung tumors, whereby tumor patients are mostly older and often suffer from chronic obstructive pulmonary disease. Therefore, these results should be interpreted with caution. Our DLT manufactured for pigs was longer and had a smaller ID than the preferred DLT's for most humans. It should be considered that a higher tube resistance compared with the human DLT could occur[36]. The total duration of the SHFJV was 45 min, but not continuously, because 15 min in each body position was switched to the PCV mode. Thus, the maximum duration of SHFJV that can be safely performed cannot be determined in the present

work. We believe that a duration of 15 min is sufficient for HIFU ablation of a lung tumor up to 3 cm in diameter since in a simulation study, 10 min was calculated for the ablation of such a tumor size[37]. The ventilation procedure requires appropriate equipment and experienced users. Finally, to the best of our knowledge, studies on unilateral SHFJV as an OLV method with or without OLF to compare these findings with those of other studies are lacking.

CONCLUSION

In porcine model, unilateral SHFJV provided adequate ventilation in different animal positions during OLF. The lateral position with the flooded lung above it was the most unfavorable. The very low DPs for the low- and high-frequency jet stream components were due to a compromise between sufficient gas exchange and maximum movement reduction. The slight decrease in oxygenation and CO_2 removal compared to PCV did not lead to hypoxia or hypercapnia and was completely reversible. The SHFJV can be safely used for lung tumor ablation to minimize lung motion. The maximum safe duration of SHFJV could not be determined in this study.

ARTICLE HIGHLIGHTS

Research background

Lung cancer prognosis is among the most unfavourable of all cancers. This is reflected in its relatively low 5-year survival rate. Therefore, there is a need to improve local tumour therapy while avoiding surgery. High-intensity focused ultrasound (HIFU) is the only highly effective non-invasive approach to ablating tumours in parenchymal organs outside the chest. A new method one-lung flooding (OLF) for complete lung sonography was developed that allows ultrasound-mediated lung tumour ablation. OLF involves unilateral lung filling with saline, which generates a suitable acoustic pathway for transthoracic application of HIFU in the lung. Saline filling of one lung requires one-lung ventilation of the contralateral lung.

Research motivation

Breathing and lung movement during HIFU procedures can result in incomplete tumour ablation or collateral damage. Superimposed high-frequency jet ventilation (SHFJV) can reduce respiratory motion. However, it is unclear whether unilateral SHFJV allows adequate haemodynamics and gas exchange.

Research objectives

This study aimed to compare SHFJV with pressure-controlled ventilation (PCV) during OLF by assessing hemodynamics and gas exchange relative to the animal position.

Research methods

SHFJV or PCV were used alternately to ventilate the non-flooded lungs of 12 anaesthetised pigs during OLF in different body positions. Haemodynamic variables and arterial blood gas levels were measured using both ventilation modalities.

Research results

Unilateral SHFJV yielded lower carbon dioxide removal than PCV; however, it did not result in elevated carbon dioxide levels. SHFJV exhibited slightly decreased oxygenation in pigs in supine position and RLP compared with PCV. The lowest arterial partial oxygen pressure and arterial partial oxygen pressure/ inspired oxygen fraction (Horowitz index) values were observed in SP [13.0; interquartile range (IQR): 12.6-5.6 and 32.5 (IQR: 31.5-38.9) kPa]. Conversely, SHFJV yielded the highest shunt fractions in all animal positions (highest in the RLP: 0.30).

Research conclusions

In this porcine model, unilateral SHFJV may provide adequate ventilation to animals in different positions during OLF. Lower oxygenation and carbon dioxide removal rates compared with PCV did not lead to hypoxia or hypercapnia.

Research perspectives

SHFJV can safely minimise ventilation-induced lung motion during lung tumour ablation.

ACKNOWLEDGEMENTS

We thank the team at the Central Experimental Animal Facility, Jena University Hospital, especially Mrs. Dobermann, Mrs. Goebel, and Mr. Wuckelt, for their assistance with this project. We thank Dr. Martin Roskos for providing the blood gas analyzer and Dipl. Ing. F. Sick, Medicoplast International GmbH, Illingen, Germany, for providing the double-lumen endobronchial tubes. The authors gratefully acknowledge the technical support provided by Mr. R. Kölbl and Mr. M. Frank (Carl Reiner GmbH, Austria). The authors thank Drs. rer. pol. Thomas Lehmann from the Institute for Medical

Statistics, Computer Science, and Data Science, Jena University Hospital, Jena, Germany, for the statistical analyses. The authors gratefully acknowledge the support provided by SRH Wald-Klinikum Gera, particularly PD Drs. U. Leder, MBA, A. Peuke, and M. Lechner.

FOOTNOTES

Author contributions: Lesser T designed, coordinated the study, performed the experiments and wrote the manuscript; Wolfram F collected and analysed data; Braun C performed the anesthesia, monitored vital functions and was responsible for animal care; Gottschall R performed the ventilation of animals, reviewed the manuscript; all authors approved the final version of the article.

Institutional animal care and use committee statement: All procedures involving animals were reviewed and approved by the Institutional Animal Care and Use Committee of the Thuringian State Authority.

Conflict-of-interest statement: All other authors have nothing to disclose.

Data sharing statement: No additional data are available.

ARRIVE guidelines statement: The authors have read the ARRIVE guidelines, and the manuscript was prepared and revised according to the ARRIVE guidelines.

Country/Territory of origin: Germany

ORCID number: Thomas Lesser 0000-0001-7543-0193.

S-Editor: Qu XL
L-Editor: A
P-Editor: Yuan YY

REFERENCES

1 **Chu KF**, Dupuy DE. Thermal ablation of tumours: biological mechanisms and advances in therapy. *Nat Rev Cancer* 2014; **14**: 199-208 [PMID: 24561446 DOI: 10.1038/nrc3672]
2 **Ji Y**, Zhu J, Zhu L, Zhu Y, Zhao H. High-Intensity Focused Ultrasound Ablation for Unresectable Primary and Metastatic Liver Cancer: Real-World Research in a Chinese Tertiary Center With 275 Cases. *Front Oncol* 2020; **10**: 519164 [PMID: 33194582 DOI: 10.3389/fonc.2020.519164]
3 **Fite BZ**, Wang J, Kare AJ, Ilovitsh A, Chavez M, Ilovitsh T, Zhang N, Chen W, Robinson E, Zhang H, Kheirolomoom A, Silvestrini MT, Ingham ES, Mahakian LM, Tam SM, Davis RR, Tepper CG, Borowsky AD, Ferrara KW. Immune modulation resulting from MR-guided high intensity focused ultrasound in a model of murine breast cancer. *Sci Rep* 2021; **11**: 927 [PMID: 33441763 DOI: 10.1038/s41598-020-80135-1]
4 **Ning Z**, Xie J, Chen Q, Zhang C, Xu L, Song L, Meng Z. HIFU is safe, effective, and feasible in pancreatic cancer patients: a monocentric retrospective study among 523 patients. *Onco Targets Ther* 2019; **12**: 1021-1029 [PMID: 30774386 DOI: 10.2147/OTT.S185424]
5 **de Senneville BD**, Moonen C, Ries M. MRI-Guided HIFU Methods for the Ablation of Liver and Renal Cancers. *Adv Exp Med Biol* 2016; **880**: 43-63 [PMID: 26486331 DOI: 10.1007/978-3-319-22536-4_3]
6 **Aminzadeh P**, Alibrahim E, Dobrotwir A, Paul E, Goergen S. Multiparametric MR evaluation of uterine leiomyosarcoma and STUMP *vs* leiomyoma in symptomatic women planned for high frequency focussed ultrasound: accuracy of imaging parameters and interobserver agreement for identification of malignancy. *Br J Radiol* 2021; **94**: 20200483 [PMID: 33507806 DOI: 10.1259/bjr.20200483]
7 **Ghai S**, Finelli A, Corr K, Chan R, Jokhu S, Li X, McCluskey S, Konukhova A, Hlasny E, van der Kwast TH, Incze PF, Zlotta AR, Hamilton RJ, Haider MA, Kucharczyk W, Perlis N. MRI-guided Focused Ultrasound Ablation for Localized Intermediate-Risk Prostate Cancer: Early Results of a Phase II Trial. *Radiology* 2021; **298**: 695-703 [PMID: 33529137 DOI: 10.1148/radiol.2021202717]
8 **McWilliams JP**, Lee EW, Yamamoto S, Loh CT, Kee ST. Image-guided tumor ablation: emerging technologies and future directions. *Semin Intervent Radiol* 2010; **27**: 302-313 [PMID: 22550370 DOI: 10.1055/s-0030-1261789]
9 **Brandner ED**, Chetty IJ, Giaddui TG, Xiao Y, Huq MS. Motion management strategies and technical issues associated with stereotactic body radiotherapy of thoracic and upper abdominal tumors: A review from NRG oncology. *Med Phys* 2017; **44**: 2595-2612 [PMID: 28317123 DOI: 10.1002/mp.12227]
10 **Elen Evans**, Peter Biro, Nigel Bedforth. Continuing Education in Anaesthesia Critical Care and Pain. *Jet vent* 2007; **7**: 2-5 [DOI: 10.1093/bjaceaccp/mkl061]
11 **Biro P**, Spahn DR, Pfammatter T. High-frequency jet ventilation for minimizing breathing-related liver motion during percutaneous radiofrequency ablation of multiple hepatic tumours. *Br J Anaesth* 2009; **102**: 650-653 [PMID: 19346232 DOI: 10.1093/bja/aep051]
12 **Abderhalden S**, Biro P, Hechelhammer L, Pfiffner R, Pfammatter T. CT-guided navigation of percutaneous hepatic and renal radiofrequency ablation under high-frequency jet ventilation: feasibility study. *J Vasc Interv Radiol* 2011; **22**: 1275-1278 [PMID: 21703873 DOI: 10.1016/j.jvir.2011.04.013]

13 **Galmén K**, Jakobsson JG, Freedman J, Harbut P. High Frequency Jet Ventilation during stereotactic ablation of liver tumours: an observational study on blood gas analysis as a measure of lung function during general anaesthesia. *F1000Res* 2019; **8**: 386 [PMID: 31583085 DOI: 10.12688/f1000research.18369.1]

14 **Galmén K**, Jakobsson JG, Perchiazzi G, Freedman J, Harbut P. Quantitative assessment of atelectasis formation under high frequency jet ventilation during liver tumour ablation-A computer tomography study. *PLoS One* 2023; **18**: e0282724 [PMID: 37011083 DOI: 10.1371/journal.pone.0282724]

15 **Biro P**, Gottschall R, Klein U, Wiedemann K. Jet-Ventilation. Grundlagen und klinische Anwendung der Jet-Beatmungstechnik. 2001. Available from: https://www.ifm-medical.de/wp-content/uploads/2015/10/booklet-jv-ebook.pdf

16 **Lesser T**, Klinzing S, Schubert H, Klein U, Bartel M. Lung flooding--a new method for complete lung sonography. *Res Exp Med (Berl)* 1998; **198**: 83-91 [PMID: 9782528 DOI: 10.1007/s004330050092]

17 **Wolfram F**, Boltze C, Schubert H, Bischoff S, Lesser TG. Effect of lung flooding and high-intensity focused ultrasound on lung tumours: an experimental study in an *ex vivo* human cancer model and simulated *in vivo* tumours in pigs. *Eur J Med Res* 2014; **19**: 1 [PMID: 24393333 DOI: 10.1186/2047-783X-19-1]

18 **Lesser TG**, Boltze C, Schubert H, Wolfram F. Flooded Lung Generates a Suitable Acoustic Pathway for Transthoracic Application of High Intensity Focused Ultrasound in Liver. *Int J Med Sci* 2016; **13**: 741-748 [PMID: 27766022 DOI: 10.7150/ijms.16411]

19 **Aloy A**, Schachner M, Spiss CK, Cancura W. Tube-free translaryngeal superposed jet ventilation. *Anaesthesist* 1990; **39**: 493-498 [PMID: 2278368]

20 **Bacher A**, Pichler K, Aloy A. Supraglottic combined frequency jet ventilation *vs* subglottic monofrequent jet ventilation in patients undergoing microlaryngeal surgery. *Anesth Analg* 2000; **90**: 460-465 [PMID: 10648340 DOI: 10.1213/00000539-200002000-00041]

21 **Leiter R**, Aliverti A, Priori R, Staun P, Lo Mauro A, Larsson A, Frykholm P. Comparison of superimposed high-frequency jet ventilation with conventional jet ventilation for laryngeal surgery. *Br J Anaesth* 2012; **108**: 690-697 [PMID: 22258205 DOI: 10.1093/bja/aer460]

22 **Kraincuk P**, Körmöczi G, Prokop M, Ihra G, Aloy A. Alveolar recruitment of atelectasis under combined high-frequency jet ventilation: a computed tomography study. *Intensive Care Med* 2003; **29**: 1265-1272 [PMID: 12879246 DOI: 10.1007/s00134-003-1828-6]

23 **Sütterlin R**, Priori R, Larsson A, LoMauro A, Frykholm P, Aliverti A. Frequency dependence of lung volume changes during superimposed high-frequency jet ventilation and high-frequency jet ventilation. *Br J Anaesth* 2014; **112**: 141-149 [PMID: 23963714 DOI: 10.1093/bja/aet260]

24 **Lesser T**, Wolfram F, Braun C, Gottschall R. Superimposed High Frequency Jet Ventilation Minimises Diaphragm, Bronchus, and Mediastinum Motion during One-Lung Flooding. *Austin J Radiol* 2021; **8**: 1150 [DOI: 10.21203/rs.3.rs-97638/v1]

25 **Lesser T**, Braun C, Wolfram F, Gottschall R. A special double lumen tube for use in pigs is suitable for different lung ventilation conditions. *Res Vet Sci* 2020; **133**: 111-116 [PMID: 32977118 DOI: 10.1016/j.rvsc.2020.09.007]

26 **Muders T**. Einfluss von Spontanatmung auf die regionale Verteilung von Belüftung und Ventilation bei experimentellem Lungenschaden. [cited 4 March 2008]. Available from: https://bonndoc.ulb.uni-bonn.de/xmlui/handle/20.500.11811/3756

27 **Kneucker A**. Funktionelle Residualkapazität und Diffusionskapazität der Lunge bei Kalb und Schwein: Physiologische Werte und Einfluss respiratorischer Infektionen. [cited 14 December 2009]. Available from: https://refubium.fu-berlin.de/handle/fub188/13904

28 **Kroegel C**, Costabel U. Klinische Pneumologie. *Thieme* 2014; **90** [DOI: 10.1055/b-002-57146]

29 **Miñana G**, Núñez J, Bañuls P, Sanchis J, Núñez E, Robles R, Mascarell B, Palau P, Chorro FJ, Llàcer A. Prognostic implications of arterial blood gases in acute decompensated heart failure. *Eur J Intern Med* 2011; **22**: 489-494 [PMID: 21925058 DOI: 10.1016/j.ejim.2011.01.014]

30 **Wang Y**, Bao Y, Zhang L, Fan W, He H, Sun ZW, Hu X, Huang SM, Chen M, Deng XW. Assessment of respiration-induced motion and its impact on treatment outcome for lung cancer. *Biomed Res Int* 2013; **2013**: 872739 [PMID: 23862160 DOI: 10.1155/2013/872739]

31 **Illing RO**, Kennedy JE, Wu F, ter Haar GR, Protheroe AS, Friend PJ, Gleeson FV, Cranston DW, Phillips RR, Middleton MR. The safety and feasibility of extracorporeal high-intensity focused ultrasound (HIFU) for the treatment of liver and kidney tumours in a Western population. *Br J Cancer* 2005; **93**: 890-895 [PMID: 16189519 DOI: 10.1038/sj.bjc.6602803]

32 **Rezaie-Majd A**, Bigenzahn W, Denk DM, Burian M, Kornfehl J, Grasl MCh, Ihra G, Aloy A. Superimposed high-frequency jet ventilation (SHFJV) for endoscopic laryngotracheal surgery in more than 1500 patients. *Br J Anaesth* 2006; **96**: 650-659 [PMID: 16574723 DOI: 10.1093/bja/ael074]

33 **Hohenforst-Schmidt W**, Zarogoulidis P, Huang H, Man YG, Laskou S, Koulouris C, Giannakidis D, Mantalobas S, Florou MC, Amaniti A, Steinheimer M, Sinha A, Freitag L, Turner JF, Browning R, Vogl T, Roman A, Benhassen N, Kesisoglou I, Sapalidis K. A New and Safe Mode of Ventilation for Interventional Pulmonary Medicine: The Ease of Nasal Superimposed High Frequency Jet Ventilation. *J Cancer* 2018; **9**: 816-833 [PMID: 29581760 DOI: 10.7150/jca.23737]

34 **Veres J**, Slavei K, Errhalt P, Seyr M, Ihra G. The Veres adapter: clinical experience with a new device for jet ventilation *via* a laryngeal mask airway during flexible bronchoscopy. *Anesth Analg* 2011; **112**: 597-600 [PMID: 21233501 DOI: 10.1213/ANE.0b013e3182080407]

35 **Reinhold P**, Rosenbruch M, Theegarten D, Dalhoff K. Pulmonary infection models--7. Workshop on work crises "Comparative pathology and pathophysiology of the respiratory system" of the German Veterinary Medical Society in co-operation with the sections of infectious diseases and tuberculosis and cell biology of the German Society of Pneumology on 17 Mar 2005 om Berlin. *Pneumologie* 2005; **59**: 411-427 [PMID: 15991078 DOI: 10.1055/s-2004-830310]

36 **Beermann M**, Lindeberg J, Engstrand J, Galmén K, Karlgren S, Stillström D, Nilsson H, Harbut P, Freedman J. 1000 consecutive ablation sessions in the era of computer assisted image guidance - Lessons learned. *Eur J Radiol Open* 2019; **6**: 1-8 [PMID: 30547062 DOI: 10.1016/j.ejro.2018.11.002]

37 **Wolfram F**, Lesser TG. A simulation study of the HIFU ablation process on lung tumours, showing consequences of atypical acoustic properties in flooded lung. *Z Med Phys* 2019; **29**: 49-58 [PMID: 30037435 DOI: 10.1016/j.zemedi.2018.06.002]

World Journal of Experimental Medicine

Submit a Manuscript: https://www.f6publishing.com

World J Exp Med 2024 March 20; 14(1): 87916

DOI: 10.5493/wjem.v14.i1.87916

ISSN 2220-315x (online)

ORIGINAL ARTICLE

Basic Study

Artificial intelligence powered glucose monitoring and controlling system: Pumping module

Sravani Medanki, Nikhil Dommati, Hema Harshitha Bodapati, Venkata Naga Sai Kowsik Katru, Gollapalli Moses, Abhishek Komaraju, Nanda Sai Donepudi, Dhanya Yalamanchili, Jasti Sateesh, Pratap Turimerla

Specialty type: Engineering, biomedical

Provenance and peer review: Invited article; Externally peer reviewed.

Peer-review model: Single blind

Peer-review report's scientific quality classification

Grade A (Excellent): 0
Grade B (Very good): B
Grade C (Good): C, C
Grade D (Fair): D
Grade E (Poor): 0

P-Reviewer: Joda BA, Iraq; Long P, China; Zhao CF, China

Received: September 2, 2023
Peer-review started: September 2, 2023
First decision: November 1, 2023
Revised: December 18, 2023
Accepted: February 3, 2024
Article in press: February 3, 2024
Published online: March 20, 2024

Sravani Medanki, Nikhil Dommati, Hema Harshitha Bodapati, Venkata Naga Sai Kowsik Katru, Gollapalli Moses, Jasti Sateesh, Pratap Turimerla, Department of Electronics and Communication Engineering, Velagapudi Ramakrishna Siddhartha Engineering College, Vijayawada 520007, Andhra Pradesh, India

Nanda Sai Donepudi, Dhanya Yalamanchili, Department of General Medicine, Siddhartha Government Medical College, Vijayawada 520008, Andhra Pradesh, India

Corresponding author: Jasti Sateesh, PhD, Academic Research, Department of Electronics and Communication Engineering, Velagapudi Ramakrishna Siddhartha Engineering College, Kanuru, 340, Vijayawada 520007, Andhra Pradesh, India. sateeshjasti441@gmail.com

Abstract

BACKGROUND

Diabetes, a globally escalating health concern, necessitates innovative solutions for efficient detection and management. Blood glucose control is an essential aspect of managing diabetes and finding the most effective ways to control it. The latest findings suggest that a basal insulin administration rate and a single, high-concentration injection before a meal may not be sufficient to maintain healthy blood glucose levels. While the basal insulin rate treatment can stabilize blood glucose levels over the long term, it may not be enough to bring the levels below the post-meal limit after 60 min. The short-term impacts of meals can be greatly reduced by high-concentration injections, which can help stabilize blood glucose levels. Unfortunately, they cannot provide long-term stability to satisfy the post-meal or pre-meal restrictions. However, proportional-integral-derivative (PID) control with basal dose maintains the blood glucose levels within the range for a longer period.

AIM

To develop a closed-loop electronic system to pump required insulin into the patient's body automatically in synchronization with glucose sensor readings.

METHODS

The proposed system integrates a glucose sensor, decision unit, and pumping module to specifically address the pumping of insulin and enhance system effectiveness. Serving as the intelligence hub, the decision unit analyzes data from the

glucose sensor to determine the optimal insulin dosage, guided by a pre-existing glucose and insulin level table. The artificial intelligence detection block processes this information, providing decision instructions to the pumping module. Equipped with communication antennas, the glucose sensor and micropump operate in a feedback loop, creating a closed-loop system that eliminates the need for manual intervention.

RESULTS

The incorporation of a PID controller to assess and regulate blood glucose and insulin levels in individuals with diabetes introduces a sophisticated and dynamic element to diabetes management. The simulation not only allows visualization of how the body responds to different inputs but also offers a valuable tool for predicting and testing the effects of various interventions over time. The PID controller's role in adjusting insulin dosage based on the discrepancy between desired setpoints and actual measurements showcases a proactive strategy for maintaining blood glucose levels within a healthy range. This dynamic feedback loop not only delays the onset of steady-state conditions but also effectively counteracts post-meal spikes in blood glucose.

CONCLUSION

The WiFi-controlled voltage controller and the PID controller simulation collectively underscore the ongoing efforts to enhance efficiency, safety, and personalized care within the realm of diabetes management. These technological advancements not only contribute to the optimization of insulin delivery systems but also have the potential to reshape our understanding of glucose and insulin dynamics, fostering a new era of precision medicine in the treatment of diabetes.

Key Words: Diabetes; Hyperglycemia; Insulin; Micropump; Closed loop systems; Artificial intelligence automation

Core Tip: This study describes an innovative diabetes management system that integrates real-time glucose monitoring with advanced artificial intelligence (AI) algorithms and closed-loop insulin delivery. This approach offers precise, personalized control of blood glucose levels, reducing the risk of complications. The simulations demonstrate the system's effectiveness in maintaining stable glucose levels, even in response to meals and exercise, thanks to the International Diabetes Federation controller and basal insulin dosage. Additionally, the study explores the use of ESP32 for monitoring input voltage levels to protect the system. Overall, this study provides a groundbreaking approach that combines AI, closed-loop control, and real-time monitoring to revolutionize diabetes care and improve patient outcomes.

Citation: Medanki S, Dommati N, Bodapati HH, Katru VNSK, Moses G, Komaraju A, Donepudi NS, Yalamanchili D, Sateesh J, Turimerla P. Artificial intelligence powered glucose monitoring and controlling system: Pumping module. *World J Exp Med* 2024; 14(1): 87916

URL: https://www.wjgnet.com/2220-315x/full/v14/i1/87916.htm

DOI: https://dx.doi.org/10.5493/wjem.v14.i1.87916

INTRODUCTION

A significant worldwide health issue, diabetes mellitus is a complex metabolic condition. Diabetes, which is characterized by high blood glucose levels, is extremely dangerous for both people's health and the global healthcare system. According to the International Diabetes Federation, there were 463 million adult diabetics worldwide in 2019, and that number is expected to more than double to 700 million by 2045[1,2]. Continuous glucose monitoring and exact glucose control are essential for efficient diabetes treatment in order to reduce the risk of consequences such as cardiovascular disease, neuropathy, nephropathy, and retinopathy[2].

A type of medical technology or procedure known as a "open-loop glucose controlling system" is intended to control a person's blood glucose levels without requiring ongoing feedback or alterations based on real-time data[3]. It has certain advantages, but it also has a number of drawbacks. The drawbacks can be avoided by using a feedback system. Recent advancements in artificial intelligence (AI) and machine learning offer a promising avenue for redefining diabetes management paradigms[4]. The fusion of AI with glucose monitoring systems presents an opportunity to enhance the precision and personalization of diabetes care. Through the integration of AI algorithms, not only can glucose levels be continuously monitored, but patterns can also be analyzed, future trends predicted, treatment plans dynamically adjusted, and interventions even automated[5]. At the heart of this research paper lies the development and comprehensive evaluation of an AI-powered glucose monitoring and controlling system poised to revolutionize the landscape of diabetes care.

This pioneering system integrates real-time glucose monitoring through continuous glucose monitoring technology with sophisticated AI algorithms, capable of learning from individual responses to a spectrum of interventions. By

harmonizing data-driven insights with automated decision-making, the system aspires to maintain glucose levels within a targeted range while simultaneously minimizing the risks of hypoglycemia and hyperglycemia.

The technological details of the AI-powered glucose monitoring and controlling system will be covered in detail in the following sections of this article. This entails a thorough investigation of data collection techniques, the careful selection and application of AI algorithms, the design of the system's architecture, and the utilized validation processes. Additionally, a thorough evaluation of the system's effectiveness will be carried out through precisely planned clinical trials, which will compare its performance to current glucose management techniques[6]. Such an innovative strategy has significant potential for transformation, promising to improve the quality of life for people with diabetes while simultaneously reducing the burden on healthcare systems around the world. By providing real-time insights, predictive abilities, and autonomous treatments, the integration of AI into glucose monitoring and management is poised to completely change the way that diabetes is treated. To treat illnesses, pharmaceutics is a major component of medical care. Injections under the skin are a simple and popular method of delivery. Manual injections, however, do not allow for continuous dosing and might be painful. They also demand frequent attention[7]. These drawbacks can be avoided *via* automated delivery. The treatment of diabetics is one common pharmacological dosing application. The patient's health depends on the tight monitoring of blood glucose levels. It is well recognized that using a micropump to give insulin continuously improves care compared to many daily injections.

One of the most exciting advancements is the development of insulin pumps that help deliver medications with ease and comfort. With the availability of two types of pumps, patch pumps, and durable pumps, patients have more options than ever before. The durable pumps used in conjunction with infusion sets are especially noteworthy as they provide a continuous supply of insulin, which reduces the need for routine disconnections. This is a notable change for patients who want to maintain their active lifestyles without having to worry about taking breaks for medication[8]. Another advantage of durable pumps is that they are more comfortable to use, thanks to the removal of tubing. Patients can now wear them without feeling self-conscious or weighed down and this helps increase patient compliance. With these innovative devices, patients can go about their daily activities without feeling like they must compromise their comfort or lifestyle.

Type 1 diabetes, characterized by an insufficient production of insulin, demands a vigilant approach to prevent dangerous fluctuations in blood sugar concentrations. Genetic predisposition, autoimmune factors, or underlying diseases can trigger the onset of this chronic condition. Managing type 1 diabetes involves a multi-faceted approach, including insulin injections, dietary adjustments, and regular exercise. However, the inherent challenge lies in the precise administration of insulin, as overdosing can lead to hypoglycemia with symptoms ranging from chills to unconsciousness. Conversely, inadequate insulin administration may result in hyperglycemia, a condition associated with severe complications such as neuropathy, retinopathy, and kidney damage. To navigate this intricate balance, individuals with type 1 diabetes often rely on frequent blood glucose monitoring using handheld meters or body-attached monitors. Based on these readings, they make critical decisions regarding insulin dosage, a process that can be both cumbersome and demanding.

Recognizing the complexities of insulin management in type 1 diabetes, there is a growing interest in automated solutions. An automated insulin pump, equipped with the capability to measure blood glucose levels and administer insulin in real-time, holds the promise of simplifying this process. Such a technological advancement could not only enhance the precision of insulin delivery but also alleviate the burden on individuals, contributing to an improved quality of life.

In pursuit of improved outcomes for those with insulin dependence, modeling blood glucose levels becomes a pivotal aspect. By developing sophisticated models that predict blood glucose fluctuations based on various factors, and refining insulin administration methods tailored to individual needs, we can aspire to maintain healthier blood glucose ranges. This not only addresses the immediate challenges of diabetes management but also contributes to the long-term well-being and overall health of individuals grappling with this chronic condition.

MATERIALS AND METHODS

The proposed system being developed comprises an AI detection block. This block acts as the brain of the device, receiving input from a glucose sensor that measures blood sugar levels. Using advanced algorithms and machine learning, the AI then analyzes this data and makes decisions on how much insulin to release into the patient's bloodstream. This closed-loop system eliminates the need for manual intervention or guesswork, providing patients with a reliable and efficient way to manage their diabetes (Figure 1).

The system's cutting-edge AI detection block serves as its central component. It orchestrates a seamless interface with a cutting-edge glucose sensor, which is in charge of continuously measuring blood sugar levels. This complex component serves as the device's intellectual hub. The AI detection block takes on the difficult duty of analyzing the incoming glucose data through the integration of complicated algorithms and cutting-edge machine learning techniques, which ultimately results in educated recommendations for the administration of insulin. A ground-breaking closed-loop system that combines real-time monitoring with AI-driven decision-making streamlines the treatment of diabetes while also vastly improving its accuracy and dependability.

At the heart of this closed-loop system is the glucose sensor, a state-of-the-art technology designed to monitor blood sugar levels in near-real-time. This sensor acquires data through non-invasive or minimally invasive means, negating the need for traditional and often uncomfortable fingerstick tests. The data acquired are then seamlessly transmitted to the AI detection block, which serves as the digital nerve center of the entire system. The transformative power of this AI de-

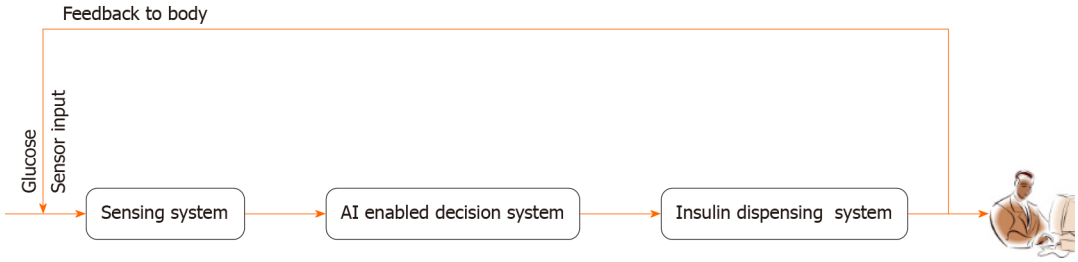

Figure 1 The block diagram encompasses a comprehensive diabetes management system: A glucose sensing component utilizes a glucose sensor, feeding data to an artificial intelligence driven decision system, which then triggers an insulin dispensing mechanism, forming an integrated framework for precise and automated diabetes control. AI: Artificial intelligence.

tection block lies in its ability to process and understand the complex glucose data streams received from the sensor. These data streams are characterized by their dynamic and fluctuating nature, influenced by factors such as food intake, physical activity, and stress.

Through the utilization of advanced algorithms, the AI is capable of discerning patterns, trends, and potential anomalies within these data streams. This intelligence allows the system to create a comprehensive and personalized understanding of the patient's glucose dynamics. A significant advantage of this closed-loop system is its ability to function autonomously, effectively reducing the reliance on manual intervention and minimizing guesswork. This empowers individuals with diabetes to actively manage their condition with a heightened level of trust and convenience. The need for constant monitoring and calculation is mitigated, as the AI detection block seamlessly maintains glucose levels within the target range.

The Bergman Minimal Model, a widely accepted framework for describing blood glucose control in individuals with type 1 diabetes.

$$\frac{dG}{dt} = -P_1 G - x(G + G_b) + D$$

$$\frac{dI}{dt} = -n(I + I_b) + \frac{U}{v_1}$$

$$\frac{dx}{dt} = -P_2 x + P_3 I$$

comprises a set of ordinary differential equations that model the dynamics of key variables: G (deviation of blood glucose concentration from basal levels), I (deviation of blood insulin concentration from basal levels), and X (proportionality variable describing insulin concentration in a remote compartment). These variables are crucial in understanding the intricate interplay of glucose and insulin in the body. The model is governed by parameters representing rates and conversions related to glucose and insulin processes. Basal blood glucose and basal blood insulin levels, along with parameters such as P1 (glucose removal rate), P2 (insulin removal rate from the remote compartment), and P3 (insulin appearance rate in the remote compartment), collectively contribute to the model's accuracy. Disturbance variable D represents the intake of glucose from external sources, while U accounts for insulin input from an external source. To better mimic real-world scenarios, the disturbance variable D is time-dependent and represents glucose intake from external sources, primarily food. Its formulation includes factors like glucose distribution volume, determined by an individual's weight and size, and the rate of glucose infusion, influenced by meal content, weight, and size. On the other hand, U represents external insulin input into the bloodstream.

The study introduces a proportional-integral-derivative (PID) controller to maintain blood glucose (G) at a desired setpoint. The PID controller involves terms such as Uff (feedforward controller output), Kp (proportional controller gain), Kd (derivative controller gain), and Ke (integral controller gain). This setup allows for a comprehensive and adaptive control mechanism, responding to deviations from the setpoint by adjusting insulin administration.

$$u = \bar{U}_{ff} + k_P\left(G - G_{sp}\right) + k_d \frac{dG}{dt} + k_e \int_0^\infty \left(G - G_{sp}\right) dt$$

Additionally, the study explores an alternative input mechanism, a high-concentration insulin injection modeled similarly to the glucose disturbance function. This injection mechanism, represented by Uinject, involves an exponential decay with a decay rate of 10. The sharpness of the injection peak, denoted by Uinject, is estimated to scale with glucose intake from corresponding meals, providing a nuanced representation of real-world insulin injections the Bergman Model, coupled with PID control and alternative insulin injection mechanisms, provides a robust foundation for simulating and understanding the complexities of blood glucose control in type 1 diabetes. These models and control strategies aim to enhance our ability to predict, manage, and ultimately improve the lives of individuals with diabetes.

$$u = \bar{U}_\iota e^{-10t}$$

The Bergman Model, coupled with PID control and alternative insulin injection mechanisms, provides a robust foundation for simulating and understanding the complexities of blood glucose control. These models and control

strategies aim to enhance our ability to predict, manage, and ultimately improve the lives of individuals with diabetes. Furthermore, the integration of the Bergman Model with PID control and innovative insulin injection methods represents a significant step toward personalized and precise diabetes management. By capturing the intricate dynamics of glucose-insulin interactions, these models offer a more nuanced understanding of the disease's complexities. The application of PID control introduces a dynamic and adaptive approach to insulin administration, allowing for real-time adjustments to deviations from target glucose levels. Exploring alternative insulin injection mechanisms adds versatility to treatment options, potentially catering to individual variations in insulin needs. This comprehensive approach not only advances our theoretical understanding of diabetes physiology but also holds promise for the development of more effective and patient-tailored therapeutic interventions. Ultimately, these advancements contribute to the overarching goal of improving the quality of life for individuals living with diabetes through enhanced predictive capabilities and refined management strategies.

Methodology for wi-fi controller to pump insulin

The comprehensive methodology for implementing an insulin pump system with the ESP32 goes beyond mere integration and data analysis. It encompasses a multifaceted approach to address the various aspects crucial for the system's accuracy, reliability, and safety. Sensor integration forms the foundation, with the ESP32 connecting seamlessly to glucose sensors to capture real-time data. The microcontroller's processing capabilities are then harnessed to not only analyze glucose levels but also to implement sophisticated algorithms that intelligently calculate the precise insulin dosage required. This iterative process of data interpretation ensures that the insulin pump responds dynamically to the user's changing physiological needs. Communication protocols play a pivotal role in ensuring the effectiveness of the system. The ESP32 employs wireless technologies like Bluetooth or Wi-Fi to establish robust connections between the microcontroller and user interfaces, which can include liquid crystal displays or mobile applications. This facilitates real-time monitoring of glucose levels, user input for dosage adjustments, and the reception of alerts or notifications, enhancing the overall user experience. Safety is paramount in insulin pump systems, and the ESP32 is programmed to incorporate multiple layers of protection. Fail-safes and redundant checks are meticulously designed to prevent over-dosage or any potential risks, ensuring the user's safety and peace of mind. The system undergoes rigorous testing and calibration, including simulated scenarios with varying glucose levels and hardware stress tests, to validate its accuracy and reliability across diverse conditions. User interface design extends beyond functionality, focusing on creating an intuitive and user-friendly experience. The ESP32 facilitates the development of interfaces that not only provide essential information but also allow users to customize settings, track historical data, and receive timely notifications, fostering a sense of control over their health management. Efficient power management is a key consideration, especially in portable insulin pump systems. The ESP32's capabilities are leveraged to optimize power consumption, extending the lifespan of the battery and ensuring uninterrupted operation. This is essential for users who rely on the portability of the insulin pump for their daily activities. In conclusion, the methodology for implementing an insulin pump system with the ESP32 is a holistic process that integrates cutting-edge technology, prioritizes user experience and safety, and undergoes meticulous testing and validation. The result is a sophisticated and effective insulin delivery system that empowers users to manage their health with confidence and convenience.

Flow chart

The necessary amount of insulin is pumped using a micropump combined with a microneedle, and the insulin is supplied to the body based on a choice using the pre-existing glucose and insulin levels. The control algorithm, which directs insulin delivery in accordance with glucose levels, is a crucial part. A gadget with a control algorithm receives data from a sensor concerning interstitial glucose levels. Subcutaneously, rapid-acting insulin is administered by an insulin pump. The control algorithm modifies the insulin supply. Wireless technology is used for system component communication (Figure 2).

Simulation

The WiFi-controlled voltage controller plays a vital role in pumping insulin. The ESP32 is a highly versatile, low-cost SoC chip that has a built-in microprocessor, a full TCP/IP protocol stack, and can connect straight to your Wi-Fi network.

This chip has a built-in Microcontroller Unit, so you can either program it with your application code or just utilize the module as a Wi-Fi transceiver, which is what we do in this project. Using the same module as a transmitter and controller will be more effective. Here, we have utilized the ESP32 development board to create a monitoring system for input voltage levels. The primary objective of this project is to ensure that the input voltage level does not exceed the safe operating voltage of the ESP32, which is typically 3.3V. This is achieved by connecting a potentiometer as a voltage divider, allowing us to measure and monitor the input voltage in real time. If the voltage exceeds 3.3V, the system takes corrective action to prevent potential damage to the ESP32.

The integration of a WiFi-controlled voltage controller, specifically leveraging the ESP32 SoC chip, plays a crucial role in enhancing the efficiency and safety of the insulin pumping system (Figure 3). The ESP32, known for its versatility and cost-effectiveness, serves as a powerful tool to connect the insulin pumping system to a Wi-Fi network, enabling seamless communication and control. In the context of insulin delivery systems, maintaining the stability of the input voltage is paramount to the reliable operation of the ESP32. The ESP32, being a sensitive electronic component, typically operates at a safe voltage level of 3.3V. The implemented solution involves using the ESP32 development board to establish a real-time monitoring system for input voltage levels. To achieve this, a potentiometer is employed as a voltage divider, allowing continuous monitoring of the input voltage levels. This monitoring is critical to ensuring that the voltage does not surpass the safe operating threshold of 3.3V. In the event that the voltage exceeds this limit, the WiFi-controlled voltage

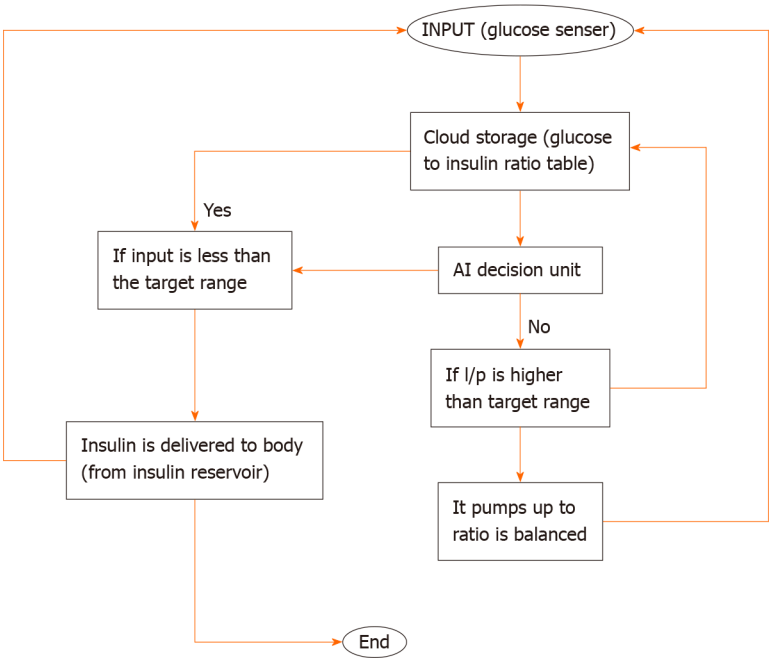

Figure 2 The flow chart illustrates a closed-loop diabetes management system that optimizes patient care.

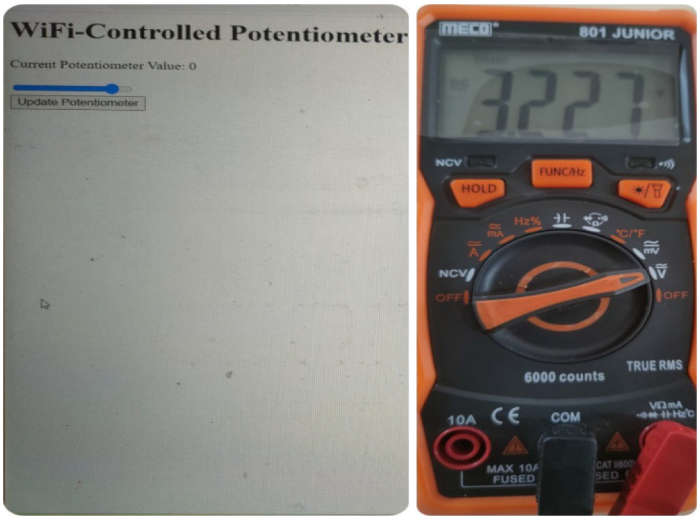

Figure 3 Wi-Fi controller for the pumping system.

controller, based on the ESP32, takes immediate corrective action to prevent potential damage to the ESP32 and, consequently, to the entire insulin pumping system. By leveraging the ESP32's capabilities as both a transmitter and a controller, the system gains enhanced effectiveness. The WiFi connectivity enables remote monitoring and control, providing healthcare professionals and patients with real-time insights into the status of the insulin delivery system. This connectivity ensures prompt responses to any voltage irregularities, contributing to the overall safety and reliability of the system. The incorporation of the WiFi-controlled voltage controller powered by the ESP32 significantly improves the insulin pumping system's functionality. It introduces a proactive approach to voltage monitoring, allowing for timely interventions to maintain the system within its safe operational parameters. This technological advancement not only safeguards the integrity of the ESP32 but also contributes to the overall reliability and safety of the insulin delivery process.

RESULTS

Evaluation of System Performance using the Bergman Equation as outlined in the Methodology

With no controller: Without a controller, this simulation replicates, the rapid blood glucose rise with respect to time and there is no control over it, which has a dangerous effect on people. In the absence of a controller within a blood glucose

regulation simulation, a concerning scenario unfolds where blood glucose levels surge uncontrollably over time. This unchecked escalation poses significant risks to individuals, particularly those with diabetes. Without the mechanisms to modulate these fluctuations, blood glucose levels can spike rapidly, leading to a state known as hyperglycemia. Hyperglycemia, characterized by elevated blood sugar levels, can manifest in symptoms like excessive thirst, frequent urination, fatigue, and impaired vision.

This situation becomes even more critical for individuals with diabetes, potentially culminating in life-threatening diabetic ketoacidosis (DKA). DKA arises when the body resorts to breaking down fats for energy due to insufficient glucose utilization, resulting in the production of acidic ketones and severe symptoms such as vomiting and confusion. Prolonged exposure to uncontrolled hyperglycemia can also give rise to debilitating long-term complications, including cardiovascular issues, kidney problems, neuropathy, and retinopathy. Managing high blood sugar levels becomes an arduous task, affecting an individual's overall well-being, daily routines, and incurring substantial healthcare expenses. In essence, the absence of a controller in this simulation mimics the dangerous consequences of unregulated blood glucose, underscoring the critical importance of effective blood glucose management strategies for those affected by diabetes (Figure 4).

With dosage of basal insulin: The graph depicting the correlation between glucose concentration and basal insulin dosage offers valuable insights into the efficacy of the basal insulin regimen in the context of blood glucose level maintenance (Figure 5). This visual representation provides a clear understanding of how changes in the basal insulin dosage relate to fluctuations in glucose concentration. Basal insulin, which serves as the foundation of diabetes management, plays a pivotal role in stabilizing blood sugar levels between meals and during periods of fasting. As we examine the graph, patterns and trends become discernible. A rise in basal insulin dosage typically corresponds to a decline in glucose concentration, suggesting that an increase in basal insulin can effectively lower blood sugar levels. Conversely, a reduction in basal insulin dosage tends to result in an uptick in glucose concentration. These correlations underscore the delicate balance required in diabetes management, where the fine-tuning of basal insulin dosages is crucial for achieving and maintaining stable glucose levels. Furthermore, this graph can aid healthcare professionals and individuals with diabetes in optimizing their treatment plans. It provides a quantitative basis for adjusting basal insulin dosages to achieve target glucose levels, thus enhancing the precision of diabetes care. The data gleaned from this graphical representation can inform personalized insulin regimens tailored to individual needs, promoting better glycemic control and ultimately improving the quality of life for those managing diabetes. In summary, the glucose concentration *vs* basal insulin dosage graph serves as a powerful tool in diabetes management, offering insights that can lead to more effective treatment strategies and enhanced glucose level stability.

DISCUSSION

Basal dose along with high concentration injections

The simulation's ability to keep blood glucose levels steady and in an acceptable range is a significant breakthrough in diabetes management. Maintaining steady-state over extended periods of time is a critical aspect of diabetes management, as it reduces the risk of developing complications such as kidney failure, blindness, and nerve damage. The basal dosage works in tandem with the fast-acting insulin injection to provide a more comprehensive solution that is tailored towards an individual's needs. This simulation provides a more personalized approach that takes into account the unique characteristics of each patient, making it a more efficient and effective way of managing diabetes (Figure 6).

The simulation's remarkable capacity to maintain blood glucose levels within a steady and acceptable range represents a monumental leap forward in the field of diabetes management. This achievement holds profound implications for the well-being of individuals grappling with this chronic condition. The ability to sustain a steady-state of glucose levels over extended periods is a cornerstone of effective diabetes care. This stability significantly diminishes the risk of debilitating complications, including but not limited to kidney failure, vision impairment, and nerve damage, all of which can have profoundly negative impacts on an individual's quality of life.

Central to the success of this simulation is the seamless integration of basal insulin dosage with fast-acting insulin injections. This synergistic combination forms a holistic solution finely tuned to an individual's specific requirements. The basal dosage serves as the foundational support, providing a steady release of insulin that acts as a stabilizing force between meals and during periods of fasting. Complementing this, the fast-acting insulin injection steps in to address post-meal spikes in blood sugar, ensuring a comprehensive coverage of insulin needs throughout the day. What sets this simulation apart is its ability to offer a highly personalized approach to diabetes management. It takes into account the unique physiological and lifestyle characteristics of each patient, allowing for a level of customization that was previously unprecedented. By tailoring treatment strategies to the individual, this simulation maximizes the effectiveness of diabetes management, ultimately leading to improved outcomes and a higher quality of life. Moreover, the potential ripple effects of this breakthrough are immense. It not only empowers individuals with diabetes to take more control over their health but also represents a leap forward in the broader landscape of healthcare. This personalized approach sets a precedent for the development of tailored treatments in other areas of medicine, potentially revolutionizing how we approach a range of chronic conditions. The simulation's ability to maintain steady blood glucose levels is a game-changer in diabetes management. It not only mitigates the risk of serious complications but also ushers in a new era of personalized care, underscoring its profound significance in the field of healthcare and the lives of those affected by diabetes.

Meal with basal dose

With the ability to see how blood glucose and insulin levels fluctuate in response to different inputs, this simulation

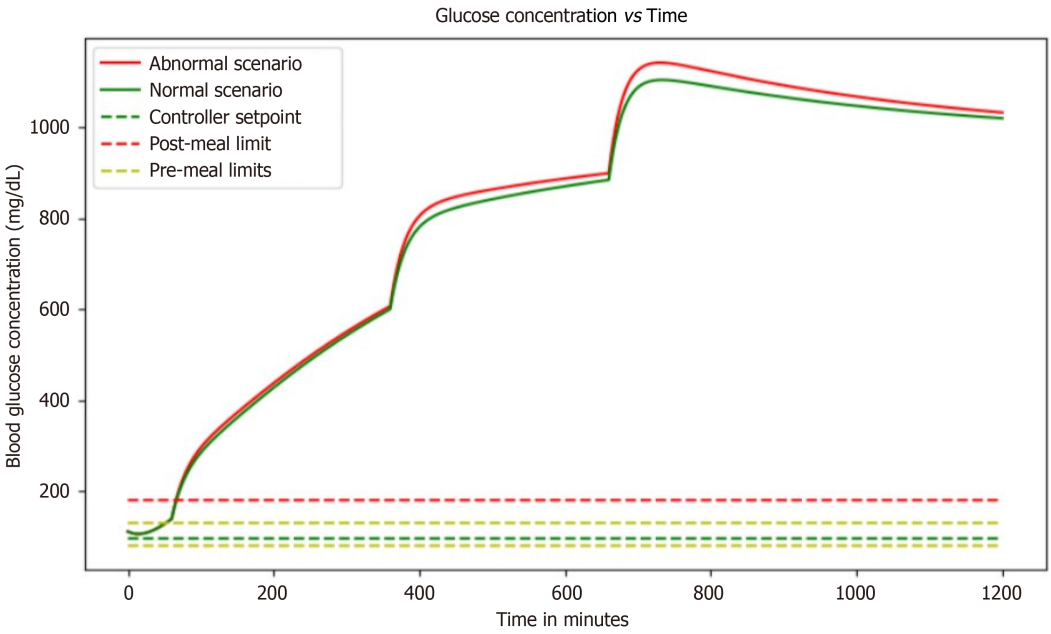

Figure 4 Graph depicts the dynamic relationship between glucose concentration and time, revealing fluctuations that highlight the critical need for precise glucose management in diabetes care.

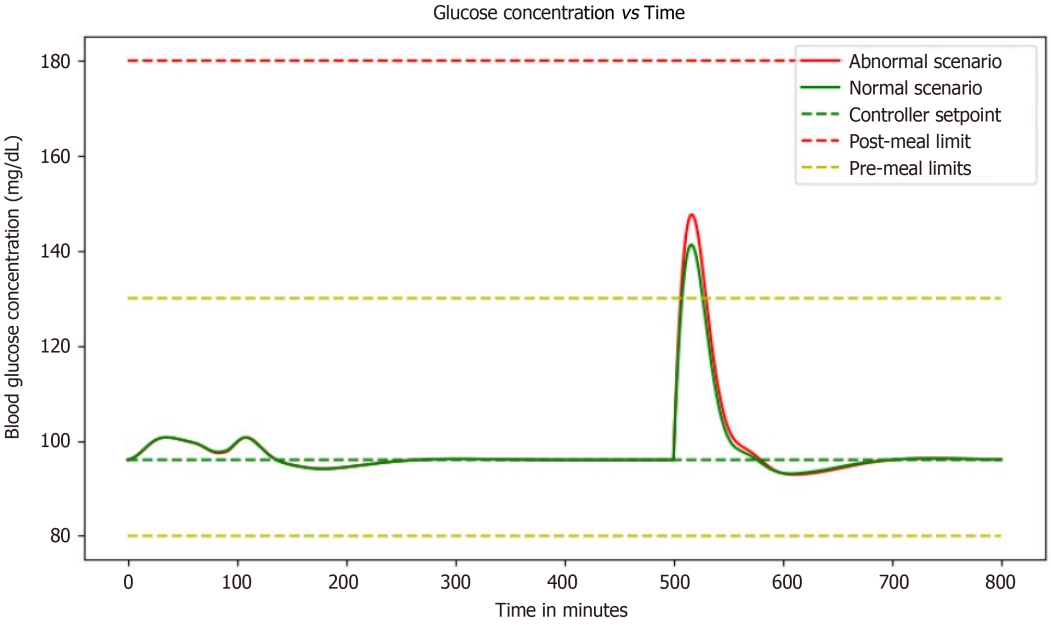

Figure 5 Graph showcases the correlation between glucose concentration and basal insulin dosage, providing insights into the effectiveness of the basal insulin regimen in maintaining stable glucose levels.

provides an invaluable tool for healthcare professionals and patients alike. In particular, the scenario of a diabetic patient vigorously exercising before eating a small meal is fascinating. The simulation illustrates just how complex diabetes management can be. Even with only a basal dosage as a controller input, the patient's blood glucose and insulin concentrations are constantly changing. It is incredible to see how the addition of a small meal or some exercise can impact these levels so dramatically. As someone who's never had to manage diabetes, it is eye-opening to see just how much work goes into keeping blood glucose levels within a healthy range (Figure 7).

The ability of this simulation to visually represent the intricate dance between blood glucose and insulin levels in response to various inputs is an invaluable asset for both healthcare professionals and individuals navigating diabetes. It offers a dynamic and illuminating window into the complexities of managing this chronic condition. One particularly captivating scenario within this simulation involves a diabetic patient engaging in vigorous exercise before consuming a small meal.

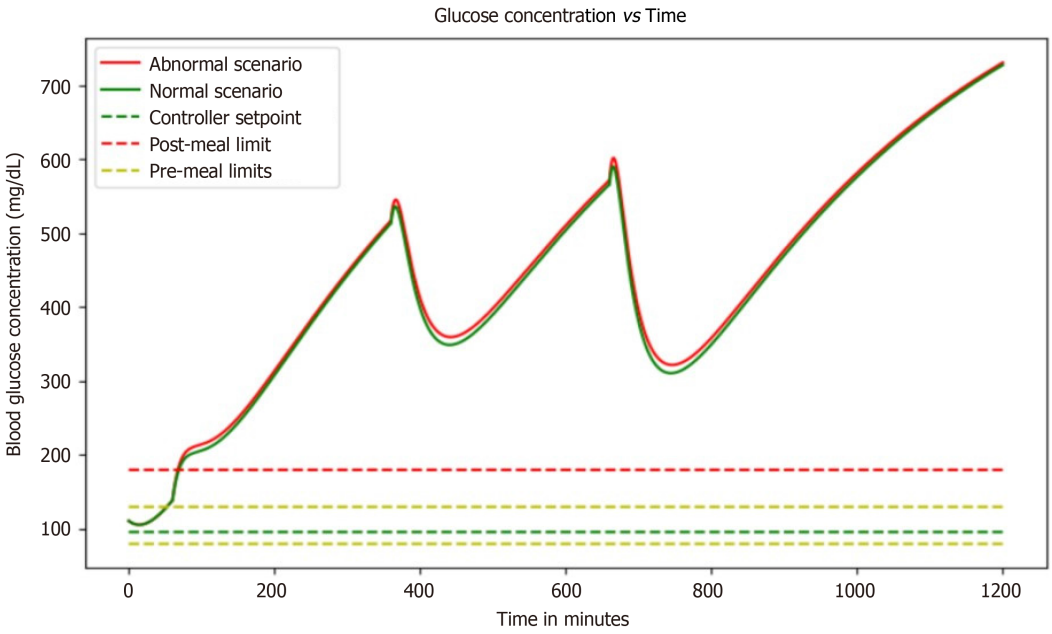

Figure 6 Graph highlights the impact of high glucose concentrations, revealing the critical importance of effective interventions to prevent hyperglycemia-related complications in diabetes management, but after a certain period of time glucose levels increases abnormally.

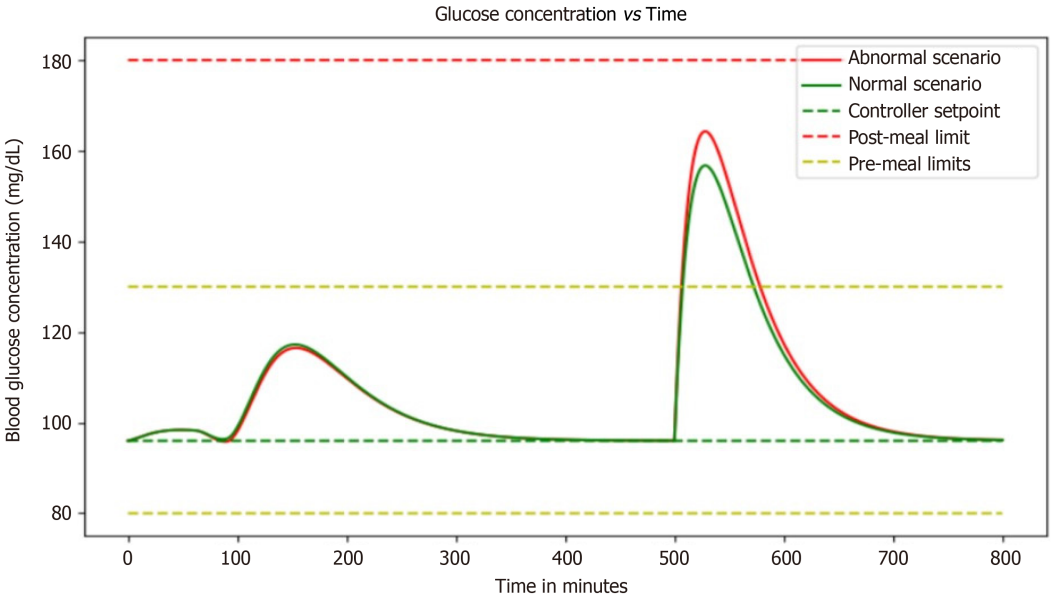

Figure 7 Graph illustrates the dynamic interaction between meal intake and basal insulin dose, showcasing the intricate balance required for optimal glucose control in diabetes management.

This scenario vividly underscores the multifaceted nature of diabetes management. What stands out is the dynamic nature of blood glucose and insulin concentrations, even with the sole input of a basal dosage. It highlights the constant ebb and flow of these critical biomarkers, emphasizing that diabetes management is far from a static process. The intricate interplay between insulin, glucose, and external factors such as exercise and meal timing is on full display. Witnessing how even minor changes, like a small meal or a burst of physical activity, can exert profound effects on these levels is nothing short of astonishing. For individuals fortunate enough not to grapple with diabetes, this simulation serves as an eye-opening revelation. It sheds light on the immense effort and vigilance required to maintain blood glucose within a healthy range.

It underscores that diabetes management is not a one-size-fits-all endeavor but a highly individualized and nuanced process. Each person's response to various inputs can be unique, demanding a personalized approach that takes into account factors like lifestyle, dietary choices, and exercise routines. Moreover, the simulation's utility extends beyond raising awareness. It offers a practical tool for healthcare professionals to fine-tune treatment plans for their patients. By visually assessing how different scenarios impact blood glucose and insulin levels, healthcare providers can make more

informed decisions about medication adjustments, dietary recommendations, and lifestyle modifications. This empowers individuals with diabetes to actively participate in their own care and enables healthcare teams to offer more tailored and effective guidance.

This simulation unveils the intricate web of factors influencing blood glucose and insulin dynamics, making it an essential resource for healthcare professionals and a revealing educational tool for those unfamiliar with the complexities of diabetes management. It underscores the relentless effort required to maintain blood glucose within a healthy range and the critical role of personalized care in this ongoing endeavor.

PID controller

In this simulation, a PID controller was used to model the changing blood glucose and insulin levels in individuals with diabetes. Imagine being able to see how your body responds to different foods and activities without actually having to undergo those experiences in real life (Figure 8).

The goal of this simulation is to develop a way to effectively manage blood glucose levels in people with diabetes. The PID controller used in this simulation is a control mechanism that adjusts the input based on the error between the setpoint and the actual output.

In this case, the setpoint is the desired blood glucose level, and the actual output is the measured blood glucose level. By adjusting the insulin dosage based on these measurements, researchers hope to delay reaching a steady-state and counteract any spikes in blood glucose that occur after meals. It is fascinating to think about how this simulation can help better understand how the body processes glucose and insulin.

This simulation emerges as a captivating tool, offering an unprecedented opportunity to gain insights into the intricate processes of glucose and insulin regulation within the body. The PID-controlled insulin dosage adjustments create a dynamic feedback loop, mimicking the complexities of real-life physiological responses. It is not just a simulation; it is a window into the nuanced world of diabetes management, enabling researchers to explore, in a controlled virtual environment, the multifaceted factors influencing blood glucose dynamics.

By modeling these complex systems, predictions can be made about how different interventions will affect blood glucose levels. They can also test different scenarios and see how the body responds over time. This can lead to improved treatment options for people with diabetes, as well as a better understanding of the disease itself.

PID controller with basal dose

The simulation of the evolution of insulin and blood glucose levels in diabetic patients is an incredible technological advancement. With the help of a PID controller coupled with the basal input for steady-state, it has become possible to control the controller's input and mitigate the effects of blood sugar increase brought on by meals (Figure 9).

The simulation aims to delay the controller's arrival at a steady-state, which ultimately leads to little to no variation from the setpoint value. This means that diabetic patients can now have better control over their blood glucose levels, which is a huge relief for them. The use of a PID controller coupled with the basal input for steady-state is an excellent approach to modeling the evolution of insulin and blood glucose levels. The simulation enables diabetic patients to have a better understanding of their blood glucose levels and how they can manage them effectively. With the help of this simulation, patients can now avoid sudden spikes in their blood sugar levels that can be harmful to their health. This simulation brings hope to millions of people suffering from diabetes worldwide. By taking into account the basal dose in the expression, it is expected that a steady state would be attained with little to no variation from the setpoint value. This means that diabetic patients can now live healthier and happier lives without having to worry about fluctuating blood sugar levels. The simulation has made it possible for people with diabetes to have better control over their lives and health. It has given them a new lease on life, where they can enjoy their favorite foods without worrying about the consequences.

CONCLUSION

Blood glucose control is an essential aspect of managing diabetes and finding the most effective ways to control it. The latest findings suggest that a basal insulin administration rate and a single, high-concentration injection before a meal may not be sufficient to maintain healthy blood glucose levels. While the basal insulin rate treatment can stabilize blood glucose levels over the long term, it may not be enough to bring the levels below the post-meal limit after 60 min. The short-term impacts of meals can be greatly reduced by high-concentration injections, which can help stabilize blood glucose levels. Unfortunately, they cannot provide long-term stability to satisfy the post-meal or pre-meal restrictions. However, PID control with basal dose maintains the blood glucose levels within the range for a longer period of time.

In conclusion, the WiFi-controlled voltage controller used for insulin pumping systems, leveraging the ESP32 SoC chip, represents a remarkable advancement in the field of healthcare technology. The integration of this controller addresses a critical aspect of insulin delivery systems by ensuring the stability of the input voltage, a factor pivotal to the safe and reliable operation of the ESP32 microcontroller. By employing the ESP32's capabilities for real-time monitoring and corrective actions, the system demonstrates an innovative approach to safeguarding sensitive electronic components, preventing potential damage, and ultimately enhancing the overall performance and safety of insulin delivery.

Furthermore, the incorporation of a PID controller to assess and regulate blood glucose and insulin levels in individuals with diabetes introduces a sophisticated and dynamic element to diabetes management. The simulation not only allows for the visualization of how the body responds to different inputs but also offers a valuable tool for predicting and testing the effects of various interventions over time. The PID controller's role in adjusting insulin dosage based on

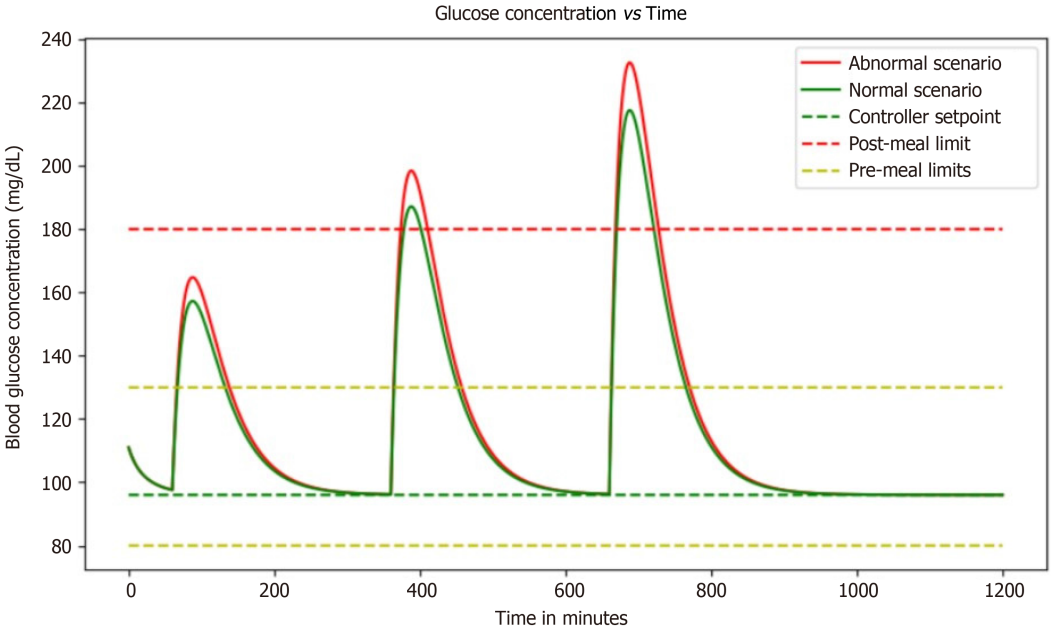

Figure 8 Graph demonstrates the performance of the proportional-integral-derivative controller, showcasing its ability to efficiently regulate a system's output by continuously adjusting the control parameters.

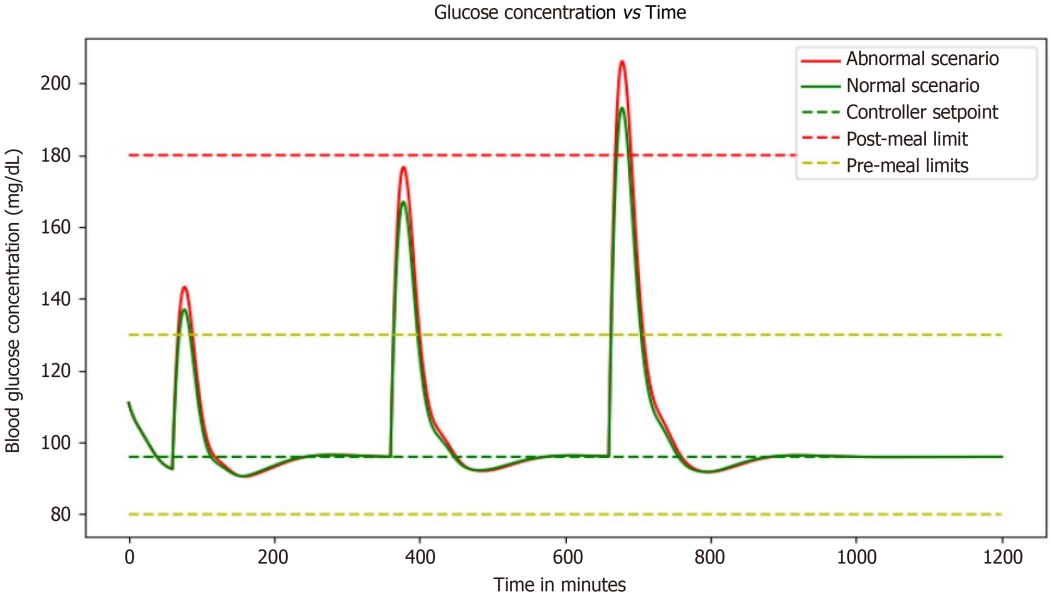

Figure 9 Graph illustrating the combined effect of proportional-integral-derivative controller with basal dose which is measured to evaluate the ability to effectively regulate glucose levels.

the discrepancy between desired setpoints and actual measurements showcases a proactive strategy for maintaining blood glucose levels within a healthy range. This dynamic feedback loop not only delays the onset of steady-state conditions but also effectively counteracts post-meal spikes in blood glucose.

In essence, the WiFi-controlled voltage controller and the PID controller simulation collectively underscore the ongoing efforts to enhance efficiency, safety, and personalized care within the realm of diabetes management. These technological advancements not only contribute to the optimization of insulin delivery systems but also hold the potential to reshape our understanding of glucose and insulin dynamics, fostering a new era of precision medicine in the treatment of diabetes.

ARTICLE HIGHLIGHTS

Research background

The system in the future will be made more robust by integrating with the Internet of Things (IoT), and will be made customizable to the patient's needs.

Research motivation

This study proposes a novel approach to reduce the circuitry to be carried by the patient while using an automated glucose-controlling system by adopting cloud storage. The system uses a micropump and microneedle to pump the insulin into the body making it comfortable and affordable.

Research objectives

The system was successful in delivering the required amount of insulin in accordance with the glucose sensor readings.

Research methods

Techniques like the IoT and artificial intelligence were used to design and work with the proposed system.

Research results

A closed-loop diabetes control system was designed, which was validated with several glucose sensor readings.

Research conclusions

This system will provide a better and affordable solution for diabetic patients to control glucose levels in the body which can extend the life expectancy.

Research perspectives

There exist very few but expensive closed-look automated diabetes detection control systems presenting a research gap for technical research.

ACKNOWLEDGEMENTS

The authors would like to thank Velagapudi Ramakrishna Siddhartha Engineering College, Sponsored by Siddhartha Academy of General Technical Education (SAGTE) m Vijayawada, for the financial support extended to carry out the project.

FOOTNOTES

Author contributions: Sateesh J designed the research idea and supervised the project; Medanki S, Dommati N, Bodapati HH, Komaraju A, Katru VNSK, and Moses G performed the research; Donepudi NS and Yalamanchili D validation of idea and research supervision; Turimerla P design and supervision; All authors contributed equally.

Institutional review board statement: This work does not involve any animal or human samples and no experimentation was carried out on animals or humans. The authors feel this research does not necessitate institutional review board approval.

Conflict-of-interest statement: All the authors declare no conflicts of interest.

Data sharing statement: Data will be shared by the authors upon reasonable request.

Country/Territory of origin: India

ORCID number: Jasti Sateesh 0000-0002-3459-8253.

S-Editor: Liu JH
L-Editor: Webster JR
P-Editor: Zhao YQ

REFERENCES

1 **International Diabetes Federation Guideline Development Group**. Global guideline for type 2 diabetes. *Diabetes Res Clin Pract* 2014; **104**: 1-52 [PMID: 24508150 DOI: 10.1016/j.diabres.2012.10.001]

2 **Sakudo A**. Near-infrared spectroscopy for medical applications: Current status and future perspectives. *Clin Chim Acta* 2016; **455**: 181-188 [PMID: 26877058 DOI: 10.1016/j.cca.2016.02.009]

3 **Khan MAB**, Hashim MJ, King JK, Govender RD, Mustafa H, Al Kaabi J. Epidemiology of Type 2 Diabetes - Global Burden of Disease and Forecasted Trends. *J Epidemiol Glob Health* 2020; **10**: 107-111 [PMID: 32175717 DOI: 10.2991/jegh.k.191028.001]

4 **Villena Gonzales W**, Mobashsher AT, Abbosh A. The Progress of Glucose Monitoring-A Review of Invasive to Minimally and Non-Invasive Techniques, Devices and Sensors. *Sensors (Basel)* 2019; **19** [PMID: 30781431 DOI: 10.3390/s19040800]

5 **Bazaev NA**, Masloboev IuP, Selishchev SV. [Optical methods for noninvasive blood glucose monitoring]. *Med Tekh* 2011; 29-33 [PMID: 22312873]

6 **Bruen D**, Delaney C, Florea L, Diamond D. Glucose Sensing for Diabetes Monitoring: Recent Developments. *Sensors (Basel)* 2017; **17** [PMID: 28805693 DOI: 10.3390/s17081866]

7 **Nathan DM**; DCCT/EDIC Research Group. The diabetes control and complications trial/epidemiology of diabetes interventions and complications study at 30 years: overview. *Diabetes Care* 2014; **37**: 9-16 [PMID: 24356592 DOI: 10.2337/dc13-2112]

8 **Shokrekhodaei M**, Quinones S. Review of Non-invasive Glucose Sensing Techniques: Optical, Electrical and Breath Acetone. *Sensors (Basel)* 2020; **20** [PMID: 32106464 DOI: 10.3390/s20051251]

World Journal of Experimental Medicine

Submit a Manuscript: https://www.f6publishing.com

World J Exp Med 2024 March 20; 14(1): 91271

DOI: 10.5493/wjem.v14.i1.91271

ISSN 2220-315x (online)

ORIGINAL ARTICLE

Basic Study

Hepatic and renal effects of oral stingless bee honey in a streptozotocin-induced diabetic rat model

Suriati Mohd Nasir, Anis Farihan Ismail, Tuan Salwani Tuan Ismail, Wan Faiziah Wan Abdul Rahman, Wan Amir Nizam Wan Ahmad, Tengku Ahmad Damitri Al- Astani Tengku Din, Kuttulebbai Nainamohammed Salam Sirajudeen

Specialty type: Health care sciences and services

Provenance and peer review: Invited article; Externally peer reviewed.

Peer-review model: Single blind

Peer-review report's scientific quality classification

Grade A (Excellent): 0
Grade B (Very good): B
Grade C (Good): 0
Grade D (Fair): 0
Grade E (Poor): 0

P-Reviewer: Roomi AB, Iraq

Received: December 26, 2023
Peer-review started: December 26, 2023
First decision: January 11, 2024
Revised: January 24, 2024
Accepted: March 1, 2024
Article in press: March 1, 2024
Published online: March 20, 2024

Suriati Mohd Nasir, Anis Farihan Ismail, Tengku Ahmad Damitri Al- Astani Tengku Din, Department of Chemical Pathology, School of Medical Sciences, Universiti Sains Malaysia, Kota Bharu 16150, Kelantan, Malaysia

Tuan Salwani Tuan Ismail, Endocrinology Laboratory, Department of Chemical Pathology, School of Medical Sciences, Universiti Sains Malaysia, Kota Bharu 16150, Kelantan, Malaysia

Wan Faiziah Wan Abdul Rahman, Department of Pathology, School of Medical Sciences, Universiti Sains Malaysia, Kota Bharu 16150, Kelantan, Malaysia

Wan Amir Nizam Wan Ahmad, Biomedicine Program, School of Health Sciences, Health Campus, Universiti Sains Malaysia, Kota Bharu 16150, Kelantan, Malaysia

Kuttulebbai Nainamohammed Salam Sirajudeen, Department of Basic Medical Sciences, Kuliyyah of Medicine, International Islamic University Malaysia, Bandar Indera Mahkota, Kuantan 25200, Pahang, Malaysia

Corresponding author: Tuan Salwani Tuan Ismail, MBBS, Associate Professor, Doctor, Endocrinology Laboratory, Department of Chemical Pathology, School of Medical Sciences, Universiti Sains Malaysia, Kubang Kerian, Kota Bharu 16150, Kelantan, Malaysia.
tusti@usm.my

Abstract

BACKGROUND

Diabetes is known damage the liver and kidney, leading to hepatic dysfunction and kidney failure. Honey is believed to help in lowering the blood glucose levels of diabetic patients and reducing diabetic complications. However, the effect of stingless bee honey (SBH) administration in relieving liver and kidney damage in diabetes has not been well-studied.

AIM

To investigate the effect of SBH administration on the kidney and liver of streptozotocin-induced (STZ; 55 mg/kg) diabetic Sprague Dawley rats.

METHODS

The rats were grouped as follows (n = 6 per group): non-diabetic (ND), untreated

diabetic (UNT), metformin-treated (MET), and SBH+metformin-treated (SBME) groups. After successful diabetic induction, ND and UNT rats were given normal saline, whereas the treatment groups received SBH (2.0 g/kg and/or metformin (250 mg/kg) for 12 d. Serum biochemical parameters and histological changes using hematoxylin and eosin (H&E) and periodic acid–Schiff (PAS) staining were evaluated.

RESULTS

On H&E and PAS staining, the ND group showed normal architecture and cellularity of Bowman's capsule and tubules, whereas the UNT and MET groups had an increased glomerular cellularity and thickened basement membrane. The SBH-treated group showed a decrease in hydropic changes and mild cellularity of the glomerulus *vs* the ND group based on H&E staining, but the two were similar on PAS staining. Likewise, the SBME-treated group had an increase in cellularity of the glomerulus on H&E staining, but it was comparable to the SBH and ND groups on PAS staining. UNT diabetic rats had tubular hydropic tubules, which were smaller than other groups. Reduced fatty vacuole formation and dilated blood sinusoids in liver tissue were seen in the SBH group. Conversely, the UNT group had high glucose levels, which subsequently increased MDA levels, ultimately leading to liver damage. SBH treatment reduced this damage, as evidenced by having the lowest fasting glucose, serum alanine transaminase, aspartate transaminase, and alkaline phosphatase levels compared to other groups, although the levels of liver enzymes were not statistically significant.

CONCLUSION

The cellularity of the Bowman's capsule, as well as histological alteration of kidney tubules, glomerular membranes, and liver tissues in diabetic rats after oral SBH resembled those of ND rats. Therefore, SBH exhibited a protective hepatorenal effect in a diabetic rat model.

Key Words: Diabetes; Streptozotocin; Stingless bee honey; Hematoxylin and eosin; Periodic acid–Schiff; Liver; Kidney

Core Tip: Honey products are widely recognized for their abundant vitamin content and bioactive components, which enhance their potential therapeutic benefits in the management of diabetes. This study demonstrated the hepatic and renal protective properties of stingless bee honey, which improved the architecture of the kidney and liver in diabetic rats. Thus, stingless bee honey could be useful in the treatment or prevention of liver and kidney impairment in diabetes.

Citation: Mohd Nasir S, Ismail AF, Tuan Ismail TS, Wan Abdul Rahman WF, Wan Ahmad WAN, Tengku Din TADAA, Sirajudeen KNS. Hepatic and renal effects of oral stingless bee honey in a streptozotocin-induced diabetic rat model. *World J Exp Med* 2024; 14(1): 91271

URL: https://www.wjgnet.com/2220-315x/full/v14/i1/91271.htm

DOI: https://dx.doi.org/10.5493/wjem.v14.i1.91271

INTRODUCTION

Diabetes mellitus (DM) is becoming an increasingly prevalent major health concern, characterized by hyperglycemia secondary to insulin deficiency or resistance[1]. In 2019, 9.3% (463 million) of individuals worldwide had diabetes, according to the International Diabetes Federation[2], and this is expected to increase to 10.2% (578 million) by 2030 and 10.9% (700 million) by 2045 if effective prevention strategies are not applied[3]. In particular, Malaysia has the highest rate of diabetes in the Western Pacific region and one of the highest in the world, costing around 600 million United States dollars per year[2]. Diabetics are predisposed to macrovascular problems, such as cardiovascular, cerebrovascular, and peripheral vascular illnesses, as well as microvascular consequences, such as retinopathies, nephropathies, and neuropathies[4].

One complication of uncontrolled diabetes is diabetic nephropathy, characterized by pathological quantities of urine albumin excretion, diabetic glomerular lesions, and loss of glomerular filtration rate in diabetics[5]. DM has also been associated with many liver abnormalities, such as abnormal glycogen deposition, nonalcoholic fatty liver disease, fibrosis, cirrhosis, hepatocellular carcinomas, abnormal elevated hepatic enzymes, acute liver disease, and viral hepatitis[6]. This worsens insulin resistance and leads to severe metabolic dysfunction. Moreover, it can destroy hepatocytes and contribute to increased morbidity and mortality among diabetic patients.

Regulating blood glucose levels is essential for reducing the risk of diabetic complications and improving the health of diabetic patients[7]. Until recently, conventional therapies have only attempted to manage blood glucose levels, but efforts to control diabetic complications have been unsuccessful[8]. Honey is a natural substance that consists of carbohydrates, water, organic acids, amino acids, enzymes, pigment, and pollens with antibacterial and antiinflammatory features[9,10]. Clinically speaking, honey is believed to help lower the blood glucose levels of diabetic patients and

reduce diabetic complications[11]. Despite many studies on the therapeutic properties of different types of honey, it is still not regularly applied in practice, since there is still controversy regarding glycemic control in individuals with oral honey supplementation and the role of honey in diabetic complications.

Oxidative stress plays a vital role in the development of diabetic complications[12]. Honey has been studied in various ailments in animal and human models and has been discovered as a novel antioxidant agent[13]. The composition of honey depends primarily on its floral source and seasonal and environmental factors[14-16], and thus its different varieties may exhibit various health-promoting properties. In particular, SBH includes various compounds (*i.e.*, phenolic acids, flavonoid enzymes, organic acids, and other minor compounds) that act as antioxidants, which are believed to have a synergistic effect. The phenolic and anti-inflammatory properties of SBH are believed to have a hepatorenal protective effect against diabetes. This study aimed to evaluate the effects of oral SBH on serum biochemical parameters and histological changes in the liver and kidney in a streptozotocin (STZ)-induced diabetic Sprague Dawley (SD) rat model.

MATERIALS AND METHODS

Animal model

The experimental animals in this study were male SD rats (n = 30), 8-10 wk old, weighing 200-250 g, purchased from the Animal Research and Service Centre (ARASC), University Sains Malaysia, Health Campus, Kubang Kerian. All rats were housed in plastic cages and maintained under standard laboratory conditions (21°C ± 2°C) with a 12 h light/dark cycle. Rats were given free access to normal standard rat pellet diet (10%/kg) supplied by ARASC USM and water *ad libitum*. The rats were acclimatized for one week before the experiment to reduce stress and familiarize them with human contacts. This study was conducted in accordance with the Institutional Guidelines for the Care and Use of Animals for Scientific Purposes (IACUC @ USM V4.Apr18).

Induction of STZ in diabetic rat model

The rats were divided into five groups based on the treatment given: non-diabetic (ND) rats as the control group (given normal saline), untreated diabetic (UNT) rats (given normal saline), SBH-treated (2.0 g/kg) diabetic rats, metformin-treated (MET) (250 mg/kg) diabetic rats, and SBH+metformin-treated (SBME) diabetic rats. In all except the ND group, Diabetes was induced by a single intraperitoneal injection of a freshly prepared solution of STZ (Sigma Aldrich, United States) 50 mg/kg BW in 0.1 M cold sodium citrate buffer (pH 4.5) after overnight fasting[17]. Diabetes was confirmed based on elevated fasting capillary plasma glucose (CPG) levels determined on days 3 and 7 after STZ injection; those persistently exhibiting CPG > 11.1 mmol/L were used for the experiment[18]. In this study, the range of CPG before treatment was 15.02-19.95 mmol/L, which was not more than 21.0 mmol/L. No mortality was observed during DM induction. The treatment was given *via* oral gavage by means of a tube inserted into the stomach through the mouth.

Histological analysis

Rats were euthanized *via* cervical dislocation under anesthesia using ketamine plus xylazin. The kidneys and livers of all rats were harvested and preserved in 10% formalin. Samples then underwent a standard dehydration process in a series of increasing ethanol concentrations for 24 h using a processing machine. The tissue was then degreased with xylene, embedded in paraffin, and sectioned using a histological microtome. Afterward, 2.5-μm tissue sections were mounted on a glass slide, stained using hematoxylin and eosin (H&E) and periodic acid–Schiff (PAS) staining, then visualized under a light microscope at 40× magnification (Olympus BX41) and image analyzer.

Biochemical analysis

CPG was measured using a URight blood glucometer (Uright, TD 4279) using the tail-prick technique to obtain tail vein blood. To collect fresh small medium of blood, an appropriate restraint device was used, and the withdrawal site was cleaned with alcohol. A finger prick lancet was used on the tail vein, and then capillary blood glucose was measured using a glucometer. After 12 d of treatment, the rat was euthanized before blood collection using cardiac puncture. The blood samples were then centrifuged at 4500 rpm for 10 min, and the serum samples were stored at 80°C until further analysis. Serum urea, creatinine, sodium (Na^+), potassium (K^+), calcium (Ca), magnesium (Mg), albumin, total protein, alanine transaminase (ALT), aspartate transaminase (AST), and alkaline phosphatase (ALP) were analyzed using an auto analyzer (Abbott ARCHITECT analyzer). Serum MDA was analyzed using the MDA ELISA Kit from Elabscience, USA, which uses the Sandwich-ELISA principle. All procedures were performed according to the manufacturer's instructions.

Statistical analysis

Experimental data are presented as the mean ± SE of the mean in this study. One-way and two-way repeated measures of analysis of variance (ANOVA) were used to analyze CPG. Biochemical results were compared between groups by one-way ANOVA. All the analyses conducted were followed by Tukey's post-test and performed using GraphPad Prism, v9.0 software (GraphPad, San Diego, CA, United States; alkaline phosphatase), with $P < 0.05$ denoting statistical significance.

Table 1 Mean fasting capillary blood glucose (day 0 and day 13) in response to different treatments over 12 d

Group	Fasting capillary plasma glucose (mmol/L)	
	Day 0	Day 13
Non-diabetic	4.85 ± 0.26	4.48 ± 0.38
Untreated diabetic	20.00 ± 1.69	21.38 ± 2.94
Stingless bee honey	14.74 ± 2.25	7.66 ± 1.60
Metformin-treated	13.78 ± 1.18	7.00 ± 2.44
Stingless bee honey plus metformin	12.25 ± 2.43	9.73 ± 3.72

Data was analyzed using one-way and two-way repeated measures ANOVA, followed by Tukey's post-test. Data are expressed as mean + SEM.

Table 2 Biochemical evaluation of renal function in response to different treatments over 12 d

Analytes	ND	UNT	SBH	MET	SBME
Urea (mmol/L)	8.28 ± 0.59	14.28 ± 4.92	7.95 ± 1.85	9.70 ± 0.30	7.30 ± 3.20
Creatinine (μmol/L)	46.00 ± 1.73	50.67 ± 1.80	46.17 ± 2.48	37.82 ± 8.62	40.80 ± 11.91
Na^+ (mmol/L)	135.30 ± 1.93	138.40 ± 0.68	136.30 ± 0.88	134.40 ± 1.12	135.00 ± 1.23
K^+ (mmol/L)	4.68 ± 0.12	4.45 ± 0.10	4.56 ± 0.32	4.52 ± 0.17	4.48 ± 0.11
Ca^{2+} (mmol/L)	2.36 ± 0.06	2.28 ± 0.04	2.35 ± 0.05	2.32 ± 0.04	2.36 ± 0.03
Mg^{2+} (mmol/L)	0.95 ± 0.03	0.88 ± 0.03	1.07 ± 0.05	0.93 ± 0.05	1.01 ± 0.14

Data were analyzed using one-way ANOVA, followed by Tukey's post-test. Data were expressed as mean + SEM. Among these five groups, there were no statistically significant differences in all parameters.

RESULTS

To evaluate the antihyperglycemic effects of SBH, changes in CPG levels were measured on days 0 and 13 of treatment. Table 1 shows the effect of SBH and SBME on fasting blood glucose (FBG) concentrations in the diabetic rat groups on days 0 and 13 of treatment. The SBH, MET, and SBME groups had consistently reduced FBG levels throughout the treatment period. On day 13, the SBH- and MET-treated groups showed lower FBG levels than the SBME group. Meanwhile, UNT diabetic rats had the highest FBG compared to the other groups at all time points.

Biochemical analysis

Serum urea and creatinine levels were measured to assess renal function and injury (Table 2). UNT diabetic rats showed the highest serum urea (14.28 + 4.92 mmol/L) and creatinine levels and (50.67 + 1.80 μmol/L) compared with ND rats. The SBH group had a lower serum urea compared with UNT diabetic rats. However, across the different treatment groups, SBME had the lowest serum urea level, followed by the SBH and MET groups. Meanwhile, for serum creatinine level, MET-treated diabetic rats had the lowest level of creatinine followed by SBME- and SBH-treated groups, but none of them were statistically significant.

Na^+ levels in all diabetic rats were not significantly different compared to ND rats, but this was highest in UNT diabetic rats. The SBH group had a lower Na^+ level compared to the UNT group. However, the MET groups had the lowest Na^+ levels compared to all the treatment groups. The UNT group had a lower level of K^+ (4.45 + 0.10 mmol/L) *vs* controls. Compared to the UNT group, the highest level of K^+ was seen in the MET group (4.56 + 0.32 mmol/L), followed by the MET (4.52 + 0.17 mmol/L) and SBME (4.48 + 0.11 mmol/L) groups. The serum Ca^{2+} level of the UNT group was also lower than controls. The SBH, SBME, and MET groups had higher Ca^{2+} levels than that the UNT group, but this was not statistically significant. Meanwhile, serum Mg^{2+} levels were reduced in UNT rats *vs* ND rats. Serum Mg^{2+} was highest in the SBG group, followed by the SBME and MET groups.

Serum albumin in the SBH and SBME groups was higher than that of the UNT group, but lower than that of the ND group. The MET group had the lowest albumin level (28.40 + 0.51 g/L) out of all the groups of rats, but this was not significantly different. UNT rats had lower serum total protein than the ND rats. The SBME group, as well as the SBH and MET groups, had a higher total protein level than UNT diabetic rats, but this was not statistically significant.

Serum ALT was higher in the UNT group (75.50 + 33.18 U/L) *vs* ND rats. The SBH group had a lower serum ALT *vs* the UNT group. Conversely, serum AST (121.00 + 7.44 U/L) and ALP (162.00 + 25.65 U/L) were highest in the UNT group, compared to the ND and treatment groups. Meanwhile, the lowest serum ALP was seen in the MET group (126.70 + 14.84 U/L), followed by the SBH (131.70 + 23.92 U/L) and SBME (149.30 + 7.75 U/L) groups. The biochemical

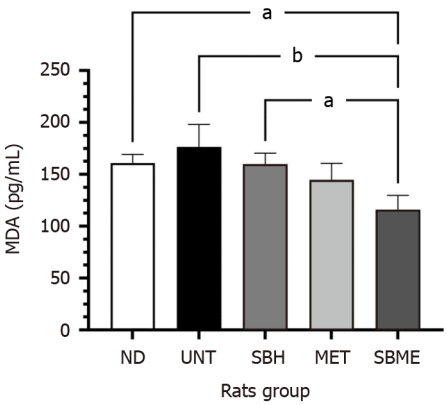

Figure 1 MDA level in diabetic rats in response to different treatments over 12 d. Data were analyzed using one-way analysis of variance, followed by Tukey's post-test. Data showed in mean ± SEM; $^{a,b}P < 0.05$. ND: Non-diabetic group; UNT: Untreated diabetic group; SBH: Stingless bee honey group; MET: Metformin group; SBME: Stingless bee honey plus metformin group.

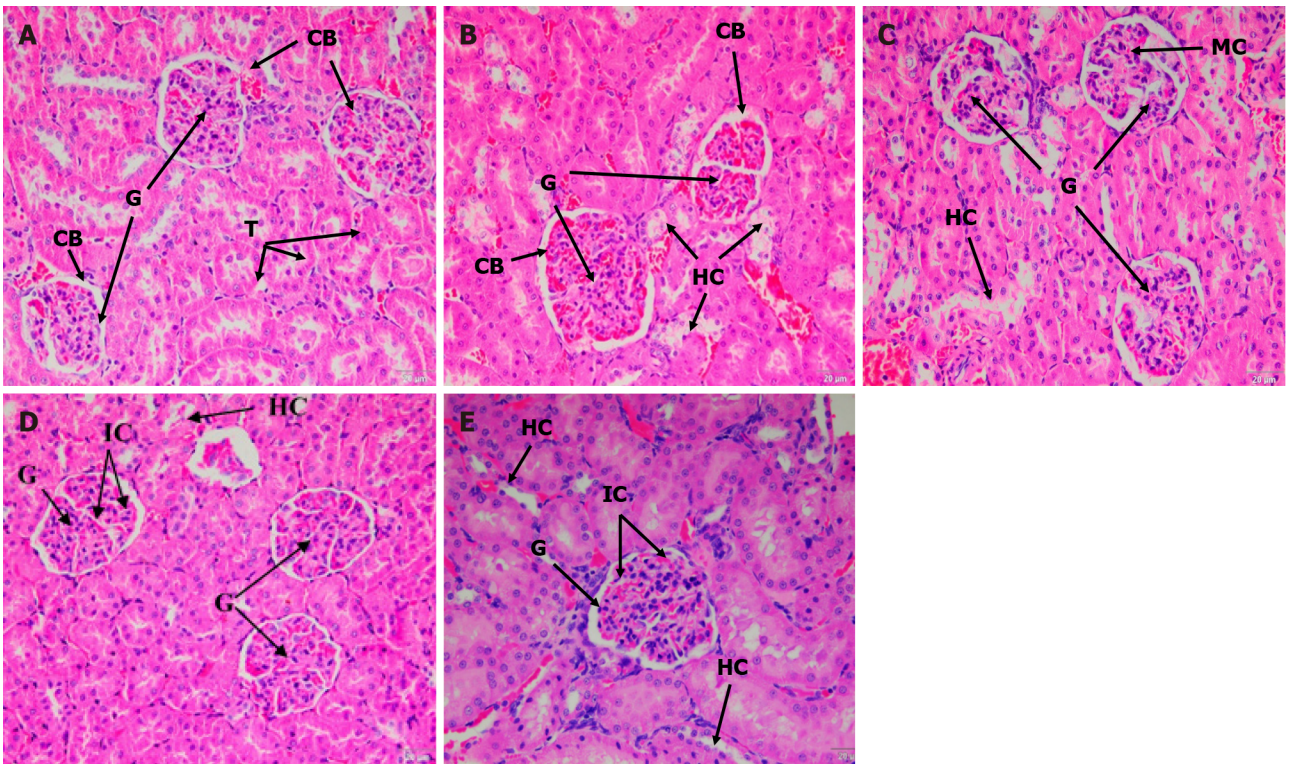

Figure 2 H&E staining of kidney tissue samples on day 13. A: Tissue sample for the non-diabetic control group; B: Untreated (UNT) diabetic group; C: Stingless bee honey (SBH) treatment group; D: Metformin (MET) treatment group; E: Stingless bee honey plus metformin (SBME) treatment group. The UNT group showed an increase in glomerular cellularity and tubular hydropic changes. The MET and SBME groups showed high cellularity and mesangial matrix expansion. The SBH group showed a decrease in hydropic changes and mild cellularity of the glomerulus (H&E staining, 40 ×). G: Glomerulus; CB: Capsule Bowman; T: Tubules; HC: Hydropic changes; IC: Increased cellularity; C: Capillary; M: Mesangial cell; MC: Mild cellularity.

evaluation of liver function tests in rats treated with different treatments for 12 d are shown in Table 3.

An MDA assay was performed to determine the role of SBH supplementation in the lipid peroxidation process. Figure 1 shows the MDA levels after 12 d of treatment. The MDA level was significantly higher in the UNT group *vs* ND rats ($P < 0.05$), whereas it was significantly lower in the treatment groups than in the UNT group ($P < 0.01$). The SBME group had significantly lower MDA levels compared to the SBH group ($P < 0.05$).

Hematoxylin and eosin staining of the kidneys

ND rats showed a normal architecture of Bowman's capsule and tubules; the glomeruli had normal cellularity and no hydropic changes of the tubules (Figure 2A). Contrarily, the UNT group had increased glomerular cellularity and tubular hydropic changes was also observed (Figure 2B). In the SBH-treated groups, the kidney architecture showed a decrease in hydropic changes and mild cellularity of the glomerulus compared with the ND group (Figure 2C). The MET and SBME groups had higher cellularity than the SBH group as well as tubular hydropic changes were seen (Figure 2D and E).

Table 3 Biochemical evaluation of liver function in response to different treatments over 12 d

Group	Analytes				
	Albumin (g/L)	Total Protein (g/L)	ALT (U/L)	AST (U/L)	ALP (U/L)
Non-diabetic	32.00 ± 1.10	54.25 ± 0.75	58.00 ± 5.40	110.40 ± 12.14	134.60 ± 5.59
Untreated diabetic	28.50 ± 0.65	49.67 ± 2.19	75.50 ± 33.18	121.00 ± 7.44	162.00 ± 25.65
Stingless bee honey	29.33 ± 0.71	52.67 ± 2.32	64.20 ± 0.80	108.30 ± 11.46	131.70 ± 23.92
Metformin	28.40 ± 0.51[a]	50.33 ± 0.33	69.00 ± 7.41	110.30 ± 6.921	126.70 ± 14.84
Stingless bee honey plus metformin	29.50 ± 0.87	53.67 ± 1.20	71.50 ± 15.50	116.00 ± 11.41	149.30 ± 7.75

[a]$P < 0.05$ compared with non-diabetic.

Data were analyzed using one-way ANOVA, followed by Tukey's post-test. Data were expressed as mean + SEM. ALT: Alanine transaminase; AST: Aspartate transaminase; ALP: Alkaline phosphatase.

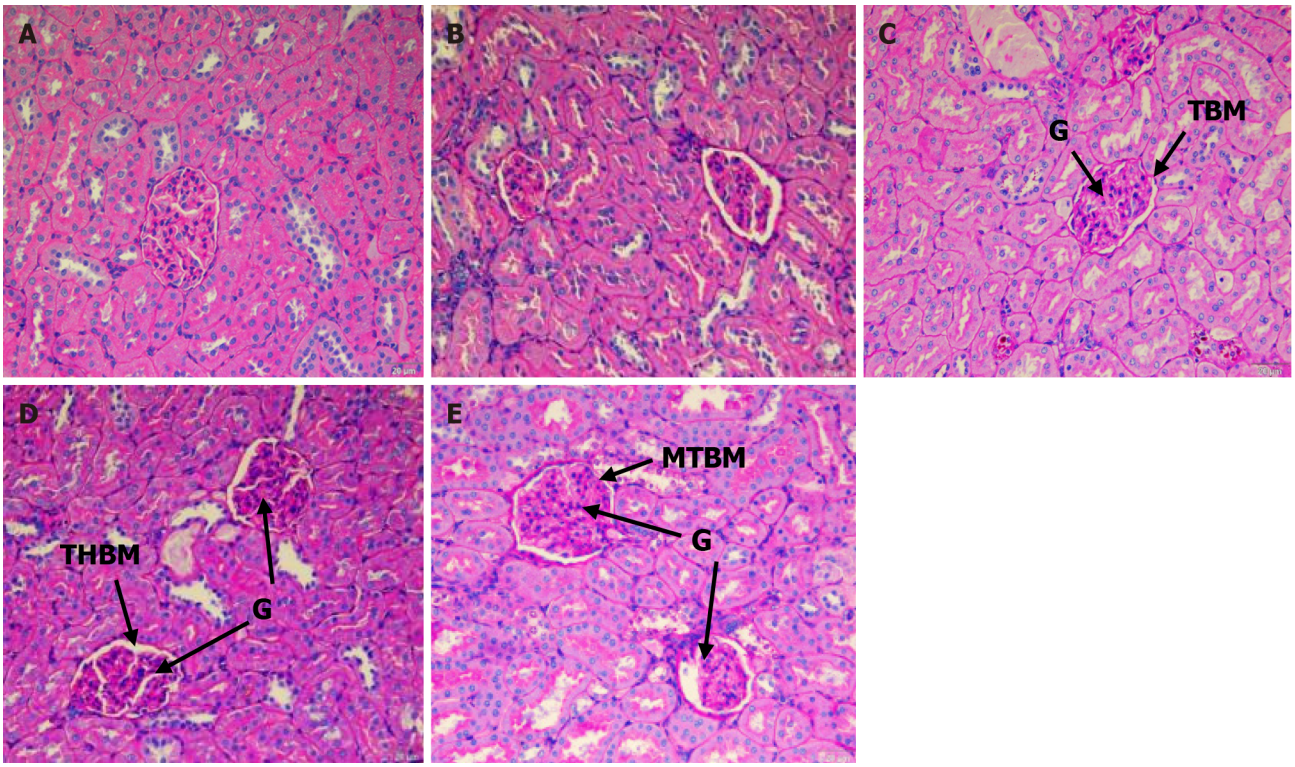

Figure 3 Periodic acid–Schiff staining of kidney tissue sample on day 13. A: Tissue sample for the non-diabetic (ND) control group; B: Untreated (UNT) diabetic group; C: Stingless bee honey plus metformin (SBME) treatment group; D: Stingless bee honey (SBH) treatment group; E: Metformin (MET) treatment group. The ND control group showed normal kidney tissue architecture. The UNT group had hydropic tubules and thickened basement membrane of the glomeruli, tubules, and blood capillaries. The SBH group showed improvement in these basement membrane changes. The MET group showed mild thickening of the glomerular basement membrane. The SBME group showed improvement of the basement membrane (PAS staining, 40 ×). G: Glomerulus; TBM: Thin layer basement membrane of glomeruli; T: Tubules; THBM: Thickening basement membrane of glomeruli; TT: Thickening basement membrane of tubules; AT: Atrophic tubules; MTBM: Mild thickening basement membrane of glomeruli.

Mesangial matrix expansion was observed in the kidneys of both MET and SBME rats.

PAS

The ND rats showed a thin layer of glomeruli basement membrane when stained with PAS (Figure 3A). UNT diabetic rats showed tubular hydropic tubules, which appeared to be smaller than that of other groups. Figure 3B also indicates thickening of the basement membrane of glomeruli, tubules, and blood capillaries as the intensity of PAS stain increased. The basement membrane of the SBH-treated rat kidney (Figure 3C) appears to resemble the ND rat kidney. The MET-treated rat kidney (Figure 3D) showed mild thickening of the glomeruli basement membrane. The basement membrane of the rat kidney in the SBME-treated group (Figure 3E) was also comparable to that of the SBH and ND groups.

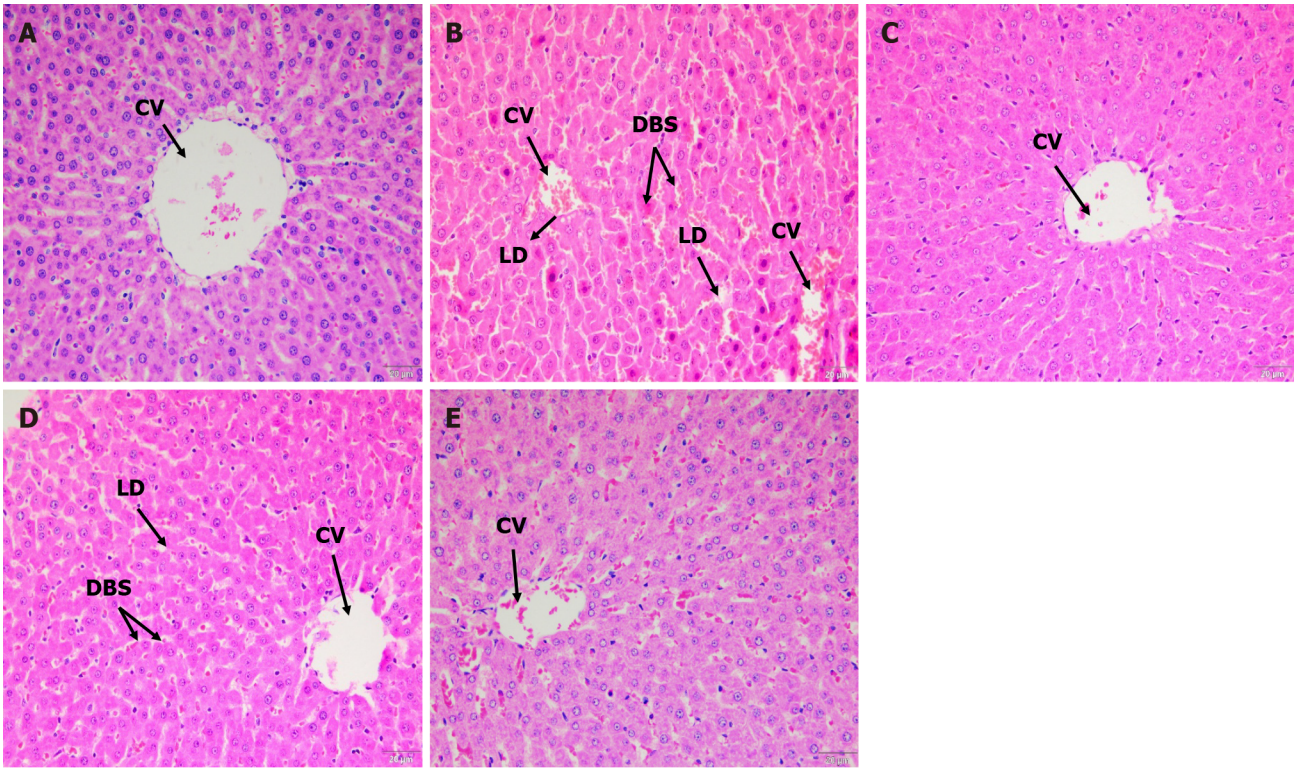

Figure 4 H&E staining of liver tissue sample on day 13. A: Tissue sample for the non-diabetic (ND) control group; B: Untreated (UNT) diabetic group; C: Stingless bee honey (SBH) treatment group; D: Metformin (MET) treatment group; E: Stingless bee honey plus metformin (SBME) treatment group. The ND control group showed normal liver architecture. The UNT group had lipid droplet formation in hepatocytes with dilated blood sinusoids and congestion surrounding central veins. The SBH group showed significant reduction in steatosis and sinusoid congestion. The MET group showed a reduction in steatosis, but sinusoids congestion was still present. The SBME group had decreased lipid droplet formation and dilated blood sinusoids (H&E staining, 40 ×). CV: Central vein; BS: Blood sinusoids; H: Hepatocytes; LD: Lipid droplet; DBS: Dilated blood sinusoids.

Effect of SBH on rat liver after treatment

Hematoxylin and eosin staining: Compared to controls (Figure 4A), histological alterations were detected in the liver tissue of UNT diabetic rats, which revealed significant steatosis harboring lipid droplet formation in hepatocytes with dilated blood sinusoids and congestion surrounding the central veins (Figure 4B). This was in accordance with an increase in the serum ALT and AST, which are indicators of hepatocyte damage. However, these pathological alterations were reduced after treatment with SBH (Figure 4C), which showed a normal structure of the hepatic cells, specifically, reduced steatosis and congestion of sinusoids. MET-treated rats still showed dilation of sinusoids but had reduced formation of lipid droplets compared to the UNT group (Figure 4D). The SBME group had similar liver structure to the SBH group, wherein the fatty vacuoles and dilation of sinusoids were decreased *vs* UNT diabetic rats (Figure 4E). Thus, SBH administration ameliorated STZ-induced diabetic hepatic toxicity and hyperlipidemia.

Periodic acid–Schiff staining: The ND rat liver showed normal staining of glycogen content on PAS (Figure 5A). In the UNT group, the glycogen content in the liver structure of rats can be observed clearly (Figure 5B). Interestingly, after treatment with SBH for 12 consecutive days, the glycogen content was decreased, as only some cells were maintained (Figure 5C). Similarly, in the SBME group, only some cells had a positive PAS stain effect (Figure 5D). Treatment with MET (Figure 5E) did not change the rat liver structure, since it was still similar to that of the UNT group, wherein the intensity of glycogen stain increases in almost all hepatocytes.

DISCUSSION

The International Diabetes Federation estimates that 537 million people were living with diabetes in 2021, with an expected increase to 784 million by the year 2045[19]. The association between liver illness and diabetes mellitus (DM) is well established[20]. Diabetes is the most common cause of kidney failure requiring kidney transplantation or dialysis worldwide[21].

In this study, after 12 d of treatment, the concentrations of serum urea and creatinine for all groups of rats were within a normal reported range. UNT rats had the highest level of serum urea and creatinine compared with ND rats, suggesting that STZ-induced toxic effects on the kidneys[22]. Tavafi[23] reported significantly high levels of serum urea and creatinine in diabetic rats (induced by alloxan) compared with normal control rats after 8 wk, which might be due to a longer period of treatment taken for treating DM rats than in our current study of only 12 d.

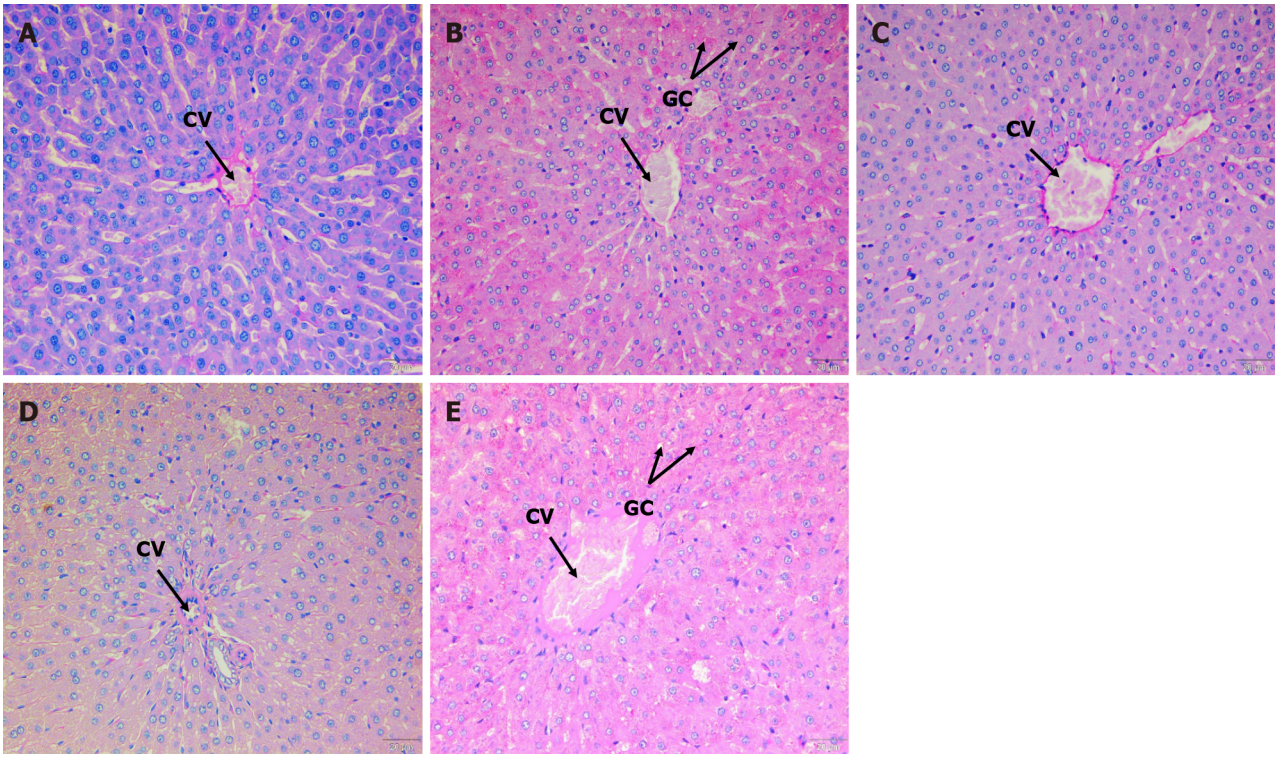

Figure 5 Periodic acid–Schiff staining of liver tissue sample on the 13th day of study. A: Tissue sample for the non-diabetic (ND) control group; B: Untreated diabetic (UNT) group; C: Stingless bee honey (SBH) treatment group; D: Stingless bee honey plus metformin (SBME) treatment group; E: Metformin treatment (MET) group. The ND control group showed normal architecture. The UNT group showed an increase in glycogen content. The SBH diabetic group showed a reduction in glycogen content. The MET group showed an increase in glycogen content. The SBME group showed a reduction in glycogen content (PAS staining, 40 ×). CV: Central vein; GC: Glycogen content showed an increase in glycogen content.

Histological findings revealed tubular hydropic alterations and an increase in glomerular cellularity of kidney sections in UNT diabetic rats *vs* ND rats. Structural changes in the kidney could be related to diabetic metabolic changes. After staining with H&E and PAS, kidney sections from STZ-induced diabetic rats showed significant vacuolar degeneration of tubules, increased glomerular cellularity, mesangial matrix enlargement, and basement membrane thickening, likely caused by the extreme hyperglycemia from STZ induction. In line with this, Obi-Ezeani *et al*[24] described tubular epithelial alterations, increased capsular space, and glomerular degeneration in diabetic rats. Treatment with SBH had a favorable effect in mitigating renal injury by reducing hydropic alterations and improving basement membrane integrity. Compared to SBH-treated diabetic rats, high glomerular cellularity and mesangial matrix growth can still be detected with MET and SBME treatment. Furthermore, after staining with PAS, MET-treated rat kidneys had a slightly thickened glomeruli basement membrane. SBME-treated animals had similar basement membranes to those of the SBH and ND groups. Thus, therapy with SBH alone considerably reduced the changes identified on H&E and PAS staining, indicating its preventive role in renal injury.

MDA is a highly toxic aldehyde produced as a result of polyunsaturated fatty acid peroxidation, and it is a common indicator of lipid peroxidation[24]. DM can cause tissue damage through lipid peroxidation. Our findings revealed that the UNT group had the highest serum MDA level, likely from an increase in reactive oxygen species production caused by persistent hyperglycemia in UNT diabetic rats. Hyperglycemia reduces antioxidant levels in rats while increasing free radicals. However, treatment with SBME in our study significantly suppressed MDA levels in STZ-induced diabetic rats; this could help reduce oxidative stress. Our findings were consistent with those of other studies that indicated that SBH improved the MDA level in diabetic rats[25].

Elevated serum aminotransferase activity is a common indicator of liver illness. ALT and AST are common serum biochemical indicators that are regularly examined to diagnose liver injury and abnormalities[24,26]. The biochemical data in our study agreed with our histological observations using H&E and PAS staining. In UNT diabetic rats, lipid droplets accumulated in the cytoplasm of hepatocytes (Figure 4B and D). STZ caused acute liver injury in the current investigation, as evidenced by an increase in liver enzymes and histological abnormalities in the liver tissue of UNT diabetic rats (Figure 5B) after 12 d compared with ND rats, but these differences were not statistically significant. Nevertheless, after 12 d of SBH and MET treatment, ALT, AST, and ALP activity were all reduced, possibly because of the hepatoprotective effects of SBH and MET. Thus, even if hyperglycemia increased the MDA levels, causing oxidative liver damage, treatment with SBH was able to protect the liver by lowering blood ALT, AST, and ALP levels, possibly due to its hypoglycemic and antioxidant properties. Therefore, SBH can help improve impaired liver function in STZ-induced diabetic rats.

The current study has some limitations. The short treatment period may have contributed to the non-significant changes in biochemical results, despite clear histological changes seen in the liver and kidneys of diabetic rats. Moreover,

during the 12-d treatment period, the ND rats did not receive SBH treatment. Future studies should explore the potential benefits and effects of oral SBH delivery in ND rats.

CONCLUSION

Although there were no significant variations in serum creatinine and urea levels between the groups, kidneys from the SBH group showed a normal thin layer of glomeruli basement membrane, equivalent to that of ND rats, and less hydropic alteration than the other groups. Although the decrease serum ALT, AST, and ALP levels were not significant, SBH treatment caused a histologically evident improvement in hepatocytes and reduced the formation of fatty vacuoles and dilatations of blood sinusoids in diabetic rat livers.

ARTICLE HIGHLIGHTS

Research background

Studies have demonstrated an inverse relationship between honey consumption and the risk of diabetes and its complications. The argument about using honey to lower blood glucose and prevent hepatorenal diabetic complications however, continued.

Research motivation

Recent research has focused on exploring the biochemical and histological effects on kidney and liver of diabetic rats given oral stingless bee honey (SBH) and compared with rats given metformin (MET), combination SBH+MET, untreated and non-diabetic rats.

Research objectives

We investigated the effect of SBH administration on the serum biochemical parameters and the histological changes in streptozotocin induced diabetic rats' kidney and liver using hematoxylin and eosin (H&E), Periodic Acid Schiff (PAS) staining.

Research methods

Sprague Dawley rats (n = 30) grouped into 5, *i.e.* SBH-treated, metformin-treated (MET) and SBH+metformin-treated (SBME) non-diabetic (ND) and untreated diabetic (UNT) groups. The rats were sacrificed after 12 d of treatment, and serum, kidney and liver collected from the rats were used for biochemical parameters assessment.

Research results

SBH-treated group showed reduce in hydropic changes and mild cellularity of glomerulus as compared to ND group on H&E staining, but resembled ND group on PAS staining. Liver tissues of SBH-treated groups revealed lower fatty vacuoles formation and dilatation of blood sinusoids as compared to other groups. Biochemically, glucose reduction and lowest serum MDA, AST, ALT and ALP observed in SBH-treated compared to MET, SBME and UNT groups.

Research conclusions

The oral SBH prevent diabetic complications development indicated by liver and kidney histology of SBH-treated diabetic rats. This finding offers a good perspective of honey role in managing diabetes.

Research perspectives

Longer duration of treatment might improve the biochemical parameters. Future study on honey role in diabetic patients and metabolomic analysis to profile the serum of human treated with SBH and MET is necessary to uncover the underlying mechanisms.

ACKNOWLEDGEMENTS

We extend our heartfelt gratitude and appreciation to the personnel and staff of ARASC and Endocrine laboratory and Chemical Pathology laboratory staff, Universiti Sains Malaysia for their invaluable support throughout this research endeavor.

FOOTNOTES

Author contributions: Mohd Nasir S and Ismail AF conducted animal study and laboratory analysis; Tuan Ismail TS and Sirajudeen KNS designed the study objective and methodology; Wan Ahmad WAN and Wan Abdul Rahman WF reviewed and validated the histological

analysis; Tengku Din TADAA conducted statistical analysis and guided the animal and laboratory study; All the authors contributed to manuscript writing; Tuan Ismail TS edited and proofread the manuscripts.

Supported by Ministry of Higher Education, Malaysia for Fundamental Research Grant Scheme FRGS/1/2019/SKK06/USM/03/6, No. 291983-329281.

Institutional animal care and use committee statement: This study was approved by the Institutional Animal Care and Use Committee USM, Kubang Kerian [USM/IACUC/2019/(120) (1020)].

Conflict-of-interest statement: All the authors declare no conflict of interest in conducting this research.

Data sharing statement: No additional data is available.

ARRIVE guidelines statement: The authors have read the ARRIVE guidelines, and the manuscript was prepared and revised according to the ARRIVE guidelines.

Country/Territory of origin: Malaysia

ORCID number: Tuan Salwani Tuan Ismail 0000-0002-7739-8323.

S-Editor: Liu JH
L-Editor: A
P-Editor: Yuan YY

REFERENCES

1 **Thangavel P**, Ramachandran B, Chakraborty S, Kannan R, Lonchin S, Muthuvijayan V. Accelerated Healing of Diabetic Wounds Treated with L-Glutamic acid Loaded Hydrogels Through Enhanced Collagen Deposition and Angiogenesis: An In Vivo Study. *Sci Rep* 2017; **7**: 10701 [PMID: 28878327 DOI: 10.1038/s41598-017-10882-1]

2 **Akhtar S**, Nasir JA, Ali A, Asghar M, Majeed R, Sarwar A. Prevalence of type-2 diabetes and prediabetes in Malaysia: A systematic review and meta-analysis. *PLoS One* 2022; **17**: e0263139 [PMID: 35085366 DOI: 10.1371/journal.pone.0263139]

3 **Wang H**, Li N, Chivese T, Werfalli M, Sun H, Yuen L, Hoegfeldt CA, Elise Powe C, Immanuel J, Karuranga S, Divakar H, Levitt N, Li C, Simmons D, Yang X; IDF Diabetes Atlas Committee Hyperglycaemia in Pregnancy Special Interest Group. IDF Diabetes Atlas: Estimation of Global and Regional Gestational Diabetes Mellitus Prevalence for 2021 by International Association of Diabetes in Pregnancy Study Group's Criteria. *Diabetes Res Clin Pract* 2022; **183**: 109050 [PMID: 34883186 DOI: 10.1016/j.diabres.2021.109050]

4 **Ganasegeran K**, Hor CP, Jamil MFA, Loh HC, Noor JM, Hamid NA, Suppiah PD, Abdul Manaf MR, Ch'ng ASH, Looi I. A Systematic Review of the Economic Burden of Type 2 Diabetes in Malaysia. *Int J Environ Res Public Health* 2020; **17** [PMID: 32784771 DOI: 10.3390/ijerph17165723]

5 **Lim AKh**. Diabetic nephropathy - complications and treatment. *Int J Nephrol Renovasc Dis* 2014; **7**: 361-381 [PMID: 25342915 DOI: 10.2147/IJNRD.S40172]

6 **Mohamed J**, Nazratun Nafizah AH, Zariyantey AH, Budin SB. Mechanisms of diabetes-induced liver damage: The role of oxidative stress and inflammation. *Sultan Qaboos Univ Med J* 2016; **16**: el32-el41

7 **Yang DK**, Kang HS. Anti-Diabetic Effect of Cotreatment with Quercetin and Resveratrol in Streptozotocin-Induced Diabetic Rats. *Biomol Ther (Seoul)* 2018; **26**: 130-138 [PMID: 29462848 DOI: 10.4062/biomolther.2017.254]

8 **Du M**, Hu X, Kou L, Zhang B, Zhang C. Lycium barbarum Polysaccharide Mediated the Antidiabetic and Antinephritic Effects in Diet-Streptozotocin-Induced Diabetic Sprague Dawley Rats *via* Regulation of NF-κB. *Biomed Res Int* 2016; **2016**: 3140290 [PMID: 27200371 DOI: 10.1155/2016/3140290]

9 **Nikpour M**, Shirvani MA, Azadbakht M, Zanjani R, Mousavi E. The effect of honey gel on abdominal wound healing in cesarean section: a triple blind randomized clinical trial. *Oman Med J* 2014; **29**: 255-259 [PMID: 25170405 DOI: 10.5001/omj.2014.68]

10 **Mohd Rafie AZ**, Syahir A, Wan Ahmad WAN, Mustafa MZ, Mariatulqabtiah AR. Supplementation of Stingless Bee Honey from Heterotrigona itama Improves Antiobesity Parameters in High-Fat Diet Induced Obese Rat Model. *Evid Based Complement Alternat Med* 2018; **2018**: 6371582 [PMID: 30643535 DOI: 10.1155/2018/6371582]

11 **Biluca FC**, Braghini F, Gonzaga LV, Costa ACO, Fett R. Physicochemical profiles, minerals and bioactive compounds of stingless bee honey (Meliponinae). *J Food Compos Anal* 2016; **50**: 61-69 [DOI: 10.1016/j.jfca.2016.05.007]

12 **Ali H**, Abu Bakar MF, Majid M, Muhammad N, Lim SY. In vitro anti-diabetic activity of stingless bee honey from different botanical origins. *Food Res* 2020; **4**: 1421-1426 [DOI: 10.26656/fr.2017.4(5).411]

13 **Ahmed S**, Sulaiman SA, Baig AA, Ibrahim M, Liaqat S, Fatima S, Jabeen S, Shamim N, Othman NH. Honey as a Potential Natural Antioxidant Medicine: An Insight into Its Molecular Mechanisms of Action. *Oxid Med Cell Longev* 2018; **2018**: 8367846 [PMID: 29492183 DOI: 10.1155/2018/8367846]

14 **Erejuwa OO**, Nwobodo NN, Akpan JL, Okorie UA, Ezeonu CT, Ezeokpo BC, Nwadike KI, Erhiano E, Abdul Wahab MS, Sulaiman SA. Nigerian Honey Ameliorates Hyperglycemia and Dyslipidemia in Alloxan-Induced Diabetic Rats. *Nutrients* 2016; **8**: 95 [PMID: 26927161 DOI: 10.3390/nu8030095]

15 **Alvarez-Suarez JM**, Gasparrini M, Forbes-Hernández TY, Mazzoni L, Giampieri F. The Composition and Biological Activity of Honey: A Focus on Manuka Honey. *Foods* 2014; **3**: 420-432 [PMID: 28234328 DOI: 10.3390/foods3030420]

16 **Zakaria F**, Rosli W, Ishak W, Sze N, Shazwan M. Assessment of Glycaemic Effect of Benincasa hispida Aqueous Extract in Streptozotocin Diabetic Rats 2016; 1-12. Available from:https://www.researchgate.net/publication/307974568_Assessment_of_Glycaemic_Effect_of_Benincasa_hispida_Aqueous_Extract_in_Streptozotocin_Diabetic_Rats

17 **Nain P**, Saini V, Sharma S, Nain J. Antidiabetic and antioxidant potential of Emblica officinalis Gaertn. leaves extract in streptozotocin-induced type-2 diabetes mellitus (T2DM) rats. *J Ethnopharmacol* 2012; **142**: 65-71 [PMID: 22855943 DOI: 10.1016/j.jep.2012.04.014]

18 **Shamsudin S**, Selamat J, Sanny M, A R SB, Jambari NN, Khatib A. A Comparative Characterization of Physicochemical and Antioxidants Properties of Processed Heterotrigona itama Honey from Different Origins and Classification by Chemometrics Analysis. *Molecules* 2019; **24** [PMID: 31671885 DOI: 10.3390/molecules24213898]

19 **Weng J**, Zhou J, Liang L, Li L. UHPLC/QTOF-MS-based metabolomics reveal the effect of Melastoma dodecandrum extract in type 2 diabetic rats. *Pharm Biol* 2019; **57**: 807-815 [PMID: 31794270 DOI: 10.1080/13880209.2019.1693605]

20 **de Boer IH**, Khunti K, Sadusky T, Tuttle KR, Neumiller JJ, Rhee CM, Rosas SE, Rossing P, Bakris G. Diabetes Management in Chronic Kidney Disease: A Consensus Report by the American Diabetes Association (ADA) and Kidney Disease: Improving Global Outcomes (KDIGO). *Diabetes Care* 2022; **45**: 3075-3090 [PMID: 36189689 DOI: 10.2337/dci22-0027]

21 **Hamed AE**, Elsahar M, Elwan NM, El-Nakeep S, Naguib M, Soliman HH, Ahmed Aboubakr A, AbdelMaqsod A, Sedrak H, Assaad SN, Elwakil R, Esmat G, Salh S, Mostafa T, Mogawer S, Sadek SE, Saber MM, Ezelarab H, Mahmoud AA, Sultan S, El Kassas M, Kamal E, ElSayed NM, Moussa S. Managing diabetes and liver disease association. *Arab J Gastroenterol* 2018; **19**: 166-179 [PMID: 30420265 DOI: 10.1016/j.ajg.2018.08.003]

22 **Nørgaard SA**, Søndergaard H, Sørensen DB, Galsgaard ED, Hess C, Sand FW. Optimising streptozotocin dosing to minimise renal toxicity and impairment of stomach emptying in male 129/Sv mice. *Lab Anim* 2020; **54**: 341-352 [PMID: 31510860 DOI: 10.1177/0023677219872224]

23 **Tavafi M**. Diabetic nephropathy and antioxidants. *J Nephropathol* 2013; **2**: 20-27 [PMID: 24475422 DOI: 10.5812/nephropathol.9093]

24 **Obi-Ezeani NC**. Evaluation of oxidative stress-induced diabetic complications on alloxan-treated hyperglycaemic rats, using some biochemical parameters and histological profiles of three major organs. *MOJ Toxicol* 2018; **4**: 59-67 [DOI: 10.15406/mojt.2018.04.00091]

25 **Touzani S**, Al-Waili N, Imtara H, Aboulghazi A, Hammas N, Falcão S, Vilas-Boas M, Arabi IE, Al-Waili W, Lyoussi B. Arbutus Unedo Honey and Propolis Ameliorate Acute Kidney Injury, Acute Liver Injury, and Proteinuria *via* Hypoglycemic and Antioxidant Activity in Streptozotocin-Treated Rats. *Cell Physiol Biochem* 2022; **56**: 66-81 [PMID: 35218633 DOI: 10.33594/000000496]

26 **Ahmed Z**, Ahmed U, Walayat S, Ren J, Martin DK, Moole H, Koppe S, Yong S, Dhillon S. Liver function tests in identifying patients with liver disease. *Clin Exp Gastroenterol* 2018; **11**: 301-307 [PMID: 30197529 DOI: 10.2147/CEG.S160537]

Published by **Baishideng Publishing Group Inc**
7041 Koll Center Parkway, Suite 160, Pleasanton, CA 94566, USA
Telephone: +1-925-3991568
E-mail: office@baishideng.com
Help Desk: https://www.f6publishing.com/helpdesk
https://www.wjgnet.com